Role of Protein *N*-glycosylation during the Pollen Tube Reception in *Arabidopsis thaliana*

Dissertation

zur

Erlangung der naturwissenschaftlichen Doktorwürde
(Dr. sc. nat.)

vorgelegt der

Mathematisch-naturwissenschaftlichen Fakultät

der

Universität Zürich

von

Andrea Zupunski

aus

Serbien

Promotionskommission

Prof. Dr. Ueli Grossniklaus
(Vorsitz und Leitung der Dissertation)

Prof. Dr. Joop Vermeer

Dr. Aurélien Boisson-Dernier

Prof. Dr. Lucia Colombo

Zürich, 2020

In loving memory of Đura Župunski

Zusammenfassung

In Blütenpflanzen ist die Befruchtung von der erfolgreichen Navigation des Pollenschlauches (PT) abhängig, der die Spermienzelle vom Stigma durch den Griffel zum weiblichen Gametophyten transportiert. Auf dem langen Weg des Pollenschlauches spielen rezeptorähnliche Kinasen (RLKs) eine wichtige Rolle. In *Arabidopsis thaliana* existieren über 600 solcher rezeptorähnlichen Kinasen. FERONIA (FER) ist eine solche RLK und spielt eine Schlüsselrolle in der Kommunikation zwischen Pollenschlauch und Gametophyt und in der erfolgreichen Aufnahme des Pollenschlauches. In *fer* Mutanten bleiben fast 80% der Samenanlagen unbefruchtet, da der Pollenschlauch nicht platzt und somit die Spermienzellen nicht freigesetzt werden, stattdessen wachsen Pollenschläuche auch im Embryosack weiter, dieser Phänotyp eines übermässigen Wachstums des Pollenschlauches wird Pollen Tube Overgrowth (PTO) bezeichnet. Wenn nahverwandte Spezies der *Brassicaceae* Familie miteinander gekreuzt werden kann man mitunter ein Phänotyp beobachten der, desjenigen der *fer*-Mutante gleicht. Deshalb könnte der FER Signalweg auch in die zwischenartliche Pollenschlaucherkennung involviert sein. Seit der Erstentdeckung von FER vor 17 Jahren konnten nur wenige weiblich gametophytischen Mutanten mit einem *fer* ähnlichen Phänotypen entdeckt werden und keine FER Liganden, die in die Pollenschlauchaufnahme involviert sind, konnten identifiziert werden. Mithilfe eines EMS-Mutagenese-Screens, der gemacht wurde, um neue Komponenten im FER Signalweg zu identifizieren, konnten zwei Mutationen in Mutanten mit PTO-Phänotyp gemappt werden; eine in einer UDP-Glycosyltransferase die TURAN (TUN) genannt wurde, und eine in einer Dolichol Kinase namens EVAN (EVN). Durch SNP Ratio Mapping (SRM) und Next Generation Sequencing konnten drei weitere potenzielle Mutationen identifiziert werden. Wir konnten eine der drei Mutationen einem neuen Allel von *TURAN (TUN)* zuordnen. Dies zeigt, dass SRM die Methode der Wahl ist um letale Mutationen und Mutationen mit niedriger Penetranz zu mappen. Eine weitere der drei Kandidaten, hatte einen kausalen SNP im Gen *ALG11 (ASPARAGINE LINKED GLYCOSYLATION 11)*; dieses Gen kodiert für ein Enzym, das im Endoplasmatischen Retikulum lokalisiert ist und in den N-Glykosylierung Signalweg involviert ist. ALG11 ist eine alpha-1,2-mannosyltransferase, dessen funktionale Charakterisierung zeigte, dass, zusätzlich zur weiblich gametophytischen PTO, die Integrität des Pollenschlauches auch in einem alg11/ALG11 Hintergrund beeinträchtigt ist und die Pollenschläuche zu früh platzen. Die Biogenese von FER war interessanterweise nicht beeinträchtigt im alg11/ALG11 Hintergrund und FER war korrekterweise am Filiform Apparat (FA), wo der Austausch molekularer Signale zwischen den Gametophyten stattfindet der zum Wachstumsstopp des Pollenschlauches, seiner Erkennung und dem Platzen des Schlauches führt. Ausserdem konnten wir sehen, dass der Verlust von ALG11 dazu führt, dass Pollen der nahverwandten Art *Arabidopsis lyrata*, schlechter erkannt wird. Die korrekte N-Glykosylierung spielt eine wichtige Rolle in der Erkennung des Gametophyten, wir versuchten deshalb unter Verwendung eines Reverse Genetic Approach die Bedeutung der N-Glykosylierung für die Pollenschlaucherkennung und den N-Glykosylierung Signalweg besser zu untersuchen. Wir fanden heraus, dass der Verlust der beiden im ER lokalisierten Enzyme ALG3 und ALG10 dazu führten, dass nur die zwischenartliche Pollenschlaucherkennung beeinträchtigt wurde. Ausserdem konnten wir eine Verbindung herstellen zwischen Golgi assozierter N-Glycan maturation und gametphyt Erkennung während der zwischenartlichen Pollenschlauchaufnahme in *A. thaliana*. Da mehrere Mutanten des N-Glykosylierung Signalweg einen *fer*-ähnlichen Phänotyp mit PTO besitzen, und FER zehn an zehn Stellen in der extrazellulären Domäne (ECD) N-glykosyliert werden könnte, wollten wir herausfinden welche Rolle spezifische N-Glykane für die Funktion des FER Proteins spielen. Des Weiteren spielt FER nicht nur eine wichtige Rolle für die Reproduktion, FER hat auch

regulatorische Aufgaben für die Kontrolle des Zellwachstums, in Hormon Signalwegen und schliesslich ist FER auch involviert in Stressantworten gegen biotischen und abiotischen Stress; FER ist essenziell für alle Aspekte eines Pflanzenleben. Eine massenspektrometrische (MS) Analyse zeigte, dass vier der zehn potenziell N-Glykolysierbaren Stellen in FER glykolisiert sind. Basierend auf dem Glykosylierung Status *in planta*, wurde die Funktionalität der N-Glykane im FER Signalweg überprüft mittels eines Stellenspezifischen Mutagenese Screens. Insgesamt wurden durch den Screen Dreissig FER N-Glykosylierung Varianten generiert, einschliesslich Einzelmutanten und Kombinationen von mehreren Mutanten. Schon der Verlust eines N-Glycans führt dazu, dass FER gegenüber hohem Salzstress intolerant wird. Andererseits war die Funktion von FER für die Entwicklung und das Wachstum der Wurzelhaare erst beeinträchtigt, nachdem gleichzeitig sechs N-Glyocsylation Motive verloren worden waren. Die vegetativen Phänotypen der *fer* Mutante konnten komplementiert werden durch eine FER Variante der acht der N-Glykosilierungsmotive fehlten, deshalb scheint es, dass der Verlust von N-Glykanen keine grosse Rolle spielt für die Funktion FERs in der vegetativen Entwicklung. Ausserdem fanden wir heraus, dass N-Glykosylierung von FER für die Erkennung von eigenem Pollen überflüssig ist, da eigener Pollen auch erkannt wurde, wenn acht Glykosilierungsmotive gefehlt haben. Im Gegensatz dazu konnte die Erkennung von Fremdpollen der nahverwandten Art *A. lyrata* stark beeinträchtigt werden, wenn N-Glykane nicht vorhanden waren, an mehreren einzelnen Motiven. Diese Studie liefert erste Evidenz, dass N-Glykosylierung von einem Protein mit Funktion in der Reproduktion essentiell ist für die Errichtung reproduktiver Barrieren. Ausserdem zeigt diese Studie die Bedeutung des N-Glykosilierungs-Signalweg für die erfolgreiche Perzeption des Pollenschlauches durch den weiblichen Gametophyten in *A. thaliana* auf.

Abstract

In flowering plants, the delivery of sperm cells to the female gametophyte is highly dependent on the successful navigation of pollen tubes (PTs) from the stigma, through the transmitting tract to the female gametophyte. Receptor like kinases (RLK), of which there are over 600 in *Arabidopsis thaliana*, play essential roles during each step of the PTs lengthy journey. The receptor-like kinase FERONIA (FER) is a key determinant of proper gametophyte communication and PT reception. In *fer* mutants, almost 80% of ovules remain unfertilized due to the inability of PTs to burst and release sperm cells. Instead, PTs continue to grow inside the embryo sack, a phenotype commonly described as PT overgrowth (PTO). A phenotype similar to *fer's* PTO occurs during interspecific pollinations among closely related species of the *Brassicaceae* family, thus also implicating the FER pathway in interspecific PT recognition. Since the initial discovery of FER almost 17 years ago, only a handful of female gametophytic mutants with *fer*-like PTO phenotype have been discovered, and the identification of FER ligands involved in PT reception has remained elusive. Previously, an EMS screen was performed to find novel components of the FER-mediated signaling pathway. Two mutants with PTO phenotypes were mapped to a UDP glycosyltransferase and a dolichol kinase, named TURAN (TUN) and EVAN (EVN) respectively. SNP ratio mapping (SRM) using next-generation sequencing (NGS) was utilized to identify three additional EMS mutant candidates. We mapped one of these candidates to a novel allele of *TURAN (TUN)*, thus further establishing SRM as the method of choice for the mapping of lethal and low penetrance mutations. Another of the candidates carried a causative SNP that mapped to *ALG11* (*ASPARAGINE LINKED GLYCOSYLATION 11*), which encodes an endoplasmic reticulum (ER)-resident enzyme of the *N*-glycosylation pathway. Functional characterization of ALG11, an alpha-1,2-mannosyltransferase, was performed and in addition to female gametophytic PTO, PT integrity was also compromised in the *alg11/ALG11* background resulting in a premature PT bursting. Interestingly, biogenesis of FER was not affected in *alg11/ALG11*. Rather, FER was correctly targeted to the filiform apparatus (FA), the site of extensive molecular crosstalk between gametophytes during PT arrest, recognition, and bursting. We also found that loss of *ALG11* caused impaired recognition of interspecific pollen from the closely related *Arabidopsis lyrata*. Given the importance of accurate *N*-glycosylation for gametophyte recognition, we performed a reverse genetic approach in order to further dissect the *N*-glycosylation pathway, and assess its importance during PT reception. We found that loss of the ER-localized *N*-glycosylation enzymes ALG3 and ALG10 resulted in an exclusive impairment of interspecific PT recognition. Furthermore, we identified a novel connection between Golgi associated *N*-glycan maturation and gametophyte recognition during interspecific PT reception in *A. thaliana.* Based on the observation that several mutants in the *N*-glycosylation pathway display *fer*-like PTO and FER has ten putative *N*-glycosylation sites in the extracellular domain (ECD), we set out to assess the importance of specific *N*-glycans for proper FER protein functionality. In addition to being a key reproductive regulator, FER is involved in cell growth control, hormone signaling, abiotic and biotic stress responses, and is overall essential for the key aspects of a plant life. Mass spectrometry (MS) analysis revealed that four of FER's ten *N*-glycosylation sites were *N*-glycosylated. Once FER's *N*-glycosylation status *in planta* was confirmed, a systematic site-directed mutagenesis screen was carried out to assess the functional importance of *N*-glycans for FER-mediated signaling. A total of thirty FER *N*-glycosylation variants were generated in the mutagenesis screen, including both single and higher-order *N*-glycosylation site mutant combinations. Remarkably, we found that even the loss of a single *N*-glycan renders FER completely intolerant to high salinity stress. On the other hand,

FER regulation of root hair development and growth was only affected after the simultaneously loss of six *N*-glycosylation motifs. FER's role in vegetative development appears to be even less sensitive to loss of *N*-glycans, as the FER variant lacking eight *N*-glycosylation sites was sufficient to restore the *fer* mutant's vegetative phenotypes. We found *N*-glycosylation of FER during the recognition of self-pollen to be essentially superfluous, with proper reception of self-pollen occurring even in FER variants lacking up to eight *N*-glycosylation sites. In contrast to the intraspecific pollinations, recognition of foreign pollen from the closely related *A. lyrata* was dramatically hindered by loss of *N*-glycans at several single positions. This study constitutes the first evidence that *N*-glycosylation of a reproductive protein is essential for reproductive barrier establishment, and reveals the importance of the *N*-glycosylation pathway for successful pollen tube reception by the female gametophyte in *A. thaliana.*

Acknowledgements

I firstly would like to express my gratitude to **Ueli Grossniklaus** for giving me the chance to do my PhD in his group and to work on such an interesting topic. I am thankful for helpful discussions, guidance, support, but also for giving me the freedom in my projects which helped me to develop both scientifically and personally. I am also grateful for creating such a stimulating and positive working atmosphere.

I am very thankful to **Aurélien Boisson-Dernier** (University of Cologne), **Joop Vermeer** (University of Zurich), and **Lucia Colombo** (University of Milan) for being the part of my thesis committee, for being supportive and giving very insightful feedback. Additionally, I would like to thank to **Aurélien Boisson-Dernier** for kindly providing plant material and plasmids, as well for all ideas and helpful suggestions.

I am very grateful to **Andrea Martínez Bernardini** for the immense help throughout my entire PhD, for always being extremely supportive and encouraging, and for introducing me to the world of *N*-glycosylation. I would like to thank you for being so generous with your time even after leaving the lab, and for careful reading of thesis. Thanks for all the fun times we had inside and outside the lab, but also for being there during the hard times, I am so grateful to have you as a friend! :)

I am very thankful to **Martin Mecchia** for all the invaluable scientific discussions we had, for the infinite input and exciting ideas over the years. Additionally, I am very grateful for such a dedicated reading and extensive input regarding my thesis. Thanks for being a good friend and always such a fun to be around! :)

I am very grateful to **Stefano Bencivenga** for being always ready to help, for all the troubleshooting with the technical problems, as well for countless useful suggestions regarding my projects. Thank you also for reading parts of the thesis and providing helpful input. Thanks for being a great lab neighbour, as well on the weekends!

I am very thankful to **Kinga Rutowicz** for your patience and readiness to help, for all the discussions and ideas over the years. Thanks for being so positive and kind, I am grateful to be your friend! :)

I am very grateful to **Wei W(h)en Chong** and **Kati(y)a Taylor** for being not only amazing lab mates but also for becoming such a great friends. Thanks for all the fun times and for making my last year of PhD so much better than I could have ever imagined! :)

I am very thankful to **Miloslawa Jaciubek**, **Ethel Mendocilla Sato, Ana Marcela Florez Rueda,** and **Ulrike Nienhaus** for all the coffee breaks and loughs, thanks for being such a lovely company and good friends! :)

I would also like to thank to **Stefan Wyder** for providing invaluable help regarding the NGS data analysis, and for the careful reading of part of my thesis. Also, thanks for being nice lab neighbour in the first years of my PhD.

I would like to thank to **Alejandro Giraldo Fonseca** for reading and giving useful input regarding part of the thesis, for always being helpful with bioinformatics and for being a great member of the Sex club. Also, thanks for being the best DJ and for always having such a positive attitude!

I am very thankful to **Tiago Meier** for translating lengthy abstract of my thesis to german, for being very encouraging and supportive and a great lab mate!

I would like to thank to **Nicholas Desnoyer** for always being ready to engage into scientific discussions and for useful suggestions regarding my projects. Thanks for teaching me how to play beer pong :), and for being a nice company!

I am very grateful to **Benoit Mermaz** for being such a awsome lab mate during the first sixs months of my PhD, as well for all the fun times we had outside the lab! :)

I would also like to thank to the all past and current members of the Sex club (**Lena, Anna, Roger, Evelyne, Andrea, Moritz, Dario, Gorka, Alejandro, Tiago, Stefano, Martin, Nadine, Philippe, Katia, Nick, Nicolas**) for having engaging discussions every second week, while enjoying the morning gipfeli.

I am also thankful to the TA Team: **Valeria Gagliardini, Frédérique Pasquer, Peter Kopf, Arturo Bolaños,** and **Christof Eichenberger**. I am very grateful to **Valeria Gagliardini** for always having great tips and tricks, for performing ddPCR analysis and for making the best tiramisu! I would like to thank to **Frédérique Pasquer** for all the sequencing preparation, always making great competent cells and being a nice greenhouse neighbour. Also, thanks for all the fun times throughout the years! I am very thankful to **Daniel Prata** for being awesome lab technician and simply the best $C_{12}H_{22}O_{11}$ provider. :)

The best part of my PhD time was definitely meeting my Vinzenz crew which has become over the years Züri family, so thank you **Mattia**, **Sara**, **Dimitris**, **Gloria**, **Joana**, **Alek**, **Jessica**, **Caterina** for making me feel like at home. I cannot find the right words to express the gratitude to my flatmate and friend **Elena**. Thanks for making life in the "ghetto" so amazing!

I also would like to thank to **Sandra**, **Mila**, **Majda**, **Bojana**, and **Jelena** for making me not forget Serbian :), and for helping me to miss home a bit less. Thanks, **Sandra**, for being always such a good friend, I am so happy for meeting you!

I would like to express my gratitude to my friends, who have been there through the good times, but also for some of the hardest moments I had faced. Even though we are far, I feel that we are always connected, and distance has only proven how strong our bond really is. I am so happy for having you in my life, so thank you **Jovana**, **Kornelija**, **Natasa** and **Sanja**.

Finally, I feel immensely blessed for having my family, thank you for your endless support, encouraging, patience, I do not know where I would be without your infinite love. To my mom, my entire world, I can say huge thank you for shaping me into the person I am today, volim te najvise!

TABLE OF CONTENTS

Scope of the thesis

Flowering plants (angiosperms) are the most successful and ubiquitously present group of land plants (Sprunck, 2020). Double fertilization in angiosperms and subsequent seed production rely on the successful transfer of sperm cells by pollen tubes (PT) to the embryo sack (Kessler and Grossniklaus, 2011). In the absence of FERONIA (FER), PTs fail to burst in the synergid cells leading to the continuous growth of PT inside the embryo sack (Escobar-Restrepo et al., 2007; Huck, 2003). A similar *fer-like* PT overgrowth (PTO) phenotype was observed in the interspecific crosses between closely related *Brassicaceae* species *A. thaliana* and *A. lyrata.* Interestingly the degree of interspecific PTO correlates with the sequence divergence of the FER extracellular domain (Escobar-Restrepo et al., 2007). FER is the first functionally characterized member of the *Cr*RLK1L subfamily comprised of 17 closely related proteins with a variable extracellular domain (ECD), transmembrane (TM) domain and an intracellular (ICD) S/T kinase domain (Boisson-Dernier et al., 2011). *Cr*RLK1L ECDs were showed to contain two malectin domains (MLDs) with several putative *N*-glycosylation sites (Lindner et al., 2012). Our group has previously demonstrated that disturbance of three enzymes of the *N*-glycosylation pathway caused PTO either in intra- or inter- specific pollinations (Lindner et al., 2015; Müller et al., 2016).

With the purpose of gaining better understanding of molecular mechanisms underlying PT reception, several research questions were addressed in this thesis utilizing different methodological approaches:

- **Which other molecular factors are required during the FER mediated PT reception?** In order to answer this question, uncharacterized EMS mutants from the forward genetic screen for the *fer*-like PTO were mapped using SNP ratio mapping approach (SRM). We have successfully discovered a novel component of the PT reception pathway *ALG11* encoding an enzyme of endoplasmic reticulum (ER) *N*-glycosylation pathway. Additionally, a novel allele of *TUN* as well as RNA helicase *RID1* were identified. Detail description can be found in the Chapter 2 of this thesis.

- **What is the role of protein *N*-glycosylation during the female and male gametophyte interaction?** We have dissected ER and Golgi mediated *N*-glycosylation pathway and found ALG3, ALG10 and CGL1 to be involved in the recognition of interspecific pollen in crosses with *A. lyrata*. Additionally, functional characterization of ALG11 (identified in Chapter 2) was performed. ALG11 is essential for both intra- and inter- specific PT recognition as well as for the maintenance of PTs cell wall integrity. Detail explanation is provided in the Chapter 3 of the thesis.

- **Are putative *N*-glycosylation sites of the FER ECD utilized *in planta*, and if so, what is their functional importance?** Mass spectrometry analysis was carried out, and four out of the ten putative *N*-glycosylation sites were found to be occupied with *N*-glycans. Having validation of FER being *N*-glycosylated, a large-scale site-directed mutagenesis screen was performed to assess importance of all ten *N*-glycosylation sites located in the FER`s ECD. Detail description of the systematic characterization of *N*-glycans` role for the mediation of FER signaling responses during vegetative growth, abiotic stress, and PT reception can be found in the Chapter 4 of this thesis.

Each chapter is written in a form of publication with its respective introduction, methods, results, discussion, and references used in the chapter. Chapter 1 is giving a broad overview of the plant reproduction field as well as the biological significance of the protein *N*-glycosylation. Chapter 5 comprises a general discussion with future directions and potential experiments for the results obtained in Chapter 2 and Chapter 3, while the results from Chapter 4 were discussed within respective paper.

References

Boisson-Dernier, A., Kessler, S.A., and Grossniklaus, U. (2011). The walls have ears: the role of plant CrRLK1Ls in sensing and transducing extracellular signals. Journal of Experimental Botany *62*, 1581–1591.

Escobar-Restrepo, J.-M., Huck, N., Kessler, S., Gagliardini, V., Gheyselinck, J., Yang, W.-C., and Grossniklaus, U. (2007). The FERONIA Receptor-like Kinase Mediates Male-Female Interactions During Pollen Tube Reception. Science *317*, 656–660.

Huck, N. (2003). The Arabidopsis mutant feronia disrupts the female gametophytic control of pollen tube reception. Development *130*, 2149–2159.

Kessler, S.A., and Grossniklaus, U. (2011). She's the boss: signaling in pollen tube reception. Current Opinion in Plant Biology *14*, 622–627.

Lindner, H., Müller, L.M., Boisson-Dernier, A., and Grossniklaus, U. (2012). CrRLK1L receptor-like kinases: not just another brick in the wall. Current Opinion in Plant Biology *15*, 659–669.

Lindner, H., Kessler, S.A., Müller, L.M., Shimosato-Asano, H., Boisson-Dernier, A., and Grossniklaus, U. (2015). TURAN and EVAN Mediate Pollen Tube Reception in Arabidopsis Synergids through Protein Glycosylation. PLoS Biol *13*, e1002139.

Müller, L.M., Lindner, H., Pires, N.D., Gagliardini, V., and Grossniklaus, U. (2016). A subunit of the oligosaccharyltransferase complex is required for interspecific gametophyte recognition in Arabidopsis. Nat Commun *7*, 10826.

Sprunck, S. (2020). Twice the fun, double the trouble: gamete interactions in flowering plants. Current Opinion in Plant Biology *53*, 106–116.

CHAPTER 1 - INTRODUCTION

1.1 Sexual reproduction in flowering plants

Plants are essential for the maintenance of life on earth by not only providing us with oxygen through the photosynthesis, but additionally serving as the primary energy source. The most abundant and ecologically successful group of plants on earth nowadays are flowering plants (angiosperms). Having in mind that most of them reproduce sexually, it is not an underestimation that successful fertilization of flowering plants is necessary to sustain life as we know it. Double fertilization of angiosperms is a key evolutionary feature that set them apart from the other land plants, and allowed them to take a myriad of habitats with astonishing 350 000 species (Crepet, 2000). Basis of such a rapid diversification of angiosperms were thought provoking for evolutionary biologist ever since Charles Darwin. Most of the defining features of flowering plants are thought to have evolved under a strong selection pressure to achieve a faster reproductive cycle (Williams, 2008).

Double fertilization is extremely complex process which relies on two fertilization events between two sperm cells and two female gametes, the egg and the central cell, to initiate seed development (Bleckmann et al., 2014). Since its discovery at the end of the nineteenth century by Nawaschin and Guignard, it remains to be one of the most puzzling fields of the plant biology (Berger et al., 2008). Using the model plant *Arabidopsis thaliana* tremendous progress has been made during the last decade in the better understanding of the cellular and molecular mechanisms that regulate each step of double fertilization (Adhikari et al., 2020; Sprunck, 2020; Zheng et al., 2018). One of the remarkable features of angiosperms' double fertilization is the fact that pollen tubes have evolved to precisely deliver immobile sperm cells to the female gametophyte. Male gametophyte is a tri-cellular structure, comprised of a vegetative cell and of two immotile sperm cells, which develop in anthers (Fig. 1). These cells are well protected by three cell wall layers, intine, outer exine as well as the pollen coat, which all together makes male gametophyte highly resistant to a vast range of environmental stresses (Lou et al., 2014).

Unlike mammals and many other lower plants, angiosperms sperm cells are immotile, and they are delivered as a cargo by the pollen vegetative cell. This was another key evolutionary feature that enabled angiosperms to be independent from the water (syphonogamy) (Kessler and Grossniklaus, 2011). Moreover, male gametes can be dispersed over long distances, with pollen carried by wind or various animal pollinators (Dresselhaus and Franklin-Tong, 2013). During anthesis pollen grains are released from anthers and can adhere to stigma, where in case of compatible pollinations they are allowed to hydrate and germinate (Johnson et al., 2019). In angiosperms, successful fertilization depends on the extensive communication between the male gametophyte and both the sporophytic and gametophytic tissues of the female. Pollen tubes evolved an astonishing capability to grow fast, with an incredible speed of 1 cm per hour, while also being able to maintain their integrity along the long journey from stigma to embryo sack (Vogler et al., 2016). Another evolutionary innovation observed only in angiosperms is the reinforcement of pollen tube walls with the callose plugs to ensure their integrity (Williams, 2008).

Another unique characteristic of angiosperms is that multicellular female gametophyte (embryo sack) is deeply protected in the pistil tissue (Fig. 1). In the majority of angiosperms, including *A. thaliana*, embryo sack consists of four cell types: the two synergid cells which are located at the entrance of ovule (micropyle), two gametes: egg cell (located at micropyle) and the central cell (residing in the middle part) as well as three antipodal cells at the chalazal part of the ovule (Skinner and Sundaresan, 2018; Yang et al., 2010). Female gametophyte is controlling final stages of the pollen tube journey

with the secretion of attractants to promote correct targeting of the pollen tubes (Higashiyama and Takeuchi, 2015; Higashiyama and Yang, 2017). The pollen tube enters the ovule through the micropyle opening, and ruptures in the receptive synergid to release the sperm cells. Sperm cells fertilize egg or central cells, forming a diploid embryo and triploid endosperm, respectively. This fertilization mechanism, unique to angiosperms, is known as double fertilization (Beale and Johnson, 2013; Dresselhaus and Franklin-Tong, 2013; Palanivelu and Tsukamoto, 2012).

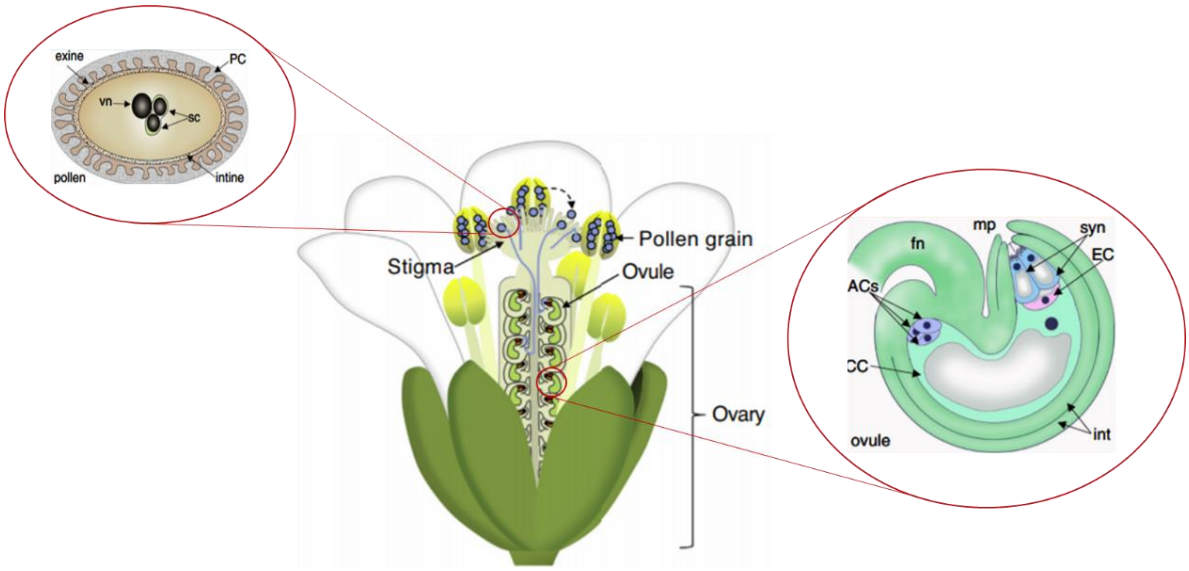

Figure 1. Schematic representation of the *A. thaliana* flower with its gametes. Male gametophytes (pollen grains) are developing within anthers, while the female gametophyte develop in the ovules, deeply embedded in ovary tissue. Once pollen grains lend on the stigma of self-compatible *A.thaliana*, they start their long journey through the transmitting tract towards the ovule. Pollen is comprised of vegetative cell which will upon germination develop into pollen tube as well of two immotile sperm cells. Ovules contain seven-celled female gametophyte. Legend (from left to the right): **vn** vegetative nucleus; **sc** sperm cell; **PC** pollen coat; **fn** funiculus, **ACs** antipodal cells; **CC** central cell, **mp** micropyle, **syn** synergid cell, **EC** egg cell, **int** integuments (inner and outer). Images adapted from reviews (Adhikari et al., 2020; Sprunck, 2020).

Plant double fertilization can be viewed as a step wise process and further subdivided into following stages: A) pollen adhesion, recognition and hydration on stigma; B) pollen tube growth through the transmitting tract C) gametophytic guidance D) pollen tube reception E) double fertilization and polyspermy block. In the following sections all stages of double fertilization will be described in more detail.

1.2 Pollen adhesion, hydration and germination

Once pollen has landed on the stigma either by contact, wind or different type of pollinators the process of attachment to the papillae cells, termed as a pollen capture can begin. The initial stages of pollen capture are mediated by the cell wall components of pollen (Chapman and Goring, 2010). Pollen wall is comprised of inner intine and outer exine (Fig. 1), with exine being primarily composed of sporopollenin making pollen grains extremely robust and resistant to enzymatic or chemical degradation (Yang, 2016). Exine is not only providing excellent protection to the male gametophyte but is also essential during the pollen capture. Class of mutants with a malformed exine, generally termed as *less adhesive pollen*, display severely reduced capability to adhere to stigmatic surface

(Dobritsa et al., 2009; Yang, 2016). Additionally, there is a high species-specific variability in exine structure and even isolated *A. thaliana* exine on its own shows high preference to adhere to *A. thaliana* compared to any other *Brassicaceae* species (Zinkl et al., 1999). Stigmas of *Brassicaceae, Asteraceae,* and *Gramineae* are considered as 'dry' type of stigma, with a proteinic surface and tight species-specific regulation of pollen adhesion and hydration, compared to 'wet' type stigmas which are coated with viscous secretions and are allowing non-species specific pollen hydration (Chapman and Goring, 2010; Swanson et al., 2004).

Upon pollen adhesion on the papillae cells of 'dry' stigma such as *A. thaliana* (Fig. 2), complex interplay between protein and lipids from both surfaces are initiated in a process termed as a 'foot formation'. This is not a passive process and active signaling pathway is required to trigger hydration and germination of compatible pollen (Doucet et al., 2016). More than half of angiosperms species are self-incompatible (SI) and a crucial role during recognition of self vs non-self-pollen is controlled by S-locus which contains S-RECEPTOR KINASE (SRK), S-LOCUS PROTEIN 11 (SP11) and S-LOCUS GLYCOPROTEIN (SLG) (Iwano and Takayama, 2012; Takayama et al., 2001). This SI system is found in both *Brassicaceae* and *Papaveraceae* and it relies on the specific interplay of male and female S-proteins derived from the same S-haplotype (Iwano and Takayama, 2012). Successful interaction of SRK-SCR causes proteasome mediated degradation of EXO70A1 (component of exocyst subunit) which further promotes inhibition of pollen hydration at stigma (Dresselhaus and Franklin-Tong, 2013). Therefore EXO70A1 is a stigmatic compatibility factor, for instance *B. napus* and *A. thaliana* depleted of EXO70A1 lost any ability to accept compatible pollen (Samuel et al., 2009). On the other hand, in the self-compatible species such as *A. thaliana* SRK and SRC alleles are no longer functional therefore there is no activation of pollen rejection (Li and Yang, 2016). When *A. lyrata* signaling pair SRK-SCR is introduced to the self-fertile *A. thaliana* self-incompatibility response is reestablished. (Nasrallah, 2002). Upon compatible pollinations stigma provides water to the highly desiccated pollen grains which happens within minutes (Doucet et al., 2016).

During pollen hydration lipids and proteins from both pollen coat and stigma play a crucial role. Several mutants defective in the synthesis of either long chain lipids or fatty acids as well as of glycine-rich proteins (GRPs) all fail to hydrate on stigma (Mayfield and Preuss, 2000; Preuss et al., 1993). Additionally, KINβγ subunit of SNRK1 complex controls pollen germination via regulation of ROS signaling, hence *kinβγ* mutant pollen could not hydrate on stigma (Gao et al., 2016b). Another maternal component required for the proper pollen hydration is undisturbed level of the PHOSPHATIDYLINOSITOL-4-PHOSPHATE (PI4P) in the stigma, with mutants displaying reduced rate of pollen hydration on the stigma as well as additional defects at the later stages of pollen-pistil interactions (Chapman and Goring, 2011).

Once the pollen grain is successfully hydrated, the pollen germinates in less than 30 minutes and a pollen tube (PT) emerges (Fig. 2) (Fiebig et al., 2004). Live imagining studies revealed that Ca^{2+} gradient is being established soon upon pollen hydration, with the highest concentration at the potential germination site (Palanivelu and Tsukamoto, 2012; Steinhorst and Kudla, 2013). The vast importance of the Ca^{2+} mediated signaling responses is indisputable having in mind that several mutants affected in either Ca^{2+} pump, Ca^{2+} channel or even in downstream components such as calmodulin (Ca^{2+} binding protein), all display pollen germination defects (Gu et al., 2017; Landoni et al., 2010; Li et al., 2018). Germinated PTs grow through stigma towards the style (Fig. 2), which is mediated by signaling factors such as chemocyanins, firstly discovered in lily in which they caused redirection of PTs growth *in vitro* (Kim et al., 2003). Once on the right track PTs also must penetrate

stigma and style tissues before reaching the transmitting tract. Only recently it was reported that O-FUCOSYLTRANSFERASE1 (OFT1), which is a Golgi apparatus resident protein plays an essential role during PTs penetrance through the stigma-style interface. Mutant PTs of *oft1-1* can germinate and grow normally *in vitro*, however when deposited on stigma they display severely reduced ability to penetrate the stigma-style interface (Smith et al., 2018).

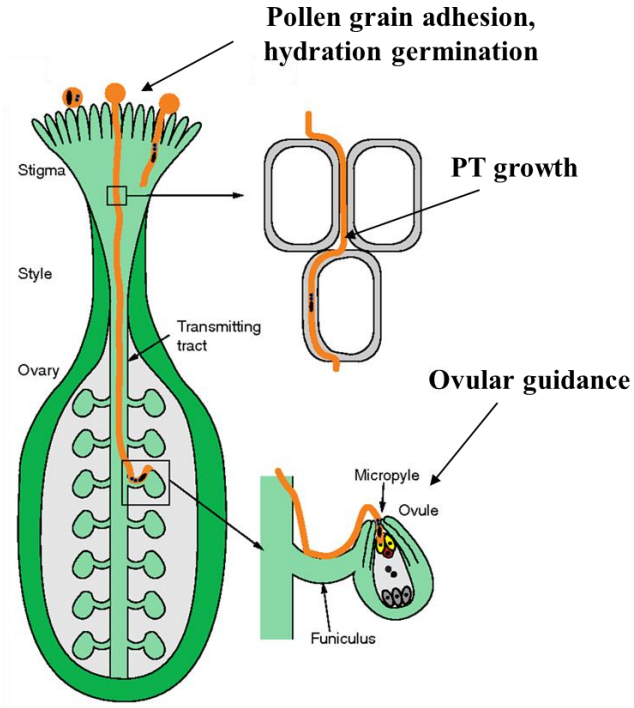

Figure 2. Stages of the pollen tube journey. The carton represents a generalized model of a pollinated pistil. Once the compatible pollen grains (orange) land on a suitable stigmatic papilla cells they adhere, hydrate, and germinate. Fast growing pollen tubes (PTs) invade stigmatic tissue, continue directional growth through the style and transmitting tract (TT). During PTs growth extracellular surrounding is modulated to allow continuous growth either between cells (grey rectangles) or within their cell walls. TT provides PTs with essential nutrients as well chemotropic cues that assist with the focused PT growth. Typically, only one PT is attracted by secreted peptides to the female gametophyte. Guided PT grow along the funiculus (connects ovule to septum) towards the micropyle where upon an extensive molecular communication PT bursts and releases sperm cells. Image adapted from a review (Vogler et al., 2016).

1.3 Pollen tube journey through the transmitting tract

Once the PTs grow through the style, they penetrate the transmitting tract (TT) tissue which consists of cylindrical cells surrounded by the nutrient rich extracellular matrix (ECM) on their ways to ovules (Fig. 2). PTs growth and invasion through stigmatic and stylar tissue is supported by the PECTIN METHYLESTERASE (PME) which are remodeling cell wall and thus enhancing fast growth of PTs on their way to ovules (Fig. 2) (Bosch and Hepler, 2005). For instance disruption of pollen-specific PME-homologous protein *VANGUARD1* (*VGD1*) caused disruption of PTs growth in the TT and subsequently fertility was significantly impaired (Jiang et al., 2005). More recently it was reported that loss of male gametophyte specific PECTIN METHYLESTERASE48 (PME48) caused an obstruction of pollen germination both *in vitro* and *in vivo*, with many pollen grains displaying two pollen tips compared to the one present in wild type (Leroux et al., 2015).

The proper formation of the TTs is essential for the PTs guidance, since in mutants without TT such as NO TRANSMITTING TRACT (NTT) or HALF FILLED (HAF), growth of PTs is either severely slowed down or prematurely stopped. NTT encodes a zinc finger transcription factor essential for ECM production as well as the programmed cell death (PCD) after pollination. HAF encodes a bHLH transcription factor and together with NTT regulates specification of TT tissues (Crawford and Yanofsky, 2011; Crawford et al., 2007). Recently it was found that NTT interacts with a MADS-box protein SEEDSTICK (STK), and that *ntt/stk* double mutants impair polysaccharide and lipid deposition as well as septum fusion, followed by delayed degradation of septum cells (Herrera-Ubaldo et al., 2019). Additionally, mutants depleted of two AUXIN RESPONSE FACTORS (ARF6 and ARF8), which are strongly expressed in the style and TT, led to the inability of wild-type pollen to grow through *arf6/arf8* gynoecia (Wu et al., 2006). Taken together, disrupted development of the TT severely impairs PTs growth and subsequently leads to the overall hindered fertilization and seed production.

The TT is also capable of arresting further growth of the non-self pollen in species that have evolved gametophytic self-incompatibility (SI) system. Unlike the previously mentioned sporophytic SI system of *Brassicaceae*, gametophytic SI systems are non-self recognition based and therefore interaction between male and female relies on the different S-haplotypes (Iwano and Takayama, 2012). For instance, pistil secreted RNases are crucial for the barrier establishment in gametophytic SI species of the *Solanaceae* family (Bedinger et al., 2017). Besides being a physical gateway on the PTs way to the ovule, the ECM of TT contains a diverse mixture of polysaccharides, glycoproteins and glycolipids which enable the fast and directed growth of PTs (Lennon et al., 1998).

Arabinogalactan protein (AGP) are hydroxyproline-rich glycoproteins, with a glycosylphosphatidylinositol (GPI) anchor either tethering them to the plasma membrane, or if it gets cleaved releasing them to the extracellular environment where they act as a signaling components, morphogens or nutrients (Pereira et al., 2015). More than 25 years ago role of arabinogalactan proteins in the plant reproduction was discovered in two Solanaceous species. TRANSMITTING TRACT-SPECIFIC (TTS) arabinogalactan proteins TTS1 and TTS2 from *Nicotiana tabacum* as well as alTTS *Nicotiana alata* were found to stimulate directional PTs growth *in vitro* (Cheung et al., 1995; Wu et al., 2000). Even though there are potential orthologs in *A. thaliana* their roles remain to be assessed. Very recently a study in pear demonstrated that PbrTTS1 interacts with a Ca^{2+} binding C2 domain containing PbrPCCP1 to together promote the PT growth (Jiao et al., 2019). Not long ago it was discovered that a pistil extensin-like (PELPIII) arabinogalactan protein from *N. tabacum* plays a vital role in the regulation of interspecific PT growth. Furthermore, a single amino acid change in the more divergent N-terminal domain (NTD) could not compliment RNAi line with a reduced PELPIII expression. Taken together PELPIII is essential for the inhibition of *N. obtusifolia* PTs growth (Alves et al., 2019). Arabinogalactans have also been shown to play important roles during pollen development. Loss of two pollen-specific AGPs caused premature germination of PTs inside the anthers as well as reduced germination and PT growth *in vivo* (Costa et al., 2013). Furthermore, disturbance of PECTIC ARABINOGALACTAN SYNTHESIS-RELATED (PAGR), involved in the pectin biosynthesis, led to drastically reduced pollen germination rates (Stonebloom et al., 2016).

In addition to the highly glycosylated proteins, chemoattractant gradients of cysteine rich peptides (CRPs), as well as the rare amino acids GABA and D-serine are essential for the guided growth of PTs towards the ovule (Palanivelu and Tsukamoto, 2012; Zheng et al., 2018). Small CPRs cysteine-rich adhesin (SCA) in lily regulates directed PT growth as well as binding to cell wall pectin which

is essential for the adhesion-mediated guidance. It is interesting that PTs *in vivo* adhere to each other, while that is not the case when pollen is germinated *in vitro*. Furthermore SCA is increasing activity of lily chemocyanin together ensuring polar PT growth (Chae and Lord, 2011; Park and Lord, 2003). Homolog of SCA in *A. thaliana* is LIPID TRANSFER PROTEIN5 (LPT5), pollen and TT expressed protein, which when overexpressed leads to formation of atypical ballooned PTs, abnormal elongation of PTs and all together a substantial fertility drop (Chae et al., 2009).

Uncommon amino acid γ -aminobutyric acid (GABA) is involved in both PT growth as well in PT guidance towards the ovules. Mutation of POLLEN ON PISTIL2 (POP2) transaminase important for the degradation of GABA and formation of gradient, resulted in either arrest of PTs or inability to further grow towards ovules (Palanivelu et al., 2003). Molecular mechanisms of GABA-mediated PTs growth were revealed in the whole-cell voltage clamp experiments using tobacco pollen. Application of exogenous GABA activated Ca^{2+}-permeable channels causing the influx of Ca^{2+} in the PTs. This process is tightly regulated, and glutamate decarboxylase (GAD) controls Ca^{2+}-permeable channels in a negative feedback loop to modulate GABA biosynthesis and subsequently PTs growth (Yu et al., 2014). Rare D-amino acid serine is similarly to GABA involved in the control of PTs growth via modulation of Ca^{2+} signaling in both *A. thaliana* and tobacco. D-serine activates glutamate receptor-like channels (GLRs) and leads to modulation of Ca^{2+} influx intensity hence controlling the PT growth (Michard et al., 2011). Interestingly from 20 GLRs genes in *A. thaliana* genome, six are expressed in pollen, however already in single knockout mutants PT growth is decreased resulting in reduced fertility (Michard et al., 2011).

POLLEN-SPECIFIC RECEPTOR KINASES (PRKs) are leucine-rich repeat (LRR) type of receptor like kinases firstly investigated in tomato. For instance, LePRK1 and LePRK2 bind each other but when treated with pistil exudates they begin to dissociate. lePRK2 binds a cysteine rich peptide LATE ANTHER TOMATO52 (LAT52) to promote protein germination. However once pollen tube germinates LAT52 starts to be replaced by the stigma secreted LeSTIG1 and PT growth is further promoted in the stigmatic tissue (Tang et al., 2002). More recently it was demonstrated that LeSTIG1 can either interact with LePERK1 or with the phosphatidylinositol 3-phosphate (PI3P) to induce the PT growth by influencing reactive oxygen species (ROS) production (Huang et al., 2014). *A. thaliana* homolog AtPRK2 controls polarized PT growth through the activation of Rho-like small GTPase from plant (ROP1) signaling pathway via the phosphorylation of the Rho guanine nucleotide exchange factors (ROP GEF) (Chang et al., 2013).

Early transcriptomics studies have revealed astonishing difference in gene expression profiles between the PTs that have grown through the stigma and style tissues in comparison to pollen or PT germinated *in vitro* (Qin et al., 2009). This indicated that PTs have a very dynamic gene expression profile which helps in navigation of PTs through the pistil and enables responsiveness to both sporophytic tissues as well later on to the gametophytic navigation cues. Another study has confirmed these observations by comparing expressional profiles of pistils at different time points during *in vivo* pollinations. Many of highly represented transcripts encoded proteins predicted to be secreted, or cell wall-related proteins which could potentially be involved in the mediation of extracellular signaling (Boavida et al., 2011). Interestingly genes encoding receptors involved in the pathogen defense were also identified (Boavida et al., 2011).

A more recent study has further established those findings by looking at differentially expressed genes (DEGs) during *Fusarium graminearum* infections. Furthermore, authors have in parallel compared pistils transcriptomes of closely related *A. thaliana* and *A. halleri* upon sef-pollinations as well as

after pollination with *A. lyrata*. Comparison of DEGs between fungal infections and different pollinations revealed almost 80% of genes to be overlapping and were prevalently including defensin-like genes. In pistils of *A. thaliana* pollinated with either *A. halleri* or *A. lyrata* a significant upregulation of thionins and defensins was detected (Mondragón-Palomino et al., 2017). Transcriptomic approach was utilized to gain the better understanding of the unilateral incompatibility (UI) within the populations of the wild tomato relative *Solanum habrochaites.* When comparing transcriptomic profiles of self-incompatible and self-compatible pistils many DEGs were found, among others putative arabinogalactan, as well as peptide hormone RAPID ALKALINIZATION FACTOR (RALF) mainly expressed in the style. Additionally authors report that many genes related to the ROS signaling pathway were among the top DEGs candidates (Broz et al., 2017).

1.4 Ovular pollen tube attraction

Once the PT exits the TT it starts growing on the surface of funiculus where it gets precisely navigated to enter the ovule micropyle. It is astonishing that typically only one PT gets targeted to the one out of the 50 ovules to achieve double fertilization (Dresselhaus and Franklin-Tong, 2013). Based on genetical experiments ovular guidance can be subdivided in the two consecutive phases: funicular guidance refers to navigated exiting of PTs from the TT until the funiculus and micropylar guidance refers to precise navigation of PT from funiculus toward the micropyle to the egg apparatus (Fig. 3) (Shimizu and Okada, 2000). Funicular guidance is controlled by both sporophyte and gametophyte in *A. thaliana*, while micropylar guidance is under the strict supervision of the female gametophyte (Higashiyama and Yang, 2017). The above mentioned uncommon amino acid GABA which plays a role in the PT growth through the TT is also involved in the PT guidance by creation of gradient with its maximum at the micropyle. Additionally PT growth is stimulated at the low concentrations of GABA while inhibited at high, thus it is likely that high concentration of GABA at micropyle has an important role in slowing down the PT elongation (Palanivelu et al., 2003; Renault et al., 2011).

Another contributor of the PT guidance is previously mentioned rare amino acid D-serine. Serine racemase 1 (SR1) is important for the synthesis of D-serine and it has the highest expression at the ovule micropyle, meaning that similarly to GABA maximal concentration of D-serine is at micropyle (Michard et al., 2011). During semi-*in vitro* fertilization assays cytosolic Ca^{2+} levels in PTs are oscillating as they are approaching synergids, which could be partially stemming from the increased serine concentration and hence stimulated influx of calcium through GLRs (Iwano et al., 2012). Once at the close proximity of wild type ovules cytoplasmic Ca^{2+} increased in the PTs, while when approaching *myb98* mutant ovules, there was no such increase in calcium, probably due to impaired micropylar targeting (Iwano et al., 2012). Even though it was well established that Ca^{2+} gradients in PT tips are crucial for the PT guidance, it took many years before putative Ca^{2+} channels were functionally characterized. Interestingly a single point mutation in the CYCLIC NUCLEOTIDE-GATED CHANNEL18 (CNGC18) led to the heavily impaired PT guidance. Furthermore, among the eight analyzed calcium channels only CNGC18 had a vital role during the micropylar PT guidance (Gao et al., 2016).

Nitric oxide (NO) plays an important role in the targeting of PTs to the micropyle. Mutants in which NO production is severely disrupted such as *atnos1* have reduced seeds set due to inability of PTs to correctly target micropyle. Additionally, in semi-*in vivo* assays with isolated ovules and lily pollen,

NO modulated downstream Ca^{2+} which subsequently affected PT growth (Prado et al., 2008). NO responsive proteins were largely unknown and only recently it was reported that pollen specific DIACYLGLYCEROL KINASE4 (DGK4) has a gas sensing region which is needed for the perception of NO during PT growth. PTs of *dgk4* mutants are partially insensitive to NO-mediated growth inhibition as well as to reorientation responses (Wong et al., 2020).

Additional components of the funicular PT guidance are two pollen expressed mitogen-activated protein kinases MPK3 and MPK6. *In vivo* pollination assay revealed that *mpk3/mpk6* mutants were not able to grow along the funiculus upon exiting from the transmitting tract, however *in vitro* they could correctly navigate towards the micropyle. These findings suggest that the funicular guidance depends on an *in vivo* signaling mechanism which is distinct from the micropyle guidance (Guan et al., 2014).

Furthermore, two CATION/PROTON EXCHANGERS CHX21 and CHX23 have been shown to play a role in the funicular guidance. Double mutant *chx21/chx23* could germinate and grow through the TT, but they failed to turn and grow towards ovules. Additionally, *chx21/chx23* fell short at entering micropyle of excised ovules in semi-*in vivo* assays. The ER localized CHX23 mediates K+ uptake in a pH dependent manner and is hypothesized to be involved in the sensing of ovular guidance cues (Lu et al., 2011). Another ER resident protein important for the ovular attraction as well as normal embryo development is POLLEN DEFECTIVE IN GUIDANCE1 (POD1). POD1 interacts with the CALRETICULIN3 (CRT3) to regulate membrane protein folding. Therefore it is likely that in *pod1* many membrane proteins such as receptors for ovular attractants are aberrantly processed resulting in disrupted targeting of the female gametophyte (Li et al., 2011).

COBRA-LIKE10 (COBL10) a glycosylphosphatidylinositol (GPI)-anchored protein localized at the PT membrane is another component necessary for the appropriate funicular guidance. Defects in COBL10 caused a reduced PT growth as well as inability to sense female secreted cues and orient towards the ovule (Li et al., 2013). Recently two pollen-specific aspartic proteases A36 and A39 containing putative GPI-anchor were found to be important for not only micropylar PT guidance but as well for the appropriate development of female gametophyte. Additionally, A36 and A39 are both membrane-anchored proteins and a strong colocalization was observed with the above mentioned COBL10 (Gao et al., 2017). Mutation of ABNORMAL POLLEN TUBE GUIDANCE1 (APTG1) mannosyltransferase involved in the GPI-anchor biosynthesis in the endoplasmic reticulum (ER) led to the severely impaired fertility. Having in mind that loss of *APTG1* disrupted the plasma membrane localization of COBL10, observed inappropriate PT guidance in *aptg1* was not surprising. APTG1 is highly expressed in the embryo sack where it plays an important role during the embryo development, with *aptg1* mutants being embryo lethal (Dai et al., 2014).

Besides the above mentioned *pod1, a36/a39, aptg1* mutants which displayed abnormal PT guidance as well as disrupted development of the female gametophyte, several other mutants affected in the house-keeping genes led to severe defects of the female gametophyte which then indirectly reflected in abrupted PT guidance (Fig. 3). Some of those mutants include *magatama1* (*maa1), maa3, proteins disulfide isomerase2-1 (pdil2-1), bell (bel1), short integuments (sin1), central cell guidance* (*ccg*), *myb98* as well as maize *disumo-like protein* (*zmdsul*) (Bleckmann et al., 2014; Dresselhaus and Franklin-Tong, 2013; Palanivelu and Tsukamoto, 2012). For instance, in maize *zmdsul* mutant embryo sack is disintegrated and PTs can arrive within the 100 µm from the micropylar opening of ovule. Therefore, in maize funicular guidance is regulated by the sporophytic tissues until the last 100 µm when micropylar guidance takes over (Lausser et al., 2009).

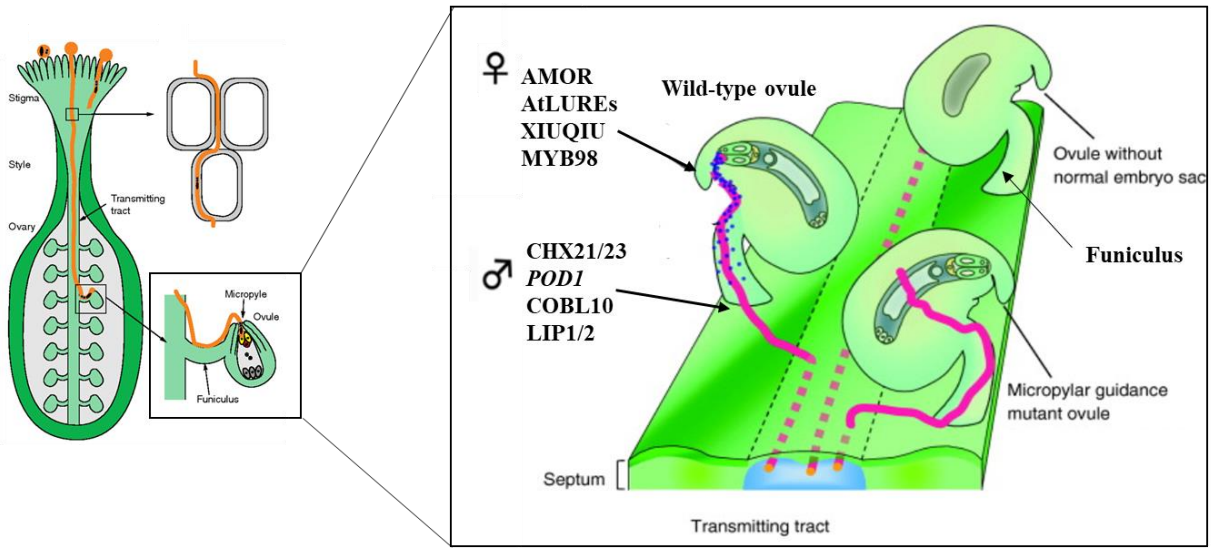

Figure 3. Ovular pollen tube guidance. The cartoon represents directed pollen tube (PT) growth from the initial adhesion to the stigma until ovule (left) with a focus on the exit of PTs from the transmitting tract (TT) to the female gametophyte (right). Several PTs emerge from the TT, however only one PT grows on the surface of funiculus and targets the ovule micropyle. Small molecular attractants such as AtLUREs (blue dots) are secreted by the ovule, mainly by synergids, to promote micropylar guidance of the PTs. These peptides are perceived by multiple receptors on the PT, leading to entrance of PT through the micropyle to the embryo sack. In the case of micropylar guidance mutants, PT can grow on the surface of funiculus, but it can no longer find micropyle, hence it continues growing on the surface of ovules. If the embryo sack is not properly developed PTs are not attracted from TT. Several key male- and female- gametophytic factors involved in the control of ovular guidance are represented. Images adapted from reviews (Takeuchi and Higashiyama, 2011; Vogler et al., 2016).

In *maa1* and *maa3* mutants central cell is not formed due to failed fusion of two polar nuclei of the embryo sack, resulting in aborted micropylar guidance (Shimizu and Okada, 2000). Important role of central cell was further corroborated with discovery of CCG central cell specific transcription factor which together with CCG BINDING PROTEIN1 (CBP1) regulates transcriptional machinery in the central cells required for the appropriate micropylar attraction (Chen et al., 2007; Li et al., 2015b). Furthermore, egg cells are involved in the PT attraction, evidential from the loss of GAMETE EXPRESSED 3 (GEX3) localized at the plasma membrane of egg cells, resulting in disrupted micropylar guidance (Alandete-Saez et al., 2008).

Finally, the majority of micropylar guidance attractants are coming from the synergids cell, more precisely from the membrane-rich region named filiform apparatus (FA). Early studies have demonstrated that either laser ablation of synergids in *Torenia fournieri* or defective FA in *A. thaliana* result in severely impaired micropylar guidance (Higashiyama and Takeuchi, 2015; Higashiyama and Yang, 2017). The first ever PT attractants released from the synergid FA were described in *T. fournieri.* LURE1 (TfCRP1) and LURE2 (TfCRP3) belong to the cysteine-rich polypeptides of the defensin-like protein group, expressed at the synergid FA from where they get secreted toward micropyle to stimulate PT guidance (Okuda et al., 2009). A recent study has demonstrated that ovular arabinogalactan polysaccharide called AMOR makes PTs fully competent to respond to LURE1/2 peptides after passing through the style tissue in *T. fournieri.* Additionally, even chemically synthesized disaccharide (4-Me-GlcA-β-(1→6)-Gal) displayed AMOR activity during *semi-in vitro* assays (Mizukami et al., 2016).

In *A. thaliana* mutation of the synergid specific MYB98 transcriptional factor caused an aberrant synergid cell differentiation as well completly abolished micropylar guidance (Kasahara et al., 2005). Furthermore, gametophytic mutants defective in the female gametophyte development (*myb98*, *maa*3, and *ccg*) do not express AtLURE1 peptides (Takeuchi and Higashiyama, 2012). Synergid specific MYB98 transcription factor regulates the expression of genes encoding cysteine-rich proteins (CRPs) of defensin-like (DEFL) polypeptides (Punwani et al., 2007; Takeuchi and Higashiyama, 2012).

By comparing duplicated defensin-like genes between closely related *A. thaliana* and *A. lyrata* six AtLURE1 peptides were identified as the PT attractants in *A. thaliana*. Having in mind that AtLURE1 has recently evolved, it is not evolutionary related to the LUREs of *T. fournieri*. AtLURE1 are secreted from synergids and attract PTs in a species-specific manner. AtLURE1 peptides attracted *A. thaliana* PTs at a higher rate in comparison to *A. lyrata* PTs. Additionally introduction of AtLURE1 into the *T. fournieri* was sufficient for the breakdown of reproductive isolation barrier between these distantly related species (Takeuchi and Higashiyama, 2012). In maize egg and synergid cell specific secreted protein *Zea mays* EGG APPARATUS1 (ZmEA1) is crucial for the micropylar guidance. *A. thaliana* transgenic plants expressing ZmEA1 could successfully guide maize PTs *in vitro* proving that hybridization barriers can be overcome even between unrelated species (Márton et al., 2012).

Male components important for the perception of guidance cues have been described more recently. Pair of receptor-like cytoplasmic kinases LOST IN POLLEN TUBE GUIDANCE1 (LIP1) and LIP2 attached to the PT plasma membrane are necessary for the micropylar guidance. Double mutants *lip1/lip2* could not grow further than funiculus *in vivo*, while *in vitro* they displayed decreased responsiveness to the synthetic AtLURE1 (Liu et al., 2013). Furthermore, two studies in parallel have shed new light into the complexity of male specific complexes required for the perception of ovular LUREs peptides. POLLEN RECEPTOR-LIKE KINASE6 (PRK6) with an extracellular leucine-rich repeat domain is essential for binding AtLURE1, with *prk6* mutant PTs being unable to respond to AtLURE1 *in vitro*. Moreover *prk3/prk6/prk8* triple mutants were not targeting ovules in the pistil. PRK6 signals through the pollen expressed ROPGEFs in cooperation with PRK3 and PRK8 upon AtLURE1 binding. PRK6 enabled responsiveness to AtLURE1 in PTs of the closely related species such as *Capsella rubella* (Takeuchi and Higashiyama, 2016).

The second study showed that AtLURE1 can also bind to the heteromeric complex consisting of MALE DISCOVERER1/2 (MDIS1) and MDIS2 as well as MDIS1-INTERACTING RECEPTOR LIKE KINASE1/2 (MIK1) and MIK2 on the PT surface. Mutant pollen *mdis1* as well as *mik1/mik2* was less sensitive to the AtLURE1 induced guidance. Similarly, to the above mentioned PRK6`s ability to confer responsiveness to AtLURE1 in *C. rubella*, also transformation of AtMDIS1 could cause partial breakdown of the reproductive isolation barrier (Wang et al., 2016). Study from the last year has identified two more genes of the AtLURE1 family, and null septuple mutants of the whole AtLURE1 family surprisingly did not impair fertility. Through the crosses with the closely related *A. lyrata* it became evident that AtLURE1-PRK6 signaling plays a role in accelerating growth of conspecific (self) pollen versus heterospecific (foreign) pollen, hence fostering reproductive isolation. Additionally, four AtLURE1-related maternal cysteine-rich peptides named XIUQIU were discovered as a non-species-specific PT attractants. XIUQIU are conserved within *Brassicaceae* family and perhaps they play a role in the formation of novel species (Zhong et al., 2019).

1.5 Pollen tube reception

Once PT makes an entrance through the micropyle, the complex and highly regulated process of PT reception takes place. Synergid cells not only mediate PTs growth into the micropyle but are also required to induce PT burst and subsequent release of the sperm cells (Dresselhaus and Franklin-Tong, 2013; Takeuchi and Higashiyama, 2012; Zheng et al., 2018). Even though the initial contact between PT and synergid is at filiform apparatus (FA) (Sandaklie-Nikolova et al., 2007), a thickened cell wall structure at the micropylar end of synergids, PT penetration occurs at zone located toward the chalazal pole named "synergid hooks" (Leshem et al., 2013). Therefore authors proposed that PT reception is two-step process, firstly PTs are primed at the FA where they slow down their growth, followed by the short-range growth until the "synergid hooks" where receptive synergid is penetrated and the PT burst occurs (Leshem et al., 2013). However live imaging studies using Ca^{2+} sensors expressed in synergids and PTs revealed that PT reception is more complicated, and it involves four distinct stages (Leydon et al., 2015).

The first phase begins with PT arrival to the micropylar pole of synergids and it is characterized with a slow PT growth with minor oscillations of $[Ca^{2+}]_{cyto}$ in the PT tip. This phase usually lasted around 34 (±15) min and $[Ca^{2+}]_{cyto}$ waves were initiated in both synergids from the contact point towards the chalazal pole (Denninger et al., 2014; Ngo et al., 2014). The second phase lasted a bit shorter (20 ± 10 min) and it constituted of strong increase of $[Ca^{2+}]_{cyto}$ at the PT tip, followed by PT growth towards the chalazal pole of the designated receptive synergid (Rsyn). Even though in both synergids a steady increase of $[Ca^{2+}]_{cyto}$ was detected, already at this stage there was an obvious difference in calcium dynamics between Rsyn and non-receptive synergid (Nsyn) (Ngo et al., 2014). The Rsyn was flooded with calcium that was typically the highest at the chalazal pole. During the third phase $[Ca^{2+}]_{cyto}$ in PT reached it maximum leading to the PT burst at "synergid hook" region and about 5-10 s later the $[Ca^{2+}]_{cyto}$ reached maximum in both synergids, followed by the collapse of Rsyn. Soon after $[Ca^{2+}]_{cyto}$ went to the basal level in Nsyn and it remained stable (Ngo et al., 2014). During the fourth phase which lasted around 1h, $[Ca^{2+}]_{cyto}$ oscillations in the Nsyn were more irregular and role of this calcium signalling could be either to repel additional PTs in the case of successful double fertilization, or the attract new PTs if there was a failure (Kasahara et al., 2012; Maruyama et al., 2013). This additionally means that both synergids have the capacity to be the receptive and further investigation is needed to elucidate how is Rsyn selected.

One of the most prominent feature of synergid cells is their filiform apparatus, the region of the extensive membrane invaginations which is significantly increasing the surface area of synergid plasma membrane (Jones et al., 2018). As previously mentioned many proteins involved in the PT guidance are secreted from the FA (Chae and Lord, 2011; Higashiyama and Takeuchi, 2015), and many proteins involved in PT reception are localized at the FA (Fig. 4). The initial evidence of PT reception being under an active signalling cascade occurring at the FA, came from the discovery of mutants in which PTs were able to reach the micropyle, but upon interaction with the synergid cells they failed to abort growth and to burst within the receptive synergid cell (Kessler and Grossniklaus, 2011). This mutant was named *feronia* (*fer*) after an Etruscan goddess of fertility, since in *fer* mutant ovules are impaired in PT reception and hence they remained unfertilized. Development of the female gametophyte was undisturbed in *fer*, but more than 80% of ovules remained unfertilized due to the PT overgrowth (PTO) within the embryo sack and a lack of PT burst and a release of sperm cells (Huck, 2003). FER is synergid expressed with the highest accumulation at the FA, and interestingly FER is broadly expressed with an exception of pollen and pollen tubes (Escobar-Restrepo et al.,

2007). FER is also playing a crucial role during the initiation and regulation of calcium signalling responses occurring in synergids upon PT arrival. In *fer* calcium signalling was distinct at all above mentioned stages of PT reception from the wild type (Ngo et al., 2014). Additionally reciprocal crosses with the wild type revealed that *fer* is a female gametophytic mutation (Huck, 2003).

FER is a plasma membrane localized receptor-like kinase belonging to the *Catharanthus rhoseus* RLK1-like *Cr*RLK1L subfamily of 17 members (Lindner et al., 2012). All members of the *Cr*RLK1Ls are composed of variable extracellular malectin-like domain, transmembrane domain, and a very conserved intracellular kinase domain. FER`s extracellular domain was proposed to be crucial for the binding of cell wall components and putative PT derived ligands (Boisson-Dernier et al., 2011). In interspecific and intergenic crosses in *Rhododendron*, a similar *fer*-like PTO was observed, indicating that PT reception is an essential prezygotic barrier to interspecific hybridization (Kaul et al., 1986; Williams et al., 1986). Furthermore, even among closely related *Brassicaceae* species for instance *A. thaliana* and *A. lyrata* there is *fer*-like phenotype in around 50% of the targeted ovules (Escobar-Restrepo et al., 2007).

Besides FER, a glycosylphosphatidylinositol (GPI)-anchored surface protein named LORELEI (LRE) also resides at the FA, where they together actively regulate PT reception (Fig. 4). Mutation of LRE led to almost 70% of PTO in the *lre* null mutants, therefore almost reaching the degree observed in *fer* (Capron et al., 2008). Modified eight-cysteine motif (M8CM) consisting of 12 amino acids is crucial for LRE`s role in PT reception. At the same time, GPI anchor is dispensable and single-pass transmembrane domain could complement *lre* female gametophytic defects (Liu et al., 2016). LRE plays additional roles during double fertilization, unfertilized *lre* egg cell degenerate leading to later seed abortion (Tsukamoto et al., 2010). LRE`s closest homolog LLG1 does not have a role during PT reception since null mutants display full seed sets (Li et al., 2015). LLG1 is strongly expressed in vegetative tissues where *llg1* phenocopies *fer* stunted growth, anthocyanin accumulation, root hair and trichome defects. LLG1 and LRE were reported to bind FER extracellular juxtamembrane (exJM) and to be responsible for FER delivery from the ER to the plasma membrane (Li et al., 2015a). However, in synergids it seems that FER localization to the FA is not completely dependent on LRE-mediated chaperoning from the endoplasmic reticulum (ER), having in mind that in *lre* certain amount of FER-GFP could still be detected at FA (Liu et al., 2016). Additionally, ectopic expression of LRE-cYFP from the PTs could complement PTO in *lre* mutants, but not in *lre/fer* double mutants indicating that LRE and FER require each other at the FA to induce PT reception (Liu et al., 2016).

Both FER and LER at the FA are required for the initiation as well as for the regulation of $[Ca^{2+}]_{cyto}$ in both synergids during PT reception (Ngo et al., 2014). Furthermore FER and LER work together in the control of reactive oxygen species (ROS) production mediated by the RAC/ROP signalling complex (Fig. 4) (Duan et al., 2014). High production of ROS at the micropylar pole of synergids is a prerequisite for the induction of PT rupture since pharmacological inhibition of ROS production caused the PTO phenotype. Furthermore ROS mediated PT burst is a Ca^{2+} mediated process, requiring Ca^{2+} channel activation (Duan et al., 2014). These observations were in line with the previous studies showing that oscillations in $[Ca^{2+}]_{cyto}$ are crucial for the complex male-female crosstalk during PT reception, and that these dynamics are heavily disrupted in both *fer* and *lre* mutants (Denninger et al., 2014; Hamamura et al., 2011; Iwano et al., 2012; Ngo et al., 2014).

Additional component of the PT reception pathway acting downstream of FER and LRE is NORTIA (NTA, MLO7) which belongs to the plant-specific MILDEW RESISTANCE LOCUS O (MLO)

family of proteins involved in barley powdery mildew (PM) susceptibility (Büschges et al., 1997). NTA encodes a seven-transmembrane protein with calmodulin (CaM)-binding domain and displays synergid specific expression. In *nta* mutants, around 24% of ovules remain unfertilized due to PTO (Kessler et al., 2010). NTA`s homooligomerization and translocation from the Golgi-associated compartments to the FA upon PT arrival is FER dependent (Fig. 4). However, FER is properly localized in *nta* ovules (Jones et al., 2017; Kessler et al., 2010). In contrast to previously mentioned roles of FER and LER for the initiation of $[Ca^{2+}]_{cyto}$, NTA is required for the fine-tuning of the intensity of calcium oscillations in both synergids (Ngo et al., 2014). NTA and FER work synergistically not only during PT reception but also during fungal infection since both mutants display increased resistance to powdery mildew infection (Kessler et al., 2010). Detailed analysis of MLO family (15 members in *A. thaliana*) revealed their expression in the pollen, stigma, central cell and synergids, raising a possibility of additional members of MLOs being involved in PT reception (Davis et al., 2017).

Recently it was reported that two members of the *Cr*RLK1L family act redundantly to control PT reception, with 90% of unfertilized ovules in *herk1/anjea* (Galindo-Trigo et al., 2019). HERCULES RECEPTOR KINASE 1 (HERK1) and ANJEA (ANJ) localize as well to the FA of synergids and associate with FER and LRE to control PT burst and sperm cell release (Fig. 4). Localization of FER and LRE remained intact in *herk1/anjea* ovules, as well as ROS accumulation at the FA. However, NTA requires both FER and LER for relocalization upon PT arrival. Therefore it was proposed that FER/LRE/HERK1 and FER/LRE/ANJEA make receptor complexes at the FA to synergistically promote PT reception (Galindo-Trigo et al., 2019).

Recently another group of female-specific proteins was found to be important during PT receptions, named EARLY NODULIN-LIKE PROTEINS (ENOLDs/ENs). ENs contain plastocyanin-like (PCNL) domain, an arabinogalactan (AG) glycomodule and LRE-like GPI-anchor motif. RNAi quintuple ENs mutant shows a PTO phenotype in 52% unfertilized ovules (Hou et al., 2016). From five ENs only EN14 strongly associates to FER extracellular domain, thus it is probable that EN14 acts together with LER to ensure polar accumulation of FER at the FA of synergid cells (Fig. 4). However single mutant *en14* had normal PT reception, and only quintuple loss-of-function RNAi-en mutants displayed *fer*-like PTO (Hou et al., 2016).

TURAN (TUN), encoding a putative UDP glycosyltransferase superfamily protein and EVAN (EVN) encoding a putative dolichol kinase act during the early stages of ER *N*-glycosylation pathway (Strasser, 2016). Both mutants display PTO phenotype with 12% (*tun/TUN*) and 20% (*evn/EVN*) of unfertilized ovules (Fig. 4). Localization of FER, LRE, and NTA at synergid`s FA remained unaffected in both *tun/TUN* and *evn/EVN* mutant ovules. Confirmation of EVN`s dolichol kinase activity, as well as reproductive phenotypes of *evn/EVN*, further validate previous findings (Kanehara et al., 2015). In a more recent study, EVN was found to be expressed in the shoot apical- and floral-meristems, and *amiDOK* lines had an early flowering time phenotype (Cho et al., 2017). Recently it was also reported that FER plays an important role in the flowering time regulation, and *fer-4* mutants displayed a substantial delay in the flowering time (Wang et al., 2020).

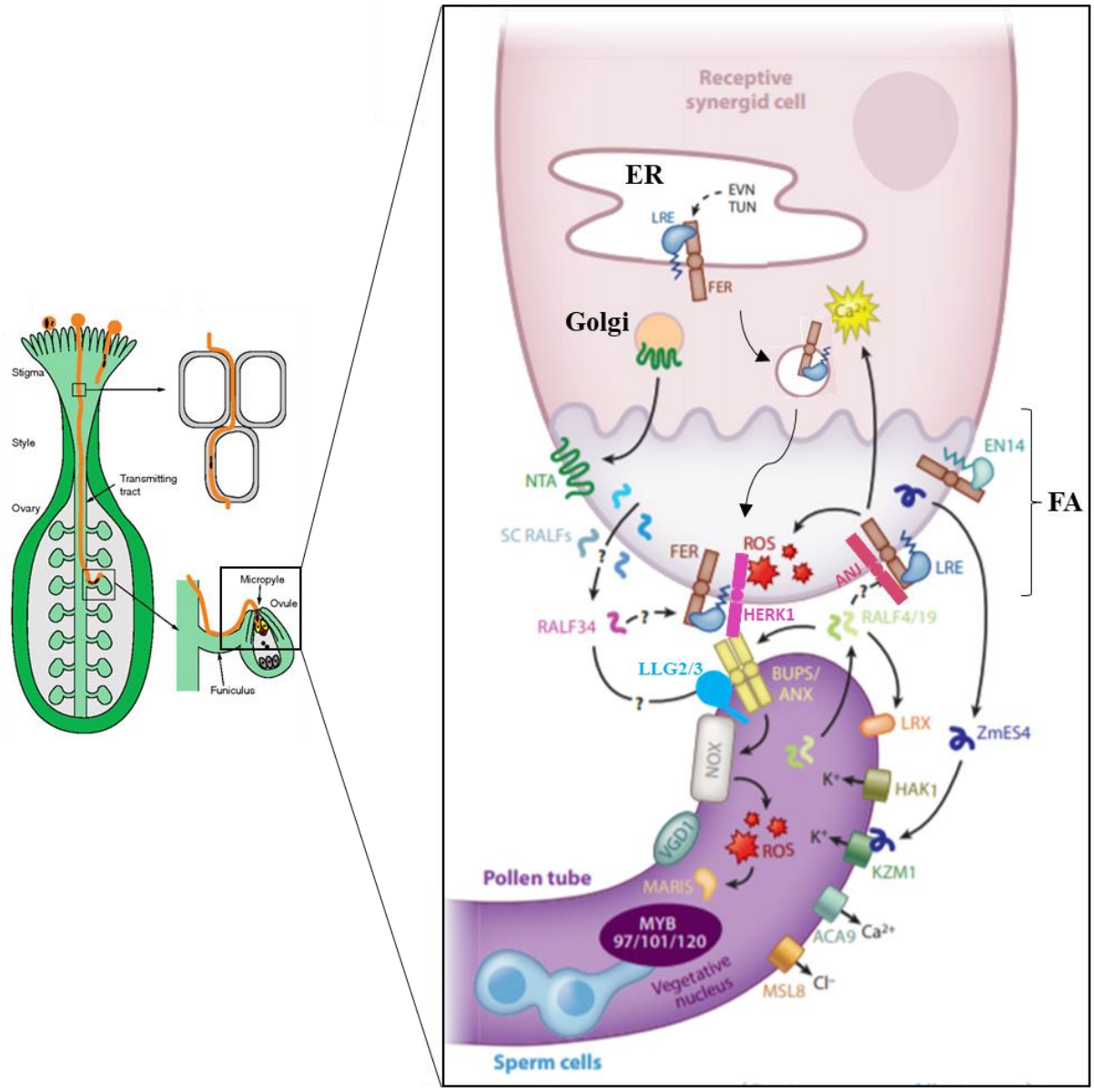

Figure 4. Molecular control of the pollen tube reception. Schematic model represents guided pollen tube (PT) growth through the pistil (left) with a focus on the PT arrival at the female gametophyte (right). FER is a key player of the PT reception pathway. LRE acts as a FER`s chaperone and promotes FER`s secretion to the FA. Additionally, EN14 could play a role in the secretion from the ER. Furthermore, ER resident TUN and EVN are important for the *N*-glycosylation of FER/other members of PT reception pathway to ensure their full functionality. Once at FA, FER forms complexes with its chaperones LRE and EN14, as well as with two other homologues from the *Cr*RLK1L subfamily, HERK1 and ANJ to bind its putative ligand. Additionally, FER is needed for the secretion of NTA from the Golgi apparatus to the FA. FER and LRE are essential for the ROS and Ca^{2+} signaling initiation upon PT arrival, while NTA is needed for the regulation of the Ca^{2+} oscillations. Unknown PT factors under the control of MYB97, MYB101, and MYB120 transcription factors are also required for the PT reception. The cell wall (CW) integrity of PTs is controlled by homologs of FER form the *Cr*RLK1L subfamily, ANX1, ANX2, BUPS1 and BUPS2. These four receptors form a complex to bind RALF4 and RALF19 to ensure maintenance of PT`s integrity until the arrival to synergids. ANX1/2 also bind to LRX proteins of the CW to mediate PT stability during growth. Additionally, they regulate NOX signalling to induce production of ROS, which in turn activates MARIS to maintain tip gradient of Ca^{2+}. Once at the synergid FA, ovule-derived RALF34 is replacing RALF4/19 from the ANX1/2-BUPS1/2 receptor complex, which is triggering the PT rupture and release of sperm cells to complete double fertilization. Abbreviations: **ACA9**, AUTOINHIBITED CALCIUM ATPASE; **ANX**, ANXURS; **ANJ**, ANJEA; **BUPS**, BUDDHA'S PAPER SEAL; **CA^{2+}**, Calcium; **EN14**, EARLY NODULIN 14; **ER**, endoplasmic reticulum; **EVN**, EVAN; **FA**, filiform apparatus; **FER**, FERONIA; **HERK1**, HERCULES1; **KZM1**, ZEA MAYS POTASSIUM TRANSPORTER 1; **LLG2/3**, LORELEI-LIKE PROTEIN 2/3; **LRE**, LORELEI; **LRX**, LEUCINE RICH REPEAT-EXTENSIN GLYCOPROTEIN; **NOX**, NICOTINAMIDE ADENINE DINUCLEOTIDE PHOSPHATE OXIDASE; **NTA**, NORTIA; **RALF**, RAPID ALKALINIZATION FACTOR;

SCRALFS, SYNERGID-DERIVED RALFS; **ROS**, REACTIVE OXYGEN SPECIES; **TUN**, TURAN; **ZMES4**, ZEA MAYS EMBRYO SAC. Images adapted from reviews (Johnson et al., 2019; Vogler et al., 2016).

Peroxin protein ABSTINENCE BY MUTUAL CONSENT (AMC) controls protein import in peroxisomes and is strongly expressed in both female and male gametophytes during double fertilization. Loss of AMC led to the PTO only if both female gametophyte as well as PT carried the *amc* mutation (Boisson-Dernier et al., 2008). This was the first study reporting that PT reception involves not only active regulation from the female side, but also undisturbed interplay between female and male gametophyte. This communication is mediated by the release of diffusible compounds such as nitric oxide and ROS from the peroxisomes (Boisson-Dernier et al., 2008). These results together with the above-mentioned involvement of NO during PT guidance further prove a vast importance of NO for the successful double fertilization.

Surprisingly, triple mutant of pollen-specific transcription factors (MYB97, MYB101, and MYB120) also displayed PTO phenotype in 70% of targeted ovules. This mutant had normal pollen development, germination, and guidance to synergids, suggesting that some of the downstream target genes play an important role in PT reception specifically (Leydon et al., 2013; Liang et al., 2013). Additionally, authors reported that the expression of MYBs was induced by their growth in the pistil. Furthermore, MYB-regulated PT expressed genes were found to include small peptides, transporters, and carbohydrate active enzymes. It still remains to be examined if any of these candidates plays an important role during FER-mediated PT reception (Leydon et al., 2013; Liang et al., 2013).

Pollen tube expressed ANX1 and ANX2 receptor kinases act redundantly to ensure PT integrity and growth towards the female gametophyte (Fig. 4). In *anx1/anx2* double mutants, this balance is disrupted, leading to the premature PT bursting and inability to deliver sperm cells to synergid cells and ensure successful double fertilization (Boisson-Dernier et al., 2009, 2013; Miyazaki et al., 2009). ANX1/2 regulate the cell wall (CW) integrity pathway through two pollen-specific NADPH-oxidases, respiratory burst oxidase homologue (Rboh) named RbohH and RbohJ, which are required for the generation of ROS and maintenance of Ca^{2+} gradient needed for the PT growth (Boisson-Dernier et al., 2013). Proper *N*-glycosylation is important not only for mediating PT reception but also for pollen development (EVN) and PT integrity maintenance (TUN). PTs of *tun/TUN* are bursting soon upon germination, and both ANX1 and ANX2 reporters could no longer be detected, suggesting TUN`s requirement for the ANX1/2 protein stability (Lindner et al., 2015). Suppressor screen was performed on the *anx1/anx2* double mutants and two novel members of the ANX1/2-mediated PT integrity pathway were described. MARIS (MRI) a plasma membrane-localized receptor-like cytoplasmic kinase was identified as a positive component of the ANX1/2 signalling pathway (Fig. 4). Loss of function *mri* mutant showed PTs as well as root hair bursting, while MRI^{R240C} mutant due to constitutively active kinase activity could partially rescue *anx1/anx2* PT burst, as well as the bursting of *fer*`s root hairs (Boisson-Dernier et al., 2015). Second suppressor from the screen a TYPE ONE PROTEIN PHOSPHATASE (TOPP), named ATUNIS1 (AUN1) turned out to be a negative regulator of the CW integrity pathway. Interestingly both AUN1 and its closest homolog AUN2 were found to function downstream of RALF4/19 and ANX1/2, but in contrast to MRI they were also in the same pathway with LEUCINE-RICH REPEAT EXTENSIN (LRX) proteins (Franck et al., 2018).

More recently two novel members of the *Cr*RLK1L subfamily were identified as the essential components of PT integrity pathway, named BUDDHA'S PAPER SEAL (BUPS). Both BUPS1 and BUPS2 are PT expressed and similarly to ANX1/2 in *bups1/bups2* double mutants PTs burst soon

upon germination both *in vitro* and *in vivo* (Fig. 4) (Ge et al., 2017; Zhu et al., 2018). BUPS1/2 interact with ANX1/2 via their extracellular domains, and this receptors complexes together bind ligands RALF4 and RALF19 to maintain PT integrity. Loss of RALF ligands, as observed from *amiRRALF4/19* presented the same PT bust phenotype, which is further establishing the key importance of this autocrine signalling pathway in the maintenance of PT integrity during growth. Additionally, RALF4/19 interact with the CW localized LRX proteins to sustain the PT`s CW integrity (Mecchia et al., 2017). Lastly it was demonstrated that ovule-expressed RALF34 which is the closest homolog of RALF4/19 caused PT burst *in vitro* at the very low concentrations (2nM) (Ge et al., 2017). Furthermore, RALF34 binds complex BUPS1/2-ANX1-2 with a high affinity, therefore it is believed that once PTs arrive to the FA, RALF34 displaces RALF4/19 which leads to the PT rupture in the receptive synergid (Fig. 4) (Ge et al., 2017). Lastly the pollen-specific LORELEI-like GPI-anchored proteins 2 and 3 (LLG2/3) were reported to be important for the secretion of ANX1/2 and BUPS1/2 to the PT plasma membrane, where they then act also as the coreceptors for RALF4 (Fig. 4). Therefore LLG2/3 is the newest found member of the complex network required for the maintenance of PT integrity during PT growth and thus ensuring the successful double fertilization (Feng et al., 2019).

In maize defensin-like cysteine-rich proteins *Zea mays* EMBRYO SAC (ZmES) 1-4 are important for the induction of PT growth arrest and burst in a species-specific manner. *ZmES1-4* genes are expressed in the female gametophyte and ZmES4 protein is accumulated in the secretory region of synergids (Amien et al., 2010). Upon PT arrival ZmES4 gets released from the synergids and binds to K+ channel (KZM1) on the PT plasma membrane (PM), leading to K+ influx, PM depolarization, water uptake and subsequent PT burst (Fig. 4). In the mutant RNAi lines directed at ZmES4, PTO was observed (Amien et al., 2010). Having in mind that pectin methylesterases (PMEs) play crucial role in the maintenance of the CW integrity, their activity is tightly regulated by the PME inhibitors (PMEI) which are especially crucial at the PT tip (Palin and Geitmann, 2012). In maize it was found that ZmPMEI1 are strongly expressed in both male and female gametophyte. Application of ZmPMEI1 protein *in vitro* did not slow down the PT growth, but it induced PT burst in a subapical region of PT. Therefore it is can be proposed that female gametophyte is releasing ZmPMI1 to destabilize PTs cell wall during PT reception (Woriedh et al., 2013).

Pollen-specific PM localized Ca^{2+} pump belonging to the family of AUTOINHIBITED Ca^{2+} ATPases (ACA), ACA9 was reported to play a vital role during PT growth and burst (Fig. 4) (Schiøtt et al., 2004). Mutant *aca9* pollen have reduced growth potential both *in vitro* and *in vivo*, however once they reach ovules PTs were competent to abort their growth. However, PT burst, and sperm cells release failed in more than 50% of targeted ovules, and overall fertility was reduced for 80%. Taken together vital importance of Ca^{2+} transporters for the pollen growth and PT reception is evident (Schiøtt et al., 2004). More recently the degree of synergid degeneration was assessed in *aca9*, and it was found to be in correlation with the extent of *aca9* PTs failure to discharge. However also ovules which contained at least one degenerated synergid despite having a PT that had not ruptured were identified, indicating that uncoupling of synergid cell death from PT discharge has taken place (Leydon et al., 2015).

The most recent findings bring up the importance of AP1G and V-ATPases mediated vacuolar acidification for the promotion of synergid degeneration and successful PT reception (Wang et al., 2017). *AP1G* encodes γ subunit of adaptor protein 1 involved in the regulation of protein sorting at *trans*-Golgi network/early endosome (TGN/EE). *VHA-A* is encoding the catalytic subunit of V-

ATPases located at the TGN/EE and tonoplast. Loss of function mutants *ap1g* and *vha-a* had severely reduced fertility and classical PTO was observed in unfertilized ovules (Wang et al., 2017). Interestingly in *ap1g* several tonoplast proteins were mistargeted, while FER was normally secreted. In *AP1G-RNAi* synergid vacuolar acidification was interrupted which is mediated by V-ATPases, suggesting that proper sorting of vacuolar cargos by AP1G is essential for the PT reception. In line with this. abolishing of the V-ATPases acidification actively caused the reminiscent PT reception defect (Wang et al., 2017).

Another component involved in the receptive synergid cell death is GFA2 encoding a J-domain containing mitochondrial matrix chaperone protein (Christensen et al., 2002). The *gfa2* mutants display intact ovular PT guidance, however due to the lack of receptive synergid degradation, ovules remained unfertilized, indicating that mitochondria play a role in cell death in *A. thaliana*. Additionally, in *gfa2* megagametogenesis is affected, and fusion of the polar nuclei does not take place (Christensen et al., 2002). A more recent study has reanalyzed *gfa2/GFA2* defects and found that in non-pollinated pistils frequency of synergid degradations is comparable to wild type after 16 hours (Leydon et al., 2015). Additionally, it was reported that PT discharge is impaired in *gfa2* embryo sacks. However more meticulous assessment revealed that among those *gfa2* ovules where PTs do manage to burst, synergid cell were either degraded or in some cases they remained intact (Leydon et al., 2015).

VERDANDI (VDD) a transcription factor belonging to the reproductive meristem (REM) family was shown to be important for the correct specification of antipodal and synergid cell (Matias-Hernandez et al., 2010). Loss of function *vdd* mutants display reduced fertility. Even though ovular guidance is undisturbed in *vdd*, PTs do not rupture and degeneration of receptive synergid does not occur. The proportion of ovule abortion was in direct correlation with the number of female gametophytes where synergid cell marker was not expressed. Therefore, VDD is essential for the regulation of synergid cell differentiation and targets of VDD remain to be elucidated further (Matias-Hernandez et al., 2010). More recent study has found a novel REM transcription factor named VALKYRIE (VAL) which interacts with VDD to regulate receptive synergid cell death. Loss of function *vdd-1/+* and *VAL_RNAi* mutants both displayed ovules with non-degenerated synergids and PTs that do not discharge. Additionally GFA2 was downregulated in both mutants ovules, while interestingly expression of FER and MYB98 remained wild type like (Mendes et al., 2016).

1.6 Double fertilization and polytubey block

Soon after the PT rupture and sperm cells delivery, one sperm cells fertilize the central cell giving the rise to endosperm, and the other egg cell to develop embryo, in a process called double fertilization (Sprunck, 2020). Intensive crosstalk between gametes occurs, and upon sperm activation and plasma membrane adhesion, gametes fuse (plasmogamy) followed by the fusion of nuclei (karyogamy) (Igawa et al., 2013). Live imaging experiments revealed that fusion events occur around 7 minutes after the sperm cells release to the receptive synergid (Hamamura et al., 2011). Additionally, there is about 2 minutes difference between two fertilizations, and even though it was initially proposed that there is no preferences in which ones takes place first (Hamamura et al., 2011), there was no clear agreement in the field. For instance, CYCLIN DEPENDENT KINASE A1 (CDKA;1) is required for the cell division of the generative cell during the male gametogenesis, and *cdka;1* mutant produced only one sperm cell (Iwakawa et al., 2006). Therefore, this mutant is a great genetic tool for the

dissection of the double fertilization. When faced with choice which cell to fertilize *cdka;1* exclusively fused with the egg cell. Since there was no central cell fertilization, endosperm does not form, and hence embryo gets arrested early on (Iwakawa et al., 2006). This was further supported by the more recent live tracking of calcium dynamic during the double fertilization where inclination towards a sperm-egg fusion was observed as well (Hamamura et al., 2014). In order to avoid reproductive failure, gametes adhesion and fusion must be accomplished with a high precision, so extensive molecular interaction between gametes must be tightly regulated (Dresselhaus et al., 2016).

Important regulator of the male germline development in *A. thaliana* is transcription factor DUO POLLEN1 (DUO1) which is needed for the correct sperm cell specification by regulating some of the key genes needed for gamete adhesion and fusion such as GAMETE EXPRESSED 2 (GEX2) and HAPLESS 2/GENERATIVE CELL SPECIFIC 1 (HAP2/GCS1) (Brownfield et al., 2009). GEX2 is localized at the sperm cells surface where it plays a vital role in the initial recognition and attachment between gametes (Mori et al., 2014). Loss of function *gex2* sperm cells are correctly delivered to ovules; however, they are unable to attach to the either egg and/or central cell resulting in failed fertilization. Additionally, it was reported that GEX2 extracellular domain is under a rapid evolution, and could be potentially involved in the mediation of species-specific gamete recognition (Mori et al., 2014). Just the close attachment and adhesion of membranes is not sufficient for their fusion, which only be accomplished by an active involvement of protein fusogens of fusion machineries (Hernández and Podbilewicz, 2017).

Upon sperm cells arrival, a small cysteine rich protein EGG CELL1 (EC1) is exocytosed from the storage vesicles in the egg cell to the apical region of degraded synergid cell. Sperm cells are getting activated and they respond by the secretion of gamete fusogen HAP2/GCS1 to the cell surface (Sprunck et al., 2012). HAP2 is exclusively expressed in the haploid sperm, and previous studies reported inability of *hap2* sperm to initiate fertilization as well as reduced ovule targeting (von Besser et al., 2006). However a more recent study reported that *hap2-1* PTs targets ovules normally based on the excess pollination experiment with *hap2-1*/*HAP2* tetrads (Takahashi et al., 2017). Previous studies revealed that before fertilization HAP2/GCS1 is predominantly localized to the ER membrane (Wong and Johnson, 2010). Interestingly only when EC1 peptides were exogenously applied to the semi-in vivo grown PTs, the HAP2-YFP signal relocated from the ER to the sperm cells plasma membrane (Sprunck et al., 2012). In the quintuple *ec1-RNAi* sperm release was intact, but gamete fusion was hindered, and multiple PTs were attracted after such failed fertilization (Sprunck et al., 2012). Very recently it was reported that two DUF679 membrane proteins DMP8 and DMP9 facilitate HAP2 role during the fusions of gametes (Cyprys et al., 2019; Takahashi et al., 2018). Furthermore, it was demonstrated that DMP8 and DMP9 act in a redundant manner, with a more prominent effect on the fusion of sperm cell with egg cell, compared to the sperm-central cell fusion (Cyprys et al., 2019). Additionally, above mentioned EC1 peptide was found to be required during the sperm cell adhesion to the membranes of both egg and central cells, followed by sperm cell separation. In *dmp8/dmp9* double mutants sperm cells remained attached to the egg cell membrane (Cyprys et al., 2019).

Central cells have also evolved an active signaling to promote its own fertilization. In the mutant affected in a BAHD acyl-transferase named *glauce* (*glc*) only the egg cell got fertilized, while central cell remained unfertilized, resulting in only embryo formation. However due to the lack of endosperm, this embryo could not develop further than globular stage (Leshem et al., 2012). Furthermore, mitochondrial ankyrin repeat protein (ANK6) was found to be vital during the gamete

recognition. ANK6 is highly expressed in both male and female gametophytes but only before and during fertilization. When both sperm cell and egg/central cell carried the *ank6* mutation the gamete recognition was impaired, leading to no homozygous zygotes formation (Yu et al., 2010).

Several studies showed that wild-type ovules almost always attract a single PT. Additionally, analysis of PT attraction *in vitro* revealed that once an ovule is targeted newly arriving PTs are getting repelled from the micropyle (Palanivelu and Preuss, 2006; Shimizu and Okada, 2000). It is still unclear if this repulsion occurs because repellents are released upon the arrival of first PT to micropyle, or if the secretion of attractants such as AtLUREs gets aborted (Adhikari et al., 2020; Dresselhaus and Franklin-Tong, 2013; Palanivelu and Tsukamoto, 2012). In line with that, hetero-fertilization in which two genetically different PTs fuse with female gametes was reported to be extremely rare in *A. thaliana* with less than 1% of ovules attracting more than one PT (Beale et al., 2012; Huck, 2003). This indicates that there are active mechanisms set up to ward off attraction of multiple PTs (polytubey), so that polyspermy is prevented which could cause a dramatic reduction of reproductive success (Spielman and Scott, 2008). Contrasting to the wild type plants, so far in a number of different female gametophytic mutants (*maa1/3, amc, fer, lre, herk1/anjea,*) with disrupted PT reception also polytubey has been detected (Boisson-Dernier et al., 2008; Capron et al., 2008; Escobar-Restrepo et al., 2007; Galindo-Trigo et al., 2019; Shimizu and Okada, 2000). These findings suggest that PT burst and/or following stages during gamete fusion are necessary to repel late arriving PTs. Additionally, mutants in which gamete fusion failed, also displayed polytubey, such as *duo1/3*, gex2, *cdka;1*, *hap2/gcs1* and *ec1-RNAi*, indicating that successful gamete fusion is needed to block the arrival of additional PTs (Beale et al., 2012; Kasahara et al., 2012; Maruyama et al., 2013; Mori et al., 2014; Sprunck et al., 2012).

These results demonstrate that there are elaborate mechanisms ensuring gamete fusion before attraction of additional PTs gets aborted (Beale and Johnson, 2013). These complex mechanisms were named "fertilization recovery" and they are important to increase chance of a successful double fertilization and subsequently to enhance reproductive success (Kasahara et al., 2012). In the same study authors reported besides polytubey, also polysiphonogamy in which different PTs discharge in the same synergid. Interestingly there are indications that such triparental progeny can be found even in wild type *A. thaliana* at extremely low rates (Nakel et al., 2017). In maize hetero-fertilization led to generation of triparental endosperm, and even though polyspermy can happen in egg cell it occurs more often in central cell (Grossniklaus, 2017). Therefore it can be concluded that there is no absolute block of polyspermy in either of gametes, which could help in gaining better understanding of polyploidy mechanisms since almost 70% of angiosperms are polyploids (Toda and Okamoto, 2020).

In ovules that attracted defective sperm cell it was observed that non-receptive synergids persisted much longer compared to the wild type fertilizations. Such persistent synergids were able of attracting up to four PTs (Beale et al., 2012). EIN3–EIN2/EIL2-dependent ethylene signalling gets activated upon gamete fusion leading to the persistent synergid cell death. Constitutive ethylene response or application of ethylene precursor resulted in premature synergid degradation (Völz et al., 2013). Additional studies demonstrated that upon a degeneration of persistent synergid cell polytubey block occurs, most likely due to the aborted secretion of PT guidance cues as well as of receptors previously present at the micropylar pole of synergid (Adhikari et al., 2020; Dresselhaus et al., 2016). Furthermore, it was elucidated that upon fertilization of egg cell activation of ethylene signalling led to the nuclear disorganization of persistent synergid, while central cell fertilization induced fusion of endosperm and persistent synergid, leading to the degradation of persistent synergid. Therefore, two

parallel pathways are utilized to accomplish the elimination of persistent synergid upon successful fertilization (Maruyama et al., 2015). Lastly an arabinogalactan protein named JAGGER is an important component of the polytubey block pathway. In *jagger* mutants persistent synergid survived which led to the impaired ability to block attraction of additional PTs. This was yet another confirmation of the vast importance of glycosylated proteins during plant reproduction (Pereira et al., 2016).

1.7 Carbohydrate mediated reproduction

N-glycosylated proteins play vital roles at every stage of extensive PT journey. First interactions between pollen and stigma are under control of heavily *N*-glycosylated receptor SRK which is important for the self-incompatibility responses of different *Brassicaceae* species (section 1.2). PTs growth through the stigma-style interface is mediated by the OFT1 which is also the first described factor involved in this process (section 1.2). OFT1 is an enzyme with *O*-fucosyltransferase activity, and even though in mammals the role of this modification is well established during the cell adhesion and cell-cell communication, almost nothing is known in plants (Smith et al., 2018). For instance, one of the OFT1 homologs named FRINGE in humans is essential for the regulation of NOTCH signalling, by mediating elongation of O-fucose residues on NOTCH, which then in turn influences its ligand binding capabilities (Brückner et al., 2000). Arabinogalactans are large group of heavily glycosylated proteins that are involved in PT growth through the transmitting tract (section 1.3), ovular PT guidance (section 1.4), and polyspermy block (section 1.6) , hence they are essential for many stages of plant reproduction. Furthermore, mutation of three enzymes of the *N*-glycosylation pathway resulted in *fer*-like PTO either intra- or inter-specifically (section 1.5). And finally, all members of *Cr*RLK1L family have several putative *N*-glycosylation sites, making them likely substrates of the previously mentioned *N*-glycosylation enzymes. Regardless considerable differences between plants and animals, there are many similarities at a molecular level, and interestingly several aspects of animal reproduction rely on glycosylated proteins as well.

On their long journey through the transmitting tract PTs become competent to perceive attracting cues from the ovule (section 1.3) and this process resembles capacitation of animal sperm which is necessary for the egg cell fertilization. In humans it was reported that *N*-glycosylation is necessary for the spermatid's differentiation during spermatogenesis (Akintayo and Stanley, 2019). Mammalian spermatozoa are surrounded with a glycocalyx which is produced during development and maturation, but it is also modified upon contact with seminal fluid. Main role of glycocalyx is to promote survival of sperm cells, to inhibit premature capacitation, to provide protection from the female`s immunity system and to render it fully capable for the fertilization. Malglycosylation is often associated with decreased fertility, which was observed in diabetic patients (Cheon and Kim, 2015; Tecle and Gagneux, 2015). Additionally, *N*-glycans are necessary for the normal oogenesis and the production of fully functional egg cells (Akintayo and Stanley, 2019).

As previously stated in plants GPI-anchor proteins are essential for several key reproductive aspects, and interestingly in humans loss of all GPI anchors significantly reduced sperm cell motility while in females it disrupted the ability of oocytes to fuse with sperm cells (Akintayo and Stanley, 2019). Very recently, a large scale glycoproteomic study has revealed pronounced differences in protein *N*-glycosylation between sexes in insects. Additionally, many of the male- or female- specific *N*-glycan occupied sites were derived from the putative reproductive proteins (Scheys et al., 2020). During

oogenesis, a glycocalyx called zona pellucida (ZP) is formed around animal oocytes, and it controls several aspects of fertilization including species-specific sperm recognition, induction of acrosome reaction and blocking of polyspermy. Using different *in vitro* de-glycosylation assays it was revealed that around 75-80% of sperm binding to oocytes is carbohydrate based in mice, with the remaining proportion being mediated by protein-protein interactions (Clark and Dell, 2006). Similar extent of carbohydrate based interactions was observed in human model, where majority of binding was stemming from lectin-lectin interactions (Ozgur et al., 1998). Mice egg cells devoid of all complex and hybrid *N*-glycans had 80% drop in sperm-zona pellucida binding and around 50% of fertility decrease (Clark and Dell, 2006). However different genetical studies in mice where either a proposed zona ligand (α1,3 galactose) or the putative sperm receptor for *N*-acetylglucosamine was lacking were fully fertile (Avella et al., 2013). Very recent study proposed that in mice sperm binding to ZP2 was not mediated by glycans, and that ZP2 N-terminus is sufficient for the efficient binding and successful fertilization (Tokuhiro and Dean, 2018). Dual adhesion model proposed that sperm-ZP interactions are mediated by both protein-protein interactions as well through carbohydrate binding, which is likely further stabilizing these interactions (Clark, 2011). Finally, fusion of gametes in mammals is mediated by sperm resident membrane glycoprotein IZUMO1 and a GPI-anchored egg cell surface localized protein JUNO. Upon IZMUO1-JUNO interaction, tetraspanin CD9 migrated and accumulated to the adhesion site, and only then fusion of gametes could finally take place (Chalbi et al., 2014). It is interesting that in plants only after EC1 is secreted from the storage vesicles upon sperm cell arrival, HAP2/GCS1 gets redistributed to the cell surface where it participates in the fusion of gametes (Section 1.6). Finally, in plants several members of tetraspanin family are expressed in plasma membrane of sperm cells as well as egg and central cells, so it could be proposed that they play a similar role to CD9 during gametes binding and fusion (Boavida et al., 2013).

2 Types of protein glycosylation in different organisms

Posttranslational modifications (PTM) of proteins can occur either spontaneously due to the exposure to cellular environment and different types of stressors, or they can be obtained enzymatically through the precise action of processing enzymes (Ryšlavá et al., 2013). PTMs also often depend on the surrounding amino acid residues, on their surface exposure as well as general chemical reactivity. PTMs are predominantly detected by mass spectrometry (MS) approaches, and the advancement of the novel technologies in the recent years have allowed for large-scale identification and hence better understanding of PTMs (Friso and van Wijk, 2015). Protein glycosylation is the most abundant co- and post-translational modification present in all three domains of life, Bacteria, Archaea and Eukarya. More than half of all proteins in eukaryotes as well one third of biopharmaceuticals are glycoproteins (Apweiler, 1999; Gomord et al., 2010). Glycosylation is enzymatic process that covalently links oligosaccharides to the amino acid residues of the nascent polypeptide chain. There are two major types of glycosylation depending on the type of bond, *N*-linked and *O*-linked glycosylation (Fig. 5) (Strasser, 2016). This covalent linkage of sugars modifies protein`s physicochemical properties and thereby affects its folding, stability, activity, which largely impacts vast array of biological process (Millar et al., 2019).

In the case of *O*-glycosylation monosaccharides are attached in a sequential manner, through an *O*-glycosidic bond to the hydroxyl group of serine and/or threonine residues predominantly (Fig. 5B). *O*-glycosylation of the other residues such as tyrosine, hydroxylysine, and hydroxyproline, has also

been reported in the recent years. *O*-glycosylation is quite common on the hydroxyproline-rich glycoproteins (HRGPs), which belong to the family of secreted cell wall proteins. HRGPs are comprised of arabinogalactan-proteins (AGPs), extensins, and proline-rich proteins. These *O*-glycosylated cell wall proteins have important roles during the plant development, reproduction, regulation of growth, cell division and expansion, abiotic and biotic stress responses, and hormonal signalling (Hijazi et al., 2014; Nguema-Ona et al., 2013; Pereira et al., 2015). It is proposed that *O*-glycans increase HRGP`s solubility, stability, and to play a protective role against proteolytic degradation (Lamport et al., 2011). *O*-glycosylation in mammals, is found on serine/threonine, proline, tyrosine and hydroxylysine amino acids, while the most abundant of these modifications being the mucin-type *O*-glycosylation (Fig. 5B) (Bennett et al., 2011). Similar with plants, mucin-type *O*-glycans have important roles in tissue structure, organization, intercellular communication, stability of hormones, additionally they are heavily present on collagen which is the most abundant protein in humans (Ricard-Blum, 2011).

N-glycosylation, which is the focus of this thesis, is the most common covalent co- and post-translational modification (Apweiler, 1999). During *N*-glycosylation preassembled oligosaccharide unit is transferred to the asparagine residues within the consensus sequence Asn-X-Ser/Thr, with X being any other amino acid besides proline (Aebi, 2013). The biosynthesis of glycoproteins is a complex task divided between the ER and the Golgi apparatus. The division of labour is such that ER is responsible for the synthesis of core oligosaccharides, followed by the covalent linking of glycan and polypeptide, as well for the initial modification of the *N*-glycans (Helenius and Aebi, 2004). Such ER attached *N*-glycans are essential for cell viability, since protein folding and quality control processes heavily affect all secreted proteins (Strasser, 2018). Once the glycoproteins have correctly folded, they move to the Golgi apparatus where they are subjected to further trimming as well as addition of new saccharides to generate the complex-type *N*-glycans present in the mature glycoproteins (Strasser, 2016). Unlike the conserved role of ER-type oligomannosidic structures, complex *N*-glycans play different protein-specific roles which are only starting to be understood in plants (Strasser, 2014).

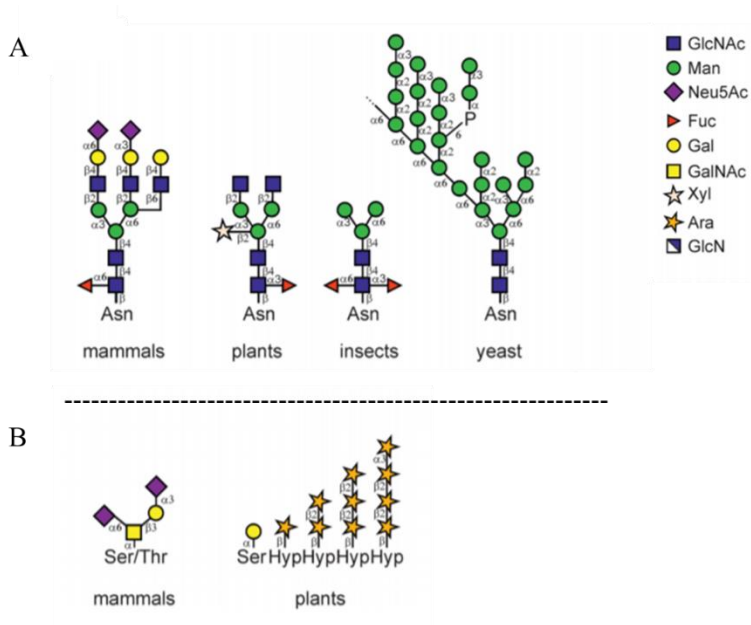

Figure 5. Types of protein linked glycans. (A) Schematic representation of different *N*-glycan structures from mammals, plants, insects, and yeast are depicted. **(B)** Schematic representation of characteristic *O*-glycans from mammals and plants. Symbols for the monosaccharides residues from schemes are displayed at the right part of the image. Adapted from a review (Strasser, 2016).

ER-mediated *N*-glycans synthesis and processing steps are largely conserved in yeasts, mammals, and plants (Wang et al., 2017). For instance, in yeast mannose residues are linked to the oligosaccharide core via α1,6 bond, followed by sequence of elongation steps catalysed by multi-enzymatic complexes, until backbone encompassing up to 50 mannose residues is synthesised (Stolz and Munro, 2002) (Fig. 5A). On the other hand, *N*-glycans of mammals and higher plants are far more variable in the monosaccharide's residues building blocks (Gupta and Shukla, 2018). The high-mannose core is synthesised similarly in plants and mammals; but further processing varies significantly in these organisms. Mammalian proteins have the most complex patterns of *N*-glycosylation, with typical tri- and tetra-antennary branched complex *N*-glycans as well sialylated *N*-glycans (Zhao et al., 2008) (Fig. 5A). Plants produce somewhat less convoluted structures compared to mammals, for instance only bi-antennary *N*-glycans can be found (Fig. 5A). Similarly to insects plants also generate a paucimannosidic type of complex *N*-glycans in which terminal *N*-acetylglucosamine is missing (Fig. 5A) (Gutternigg et al., 2007). Typical decorations of plants are present in complex *N*-glycans and consist of the addition of β1,2 xylose, α1,3-fucose as well of generation of Lewis structure formed by attachment of β1,3 galactose and α1,4 fucose to the terminal glucose residue (Fig. 5A) (Bencúr et al., 2005; Strasser, 2014; Strasser et al., 2004).

2. 1 *N*-glycosylation in the endoplasmic reticulum

N-glycosylation pathway initiates with the biosynthesis of the lipid-linked oligosaccharide precursor ($Man_5GlcNAc_2$) on the cytosolic side of the ER membrane where nucleotide sugar donors (UDP-GlcNAc and GDP-Man) serve as substrates for the number of different glycosyltransferases (Fig. 6). These glycosyltransferases are encoded by the Asparagine Linked Glycosylation (ALG) genes which were firstly characterized in yeast (*Saccharomyces cerevisiae*), and all known yeast ALG genes have plant orthologs (Lannoo and Van Damme, 2015; Lehle et al., 2006). The oligosaccharide precursor is linked to the membrane anchor dolichol pyrophosphate (Dol-PP), which availability is one of the rate-limiting factors of the entire *N*-glycosylation pathway (Schwarz and Aebi, 2011). Dolichols are a class of isoprenoids comprised of unsaturated long-chain isoprenes, which are phosphorylated before glycan attachment (Jones et al., 2009; Shridas and Waechter, 2006). This step is catalysed by a Sec59 kinase in yeast, while *A. thaliana* ortholog is EVAN (EVN), which we have previously showed to be essential for the intraspecific PT reception (Lindner et al., 2015).

The first glucose residue (GlcNAc) attachment to the Dol-PP is catalysed by the *N*-acetylglucosamine-phosphate transferase ALG7, which is a well-known target of *N*-glycosylation inhibitor tunicamycin (Elbein and Heath, 1984). ALG13 and ALG14 glycosyltransferase form a complex which is catalysing transfer of the second GlcNAc residue (Gao et al., 2005). The first mannose residue (Man) is added to Dol-PP-$GlcNAc_2$ by the mannosyltransferase ALG1, which ortholog in *A. thaliana* TURAN (TUN) similar to above mentioned EVN plays important role in the PT reception pathway (Lindner et al., 2015). Mannosyltransferases ALG2 and ALG11 then catalyse addition of four mannose residues, in which ALG2 carries out α-1,6 and α-1,3 mannosylations, followed by two ALG11 α-1,2 mannosylations to form the heptasaccharide ($Man_5GlcNAc_2$-PP-Dol), which is the final product of cytoplasmic LLO biosynthesis (Fig. 6) (Cipollo et al., 2001; O'Reilly et al., 2006). It is still not clear how is the LLO translocated across the membrane, and even though the most likely candidate is a highly conserved flippase RFT1, there is still no consensus in the field since there are some contradicting evidence of RFT1 not being required for this translocation event (Frank

et al., 2008). Upon the translocation of LLO to the luminal side of the ER membrane, further biosynthesis is catalysed by the three α-mannosyltransferases (ALG3, ALG9, and ALG12), followed by three α-glucosyltransferases (ALG6, ALG8, and ALG10). In total during luminal processing four mannose and three glucose residues are added to the LLO forming a final *N*-glycan precursor ($Glc_3Man_9GlcNAc_2$-PP-Dol) (Lannoo and Van Damme, 2015; Schwarz and Aebi, 2011). Contrasting to the initial processing steps, these six ALG transferases are using as glucosyl donors dolichylphosphate-linked monosaccharides Dol-P-Man and Dol-P-Glc. These sugar donors are synthesised by the Dol-P-Man (DPMS1) and Dol-P-Glc synthase (ALG5) present on the cytosolic part of ER membrane, and it is still not clear how are the products being flipped to the ER luminal part (Aebi, 2013; Helenius and Aebi, 2004; Larkin and Imperiali, 2011). Once the LLO is fully assembled, oligosaccharide precursor gets transferred "en bloc" from the dolichol carrier to the nascent polypeptide by an oligosaccharyltransferase (OST) complex(Gupta and Shukla, 2018). OST scans the polypeptide for the consensus sequence Asn-X-Ser/Thr (X being any amino acids besides proline) and adds through a *N*-glycosidic bond oligosaccharide to the Asn residue. In yeast OST is composed of nine trans-membrane subunits Ost1p, Ost2p, Wbp1, Swp1, Stt3p, Ost3p/Ost6p, Ost4p, and Ost5p, five of which are essential for the oligosaccharide transfer *in vivo* (Knauer and Lehle, 1999). STAUROSPORINE AND TEMPERATURE SENSITIVITY3 (STT3) is a catalytically active subunit, while the other noncatalytic subunits regulate the substrate specificity, as well as the complex assembly and stability (Nagashima et al., 2018). In mammals there are two catalytical isoforms, STT3A which is mostly involved in the co-translational *N*-glycosylation and STT3B predominantly implicated in post-translational *N*-glycosylation (Ruiz-Canada et al., 2009). In plants OST complex is also multimeric complex, and two catalytical subunits STT3A and STT3B have been identified based on the homology with yeast and mammals. Only recently it was found that *A. thaliana* OST complex is comprised of seven conserved subunits encoded by twelve genes with an overall similar complex structure to yeast (Jeong et al., 2018).

Upon transfer of the core oligosaccharide to the Asn residue in the polypeptide chain, the terminal glucoses are removed in two subsequent trimming reactions by the α-glucosidases I (GCSI) and α-glucosidases II (GCSII). Such trimmed monoglucosylated structures can be recognized by the ER resident lectin chaperones calnexin (CNX) and calreticulin (CRT), which are a part of ER quality control mechanism and promote folding of glycoproteins (Strasser, 2018). Glycoproteins that were correctly folded are finally processed by an ER-resident class I -mannosidase resulting in a glycoprotein carrying $Man_8GlcNAc_2$, which then gets exported to the Golgi apparatus for the *N*-glycans maturation. When proper folding is not accomplished, glycoprotein gets recognized by the UDP-Glc:glycoprotein glucosyltransferase (UGGT), which is re-glycosylating protein so that it can be recognized again by chaperones calnexin and calreticulin (Caramelo and Parodi, 2008). However, if after several cycles of de- and re- glycosylation folding completely fails such misfolded glycoproteins are released from the chaperones and sent for the degradation through and ER-associated degradation (ERAD) pathway (Vembar and Brodsky, 2008). Trimming of terminal mannoses from glycoproteins by the α-mannosidases MNS4 and MNS5 in the ER lumen labels misfolded glycoproteins for degradation (Hüttner et al., 2014). These final modifications are necessary for the ERAD machinery to differentiate between intermediate misfolded or terminally misfolded proteins (Hüttner and Strasser, 2012).

2.2 *N*-glycan maturation in the Golgi apparatus

Once glycoprotein passes all ER quality control checks it enters Golgi apparatus, where the vast majority of *N*-glycan modification occurs as the glycoprotein travels from the cis to medial and transcisternae (Strasser, 2016). Golgi apparatus resident glycosidases and glycosyltransferases convert oligomannosidic *N*-glycan intermediates to plant specific complex *N*-glycans (Strasser, 2014).

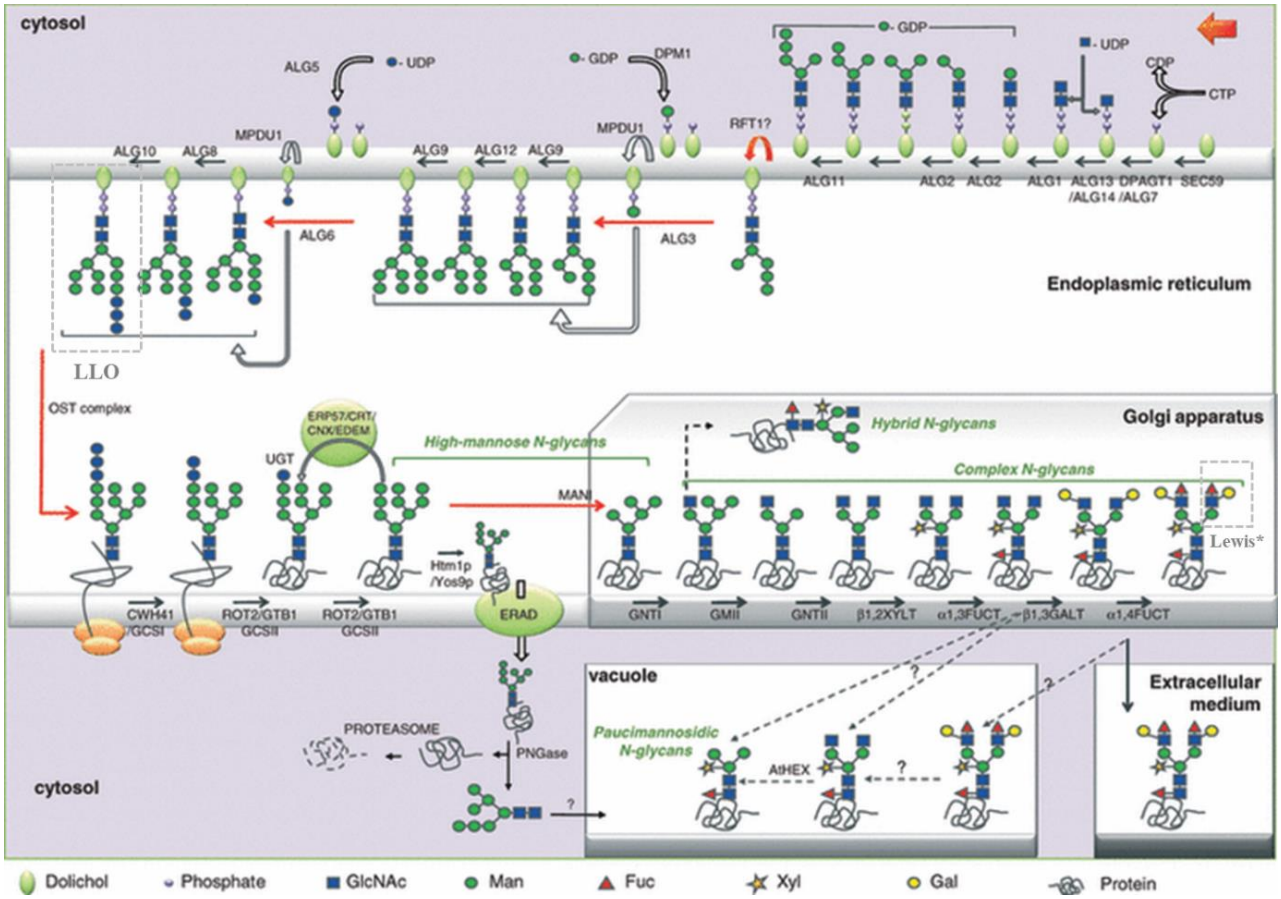

Figure 6. *N*-glycosylation pathway in *A. thaliana*. Assembly of the lipid-linked oligosaccharide (LLO) precursor starts on the cytoplasmic side of the endoplasmic reticulum membrane. Several glycosyltransferases (ALG7, ALG13/14, ALG1, ALG2, ALG11) catalyse synthesis of the dolichol-linked intermediate ($Man_5GlcNAc_2$), which is than translocated to the luminal side of ER by the putative flippase. Once in the ER lumen, α-mannosyltransferases ALG3, ALG9, and ALG12 are catalysing subsequent addition of mannose residues. The α-glucosyltransferases ALG6, ALG8, and ALG10 add terminal glucose residues and such fully assembled oligosaccharide ($Glc_3Man_9GlcNAc_2$) is transferred to the nascent protein by the oligosaccharyltransferase (OST) complex. Terminal glucoses are trimmed by the α-glucosidase I (GCSI) and II (GCSII) and such newly formed *N*-glycoprotein enters the calnexin–calreticulin (CNX–CRT) cycle, which supports protein folding. Properly folded glycoproteins can exit the ER and get exported to the Golgi apparatus. On the other hand, misfolded proteins are sent to the cytosol for the degradation by ER-associated degradation (ERAD) machinery. In Golgi apparatus several glycosidases and glycosyltransferases modify *N*-glycans, to form mature complex-type *N*-glycans. In some cases, additional processing takes place and rare Lewis epitopes are formed, which can be further processed in vacuoles to form paucimannosidic *N*-glycans. Adapted from a review (Gomord et al., 2010).

During the first processing step mannose residues (one up to four) are trimmed off by the Mannosidase I (MANI) thereby generating a $Man_5GlcNAc_2$, which is used as a substrate for the following processing steps (Fig. 6) (Kajiura et al., 2009). There are two α-mannosidases in *A. thaliana*

MNS1 and MNS2, which have probably risen from a recent duplication event, and likely act in a redundant manner (Lannoo and Van Damme, 2015). Additionally, they display sensitivity to kifunensine, which belongs to the class I α-mannosidase inhibitors. Upon cleaving of mannoses, the process of hybrid and complex *N*-glycan formation is initiated by β1,2-N-acetylglucosaminyltransferase I (GNTI) encoded by COMPLEX GLYCAN LESS1 (CGL1) in *A. thaliana*. GNTI catalyse addition of a first N-acetylglucosamine residue resulting in GlcNAc-$Man_5GlcNAc_2$ formation (Fig. 6) (von Schaewen et al., 1993). GNTI plays a central role in the Golgi-mediated pathway similar to its role in mammals, which is impacting all subsequent processing step (Gomord et al., 2010). Upon GNTI processing α-mannosidase II (GMII, encoded by HYBRID GLYCAN1) is cleaving off two more mannose residues which results in formation of hybrid maturing *N*-glycans (Fig. 6) (Strasser et al., 2006). N-acetylglucosaminyltransferase II (GNTII) is attaching terminal GlcNAc to produce complex type *N*-glycans (Strasser et al., 1999). Plant specific complex type *N*-glycans are generated when either α1,3-fucose and/or β1,2-xylose are added to the oligosaccharide core by the action of α1,3-fucosyltransferase (FUT11/FUT12) and β1,2-xylosyltransferase (XYLT) respectively (Fig. 6) (Strasser et al., 2000, 2004). FUT11/12 and XYLT work separately from each other, but both require presence of GlcNAc, which was attached by the GNTI. This complex type *N*-glycan ($GlcNAc_2XylFucMan_3GlcNAc_2$) can be further processed by addition of β1,3-galactose and α1,4-fucose catalysed by the subsequent action of the β1,3-galactosyltransferase (GALT1) and α1,4-fucosyltransferase (FUT13). Resulting structure is Lewis A epitope typical of only plant glycoproteins (Fig. 6) (Fitchette-Lainé et al., 1997). Hexosaminidases (HEXO) cleave the terminal glucose residues once the *N*-glycoproteins reach their destination (vacuole or apoplast) resulting in a formation of paucimannosidic *N*-glycans (Liebminger et al., 2011). The Golgi processing enzymes are acting on three quarters of all *N*-glycoproteins, meaning that majority of *N*-glycans (73.9%) are of complex type, with a smaller proportion of high-mannose *N*-glycans of variable sizes (Strasser, 2014).

2. 3 Biological importance of N-glycans

N-glycosylation of proteins plays essential role during the protein folding, by both increasing solubility of polypeptides and thus prohibiting protein aggregation, and by serving as marks which can be recognized by ER chaperons to further promote protein folding during ER mediated quality control (Liu and Li, 2014; Strasser, 2018). Additionally, *N*-glycans are necessary for the recognition and degradation of terminally misfolded or misassembled glycoproteins via the ERAD pathway (Hebert et al., 2010).

The early processing steps are highly conserved among different organisms; therefore, it is not surprising that perturbation of the pathway have detrimental consequences. For instance in mammals roles of *N*-glycans are well established, and over 100 diseases related to aberrant *N*-glycosylation are known, termed congenital disorders of glycosylation (CDG) (Freeze et al., 2015). CDG diseases can be further subdivided into two groups, in type I the assembly of the lipid-linked oligosaccharide is disturbed, while in type II processing of *N*-glycans upon transfer to the protein is impaired (Körner et al., 2008). With the advancement of analytical techniques field of glycobiology progressed in the last years, and it is becoming more evident that aberrant glycosylation can modulate immune responses, promote cancer metastasis, regulate apoptosis and influence function of kidneys (Reily et al., 2019).

Many aspects of plant life are severely affected by the defective *N*-glycosylation, such as embryo and gametophyte development, cell wall formation, root development, abiotic stress responses, and triggering of immune responses (Nagashima et al., 2018; Strasser, 2016). In the following paragraphs some of the most prominent examples will be given. Several studies showed that perturbation of the *N*-glycosylation pathway led to the impaired biogenesis of important receptor-like kinases (RLKs). For instance, loss of α-mannosyltransferase ALG3 led to the underglycosylation of several pattern-recognition receptors (PRRs) and a compromised calcium response upon exposure to various bacterial/fungal elicitors (Trempel et al., 2016). However, these receptors were still targeted to the plasma membrane and were able to trigger immune response, but to a lower extent compared to the wild type (Trempel et al., 2016). It is interesting that *alg3* mutant displayed no obvious phenotypes under not only standard conditions but even when challenged with increased temperature or salt and osmotic stress. Mass spectrometry analysis revealed a complete loss of high-mannose type glycans, presence of the rare *N*-glycan types and lower amount of complex-type glycans compared to the wild type (Henquet et al., 2008; Kajiura et al., 2010). Disruption of α-glucosyltransferase ALG10 caused accumulation of mainly lipid-linked $Glc_2Man_9GlcNAc_2$, exemplifying that in *alg10* plants the last step of the lipid-linked precursor biosynthesis is severely compromised. Furthermore, this pronounced protein underglycosylation led to the activation of ERAD pathway and increased salt sensitivity, as well as altered leaf size of *alg10* when grown in soil (Farid et al., 2011).

Biogenesis of BRASSINOSTEROID INSENSITIVE 1 (BRI1) receptor-like kinase was reported to be under a control of ERQC pathway, but intriguingly mutations of different components had varying effect on BRI1 secretion and functionality (Tintor and Saijo, 2014). Specificity of ERQC pathway was revealed by discovery that in contrast to BRI1, biosynthesis of immune receptor FLAGELLIN SENSITIVE 2 (FLS2) was not compromised in different mutants of ERQC (Häweker et al., 2010). Moreover complete block of the mannose trimming observed in the *mns1/mns2/mns3* triple mutant led to the severe perturbations of the root development and of the cell wall biosynthesis (Liebminger et al., 2011).

OST function is highly conserved in all eukaryotes and it presents hallmark of *N*-linked protein glycosylation. Loss of both OST1 isoforms leads to gametophytic lethality, and *ost1a* and *ost1b* mutations could only be transmitted through the female (Jeong et al., 2018). Mutation of *A. thaliana* orthologs of yeast Ost2p DEFENDER AGAINST APOPTOTIC CELL DEATH 1/2 (DAD1/2) caused male gametophyte defects. However, all single mutants (*ost1a, ost1b, dad1, dad2*) were growing normally both under standard or salt stress conditions (Jeong et al., 2018). *A. thaliana* DEFECTIVE GLYCOSYLATION 1 (DGL1) ortholog of yeast WBP1 is an essential subunit of OST complex discernible by embryo lethality of *dgl1-2* (Lerouxel et al., 2005). Weaker allele *dgl1-1/DGL-1* displayed reduced cell elongation, dwarf phenotype, and 22% of seed set abortion. Interesting pattern of cell wall composition showed non-disturbed cellulose composition but increase in arabinose, glucose and ectopic callose accumulations (Lerouxel et al., 2005).

STT3A and STT3B are *A. thaliana* orthologs of yeast catalytical subunit Stt3p involved in co-translational *N*-glycan transfer. Gametophytic lethality was observed in *stt3a/stt3b* double mutants, while in siliques of *stt3a/STT3a stt3b/STT3b* 23 % of seeds were aborted. Salt stress (NaCl) induced unfolded protein response, leading to the reduced cell division in root tips of *stt3a,* while *stt3b* showed wild type-like phenotype (Koiwa, 2003). Biosynthesis of immune receptor EF-TU RECEPTOR (EFR) was impaired in *stt3a*, while FLS2 was able to tolerate underglycosylation defects of *stt3a*

background. Loss of a single *N*-glycosylation site in the EFR ectodomain, EFR^{N143Q} led to inability to bind to its ligand and to activate downstream signaling cascade (Häweker et al., 2010).

Mutations in OST3/6, *A. thaliana* orthologs of yeast Ost3p/Ost6p, induced unfolded protein response, and caused hypersensitivity to osmotic stress (NaCl and Mannitol) as well as tunicamycin inhibition (Farid et al., 2013). Interestingly in *ost3/6* biogenesis of EFR and endo-β-1,4-glucanase KORRIGAN1 (KOR1) was severely compromised, while receptor kinase BRI1 was unaffected, exemplifying very specific substrate preferences of OST3/6 (Farid et al., 2013). Together with STT3A catalytic subunit OST3/6 is involved in the BAK1/SERK-4 regulated cell death (de Oliveira et al., 2016). We have previously discovered loss of OST3/6 (ARU) to be essential for the interspecific pollen tube reception (Müller et al., 2016).

Surprisingly, our knowledge on the plant *N*-glycan maturation in Golgi apparatus is still extremely limited. Early studies in mice revealed loss of GNTI to be embryo lethal (Ioffe and Stanley, 1994). In humans disturbance of *N*-glycan processing is implicated in several type II CDGs (Körner et al., 2008). Loss of GNTI in *Drosophila melanogaster* caused abnormal brain development as well a shorter life span (Sarkar et al., 2006), while in *Caenorhabditis elegans* development was undisturbed but immune response were compromised (Schachter, 2010). In plants the first mutant lacking complex *N*-glycans, *cgl1* was discovered more than 25 years ago (von Schaewen et al., 1993). Even though in *cgl1* all glycoproteins are exclusively of high-mannose type ($Man_5GlcNAc_2$) no obvious phenotype could be detected under range of different heat/cold/light stress conditions (Strasser et al., 2005). In agreement to *cgl1* also no evident phenotype was found in mutants which produce hybrid *N*-glycans, complex *N*-glycans devoid of β1,2-xylose and α1,3-fucose residues, or in mutants in which Lewis a epitopes were completely eliminated (Strasser, 2014).

The first evidence of complex *N*-glycans biological function was hypersensitivity of *cgl1* grown under osmotic and salt stress conditions. Salt stress led to the severe primary root growth inhibition, swelling of the root tip as well as the callose accumulation in *cgl1*, but interestingly there was no upregulation of the unfolded protein response (Kang et al., 2008). CGL1 is needed to build a tolerance to the salt exposure, and this is mediated by the correctly *N*-glycosylated KORRIGAN1 (KOR1/RSW2), necessary for the cellulose biosynthesis (Kang et al., 2008). Until nowadays the only direct target of GNTI is above mentioned KOR1, a membrane-anchored endo -β-1,4-glucanase, which contains eight putative *N*-glycosylation sites within its extracellular domain (Kang et al., 2008; Lane et al., 2001). Mutations of 4 non-conserved sites led to the lower enzymatic activity of KOR1. Similarly, single mutations of non-conserved *N*-glycan sites had lower ability to rescue *rsw2-1* compared to the highly conserved sites. KOR1 depleted of all *N*-glycans showed partial rescue of *rsw2-1* root length (Liebminger et al., 2013; Rips et al., 2014). KOR1 weaker allele *jiaoyao1* (*jia1)* caused dwarf phenotype with smaller rosette leaves, anthocyanin accumulation, shorter petioles as well as shorter siliques, however authors have not further investigated fertility issues (Lei et al., 2014).

Lastly, very exciting findings have been made in rice where loss of GNTI had profound impact leading to arrested development of seedlings and early lethality before entering the reproductive cycle. Furthermore authors reported aberrant cell wall composition and impairment of cytokine signalling (Fanata et al., 2013). These discovery highlights the vast importance of complex *N*-glycans in plants, which requirement seems to be more pronounced in monocot species.

References

Adhikari, P.B., Liu, X., Wu, X., Zhu, S., and Kasahara, R.D. (2020). Fertilization in flowering plants: an odyssey of sperm cell delivery. Plant Mol Biol.

Aebi, M. (2013). N-linked protein glycosylation in the ER. Biochimica et Biophysica Acta (BBA) - Molecular Cell Research *1833*, 2430–2437.

Akintayo, A., and Stanley, P. (2019). Roles for Golgi Glycans in Oogenesis and Spermatogenesis. Front. Cell Dev. Biol. *7*, 98.

Alandete-Saez, M., Ron, M., and McCormick, S. (2008). GEX3, Expressed in the Male Gametophyte and in the Egg Cell of Arabidopsis thaliana Is Essential for Micropylar Pollen Tube Guidance and Plays a Role during Early Embryogenesis. Molecular Plant *1*, 586–598.

Alves, C.M.L., Noyszewski, A.K., and Smith, A.G. (2019). Structure and function of class III pistil-specific extensin-like protein in interspecific reproductive barriers. BMC Plant Biol *19*, 118.

Amien, S., Kliwer, I., Márton, M.L., Debener, T., Geiger, D., Becker, D., and Dresselhaus, T. (2010). Defensin-Like ZmES4 Mediates Pollen Tube Burst in Maize via Opening of the Potassium Channel KZM1. PLOS Biology *8*, e1000388.

Apweiler, R. (1999). On the frequency of protein glycosylation, as deduced from analysis of the SWISS-PROT database. Biochimica et Biophysica Acta (BBA) - General Subjects *1473*, 4–8.

Avella, M.A., Xiong, B., and Dean, J. (2013). The molecular basis of gamete recognition in mice and humans. MHR: Basic Science of Reproductive Medicine *19*, 279–289.

Baïet, B., Burel, C., Saint-Jean, B., Louvet, R., Menu-Bouaouiche, L., Kiefer-Meyer, M.-C., Mathieu-Rivet, E., Lefebvre, T., Castel, H., Carlier, A., et al. (2011). *N* -Glycans of *Phaeodactylum tricornutum* Diatom and Functional Characterization of Its *N* -Acetylglucosaminyltransferase I Enzyme. J. Biol. Chem. *286*, 6152–6164.

Beale, K.M., and Johnson, M.A. (2013). Speed dating, rejection, and finding the perfect mate: advice from flowering plants. Current Opinion in Plant Biology *16*, 590–597.

Beale, K.M., Leydon, A.R., and Johnson, M.A. (2012). Gamete Fusion Is Required to Block Multiple Pollen Tubes from Entering an Arabidopsis Ovule. Current Biology *22*, 1090–1094.

Bedinger, P.A., Broz, A.K., Tovar-Mendez, A., and McClure, B. (2017). Pollen-Pistil Interactions and Their Role in Mate Selection. Plant Physiol. *173*, 79–90.

Bencúr, P., Steinkellner, H., Svoboda, B., Mucha, J., Strasser, R., Kolarich, D., Hann, S., Köllensperger, G., Glössl, J., Altmann, F., et al. (2005). Arabidopsis thaliana β1,2-xylosyltransferase: an unusual glycosyltransferase with the potential to act at multiple stages of the plant N-glycosylation pathway. Biochemical Journal *388*, 515–525.

Bennett, E.P., Mandel, U., Clausen, H., Gerken, T.A., Fritz, T.A., and Tabak, L.A. (2011). Control of mucin-type O-glycosylation: A classification of the polypeptide GalNAc-transferase gene family. Glycobiology *22*, 736–756.

Berger, F., Hamamura, Y., Ingouff, M., and Higashiyama, T. (2008). Double fertilization – caught in the act. Trends in Plant Science *13*, 437–443.

von Besser, K., Frank, A.C., Johnson, M.A., and Preuss, D. (2006). Arabidopsis HAP2 (GCS1) is a sperm-specific gene required for pollen tube guidance and fertilization. Development *133*, 4761.

Bleckmann, A., Alter, S., and Dresselhaus, T. (2014). The beginning of a seed: regulatory mechanisms of double fertilization. Front. Plant Sci. *5*.

Boavida, L.C., Borges, F., Becker, J.D., and Feijó, J.A. (2011). Whole Genome Analysis of Gene Expression Reveals Coordinated Activation of Signaling and Metabolic Pathways during Pollen-Pistil Interactions in Arabidopsis. Plant Physiol. *155*, 2066–2080.

Boavida, L.C., Qin, P., Broz, M., Becker, J.D., and McCormick, S. (2013). Arabidopsis Tetraspanins Are Confined to Discrete Expression Domains and Cell Types in Reproductive Tissues and Form Homo- and Heterodimers When Expressed in Yeast. Plant Physiol. *163*, 696.

Boisson-Dernier, A., Frietsch, S., Kim, T.-H., Dizon, M.B., and Schroeder, J.I. (2008). The Peroxin Loss-of-Function Mutation abstinence by mutual consent Disrupts Male-Female Gametophyte Recognition. Current Biology *18*, 63–68.

Boisson-Dernier, A., Kessler, S.A., and Grossniklaus, U. (2011). The walls have ears: the role of plant CrRLK1Ls in sensing and transducing extracellular signals. Journal of Experimental Botany *62*, 1581–1591.

Boisson-Dernier, A., Lituiev, D.S., Nestorova, A., Franck, C.M., Thirugnanarajah, S., and Grossniklaus, U. (2013). ANXUR Receptor-Like Kinases Coordinate Cell Wall Integrity with Growth at the Pollen Tube Tip Via NADPH Oxidases. PLoS Biol *11*, e1001719.

Boisson-Dernier, A., Franck, C.M., Lituiev, D.S., and Grossniklaus, U. (2015). Receptor-like cytoplasmic kinase MARIS functions downstream of *Cr* RLK1L-dependent signaling during tip growth. Proc Natl Acad Sci USA *112*, 12211–12216.

Bosch, M., and Hepler, P.K. (2005). Pectin Methylesterases and Pectin Dynamics in Pollen Tubes. Plant Cell *17*, 3219–3226.

Brownfield, L., Hafidh, S., Durbarry, A., Khatab, H., Sidorova, A., Doerner, P., and Twell, D. (2009). Arabidopsis DUO POLLEN3 Is a Key Regulator of Male Germline Development and Embryogenesis. Plant Cell *21*, 1940.

Broz, A.K., Guerrero, R.F., Randle, A.M., Baek, Y.S., Hahn, M.W., and Bedinger, P.A. (2017). Transcriptomic analysis links gene expression to unilateral pollen-pistil reproductive barriers. BMC Plant Biol *17*, 81.

Brückner, K., Perez, L., Clausen, H., and Cohen, S. (2000). Glycosyltransferase activity of Fringe modulates Notch–Delta interactions. Nature *406*, 411–415.

Büschges, R., Hollricher, K., Panstruga, R., Simons, G., Wolter, M., Frijters, A., van Daelen, R., van der Lee, T., Diergaarde, P., Groenendijk, J., et al. (1997). The Barley Mlo Gene: A Novel Control Element of Plant Pathogen Resistance. Cell *88*, 695–705.

Capron, A., Gourgues, M., Neiva, L.S., Faure, J.-E., Berger, F., Pagnussat, G., Krishnan, A., Alvarez-Mejia, C., Vielle-Calzada, J.-P., Lee, Y.-R., et al. (2008). Maternal Control of Male-Gamete Delivery in *Arabidopsis* Involves a Putative GPI-Anchored Protein Encoded by the *LORELEI* Gene. Plant Cell *20*, 3038–3049.

Caramelo, J.J., and Parodi, A.J. (2008). Getting In and Out from Calnexin/Calreticulin Cycles. J. Biol. Chem. *283*, 10221–10225.

Chae, K., and Lord, E.M. (2011). Pollen tube growth and guidance: roles of small, secreted proteins. Annals of Botany *108*, 627–636.

Chae, K., Kieslich, C.A., Morikis, D., Kim, S.-C., and Lord, E.M. (2009). A Gain-of-Function Mutation of *Arabidopsis* Lipid Transfer Protein 5 Disturbs Pollen Tube Tip Growth and Fertilization. Plant Cell *21*, 3902–3914.

Chalbi, M., Barraud-Lange, V., Ravaux, B., Howan, K., Rodriguez, N., Soule, P., Ndzoudi, A., Boucheix, C., Rubinstein, E., Wolf, J.P., et al. (2014). Binding of sperm protein Izumo1 and its egg receptor Juno drives Cd9 accumulation in the intercellular contact area prior to fusion during mammalian fertilization. Development *141*, 3732.

Chang, F., Gu, Y., Ma, H., and Yang, Z. (2013). AtPRK2 Promotes ROP1 Activation via RopGEFs in the Control of Polarized Pollen Tube Growth. Molecular Plant *6*, 1187–1201.

Chapman, L.A., and Goring, D.R. (2010). Pollen-pistil interactions regulating successful fertilization in the Brassicaceae. Journal of Experimental Botany *61*, 1987–1999.

Chapman, L.A., and Goring, D.R. (2011). Misregulation of phosphoinositides in Arabidopsis thaliana decreases pollen hydration and maternal fertility. Sex Plant Reprod *24*, 319–326.

Chen, Y.-H., Li, H.-J., Shi, D.-Q., Yuan, L., Liu, J., Sreenivasan, R., Baskar, R., Grossniklaus, U., and Yang, W.-C. (2007). The Central Cell Plays a Critical Role in Pollen Tube Guidance in Arabidopsis. Plant Cell *19*, 3563.

Cheon, Y.-P., and Kim, C.-H. (2015). Impact of glycosylation on the unimpaired functions of the sperm. Clin Exp Reprod Med *42*, 77.

Cheung, A.Y., Wang, H., and Wu, H. (1995). A floral transmitting tissue-specific glycoprotein attracts pollen tubes and stimulates their growth. Cell *82*, 383–393.

Cho, Y., Yu, C.-Y., Nakamura, Y., and Kanehara, K. (2017). Arabidopsis dolichol kinase AtDOK1 is involved in flowering time control. Journal of Experimental Botany *68*, 3243–3252.

Christensen, C.A., Gorsich, S.W., Brown, R.H., Jones, L.G., Brown, J., Shaw, J.M., and Drews, G.N. (2002). Mitochondrial GFA2 Is Required for Synergid Cell Death in Arabidopsis. Plant Cell *14*, 2215.

Cipollo, J.F., Trimble, R.B., Chi, J.H., Yan, Q., and Dean, N. (2001). The Yeast *ALG11* Gene Specifies Addition of the Terminal α1,2-Man to the $Man_5GlcNAc_2$-PP-dolichol *N* -Glycosylation Intermediate Formed on the Cytosolic Side of the Endoplasmic Reticulum. J. Biol. Chem. *276*, 21828–21840.

Clark, G.F. (2011). Molecular models for mouse sperm-oocyte binding. Glycobiology *21*, 3–5.

Clark, G.F., and Dell, A. (2006). Molecular Models for Murine Sperm-Egg Binding. J. Biol. Chem. *281*, 13853–13856.

Costa, M., Nobre, M.S., Becker, J.D., Masiero, S., Amorim, M.I., Pereira, L.G., and Coimbra, S. (2013). Expression-based and co-localization detection of arabinogalactan protein 6 and arabinogalactan protein 11 interactors in Arabidopsis pollen and pollen tubes. BMC Plant Biol *13*, 7.

Crawford, B.C.W., and Yanofsky, M.F. (2011). HALF FILLED promotes reproductive tract development and fertilization efficiency in Arabidopsis thaliana. Development *138*, 2999–3009.

Crawford, B.C.W., Ditta, G., and Yanofsky, M.F. (2007). The NTT Gene Is Required for Transmitting-Tract Development in Carpels of Arabidopsis thaliana. Current Biology *17*, 1101–1108.

Crepet, W.L. (2000). Progress in understanding angiosperm history, success, and relationships: Darwin's abominably "perplexing phenomenon." Proceedings of the National Academy of Sciences *97*, 12939–12941.

Cyprys, P., Lindemeier, M., and Sprunck, S. (2019). Gamete fusion is facilitated by two sperm cell-expressed DUF679 membrane proteins. Nature Plants *5*, 253–257.

Dai, X.R., Gao, X.-Q., Chen, G.H., Tang, L.L., Wang, H., and Zhang, X.S. (2014). ABNORMAL POLLEN TUBE GUIDANCE1, an Endoplasmic Reticulum-Localized Mannosyltransferase Homolog of GLYCOSYLPHOSPHATIDYLINOSITOL10 in Yeast and PHOSPHATIDYLINOSITOL GLYCAN ANCHOR BIOSYNTHESIS B in Human, Is Required for Arabidopsis Pollen Tube Micropylar Guidance and Embryo Development. Plant Physiol. *165*, 1544.

Davis, T.C., Jones, D.S., Dino, A.J., Cejda, N.I., Yuan, J., Willoughby, A.C., and Kessler, S.A. (2017). Arabidopsis thaliana MLO genes are expressed in discrete domains during reproductive development. Plant Reprod *30*, 185–195.

Denninger, P., Bleckmann, A., Lausser, A., Vogler, F., Ott, T., Ehrhardt, D.W., Frommer, W.B., Sprunck, S., Dresselhaus, T., and Grossmann, G. (2014). Male–female communication triggers calcium signatures during fertilization in Arabidopsis. Nat Commun *5*, 4645.

Dobritsa, A.A., Nishikawa, S.-I., Preuss, D., Urbanczyk-Wochniak, E., Sumner, L.W., Hammond, A., Carlson, A.L., and Swanson, R.J. (2009). LAP3, a novel plant protein required for pollen development, is essential for proper exine formation. Sex Plant Reprod *22*, 167–177.

Doucet, J., Lee, H.K., and Goring, D.R. (2016). Pollen Acceptance or Rejection: A Tale of Two Pathways. Trends in Plant Science *21*, 1058–1067.

Dresselhaus, T., and Franklin-Tong, N. (2013). Male–Female Crosstalk during Pollen Germination, Tube Growth and Guidance, and Double Fertilization. Molecular Plant *6*, 1018–1036.

Dresselhaus, T., Sprunck, S., and Wessel, G.M. (2016). Fertilization Mechanisms in Flowering Plants. Current Biology *26*, R125–R139.

Duan, Q., Kita, D., Johnson, E.A., Aggarwal, M., Gates, L., Wu, H.-M., and Cheung, A.Y. (2014). Reactive oxygen species mediate pollen tube rupture to release sperm for fertilization in Arabidopsis. Nat Commun *5*, 3129.

Elbein, A.D., and Heath, E.C. (1984). Inhibitors of the Biosynthesis and Processing of N-Linked Oligosaccharide. Critical Reviews in Biochemistry *16*, 21–49.

Escobar-Restrepo, J.-M., Huck, N., Kessler, S., Gagliardini, V., Gheyselinck, J., Yang, W.-C., and Grossniklaus, U. (2007). The FERONIA Receptor-like Kinase Mediates Male-Female Interactions During Pollen Tube Reception. Science *317*, 656–660.

Fanata, W.I.D., Lee, K.H., Son, B.H., Yoo, J.Y., Harmoko, R., Ko, K.S., Ramasamy, N.K., Kim, K.H., Oh, D.-B., Jung, H.S., et al. (2013). N-glycan maturation is crucial for cytokinin-mediated development and cellulose synthesis in *Oryza sativa*. Plant J *73*, 966–979.

Farid, A., Pabst, M., Schoberer, J., Altmann, F., Glössl, J., and Strasser, R. (2011). *Arabidopsis thaliana* alpha1,2-glucosyltransferase (ALG10) is required for efficient N-glycosylation and leaf growth: *Arabidopsis alpha1,2-glucosyltransferase*. The Plant Journal *68*, 314–325.

Farid, A., Malinovsky, F.G., Veit, C., Schoberer, J., Zipfel, C., and Strasser, R. (2013). Specialized Roles of the Conserved Subunit OST3/6 of the Oligosaccharyltransferase Complex in Innate Immunity and Tolerance to Abiotic Stresses. Plant Physiol. *162*, 24–38.

Feng, H., Liu, C., Fu, R., Zhang, M., Li, H., Shen, L., Wei, Q., Sun, X., Xu, L., Ni, B., et al. (2019). LORELEI-LIKE GPI-ANCHORED PROTEINS 2/3 Regulate Pollen Tube Growth as Chaperones and Coreceptors for ANXUR/BUPS Receptor Kinases in Arabidopsis. Molecular Plant *12*, 1612–1623.

Fiebig, A., Kimport, R., and Preuss, D. (2004). Comparisons of pollen coat genes across Brassicaceae species reveal rapid evolution by repeat expansion and diversification. Proceedings of the National Academy of Sciences *101*, 3286–3291.

Fitchette-Lainé, A.-C., Gomord, V., Cabanes, M., Michalski, J.-C., Saint Macary, M., Foucher, B., Cavelier, B., Hawes, C., Lerouge, P., and Faye, L. (1997). N-glycans harboring the Lewis a epitope are expressed at the surface of plant cells. The Plant Journal *12*, 1411–1417.

Franck, C.M., Westermann, J., Bürssner, S., Lentz, R., Lituiev, D.S., and Boisson-Dernier, A. (2018). The Protein Phosphatases ATUNIS1 and ATUNIS2 Regulate Cell Wall Integrity in Tip-Growing Cells. Plant Cell *30*, 1906–1923.

Frank, C.G., Sanyal, S., Rush, J.S., Waechter, C.J., and Menon, A.K. (2008). Does Rft1 flip an N-glycan lipid precursor? Nature *454*, E3–E4.

Freeze, H.H., Eklund, E.A., Ng, B.G., and Patterson, M.C. (2015). Neurological Aspects of Human Glycosylation Disorders. Annu. Rev. Neurosci. *38*, 105–125.

Friso, G., and van Wijk, K.J. (2015). Update: Post-translational protein modifications in plant metabolism. Plant Physiol. pp.01378.2015.

Galindo-Trigo, S., Blanco-Touriñán, N., DeFalco, T.A., Wells, E.S., Gray, J.E., Zipfel, C., and Smith, L.M. (2019). *Cr* RLK 1L receptor-like kinases HERK 1 and ANJEA are female determinants of pollen tube reception. EMBO Rep.

Gao, H., Zhang, Y., Wang, W., Zhao, K., Liu, C., Bai, L., Li, R., and Guo, Y. (2017). Two Membrane-Anchored Aspartic Proteases Contribute to Pollen and Ovule Development. Plant Physiol. *173*, 219.

Gao, Q.-F., Gu, L.-L., Wang, H.-Q., Fei, C.-F., Fang, X., Hussain, J., Sun, S.-J., Dong, J.-Y., Liu, H., and Wang, Y.-F. (2016a). Cyclic nucleotide-gated channel 18 is an essential Ca^{2+} channel in pollen tube tips for pollen tube guidance to ovules in Arabidopsis. Proc Natl Acad Sci USA *113*, 3096.

Gao, X.-D., Tachikawa, H., Sato, T., Jigami, Y., and Dean, N. (2005). Alg14 Recruits Alg13 to the Cytoplasmic Face of the Endoplasmic Reticulum to Form a Novel Bipartite UDP- *N* -acetylglucosamine Transferase Required for the Second Step of *N* -Linked Glycosylation. J. Biol. Chem. *280*, 36254–36262.

Gao, X.-Q., Liu, C.Z., Li, D.D., Zhao, T.T., Li, F., Jia, X.N., Zhao, X.-Y., and Zhang, X.S. (2016b). The Arabidopsis KINβγ Subunit of the SnRK1 Complex Regulates Pollen Hydration on the Stigma by Mediating the Level of Reactive Oxygen Species in Pollen. PLoS Genet *12*, e1006228.

Ge, Z., Bergonci, T., Zhao, Y., Zou, Y., Du, S., Liu, M.-C., Luo, X., Ruan, H., García-Valencia, L.E., Zhong, S., et al. (2017). *Arabidopsis* pollen tube integrity and sperm release are regulated by RALF-mediated signaling. Science *358*, 1596–1600.

Gomord, V., Fitchette, A.-C., Menu-Bouaouiche, L., Saint-Jore-Dupas, C., Plasson, C., Michaud, D., and Faye, L. (2010). Plant-specific glycosylation patterns in the context of therapeutic protein production: PMP-specific glycosylation patterns. Plant Biotechnology Journal *8*, 564–587.

Grossniklaus, U. (2017). Polyspermy produces tri-parental seeds in maize. Current Biology *27*, R1300–R1302.

Gu, L.-L., Gao, Q.-F., and Wang, Y.-F. (2017). Cyclic nucleotide-gated channel 18 functions as an essential Ca^{2+} channel for pollen germination and pollen tube growth in *Arabidopsis*. Plant Signaling & Behavior *12*, e1197999.

Guan, Y., Lu, J., Xu, J., McClure, B., and Zhang, S. (2014). Two Mitogen-Activated Protein Kinases, MPK3 and MPK6, Are Required for Funicular Guidance of Pollen Tubes in Arabidopsis. Plant Physiol. *165*, 528–533.

Gupta, S.K., and Shukla, P. (2018). Glycosylation control technologies for recombinant therapeutic proteins. Appl Microbiol Biotechnol *102*, 10457–10468.

Gutternigg, M., Kretschmer-Lubich, D., Paschinger, K., Rendić, D., Hader, J., Geier, P., Ranftl, R., Jantsch, V., Lochnit, G., and Wilson, I.B.H. (2007). Biosynthesis of Truncated *N* -Linked Oligosaccharides Results from Non-orthologous Hexosaminidase-mediated Mechanisms in Nematodes, Plants, and Insects. J. Biol. Chem. *282*, 27825–27840.

Hamamura, Y., Saito, C., Awai, C., Kurihara, D., Miyawaki, A., Nakagawa, T., Kanaoka, M.M., Sasaki, N., Nakano, A., Berger, F., et al. (2011). Live-Cell Imaging Reveals the Dynamics of Two Sperm Cells during Double Fertilization in Arabidopsis thaliana. Current Biology *21*, 497–502.

Hamamura, Y., Nishimaki, M., Takeuchi, H., Geitmann, A., Kurihara, D., and Higashiyama, T. (2014). Live imaging of calcium spikes during double fertilization in Arabidopsis. Nat Commun *5*, 4722.

Häweker, H., Rips, S., Koiwa, H., Salomon, S., Saijo, Y., Chinchilla, D., Robatzek, S., and von Schaewen, A. (2010). Pattern Recognition Receptors Require *N* -Glycosylation to Mediate Plant Immunity. J. Biol. Chem. *285*, 4629–4636.

Hebert, D.N., Bernasconi, R., and Molinari, M. (2010). ERAD substrates: Which way out? Seminars in Cell & Developmental Biology *21*, 526–532.

Helenius, A., and Aebi, M. (2004). Roles of N-Linked Glycans in the Endoplasmic Reticulum. Annu. Rev. Biochem. *73*, 1019–1049.

Henquet, M., Lehle, L., Schreuder, M., Rouwendal, G., Molthoff, J., Helsper, J., van der Krol, S., and Bosch, D. (2008). Identification of the Gene Encoding the α1,3-Mannosyltransferase (ALG3) in *Arabidopsis* and Characterization of Downstream *N* -Glycan Processing. Plant Cell *20*, 1652–1664.

Hernández, J.M., and Podbilewicz, B. (2017). The hallmarks of cell-cell fusion. Development *144*, 4481.

Herrera-Ubaldo, H., Lozano-Sotomayor, P., Ezquer, I., Di Marzo, M., Chávez Montes, R.A., Gómez-Felipe, A., Pablo-Villa, J., Diaz-Ramirez, D., Ballester, P., Ferrándiz, C., et al. (2019). New roles of NO TRANSMITTING TRACT and SEEDSTICK during medial domain development in *Arabidopsis* fruits. Development *146*, dev172395.

Higashiyama, T., and Takeuchi, H. (2015). The Mechanism and Key Molecules Involved in Pollen Tube Guidance. Annu. Rev. Plant Biol. *66*, 393–413.

Higashiyama, T., and Yang, W. (2017). Gametophytic Pollen Tube Guidance: Attractant Peptides, Gametic Controls, and Receptors. Plant Physiol. *173*, 112.

Hijazi, M., Velasquez, S.M., Jamet, E., Estevez, J.M., and Albenne, C. (2014). An update on post-translational modifications of hydroxyproline-rich glycoproteins: toward a model highlighting their contribution to plant cell wall architecture. Frontiers in Plant Science *5*, 395.

Hou, Y., Guo, X., Cyprys, P., Zhang, Y., Bleckmann, A., Cai, L., Huang, Q., Luo, Y., Gu, H., Dresselhaus, T., et al. (2016). Maternal ENODLs Are Required for Pollen Tube Reception in Arabidopsis. Current Biology *26*, 2343–2350.

Huang, W.-J., Liu, H.-K., McCormick, S., and Tang, W.-H. (2014). Tomato Pistil Factor STIG1 Promotes in Vivo Pollen Tube Growth by Binding to Phosphatidylinositol 3-Phosphate and the Extracellular Domain of the Pollen Receptor Kinase LePRK2. Plant Cell *26*, 2505–2523.

Huck, N. (2003). The Arabidopsis mutant feronia disrupts the female gametophytic control of pollen tube reception. Development *130*, 2149–2159.

Hüttner, S., and Strasser, R. (2012). Endoplasmic Reticulum-Associated Degradation of Glycoproteins in Plants. Front. Plant Sci. *3*.

Hüttner, S., Veit, C., Vavra, U., Schoberer, J., Liebminger, E., Maresch, D., Grass, J., Altmann, F., Mach, L., and Strasser, R. (2014). *Arabidopsis* Class I α-Mannosidases MNS4 and MNS5 Are Involved in Endoplasmic Reticulum–Associated Degradation of Misfolded Glycoproteins. Plant Cell *26*, 1712–1728.

Igawa, T., Yanagawa, Y., Miyagishima, S., and Mori, T. (2013). Analysis of gamete membrane dynamics during double fertilization of Arabidopsis. Journal of Plant Research *126*, 387–394.

Ioffe, E., and Stanley, P. (1994). Mice lacking N-acetylglucosaminyltransferase I activity die at mid-gestation, revealing an essential role for complex or hybrid N-linked carbohydrates. Proceedings of the National Academy of Sciences *91*, 728–732.

Iwakawa, H., Shinmyo, A., and Sekine, M. (2006). Arabidopsis CDKA;1, a cdc2 homologue, controls proliferation of generative cells in male gametogenesis. The Plant Journal *45*, 819–831.

Iwano, M., and Takayama, S. (2012). Self/non-self discrimination in angiosperm self-incompatibility. Current Opinion in Plant Biology *15*, 78–83.

Iwano, M., Ngo, Q.A., Entani, T., Shiba, H., Nagai, T., Miyawaki, A., Isogai, A., Grossniklaus, U., and Takayama, S. (2012). Cytoplasmic Ca2+ changes dynamically during the interaction of the pollen tube with synergid cells. Development *139*, 4202–4209.

Jeong, I.S., Lee, S., Bonkhofer, F., Tolley, J., Fukudome, A., Nagashima, Y., May, K., Rips, S., Lee, S.Y., Gallois, P., et al. (2018). Purification and characterization of *Arabidopsis thaliana* oligosaccharyltransferase complexes from the native host: a protein super-expression system for structural studies. Plant J *94*, 131–145.

Jiang, L., Yang, S.-L., Xie, L.-F., Puah, C.S., Zhang, X.-Q., Yang, W.-C., Sundaresan, V., and Ye, D. (2005). *VANGUARD1* Encodes a Pectin Methylesterase That Enhances Pollen Tube Growth in the Arabidopsis Style and Transmitting Tract. Plant Cell *17*, 584–596.

Jiao, H., Liu, Q., Zhang, H., Qi, K., Liu, Z., Wang, P., Wu, J., and Zhang, S. (2019). PbrPCCP1 mediates the PbrTTS1 signaling to control pollen tube growth in pear. Plant Science *289*, 110244.

Johnson, M.A., Harper, J.F., and Palanivelu, R. (2019). A Fruitful Journey: Pollen Tube Navigation from Germination to Fertilization. Annu. Rev. Plant Biol. *70*, 809–837.

Jones, D.S., Yuan, J., Smith, B.E., Willoughby, A.C., Kumimoto, E.L., and Kessler, S.A. (2017). MILDEW RESISTANCE LOCUS O Function in Pollen Tube Reception Is Linked to Its Oligomerization and Subcellular Distribution. Plant Physiol. *175*, 172–185.

Jones, D.S., Liu, X., Willoughby, A.C., Smith, B.E., Palanivelu, R., and Kessler, S.A. (2018). Cellular distribution of secretory pathway markers in the haploid synergid cells of *Arabidopsis thaliana*. Plant J *94*, 192–202.

Jones, M.B., Rosenberg, J.N., Betenbaugh, M.J., and Krag, S.S. (2009). Structure and synthesis of polyisoprenoids used in N-glycosylation across the three domains of life. Biochimica et Biophysica Acta (BBA) - General Subjects *1790*, 485–494.

Kajiura, H., Koiwa, H., Nakazawa, Y., Okazawa, A., Kobayashi, A., Seki, T., and Fujiyama, K. (2009). Two Arabidopsis thaliana Golgi α-mannosidase I enzymes are responsible for plant N-glycan maturation. Glycobiology *20*, 235–247.

Kajiura, H., Seki, T., and Fujiyama, K. (2010). Arabidopsis thaliana ALG3 mutant synthesizes immature oligosaccharides in the ER and accumulates unique N-glycans. Glycobiology *20*, 736–751.

Kanehara, K., Cho, Y., Lin, Y.-C., Chen, C.-E., Yu, C.-Y., and Nakamura, Y. (2015). Arabidopsis *DOK1* encodes a functional dolichol kinase involved in reproduction. Plant J *81*, 292–303.

Kang, J.S., Frank, J., Kang, C.H., Kajiura, H., Vikram, M., Ueda, A., Kim, S., Bahk, J.D., Triplett, B., Fujiyama, K., et al. (2008). Salt tolerance of Arabidopsis thaliana requires maturation of N-glycosylated proteins in the Golgi apparatus. Proceedings of the National Academy of Sciences *105*, 5933–5938.

Kasahara, R.D., Portereiko, M.F., Sandaklie-Nikolova, L., Rabiger, D.S., and Drews, G.N. (2005). MYB98 Is Required for Pollen Tube Guidance and Synergid Cell Differentiation in Arabidopsis. Plant Cell *17*, 2981.

Kasahara, R.D., Maruyama, D., Hamamura, Y., Sakakibara, T., Twell, D., and Higashiyama, T. (2012). Fertilization Recovery after Defective Sperm Cell Release in Arabidopsis. Current Biology *22*, 1084–1089.

Kaul, V., Rouse, J.L., and Williams, E.G. (1986). Early events in the embryo sac after intraspecific and interspecific pollinations in Rhododendron kawakamii and R. retusum. Can. J. Bot. *64*, 282–291.

Kessler, S.A., and Grossniklaus, U. (2011). She's the boss: signaling in pollen tube reception. Current Opinion in Plant Biology *14*, 622–627.

Kessler, S.A., Shimosato-Asano, H., Keinath, N.F., Wuest, S.E., Ingram, G., Panstruga, R., and Grossniklaus, U. (2010). Conserved Molecular Components for Pollen Tube Reception and Fungal Invasion. Science *330*, 968–971.

Kim, S., Mollet, J.-C., Dong, J., Zhang, K., Park, S.-Y., and Lord, E.M. (2003). Chemocyanin, a small basic protein from the lily stigma, induces pollen tube chemotropism. Proceedings of the National Academy of Sciences *100*, 16125–16130.

Knauer, R., and Lehle, L. (1999). The oligosaccharyltransferase complex from yeast. Biochimica et Biophysica Acta (BBA) - General Subjects *1426*, 259–273.

Koiwa, H. (2003). The STT3a Subunit Isoform of the Arabidopsis Oligosaccharyltransferase Controls Adaptive Responses to Salt/Osmotic Stress. THE PLANT CELL ONLINE *15*, 2273–2284.

Koprivova, A., Altmann, F., Gorr, G., Kopriva, S., Reski, R., and Decker, E.L. (2003). N-Glycosylation in the Moss Physcomitrella patens is Organized Similarly to that in Higher Plants. Plant Biology *5*, 582–591.

Körner, C., Lübbehusen, J., and Thiel, C. (2008). Congenital Disorders of Glycosylation. In Laboratory Guide to the Methods in Biochemical Genetics, N. Blau, M. Duran, and K.M. Gibson, eds. (Berlin, Heidelberg: Springer Berlin Heidelberg), pp. 379–416.

Lamport, D.T.A., Kieliszewski, M.J., Chen, Y., and Cannon, M.C. (2011). Role of the Extensin Superfamily in Primary Cell Wall Architecture. Plant Physiol. *156*, 11.

Landoni, M., De Francesco, A., Galbiati, M., and Tonelli, C. (2010). A loss-of-function mutation in Calmodulin2 gene affects pollen germination in Arabidopsis thaliana. Plant Mol Biol *74*, 235–247.

Lane, D.R., Wiedemeier, A., Peng, L., Hocart, C.H., Birch, R.J., Baskin, T.I., Burn, J.E., Arioli, T., Betzner, A.S., and Williamson, R.E. (2001). Temperature-Sensitive Alleles of RSW2 Link the KORRIGAN Endo-1,4-□-Glucanase to Cellulose Synthesis and Cytokinesis in Arabidopsis. 11.

Lannoo, N., and Van Damme, E.J.M. (2015). Review/N-glycans: The making of a varied toolbox. Plant Science *239*, 67–83.

Larkin, A., and Imperiali, B. (2011). The Expanding Horizons of Asparagine-Linked Glycosylation. Biochemistry *50*, 4411–4426.

Lausser, A., Kliwer, I., Srilunchang, K., and Dresselhaus, T. (2009). Sporophytic control of pollen tube growth and guidance in maize. Journal of Experimental Botany *61*, 673–682.

Lehle, L., Strahl, S., and Tanner, W. (2006). Protein Glycosylation, Conserved from Yeast to Man: A Model Organism Helps Elucidate Congenital Human Diseases. Angewandte Chemie International Edition *45*, 6802–6818.

Lei, L., Zhang, T., Strasser, R., Lee, C.M., Gonneau, M., Mach, L., Vernhettes, S., Kim, S.H., J. Cosgrove, D., Li, S., et al. (2014). The *jiaoyao1* Mutant Is an Allele of *korrigan1* That Abolishes Endoglucanase Activity and Affects the Organization of Both Cellulose Microfibrils and Microtubules in *Arabidopsis.* Plant Cell *26*, 2601–2616.

Lennon, K.A., Roy, S., Hepler, P.K., and Lord, E.M. (1998). The structure of the transmitting tissue of Arabidopsis thaliana (L.) and the path of pollen tube growth. Sexual Plant Reproduction *11*, 49–59.

Leroux, C., Bouton, S., Kiefer-Meyer, M.-C., Fabrice, T.N., Mareck, A., Guénin, S., Fournet, F., Ringli, C., Pelloux, J., Driouich, A., et al. (2015). PECTIN METHYLESTERASE48 Is Involved in Arabidopsis Pollen Grain Germination. Plant Physiol. *167*, 367–380.

Lerouxel, O., Mouille, G., Andème-Onzighi, C., Bruyant, M.-P., Séveno, M., Loutelier-Bourhis, C., Driouich, A., Höfte, H., and Lerouge, P. (2005). Mutants in DEFECTIVE GLYCOSYLATION, an Arabidopsis homolog of an oligosaccharyltransferase complex subunit, show protein underglycosylation and defects in cell differentiation and growth: DGL1 is required for protein N-glycosylation. The Plant Journal *42*, 455–468.

Leshem, Y., Johnson, C., Wuest, S.E., Song, X., Ngo, Q.A., Grossniklaus, U., and Sundaresan, V. (2012). Molecular Characterization of the glauce Mutant: A Central Cell–Specific Function Is Required for Double Fertilization in Arabidopsis. Plant Cell *24*, 3264.

Leshem, Y., Johnson, C., and Sundaresan, V. (2013). Pollen tube entry into the synergid cell of Arabidopsis is observed at a site distinct from the filiform apparatus. Plant Reprod *26*, 93–99.

Leydon, A.R., Beale, K.M., Woroniecka, K., Castner, E., Chen, J., Horgan, C., Palanivelu, R., and Johnson, M.A. (2013). Three MYB Transcription Factors Control Pollen Tube Differentiation Required for Sperm Release. Current Biology *23*, 1209–1214.

Leydon, A.R., Tsukamoto, T., Dunatunga, D., Qin, Y., Johnson, M.A., and Palanivelu, R. (2015). Pollen Tube Discharge Completes the Process of Synergid Degeneration That Is Initiated by Pollen Tube-Synergid Interaction in Arabidopsis. Plant Physiol. *169*, 485–496.

Li, H., and Yang, W.-C. (2016). RLKs orchestrate the signaling in plant male-female interaction. Sci. China Life Sci. *59*, 867–877.

Li, C., Yeh, F.-L., Cheung, A.Y., Duan, Q., Kita, D., Liu, M.-C., Maman, J., Luu, E.J., Wu, B.W., Gates, L., et al. (2015a). Glycosylphosphatidylinositol-anchored proteins as chaperones and co-receptors for FERONIA receptor kinase signaling in Arabidopsis. ELife *4*, e06587.

Li, H.-J., Xue, Y., Jia, D.-J., Wang, T., hi, D.-Q., Liu, J., Cui, F., Xie, Q., Ye, D., and Yang, W.-C. (2011). POD1 Regulates Pollen Tube Guidance in Response to Micropylar Female Signaling and Acts in Early Embryo Patterning in Arabidopsis. Plant Cell *23*, 3288.

Li, H.-J., Zhu, S.-S., Zhang, M.-X., Wang, T., Liang, L., Xue, Y., Shi, D.-Q., Liu, J., and Yang, W.-C. (2015b). Arabidopsis CBP1 Is a Novel Regulator of Transcription Initiation in Central Cell-Mediated Pollen Tube Guidance. Plant Cell *27*, 2880.

Li, S., Ge, F.-R., Xu, M., Zhao, X.-Y., Huang, G.-Q., Zhou, L.-Z., Wang, J.-G., Kombrink, A., McCormick, S., Zhang, X.S., et al. (2013). Arabidopsis COBRA-LIKE 10, a GPI-anchored protein, mediates directional growth of pollen tubes. Plant J *74*, 486–497.

Li, Y., Guo, J., Yang, Z., and Yang, D.-L. (2018). Plasma Membrane-Localized Calcium Pumps and Copines Coordinately Regulate Pollen Germination and Fertility in Arabidopsis. IJMS *19*, 1774.

Liang, Y., Tan, Z.-M., Zhu, L., Niu, Q.-K., Zhou, J.-J., Li, M., Chen, L.-Q., Zhang, X.-Q., and Ye, D. (2013). MYB97, MYB101 and MYB120 Function as Male Factors That Control Pollen Tube-Synergid Interaction in Arabidopsis thaliana Fertilization. PLoS Genet *9*, e1003933.

Liebminger, E., Veit, C., Pabst, M., Batoux, M., Zipfel, C., Altmann, F., Mach, L., and Strasser, R. (2011). β- *N* -Acetylhexosaminidases HEXO1 and HEXO3 Are Responsible for the Formation of Paucimannosidic *N* -Glycans in *Arabidopsis thaliana*. J. Biol. Chem. *286*, 10793–10802.

Liebminger, E., Grass, J., Altmann, F., Mach, L., and Strasser, R. (2013). Characterizing the Link between Glycosylation State and Enzymatic Activity of the Endo-β1,4-glucanase KORRIGAN1 from *Arabidopsis thaliana*. J. Biol. Chem. *288*, 22270–22280.

Lindner, H., Müller, L.M., Boisson-Dernier, A., and Grossniklaus, U. (2012). CrRLK1L receptor-like kinases: not just another brick in the wall. Current Opinion in Plant Biology *15*, 659–669.

Lindner, H., Kessler, S.A., Müller, L.M., Shimosato-Asano, H., Boisson-Dernier, A., and Grossniklaus, U. (2015). TURAN and EVAN Mediate Pollen Tube Reception in Arabidopsis Synergids through Protein Glycosylation. PLoS Biol *13*, e1002139.

Liu, Y., and Li, J. (2014). Endoplasmic reticulum-mediated protein quality control in Arabidopsis. Front. Plant Sci. *5*.

Liu, J., Zhong, S., Guo, X., Hao, L., Wei, X., Huang, Q., Hou, Y., Shi, J., Wang, C., Gu, H., et al. (2013). Membrane-Bound RLCKs LIP1 and LIP2 Are Essential Male Factors Controlling Male-Female Attraction in Arabidopsis. Current Biology *23*, 993–998.

Liu, X., Castro, C., Wang, Y., Noble, J., Ponvert, N., Bundy, M., Hoel, C., Shpak, E., and Palanivelu, R. (2016). The Role of LORELEI in Pollen Tube Reception at the Interface of the Synergid Cell and Pollen Tube Requires the Modified Eight-Cysteine Motif and the Receptor-Like Kinase FERONIA. Plant Cell *28*, 1035–1052.

Lou, Y., Zhu, J., and Yang, Z. (2014). Molecular Cell Biology of Pollen Walls. In Applied Plant Cell Biology: Cellular Tools and Approaches for Plant Biotechnology, P. Nick, and Z. Opatrny, eds. (Berlin, Heidelberg: Springer Berlin Heidelberg), pp. 179–205.

Lu, Y., Chanroj, S., Zulkifli, L., Johnson, M.A., Uozumi, N., Cheung, A., and Sze, H. (2011). Pollen Tubes Lacking a Pair of K^+ Transporters Fail to Target Ovules in Arabidopsis. Plant Cell *23*, 81.

Márton, M.L., Fastner, A., Uebler, S., and Dresselhaus, T. (2012). Overcoming Hybridization Barriers by the Secretion of the Maize Pollen Tube Attractant ZmEA1 from Arabidopsis Ovules. Current Biology *22*, 1194–1198.

Maruyama, D., Hamamura, Y., Takeuchi, H., Susaki, D., Nishimaki, M., Kurihara, D., Kasahara, R.D., and Higashiyama, T. (2013). Independent Control by Each Female Gamete Prevents the Attraction of Multiple Pollen Tubes. Developmental Cell *25*, 317–323.

Maruyama, D., Völz, R., Takeuchi, H., Mori, T., Igawa, T., Kurihara, D., Kawashima, T., Ueda, M., Ito, M., Umeda, M., et al. (2015). Rapid Elimination of the Persistent Synergid through a Cell Fusion Mechanism. Cell *161*, 907–918.

Matias-Hernandez, L., Battaglia, R., Galbiati, F., Rubes, M., Eichenberger, C., Grossniklaus, U., Kater, M.M., and Colombo, L. (2010). VERDANDI Is a Direct Target of the MADS Domain Ovule Identity Complex and Affects Embryo Sac Differentiation in Arabidopsis. Plant Cell *22*, 1702.

Mayfield, J.A., and Preuss, D. (2000). Rapid initiation of Arabidopsis pollination requires the oleosin-domain protein GRP17. Nat Cell Biol *2*, 128–130.

Mecchia, M.A., Santos-Fernandez, G., Duss, N.N., Somoza, S.C., Boisson-Dernier, A., Gagliardini, V., Martínez-Bernardini, A., Fabrice, T.N., Ringli, C., Muschietti, J.P., et al. (2017). RALF4/19 peptides interact with LRX proteins to control pollen tube growth in *Arabidopsis*. Science *358*, 1600–1603.

Mendes, M.A., Guerra, R.F., Castelnovo, B., Silva-Velazquez, Y., Morandini, P., Manrique, S., Baumann, N., Groß-Hardt, R., Dickinson, H., and Colombo, L. (2016). Live and let die: a REM complex promotes fertilization through synergid cell death in *Arabidopsis*. Development *143*, 2780–2790.

Michard, E., Lima, P.T., Borges, F., Silva, A.C., Portes, M.T., Carvalho, J.E., Gilliham, M., Liu, L.-H., Obermeyer, G., and Feijó, J.A. (2011). Glutamate Receptor–Like Genes Form Ca^{2+} Channels in Pollen Tubes and Are Regulated by Pistil d-Serine. Science *332*, 434.

Millar, A.H., Heazlewood, J.L., Giglione, C., Holdsworth, M.J., Bachmair, A., and Schulze, W.X. (2019). The Scope, Functions, and Dynamics of Posttranslational Protein Modifications. Annu. Rev. Plant Biol. *70*, 119–151.

Mizukami, A.G., Inatsugi, R., Jiao, J., Kotake, T., Kuwata, K., Ootani, K., Okuda, S., Sankaranarayanan, S., Sato, Y., Maruyama, D., et al. (2016). The AMOR Arabinogalactan Sugar Chain Induces Pollen-Tube Competency to Respond to Ovular Guidance. Current Biology *26*, 1091–1097.

Mondragón-Palomino, M., John-Arputharaj, A., Pallmann, M., and Dresselhaus, T. (2017). Similarities between Reproductive and Immune Pistil Transcriptomes of *Arabidopsis* Species. Plant Physiol. *174*, 1559–1575.

Mori, T., Igawa, T., Tamiya, G., Miyagishima, S., and Berger, F. (2014). Gamete Attachment Requires GEX2 for Successful Fertilization in Arabidopsis. Current Biology *24*, 170–175.

Nagashima, Y., von Schaewen, A., and Koiwa, H. (2018). Function of N-glycosylation in plants. Plant Science *274*, 70–79.

Nakel, T., Tekleyohans, D.G., Mao, Y., Fuchert, G., Vo, D., and Groß-Hardt, R. (2017). Triparental plants provide direct evidence for polyspermy induced polyploidy. Nature Communications *8*, 1033.

Nasrallah, M.E. (2002). Generation of Self-Incompatible Arabidopsis thaliana by Transfer of Two S Locus Genes from A. lyrata. Science *297*, 247–249.

Ngo, Q.A., Vogler, H., Lituiev, D.S., Nestorova, A., and Grossniklaus, U. (2014). A Calcium Dialog Mediated by the FERONIA Signal Transduction Pathway Controls Plant Sperm Delivery. Developmental Cell *29*, 491–500.

Nguema-Ona, E., Vicré-Gibouin, M., Cannesan, M.-A., and Driouich, A. (2013). Arabinogalactan proteins in root–microbe interactions. Trends in Plant Science *18*, 440–449.

Okuda, S., Tsutsui, H., Shiina, K., Sprunck, S., Takeuchi, H., Yui, R., Kasahara, R.D., Hamamura, Y., Mizukami, A., Susaki, D., et al. (2009). Defensin-like polypeptide LUREs are pollen tube attractants secreted from synergid cells. Nature *458*, 357–361.

de Oliveira, M.V.V., Xu, G., Li, B., de Souza Vespoli, L., Meng, X., Chen, X., Yu, X., de Souza, S.A., Intorne, A.C., de A. Manhães, A.M.E., et al. (2016). Specific control of Arabidopsis BAK1/SERK4-regulated cell death by protein glycosylation. Nature Plants *2*, 15218.

O'Reilly, M.K., Zhang, G., and Imperiali, B. (2006). In Vitro Evidence for the Dual Function of Alg2 and Alg11: Essential Mannosyltransferases in N-Linked Glycoprotein Biosynthesis †. Biochemistry *45*, 9593–9603.

Ozgur, K., Patankar, M.S., Oehninger, S., and Clark, G.F. (1998). Direct evidence for the involvement of carbohydrate sequences in human sperm-zona pellucida binding. Molecular Human Reproduction *4*, 318–324.

Palanivelu, R., and Preuss, D. (2006). Distinct short-range ovule signals attract or repel Arabidopsis thaliana pollen tubes in vitro. BMC Plant Biology *6*, 7.

Palanivelu, R., and Tsukamoto, T. (2012). Pathfinding in angiosperm reproduction: pollen tube guidance by pistils ensures successful double fertilization: Pathfinding in angiosperm reproduction. WIREs Dev Biol *1*, 96–113.

Palanivelu, R., Brass, L., Edlund, A.F., and Preuss, D. (2003). Pollen Tube Growth and Guidance Is Regulated by POP2, an Arabidopsis Gene that Controls GABA Levels. Cell *114*, 47–59.

Palin, R., and Geitmann, A. (2012). The role of pectin in plant morphogenesis. Biosystems *109*, 397–402.

Park, S.-Y., and Lord, E.M. (2003). Expression studies of SCA in lily and confirmation of its role in pollen tube adhesion. Plant Molecular Biology *51*, 183–189.

Pereira, A.M., Pereira, L.G., and Coimbra, S. (2015). Arabinogalactan proteins: rising attention from plant biologists. Plant Reprod *28*, 1–15.

Pereira, A.M., Lopes, A.L., and Coimbra, S. (2016). *JAGGER* , an AGP essential for persistent synergid degeneration and polytubey block in Arabidopsis. Plant Signaling & Behavior *11*, e1209616.

Prado, A.M., Colaço, R., Moreno, N., Silva, A.C., and Feijó, J.A. (2008). Targeting of Pollen Tubes to Ovules Is Dependent on Nitric Oxide (NO) Signaling. Molecular Plant *1*, 703–714.

Preuss, D., Lemieux, B., Yen, G., and Davis, R.W. (1993). A conditional sterile mutation eliminates surface components from Arabidopsis pollen and disrupts cell signaling during fertilization. Genes & Development *7*, 974–985.

Punwani, J.A., Rabiger, D.S., and Drews, G.N. (2007). MYB98 Positively Regulates a Battery of Synergid-Expressed Genes Encoding Filiform Apparatus–Localized Proteins. Plant Cell *19*, 2557–2568.

Qin, Y., Leydon, A.R., Manziello, A., Pandey, R., Mount, D., Denic, S., Vasic, B., Johnson, M.A., and Palanivelu, R. (2009). Penetration of the Stigma and Style Elicits a Novel Transcriptome in Pollen Tubes, Pointing to Genes Critical for Growth in a Pistil. PLoS Genet *5*, e1000621.

Reily, C., Stewart, T.J., Renfrow, M.B., and Novak, J. (2019). Glycosylation in health and disease. Nat Rev Nephrol *15*, 346–366.

Renault, H., El Amrani, A., Palanivelu, R., Updegraff, E.P., Yu, A., Renou, J.-P., Preuss, D., Bouchereau, A., and Deleu, C. (2011). GABA Accumulation Causes Cell Elongation Defects and a Decrease in Expression of Genes Encoding Secreted and Cell Wall-Related Proteins in Arabidopsis thaliana. Plant and Cell Physiology *52*, 894–908.

Ricard-Blum, S. (2011). The collagen family. Cold Spring Harb Perspect Biol *3*, a004978–a004978.

Rips, S., Bentley, N., Jeong, I.S., Welch, J.L., von Schaewen, A., and Koiwa, H. (2014). Multiple N-Glycans Cooperate in the Subcellular Targeting and Functioning of Arabidopsis KORRIGAN1. The Plant Cell *26*, 3792–3808.

Ruiz-Canada, C., Kelleher, D.J., and Gilmore, R. (2009). Cotranslational and Posttranslational N-Glycosylation of Polypeptides by Distinct Mammalian OST Isoforms. Cell *136*, 272–283.

Ryšlavá, H., Doubnerová, V., Kavan, D., and Vaněk, O. (2013). Effect of posttranslational modifications on enzyme function and assembly. Journal of Proteomics *92*, 80–109.

Samuel, M.A., Chong, Y.T., Haasen, K.E., Aldea-Brydges, M.G., Stone, S.L., and Goring, D.R. (2009). Cellular Pathways Regulating Responses to Compatible and Self-Incompatible Pollen in *Brassica* and *Arabidopsis* Stigmas Intersect at Exo70A1, a Putative Component of the Exocyst Complex. Plant Cell *21*, 2655–2671.

Sandaklie-Nikolova, L., Palanivelu, R., King, E.J., Copenhaver, G.P., and Drews, G.N. (2007). Synergid Cell Death in Arabidopsis Is Triggered following Direct Interaction with the Pollen Tube. Plant Physiol. *144*, 1753.

Sarkar, M., Leventis, P.A., Silvescu, C.I., Reinhold, V.N., Schachter, H., and Boulianne, G.L. (2006). Null Mutations in *Drosophila N* -Acetylglucosaminyltransferase I Produce Defects in Locomotion and a Reduced Life Span. J. Biol. Chem. *281*, 12776–12785.

Schachter, H. (2010). Mgat1-dependent N-glycans are essential for the normal development of both vertebrate and invertebrate metazoans. Seminars in Cell & Developmental Biology *21*, 609–615.

von Schaewen, A., Sturm, A., O'Neill, J., and Chrispeels, M.J. (1993). Isolation of a Mutant Arabidopsis Plant That Lacks N-Acetyl Glucosaminyl Transferase I and Is Unable to Synthesize Golgi-Modified Complex N-Linked Glycans. Plant Physiol. *102*, 1109.

Scheys, F., Van Damme, E.J.M., Pauwels, J., Staes, A., Gevaert, K., and Smagghe, G. (2020). N-glycosylation Site Analysis Reveals Sex-related Differences in Protein N-glycosylation in the Rice Brown Planthopper (*Nilaparvata lugens*). Mol Cell Proteomics *19*, 529–539.

Schiøtt, M., Romanowsky, S.M., Bækgaard, L., Jakobsen, M.K., Palmgren, M.G., and Harper, J.F. (2004). A plant plasma membrane Ca^{2+} pump is required for normal pollen tube growth and fertilization. Proc Natl Acad Sci U S A *101*, 9502.

Schwarz, F., and Aebi, M. (2011). Mechanisms and principles of N-linked protein glycosylation. Current Opinion in Structural Biology *21*, 576–582.

Shimizu, K.K., and Okada, K. (2000). Attractive and repulsive interactions between female and male gametophytes in Arabidopsis pollen tube guidance. Development *127*, 4511.

Shridas, P., and Waechter, C.J. (2006). Human Dolichol Kinase, a Polytopic Endoplasmic Reticulum Membrane Protein with a Cytoplasmically Oriented CTP-binding Site. J. Biol. Chem. *281*, 31696–31704.

Skinner, D.J., and Sundaresan, V. (2018). Recent advances in understanding female gametophyte development. F1000Res *7*, 804.

Smith, D.K., Jones, D.M., Lau, J.B.R., Cruz, E.R., Brown, E., Harper, J.F., and Wallace, I.S. (2018). A Putative Protein *O* -Fucosyltransferase Facilitates Pollen Tube Penetration through the Stigma – Style Interface. Plant Physiol. *176*, 2804–2818.

Spielman, M., and Scott, R.J. (2008). Polyspermy barriers in plants: from preventing to promoting fertilization. Sexual Plant Reproduction *21*, 53–65.

Sprunck, S. (2020). Twice the fun, double the trouble: gamete interactions in flowering plants. Current Opinion in Plant Biology *53*, 106–116.

Sprunck, S., Rademacher, S., Vogler, F., Gheyselinck, J., Grossniklaus, U., and Dresselhaus, T. (2012). Egg Cell–Secreted EC1 Triggers Sperm Cell Activation During Double Fertilization. Science *338*, 1093.

Steinhorst, L., and Kudla, J. (2013). Calcium - a central regulator of pollen germination and tube growth. Biochimica et Biophysica Acta (BBA) - Molecular Cell Research *1833*, 1573–1581.

Stolz, J., and Munro, S. (2002). The Components of the *Saccharomyces cerevisiae* Mannosyltransferase Complex M-Pol I Have Distinct Functions in Mannan Synthesis. J. Biol. Chem. *277*, 44801–44808.

Stonebloom, S., Ebert, B., Xiong, G., Pattathil, S., Birdseye, D., Lao, J., Pauly, M., Hahn, M.G., Heazlewood, J.L., and Scheller, H.V. (2016). A DUF-246 family glycosyltransferase-like gene affects male fertility and the biosynthesis of pectic arabinogalactans. BMC Plant Biol *16*, 90.

Strasser, R. (2014). Biological significance of complex N-glycans in plants and their impact on plant physiology. Front. Plant Sci. *5*.

Strasser, R. (2016). Plant protein glycosylation. Glycobiology *26*, 926–939.

Strasser, R. (2018). Protein Quality Control in the Endoplasmic Reticulum of Plants. Annu. Rev. Plant Biol. *69*, 147–172.

Strasser, R., Steinkellner, H., Borén, M., Altmann, F., Mach, L., Glössl, J., and Mucha, J. (1999). Molecular cloning of cDNA encoding N-acetylglucosaminyltransferase II from Arabidopsis thaliana. Glycoconjugate Journal *16*, 787–791.

Strasser, R., Mucha, J., Mach, L., Altmann, F., Wilson, I.B.H., Glössl, J., and Steinkellner, H. (2000). Molecular cloning and functional expression of β1,2-xylosyltransferase cDNA from Arabidopsis thaliana 1. FEBS Letters *472*, 105–108.

Strasser, R., Altmann, F., Mach, L., Glössl, J., and Steinkellner, H. (2004). Generation of *Arabidopsis thaliana* plants with complex *N* -glycans lacking β1,2-linked xylose and core α1,3-linked fucose. FEBS Letters *561*, 132–136.

Strasser, R., Stadlmann, J., Svoboda, B., Altmann, F., Glössl, J., and Mach, L. (2005). Molecular basis of N-acetylglucosaminyltransferase I deficiency in Arabidopsis thaliana plants lacking complex N-glycans. Biochemical Journal *387*, 385–391.

Strasser, R., Schoberer, J., Jin, C., Glössl, J., Mach, L., and Steinkellner, H. (2006). Molecular cloning and characterization of Arabidopsis thaliana Golgi α-mannosidase II, a key enzyme in the formation of complex N-glycans in plants. The Plant Journal *45*, 789–803.

Strasser, R., Bondili, J.S., Vavra, U., Schoberer, J., Svoboda, B., Glössl, J., Léonard, R., Stadlmann, J., Altmann, F., Steinkellner, H., et al. (2007). A Unique β1,3-Galactosyltransferase Is Indispensable for the Biosynthesis of N-Glycans Containing Lewis a Structures in Arabidopsis thaliana. Plant Cell *19*, 2278.

Swanson, R., Edlund, A.F., and Preuss, D. (2004). Species Specificity in Pollen-Pistil Interactions. Annu. Rev. Genet. *38*, 793–818.

Takahashi, T., Honda, K., Mori, T., and Igawa, T. (2017). Loss of GCS1/HAP2 does not affect the ovule-targeting behavior of pollen tubes. Plant Reproduction *30*, 147–152.

Takahashi, T., Mori, T., Ueda, K., Yamada, L., Nagahara, S., Higashiyama, T., Sawada, H., and Igawa, T. (2018). The male gamete membrane protein DMP9/DAU2 is required for double fertilization in flowering plants. Development *145*, dev170076.

Takayama, S., Shimosato, H., Shiba, H., Funato, M., Che, F.-S., Watanabe, M., Iwano, M., and Isogai, A. (2001). Direct ligand–receptor complex interaction controls Brassica self-incompatibility. Nature *413*, 534–538.

Takeuchi, H., and Higashiyama, T. (2011). Attraction of tip-growing pollen tubes by the female gametophyte. Current Opinion in Plant Biology *14*, 614–621.

Takeuchi, H., and Higashiyama, T. (2012). A Species-Specific Cluster of Defensin-Like Genes Encodes Diffusible Pollen Tube Attractants in Arabidopsis. PLoS Biol *10*, e1001449.

Takeuchi, H., and Higashiyama, T. (2016). Tip-localized receptors control pollen tube growth and LURE sensing in Arabidopsis. Nature *531*, 245–248.

Tang, W., Ezcurra, I., Muschietti, J., and McCormick, S. (2002). A Cysteine-Rich Extracellular Protein, LAT52, Interacts with the Extracellular Domain of the Pollen Receptor Kinase LePRK2. Plant Cell *14*, 2277–2287.

Tecle, E., and Gagneux, P. (2015). Sugar-coated sperm: Unraveling the functions of the mammalian sperm glycocalyx: F UNCTIONS OF THE M AMMALIAN S PERM G LYCOCALYX. Mol. Reprod. Dev. *82*, 635–650.

Tintor, N., and Saijo, Y. (2014). ER-mediated control for abundance, quality, and signaling of transmembrane immune receptors in plants. Front. Plant Sci. *5*.

Toda, E., and Okamoto, T. (2020). Polyspermy in angiosperms: Its contribution to polyploid formation and speciation. Molecular Reproduction and Development *87*, 374–379.

Tokuhiro, K., and Dean, J. (2018). Glycan-Independent Gamete Recognition Triggers Egg Zinc Sparks and ZP2 Cleavage to Prevent Polyspermy. Developmental Cell *46*, 627-640.e5.

Trempel, F., Kajiura, H., Ranf, S., Grimmer, J., Westphal, L., Zipfel, C., Scheel, D., Fujiyama, K., and Lee, J. (2016). Altered glycosylation of exported proteins, including surface immune receptors, compromises calcium and downstream signaling responses to microbe-associated molecular patterns in Arabidopsis thaliana. BMC Plant Biol *16*, 31.

Tsukamoto, T., Qin, Y., Huang, Y., Dunatunga, D., and Palanivelu, R. (2010). A role for LORELEI, a putative glycosylphosphatidylinositol-anchored protein, in Arabidopsis thaliana double fertilization and early seed development: LORELEI functions in fertilization and seed development. The Plant Journal *62*, 571–588.

Vembar, S.S., and Brodsky, J.L. (2008). One step at a time: endoplasmic reticulum-associated degradation. Nat Rev Mol Cell Biol *9*, 944–957.

Vogler, H., Martinez-Bernardini, A., and Grossniklaus, U. (2016). Maybe she's NOT the boss: male–female crosstalk during sexual plant reproduction. Genome Biol *17*, 96.

Völz, R., Heydlauff, J., Ripper, D., von Lyncker, L., and Groß-Hardt, R. (2013). Ethylene Signaling Is Required for Synergid Degeneration and the Establishment of a Pollen Tube Block. Developmental Cell *25*, 310–316.

Wang, J.-G., Feng, C., Liu, H.-H., Feng, Q.-N., Li, S., and Zhang, Y. (2017a). AP1G mediates vacuolar acidification during synergid-controlled pollen tube reception. Proc Natl Acad Sci U S A *114*, E4877–E4883.

Wang, L., Yang, T., Lin, Q., Wang, B., Li, X., Luan, S., and Yu, F. (2020). Receptor kinase FERONIA regulates flowering time in Arabidopsis. BMC Plant Biol *20*, 26.

Wang, P., Wang, H., Gai, J., Tian, X., Zhang, X., Lv, Y., and Jian, Y. (2017b). Evolution of protein N-glycosylation process in Golgi apparatus which shapes diversity of protein N-glycan structures in plants, animals and fungi. Sci Rep *7*, 40301.

Wang, T., Liang, L., Xue, Y., Jia, P.-F., Chen, W., Zhang, M.-X., Wang, Y.-C., Li, H.-J., and Yang, W.-C. (2016). A receptor heteromer mediates the male perception of female attractants in plants. Nature *531*, 241–244.

Williams, J.H. (2008). Novelties of the flowering plant pollen tube underlie diversification of a key life history stage. Proceedings of the National Academy of Sciences *105*, 11259–11263.

Williams, E., Kaul, V., Rouse, J., and Palser, B. (1986). Overgrowth of Pollen Tubes in Embryo Sacs of Rhododendron Following Interspecific Pollinations. Aust. J. Bot. *34*, 413–423.

Wong, J.L., and Johnson, M.A. (2010). Is HAP2-GCS1 an ancestral gamete fusogen? Trends in Cell Biology *20*, 134–141.

Wong, A., Donaldson, L., Portes, M.T., Eppinger, J., Feijó, J.A., and Gehring, C. (2020). Arabidopsis DIACYLGLYCEROL KINASE4 is involved in nitric oxide-dependent pollen tube guidance and fertilization. Development *147*, dev183715.

Woriedh, M., Wolf, S., Márton, M.L., Hinze, A., Gahrtz, M., Becker, D., and Dresselhaus, T. (2013). External application of gametophyte-specific ZmPMEI1 induces pollen tube burst in maize. Plant Reprod *26*, 255–266.

Wu, H., Wong, E., Ogdahl, J., and Cheung, A.Y. (2000). A pollen tube growth-promoting arabinogalactan protein from Nicotiana alata is similar to the tobacco TTS protein. Plant J *22*, 165–176.

Wu, M.-F., Tian, Q., and Reed, J.W. (2006). Arabidopsis microRNA167 controls patterns of ARF6 and ARF8 expression, and regulates both female and male reproduction. Development *133*, 4211–4218.

Yang, Z.-N. (2016). Regulation of sporopollenin synthesis for pollen wall formation in plant. Sci. China Life Sci. *59*, 1335–1337.

Yang, W.-C., Shi, D.-Q., and Chen, Y.-H. (2010). Female Gametophyte Development in Flowering Plants. Annu. Rev. Plant Biol. *61*, 89–108.

Yu, F., Shi, J., Zhou, J., Gu, J., Chen, Q., Li, J., Cheng, W., Mao, D., Tian, L., Buchanan, B.B., et al. (2010). ANK6, a mitochondrial ankyrin repeat protein, is required for male-female gamete recognition in Arabidopsis thaliana. Proceedings of the National Academy of Sciences *107*, 22332–22337.

Yu, G.-H., Zou, J., Feng, J., Peng, X.-B., Wu, J.-Y., Wu, Y.-L., Palanivelu, R., and Sun, M.-X. (2014). Exogenous γ-aminobutyric acid (GABA) affects pollen tube growth via modulating putative Ca2+-permeable membrane channels and is coupled to negative regulation on glutamate decarboxylase. Journal of Experimental Botany *65*, 3235–3248.

Zhao, Y., Sato, Y., Isaji, T., Fukuda, T., Matsumoto, A., Miyoshi, E., Gu, J., and Taniguchi, N. (2008). Branched N-glycans regulate the biological functions of integrins and cadherins. The FEBS Journal *275*, 1939–1948.

Zheng, Y.-Y., Lin, X.-J., Liang, H.-M., Wang, F.-F., and Chen, L.-Y. (2018). The Long Journey of Pollen Tube in the Pistil. IJMS *19*, 3529.

Zhong, S., Liu, M., Wang, Z., Huang, Q., Hou, S., Xu, Y.-C., Ge, Z., Song, Z., Huang, J., Qiu, X., et al. (2019). Cysteine-rich peptides promote interspecific genetic isolation in *Arabidopsis*. Science *364*, eaau9564.

Zhu, L., Chu, L.-C., Liang, Y., Zhang, X.-Q., Chen, L.-Q., and Ye, D. (2018). The Arabidopsis CrRLK1L protein kinases BUPS1 and BUPS2 are required for normal growth of pollen tubes in the pistil. Plant J *95*, 474–486.

Zinkl, G.M., Zwiebel, B.I., Grier, D.G., and Preuss, D. (1999). Pollen-stigma adhesion in Arabidopsis: a species-specific interaction mediated by lipophilic molecules in the pollen exine. Development *126*, 5431.

CHAPTER 2 - RESULTS

Identification of novel components of FERONIA signaling pathway using SNP-ratio mapping approach

Identification of novel components of FERONIA signaling pathway using SNP-ratio mapping approach

Andrea Zupunski, Stefan Wyder, Hiroko Shimosato-Asano, and Ueli Grossniklaus

Institute of Plant and Microbial Biology & Zurich-Basel Plant Science Center, University of Zürich, Zollikerstrasse 107, 8008 Zürich, Switzerland

Abstract

Plant receptor-like kinases (RLKs) are crucial for the perception of extracellular cues, and subsequent activation of downstream signaling components to promptly synchronize and modulate cellular responses. FERONIA (FER) and 16 closely related homologs form a group of plant malectin-like receptor kinases named *Catharanthus roseus* receptor-like kinase 1-like (*Cr*RLK1Ls). This subfamily with its key member FER is involved in the regulation of plant reproduction, growth, development, immune responses as well as adaptation to abiotic stresses. Pollen tube reception and successful fertilization largely depend on the FER-mediated signaling responses. EMS-screen for the mutants with a *fer*-like PT overgrowth (PTO) phenotype was carried out to find novel molecular players of the FER pathway. We have used a SNP-ratio mapping (SRM) approach to map three EMS mutant candidates displaying varying degrees of PTO. One of the EMS mutant carried causative SNP mapped to the *ALG11* (*ASPARAGINE LINKED GLYCOSYLATION 11*), encoding an ER-resident enzyme of the *N*-glycosylation pathway. Causative SNP led to the generation of STOP codon in the third exon (T239*). A second EMS candidates was mapped to the *RID1* (*ROOT INITIATION DEFECTIVE 1*), encoding a RNA helicase protein involved in the development of the female gametophyte, and the causative SNP resulted in a nonsynonymous amino acid change V342I. Additionally, we found a novel allele of *TURAN (TUN)*, thus further establishing SRM approach as the method of choice when it comes to the mapping of lethal and/or mutations of low penetrance.

Keywords: SNP-ratio mapping, EMS mutagenesis, pollen tube reception; FERONIA.

Introduction

Critical role of receptor-like kinases in reproduction became evident with the discovery of *feronia* mutant in which almost 80% of the ovules remain unfertilized due to the inability of PTs to burst and release sperm cells. Instead, PTs continue to grow inside the embryo sack, phenotype described as PT overgrowth (Escobar-Restrepo et al., 2007; Huck, 2003). Since initial discovery of FER almost 17 years ago, only handful of the female gametophytic mutants leading to the *fer*-like pollen tube overgrowth (PTO) have been discovered, including *scylla* (underlying gene is still unknown), *lorelei, nortia, RNAi enodls, evan, turan and herk1/anjea* double mutants (Capron et al., 2008; Galindo-Trigo et al., 2019; Hou et al., 2016; Kessler et al., 2010; Lindner et al., 2015; Rotman et al., 2008). Additionally mutation in the peroxin gene causes PTO phenotype only if both female and male gametophyte carry the *amc* mutation (Boisson-Dernier et al., 2008). Lastly male gametophytic triple mutant *myb97/myb101/myb120* presents similar PTO phenotype in 70% of targeted ovules (Leydon et al., 2015; Liang et al., 2013).

Prior to PTs arrival, FER secretion from the endoplasmic reticulum (ER) is promoted by the binding to its chaperones glycosylphosphatidylinositol (GPI)-anchored proteins LORELEI (LRE) and EARLY NODULIN-LIKE 14 (EN14) (Hou et al., 2016; Li et al., 2015; Liu et al., 2016). Mutation of LRE led to 70% of unfertilized ovules in *lre*, while RNAi quintuple ENs mutant showed a *fer-like* phenotype in 52% of ovules (Capron et al., 2008; Hou et al., 2016). Beyond roles in enabling FER localization to the filiform apparatus, it is postulated that LRE and ENs acts as coreceptors to promote putative ligand binding (Adhikari et al., 2020; Franck et al., 2018). Requirement of the functional ER processing during reproduction was revealed through the discovery of mutants with PTO phenotype as well as male gametophytic defects affected in *TURAN* (*TUN*) and *EVAN* (*EVN*) encoding enzymes of the *N*-glycosylation pathway (Lindner et al., 2015).

Both FER and LER are crucial for the activation of signaling cascade leading to the production of reactive oxygen species (ROS) at the micropyle which is required to trigger PT burst (Duan et al., 2014). FER and LRE are needed for the accurate Ca^{2+} signaling in synergid cells upon PT arrival (Ngo et al., 2014). Additionally, FER is also necessary for the Ca^{2+} dependent translocation of NORTIA (NTA) to the filiform apparatus where it contributes to the regulation of PT reception (Kessler et al., 2010; Ngo et al., 2014). NTA modulates Ca^{2+} signal magnitude once it was successfully initiated by FER and LER. In *nta* mutants approximately 24% of ovules remain unfertilized due to the *fer-like* PTO (Kessler et al., 2010). Very recently it was reported that two homologs of FER belonging to the *Cr*RLK1L subfamily act redundantly to control PT reception, with 90% of unfertilized ovules in *herk1/anjea* double mutants (Galindo-Trigo et al., 2019).

Taken together role of FER and its coreceptors at filiform apparatus is to recognize compatible pollen (self-pollen), and trigger signaling cascade leading to PT rupture, while loss of function leads to classical *fer*-like PT overgrowth. Closest homologs of FER are pollen expressed ANXUR1 (ANX1) and ANXUR2 (ANX2) which act redundantly to ensure PT cell wall integrity during the long journey of pollen from stigma to the embryo sack (Boisson-Dernier et al., 2009; Miyazaki et al., 2009). ANX1/2 similarly to FER require ROS production and Ca^{2+} gradient for the normal PT growth (Boisson-Dernier et al., 2013). Two other members of the CrRLK1L family BUDDHA'S PAPER SEAL1 (BUPS1) and BUPS2 are needed for the PT integrity maintenance. These receptors bind ANX1/2 to form a complex which binds RAPID ALKALINIZATION FACTOR 4/19 (RALF4/RALF19) to ensure polar growth of pollen tubes (Ge et al., 2017). RALF4/19 are additionally binding cell wall proteins of the LEUCINE-RICH REPEAT EXTENSIN (LRX) family and act synergistically to ensure PT cell wall integrity during growth (Mecchia et al., 2017). Once PTs are in proximity to filiform apparatus synergid released RALF34 binds to BUPS1/2-ANX1/2 and in that way replace RALF4/19, which then leads to destabilization of complex and PT burst (Ge et al., 2017).

Regardless the vast advancement of our understanding on *Cr*RLK1L signaling, ligand of FER in the light of PT reception remains a mystery. FER contains two malectin domains (MLD) in its extracellular domain, which were shown to have capability of *in vitro* binding to the pectic components of the cell wall (Feng et al., 2018). Additionally, upon PT arrival FER is regulating accumulation of nitric oxide (NO) which plays a role in repelling of supernumerary pollen tubes. However direct link between cell wall pectin state and activation of FER signaling pathway remains to be established (Duan et al., 2020). Even though it is known that FER also regulates high accumulation of reactive oxygen species (ROS) at the micropyle (Duan et al., 2014), downstream components have not been found so far. On the other hand, signaling cascade mediating polar growth

of the root hairs and leaf pavement cell growth, as well as FER-mediated suppression of abscisic acid (ABA) signaling is well established. It relies on guanine exchange factors (ROPGEFs) activation of Rho-like GTPases (RAC/ROPs) causing NADPH oxidase activation and ROS production (Duan et al., 2010; Gachomo et al., 2014; Huang et al., 2013; Li et al., 2015).

Forward genetic screens are extremely powerful tool to identify unknown gene functions in a unbiased manner (Page and Grossniklaus, 2002). In this study, we have performed a forward genetic screen in order to find novel components of FER signaling pathway and thus mapped three EMS mutants with varying degrees of *fer*-like PT overgrowth phenotype. Here, we report identification of *ASPARAGINE LINKED GLYCOSYLATION 11* (*ALG11*) encoding alpha-1,2-mannosyltransferase of *N*-glycosylation pathway as well as *ROOT INITIATION DEFECTIVE 1* (*RID1),* encoding an RNA helicase as the novel components of the pollen tube reception in the female gametophyte.

Results

Forward genetic screen for the *fer*-like PT overgrowth phenotype

Forward genetic screen was previously performed to get a better understanding of FER-mediated signaling during PT reception in *Arabidopsis thaliana*. Mutants with the highest penetrance were mapped to the genes encoding enzymes involved in the *N*-glycosylation pathway in ER, named as *TURAN* (*TUN)* and *EVAN* (*EVN)* (Lindner et al., 2015). Here the characterization of three remaining EMS mutant candidates (ADZ8, ADZ12 and ADZ17) will be described, which similarly to *tun/TUN* and *evn/EVN* were gametophytic lethal and thus homozygous individuals could not be recovered. SNP-ratio mapping (SRM) approach was employed since it has been proven as a fast and reliable strategy for the mapping of gametophytic mutants (Lindner et al., 2012, 2015).

According to the SRM approach only two rounds of backcrossing to the non-mutagenized parent (Col-0) are enough to distinguish between any unlinked ethyl methanesulfonate EMS-generated SNPs and the causative EMS-generated SNPs (Fig. 1A). After the first backcross plants were phenotyped and only mutant-like plants were used for a second round of backcrossing. Phenotyping was performed using aniline blue staining to ensure that only mutants with the classical *fer*-like PTO are being selected for the subsequent steps. Additionally, reciprocal crosses were performed, and in all three candidates PTO was due to a female gametophytic defect (Fig. 1B). F1 generation of the second backcrosses (BC2) were re-phenotyped and only the plants presenting PTO were used as the mapping population (Fig. 1A).

For each of the mutant candidates (ADZ8, ADZ12 and ADZ17) genomic DNA from the 52 individuals per mapping population was pooled and sequenced using Illumina NovaSeq 6000. We have obtained good sequencing quality for all sequenced pools, with the high base calling and per sequence quality Phred scores above 35 for the most of obtained sequences (Fig. S2). However, the GC content of the ADZ12 candidate sequences was extraordinarily high for *A. thaliana* genome, and a second peak at 60% was indicative of a bacterial contamination (Fig. S2). The other two samples (ADZ8 and ADZ17) had expected GC ratio for *A. thaliana* (36.0%) (Shangguan et al., 2013). When we analyzed the percentage of mapped reads to the reference *A. thaliana* genome (TAIR10), we detected only 50% for ADZ12 sample compared to typical values of 80-90% which were obtained for ADZ8 and ADZ17 (Fig. S2).

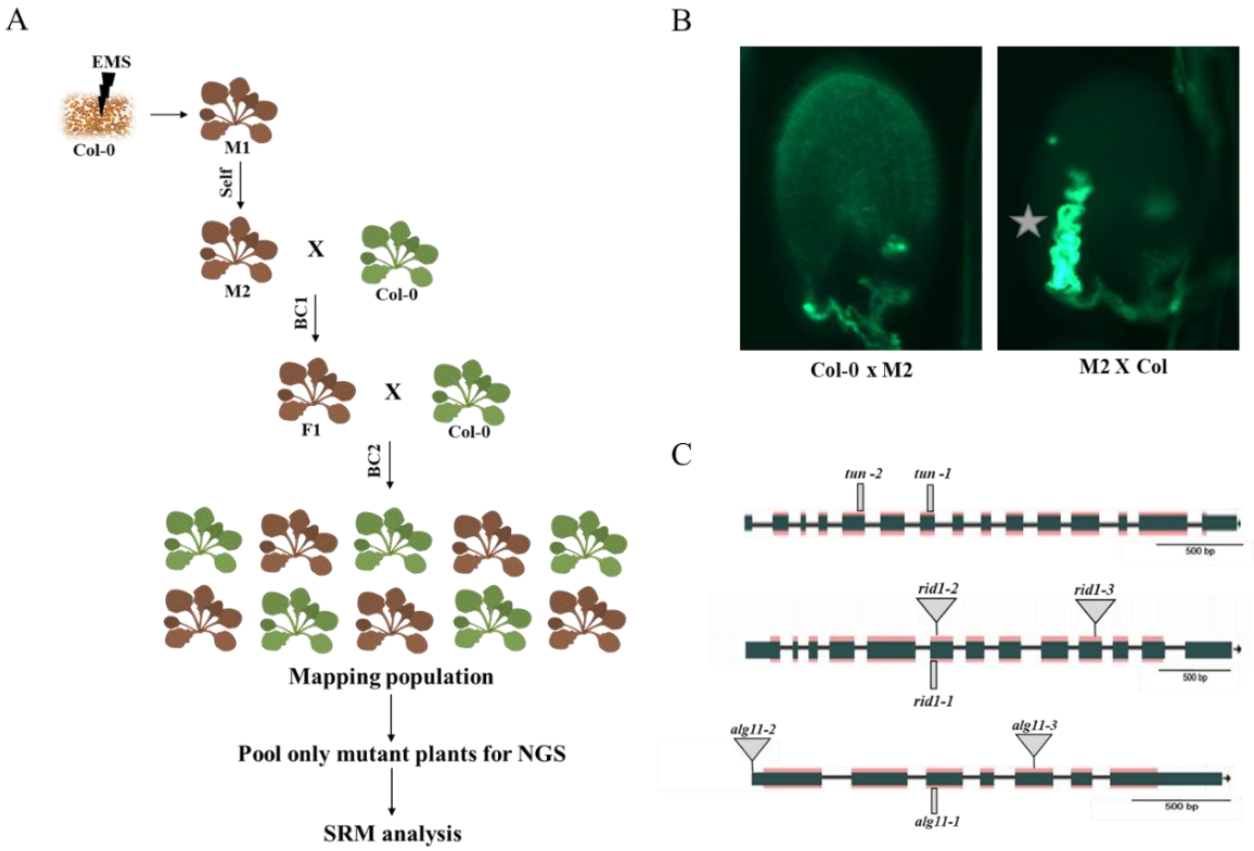

Figure 1. Application of SNP ratio mapping (SRM) approach to find novel components of pollen tube reception pathway. **(A)** EMS-treated mutants (brown plants) which present PT overgrowth phenotype were backcrossed twice to the non-mutagenized wild-type parent (Col-0) to eliminate non-causative SNPs. Genomic DNA from BC2 mutant plants (~50 plants) were pooled and sequenced. **(B)** Reciprocal crosses revealed mutants to be female gametophytic. Representative image of aniline blue stained siliques analyzed two days after pollination. Star indicates *fer*-like PT0 phenotype. **(C)** Representative scheme of genes discovered in the forward genetic screen, namely *TUN*, *RID1* and *ALG11*. Grey rectangle depicts EMS causative SNPs and grey triangle represents T-DNA insertion lines, used to confirm EMS-alleles.

Therefore, the sample ADZ12 was resequenced and subsequently around 65% of reads were mapped to the *Arabidopsis* genome, which was sufficient to proceed with the analysis. Obtained SNPs were firstly filtered to eliminate low- as well as very high-coverage SNPs, which left around 90% of the original SNPs. The total number of filtered heterozygous SNPs was 5,559 for ADZ8, 1,079 for ADZ12 and 5,188 in the case of ADZ17. The reduced mapping rate of the ADZ12 sample was evident from the lower number of obtained SNPs compared to the other two candidate samples. For each of the mutant candidates the SNP/non-SNP ratio of filtered heterozygous SNPs was determined and plotted against their chromosomal position (Fig. 2). Since causative SNPs should segregate 1:1 in the mapping population, the expected SNP to non-SNP ratio is around 0.5. SNPs which are in the proximity to a causative SNP will cosegregate together leading to ratio of >0.25. On the other hand, unlinked EMS induced SNPs should segregate 1:3 in the mapping population, meaning that their SNP to non-SNP ratio should be <0.25 (Fig. 2). Therefore, regions surrounding causative SNPs result in a rounded curve on the SNP/non-SNP ratio plot, which is easily detectable (depicted with grey boxes in Fig. 2).

For the ADZ8 candidate sample, a rounded peak putatively containing causative SNP was visually identified on the chromosome 1 (Fig. 2A). The causative SNP had a segregation ratio of 0.489 (very close to the expected ratio of 0.5) and it was a nonsynonymous GC-to-AT nucleotide change (c.321+1G>A) which resulted in a splice donor variant in the first exon of *AT1G16570* (*TURAN*). In the case of the ADZ12 sample we have observed a rounded peak at chromosome 1 (Fig. 2B). The segregation ratio of the putative causative SNP was 0.45, again very close to the anticipated ratio of 0.5, and it was a nucleotide change of GC-to-AT type (c.1024 G>A) in the *AT1G26370 ROOT INITIATION DEFECTIVE 1 (RID1),* which caused a nonsynonymous substitution of amino acid valine to isoleucine (V342I). Lastly, in the ADZ17 sample we have identified a rounded peak at chromosome 2 (Fig. 2C). The putative causative SNP had a segregation ratio of 0.46, again very close to the expected 0.5 ratio, and it was also a nonsynonymous GC-to-AT (c.716G>A) change leading to a premature STOP codon generation (p. Trp239*) in the third exon of *AT2G40190 ASPARAGINE LINKED GLYCOSYLATION 11* (*ALG11*). SNP/non-SNP ratio plots for all chromosomes for each mutant candidate can be found in the supplemental material (Fig. S4-6).

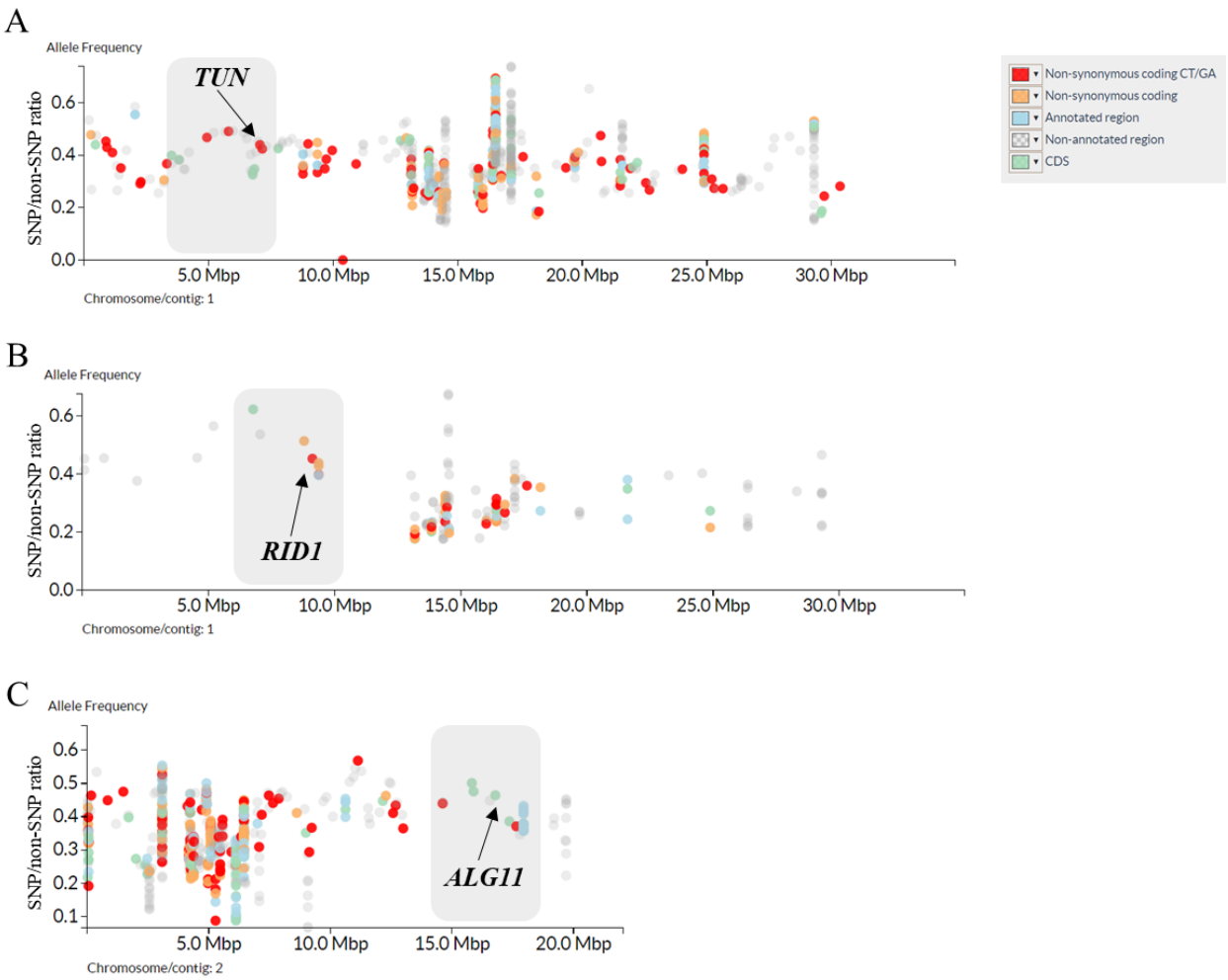

Figure 2. SNP/non-SNP ratio plots of EMS mutant candidates. Obtained SNP/non-SNP ratios of all heterozygous SNPs are plotted against respective chromosomal positions. Causative SNP should segregate with the ratio of ~0.5 (0.4 to 0.6). In the boxed areas are labelled genetically linked regions with respective causative SNPs. **(A)** SNP/non-SNP ratios of ADZ8 EMS mutant line revealed a causative SNP in *AT1G16570* (*TUN*) (arrow). **(B)** SNP/non-SNP ratios of ADZ12 EMS mutant line showed a causative SNP in *AT1G26370* (*RID1*) (arrow). **(C)** SNP/non-SNP ratios of ADZ17 EMS mutant line uncovered a causative SNP in *AT2G40190* (*ALG11*) (arrow).

To prove that the causative EMS SNPs were identified, mapped genes (*TUN, RID1* and *ALG11*) were amplified from each plant of the mapping population that was previously used for the sequencing. PCR products were then sequenced, and heterozygous causative SNPs were detected for each mapped gene in all 52 plants of the respective mutant pools. However, to have a final confirmation that the correct genes have been mapped using SRM, two independent T-DNA insertion lines were analyzed per gene candidate. In the case of ADZ17 both T-DNA lines (SALK_000886 and SALK_106951) showed the same PT overgrowth phenotype as our EMS allele, meaning that we have successfully mapped *ALG11* by SRM. Detail functional characterization of ALG11 is described in the Chapter 3 of this thesis. The rest of this chapter is dedicated to the description of ADZ12 mutant candidate phenotypes.

RID1 is necessary for both pollen tube attraction and reception

Utilizing the SRM approach on the EMS mutant candidate ADZ12, revealed a nonsynonymous nucleotide change (1024 G>A) in *ROOT INITIATION DEFECTIVE 1 (RID1)* leading to amino acid change (V342I). *RID1* was originally discovered through the screen for novel regulators of adventitious organogenesis, hence it was named root initiation defective since it failed to initiate generation of root primordia under restrictive temperatures (Konishi, 2003). *RID1* encodes a DEAH-box RNA helicase involved in pre-mRNA splicing during leaf and root morphogenesis and maintenance of meristematic tissues (Ohtani et al., 2013; Zhu et al., 2016).

Having in mind that RID1 is required for the appropriate splicing of many genes important for the development of female gametophyte (Zhu et al., 2016), we have checked tissue and cell specific expression patterns of *RID1* compared to known molecular players important for the proper reception of pollen tubes. *RID1* is expressed in synergids, and overall, it showed similar tissue expression pattern compared to *ALG11, TUN* and *FER* (Fig. S7, Tab. S1, Tab.S2).

With intention of having a validation that *RID1* was correctly mapped, two T-DNA insertion lines disrupting *RID1* were tested for the presence of PTO phenotype. Both T-DNA alleles, *rid1-2/RID1* (GABI_730B12) with an insertion in the sixth exon as well as T-DNA allele *rid1-3/RID1 (*GABI_310A05) insertion within tenth exon (Fig. 1C) have been reported to have 50% of seed abortion (Ohtani et al., 2013). In order to examine whether these mutants display defects of PT reception, we have analyzed self-pollinated siliques of EMS allele (*rid1-1/RID1*), T-DNA lines, and wild type Col-0 using aniline blue staining. Only EMS allele presented PTO in 8% of ovules, while T-DNA lines were indistinguishable to the wild type Col-0 in the level of PT overgrowth per silique (Fig. 3A). We have observed that in *rid1-2/RID1* and *rid1-3/RID1* around 50% of ovules which could no longer attract pollen tubes (Fig. 3C), leaving them unfertilized. Therefore previously reported reduction of seed set can be explained by the severely impaired PT attraction, probably caused by malfunctioning of synergid cells (Ohtani et al., 2013). However, it remains to be further investigated at precisely which stage do the PTs stop their growth.

Interestingly, in siliques of EMS allele we have observed three scenarios: wild type normal PT reception, PT overgrowth as well as around 12% of non-targeted ovules (Fig. 3C). We have also performed seed set abortion analysis on *rid1-1/RID1* allele and wild type control and found around 20% of aborted seeds in *rid1-1/RID1* mutant (Fig. 3B). Therefore, it is likely that besides impairment in PT reception, fertilization is compromised at different stages, such as PT attraction and potentially postfertilization process which remains to be further elucidated. In order to address male

gametophytic defects, we have also carried out *in vitro* pollen tube germination assays to track dynamics of PT growth (Boisson-Dernier et al., 2013). We have observed normal development of pollen and pollen tube germination was comparable to the wild-type Col-0, meaning that cell wall integrity of pollen tubes in *rid1-1/RID1* was unaffected (Fig. S1).

In a summary, we have found heterozygous *RID1* EMS SNP in all plants of the mapping population. EMS allele of RID1 displayed 8% of PTO as well as 12% of non-targeted ovules due to the most likely loss of PT attraction, resulting in 20% of seed set abortion. However, T-DNA lines disrupting *RID1* show extremely strong inability to attract PT, thus PT reception could not be assessed. Discrepancies in the observed phenotypes could stem from the fact that in T-DNA lines there is a complete loss of RID1 function, while in EMS line there is a single nonsynonymous amino acid change V342I. It is possible that this mutation has a moderate effect on protein, rendering it still partially functional.

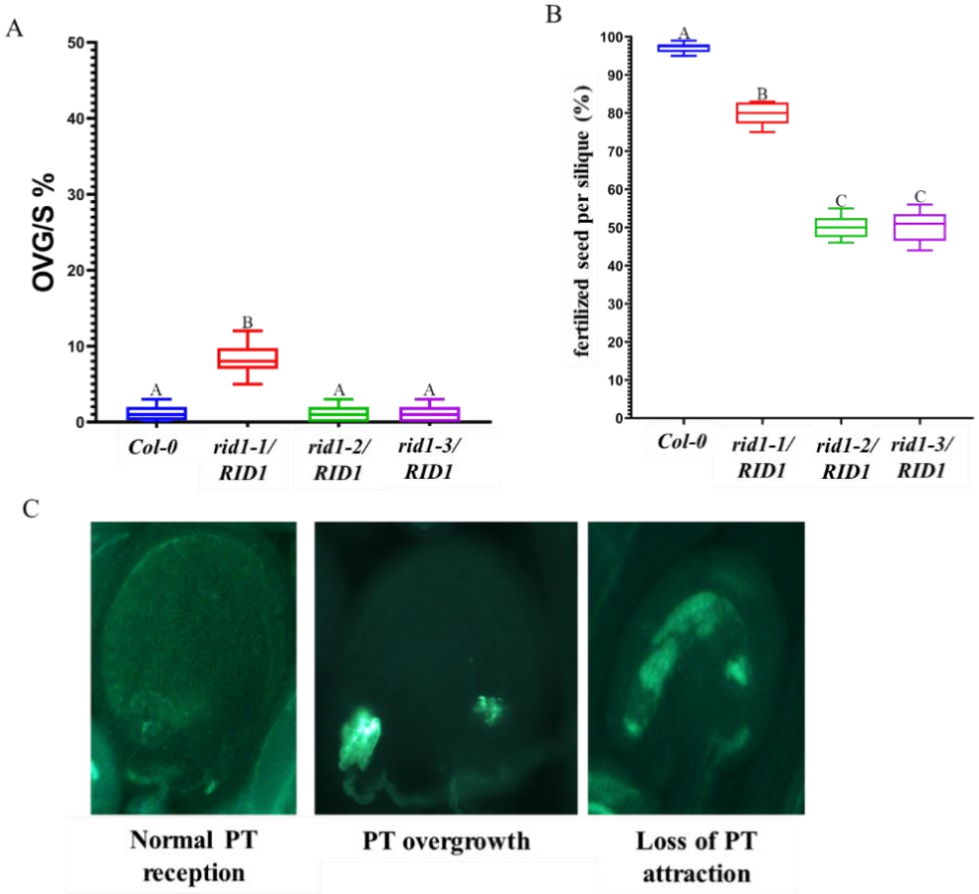

Figure 3. Pollen tube reception and pollen tube attraction is impaired in *rid1* mutants. (A) Intraspecific PT reception of Col-0 and corresponding *RID1* alleles. Box plots represent the percentage of pollen tube overgrowth per silique (OVG/S). At least ten self-pollinated siliques from five plants of Col-0 and *RID1* alleles were analyzed using aniline blue staining (n>2500 ovules per genotype). One-way ANOVA followed by Tukey's multiple comparison test (A-B ****P<0.0001). **(B)** Seed set analysis of Col-0 and *RID1* alleles was performed on the dissected mature siliques. At least five plants per line and five siliques per plant were analyzed (n>1250 seeds per line). One-way ANOVA followed by Tukey's multiple comparison test (A-B ****P<0.0001; A-C ****P<0.0001; B-C ****P<0.0001). **(C)** Representative images of *rid1-1/RID1* siliques visualized with aniline blue staining of callose in PTs and ovule cell walls. From left to right: wild-type like ovule with a normal PT reception, ovule presenting *fer*-like PT overgrowth and unfertilized ovule which lost ability to attract pollen tubes.

We have used Polymorph 1001 Genome Variant (Alonso-Blanco et al., 2016) to screen if p.V342 is conserved among the *A. thaliana* accessions. We have found p.V342 to be highly conserved and no nonsynonymous amino acids substitutions were found among all 1135 screened varieties (data not shown). This vast conversation of p.V342 is suggestive of functional importance of valine for the protein functionality. We have performed evolutionary analysis among the RID1 orthologs and found p.V342 to be conserved among the closest related species (Fig. S8). In the more divergent species also p.A342 was observed, while in rice species that was not grouping with the any of the orthologs p.I342 was detected (Fig. S8). To summarize, it was observed that the preservation of p.V342 correlates with the degree of evolutionary relatedness, suggesting that in the more closely related species this position plays similar and important role for the protein function. What remains to be done in the future to have a clear evidence of RID1 being correctly identified, is to introduce functional RID1 into the *rid-1/RID1* allele and test if reproductive phenotypes can be complemented.

Discussion

We have characterized three EMS mutants presenting *fer*-like PT overgrowth. Utilizing SNP ratio mapping approach, we have successfully discovered *ASPARAGINE LINKED GLYCOSYLATION 11 (ALG11*) as the novel component of PT reception pathway. Additionally, we have found a novel allele of *TUN*. Lastly, we have identified a region in chromosome one which was linked to the PT reception phenotypes of remaining EMS candidate (ADZ12), and we have several indications that the causative SNP is affecting *ROOT INITIATION DEFECTIVE 1* (*RID1*).

Forward genetic screens are invaluable tools when it comes to dissecting signaling pathway and gaining better understanding of a wide range of biological processes (Page and Grossniklaus, 2002). Different types of mutagenesis can be used to introduces several thousands of random mutations in the genome, including chemical, gamma-irradiation, and insertion of transgene and transposons (Kim et al., 2006). Most commonly used chemical mutagen is ethyl methanesulfonate (EMS) which is causing in the majority of cases (99%) cytosine (C) to thymine (T) C-T change further leading to GC-TA substitutions (Greene et al.; Qu and Qin, 2014). Prevalence of EMS-induced missense mutations was estimated to be around 65%, while gain of stop codon are present at much lower rate of 5% (Kim et al., 2006). In all three mutant candidates we have mapped EMS causative SNPs to be typical GC-to-AT nucleotide change, one had moderate effect on the protein leading to non-synonymous amino acid change (*RID1*), while two other were high-effect type SNPs leading to either generation of a splice donor variant (*TUN*) or a stop codon generation (*ALG11*).

We have utilized SNP ratio mapping approach since it has proven to be adequate tool for mapping of gametophytic/lethal mutations (Lindner et al., 2012). Even though we have obtained good sequencing quality for all three candidates, mapping rates were substantially lower in ADZ12 (50%). Even after resequencing we have still not obtained typical mapping rates, and hence subsequent SRM analysis was challenging as the number of mapped SNPs was five time lower compared to other candidates. After plotting of SNP/non-SNP ratios to their chromosomal positions we have observed a typical rounded curve in the first chromosome, indicative of presence of causative EMS SNP. The only two protein-coding genes in the area were *RID1* and *GAMMA CARBONIC ANHYDRASE 1* (*GAMMA CA1*), while all other SNPs in the linkage group were mapped to either transposable elements or hypothetical proteins. Therefore, we have also analyzed two T-DNA lines disrupting *GAMMA CA1*

(Tab. S3), but both alleles displayed full fertility and PT reception was identical to wild-type Col-0 (data not shown).

We have detected in all plants of the ADZ12 mapping pool heterozygous EMS SNP (c.1024 G>A) in *RID1*. Thus, we have proceeded and analyzed two independent T-DNA lines disrupting this candidate gene. PT overgrowth was not detected in either of RID1 alleles, however PT reception cannot be studied in these alleles since in heterozygous state 50% of ovules could not attract PTs, meaning that mutant ovules completely lost ability to attract PTs. However, when we analyzed EMS line, we observed not only 8% of PT overgrowth but also 12% of non-targeted ovules, leading to 20% of seed abortion. This discrepancy in the strength of phenotype can be explained by the fact that EMS line had a mild effect on protein compared to loss of function T-DNA lines.

Amino acids valine (V) and isoleucine (I) belong to the same group of nonpolar branched chain amino acids with the similar biochemical properties. In general such conservative substitutions between amino acids of the same type are producing only minor effect on the protein activity (Parker, 2001). However position within protein has to be considered as well, mutation within catalytic domains have much stronger effect, or if a change of amino acids impacts secondary structure (Parker, 2001).

Previously it was reported that loss of *RID1* leads to defective cellular specification of the female gametophyte (FG) (Ohtani et al., 2013; Zhu et al., 2016). Synergid cells are crucial for the secretion of peptides important for the PT attraction (Okuda et al., 2009; Takeuchi and Higashiyama, 2012), thus it is conceivable that due to the defect of synergids in *rid1* micropylar guidance is completely lost in the T-DNA alleles. However mild mutation of *RID1* in EMS allele caused partial impairment of PT attraction resulting in higher number of correctly targeted ovules. Additionally, RID1 was shown to bind to GAMETOPHYTIC FACTOR 1 (GFA1) and together they regulate pre-mRNA splicing of several genes important for the proper development of FG (Zhu et al., 2016). Authors also report that change of single amino acids within RID1 DEXDc domain (Y266F and T267I) impairs interaction with GFA1 and thus seed abortion phenotype of T-DNA lines could not be complemented. However EMS SNP we have detected (V3421) lies within HELICc domain which was shown to be non-essential for interaction with GFA1 (Zhu et al., 2016), which could partially explain milder defect of PT attraction in our EMS line.

However only if functional RID1 can complement our EMS line we can proceed with further mutant characterization. If proven so, using site-directed mutagenesis, EMS induced SNP could be introduced in RID1, generating $RID1^{V342I}$. Complementation capability of this variant should be compared between EMS and T-DNA alleles. It would be interesting to test whether $RID1^{V342I}$ could improve PT attraction but not PT reception of T-DNA lines, leading to comparable level of PTO. Additionally, development and cellular specification should be meticulously characterized in EMS allele. Correct localization to the filiform apparatus should be checked for several players of PT reception pathway including FER, LRE, EN14, HERK1 and ANJEA. In the case of aberrant localization, one of the first considerations should be alternative splicing of above-mentioned PT reception players, which can be further tested with qRT-PCR analysis.

Second gene mapped in this study *ALG11*, was previously identified in a EMS screen, and due to a sever reduction of primary root growth it was named *limited root growth1* (*lrg1*) (Manzano et al., 2017). EMS causative SNP in *lrg1* led to the synonymous substitution which impaired correct splicing of the fourth intron, and this missplicing was light-intensity dependent (Manzano et al., 2017). Additionally, *lrg1* roots were hypersensitive to the effects of blue light, while under normal

conditions could grow normally. Mild seeds set abortion of *lrg1* was reported, but it was not quantified since focus of the study was inhibition of root growth (Manzano et al., 2017). Therefore, more elaborated analysis of observed reproductive defects in needed to conclude if this splicing variant has differential impact on PT reception compared to EMS SNP detected in this study (T239*).

Only few months ago, FER was showed to be involved in the regulation of flowering time. Under long day conditions *fer-4* had a substantial delay of flowering time compared to the wild type Col-0. FER is functioning in a flowering transition by downregulation of key flowering genes which is achieved by regulating rates of pre-mRNA splicing (Wang et al., 2020).

Taken together alternative splicing seems to play an important role during female gametophyte development, PT attraction, PT reception as well as flowering time regulation. This complex interplay between splicing machinery, FER and ER *N*-glycosylation pathway, in ensuring reproductive success under appropriate environmental conditions just started to be understood. Since many pieces of this complicated puzzle are missing, more forward genetic screens are needed to get a better understanding of elaborate signaling necessary to ensure successful reproduction and hence seed production.

Material and methods

Plant Material and Growth Conditions

We have used for all experiments *Arabidopsis thaliana (L.) Heynh*., ecotype Col-0. T-DNA insertion lines (Tab. S3) were obtained from The European Arabidopsis Stock Center (NASC). Characterized EMS-alleles *tun-2*, *rid1-1*, *alg11-1* (Tab. S3) came from the M1 plants which were left to self, followed by two rounds of backcrossing to the Col-0 wild type accession. Seeds were sterilized using 3% NaOCl/0.01% Triton X-100 solution followed by incubation in 100% ethanol and sterile drying. Seeds were transferred to sterile half-strength Murashige and Skoog (MS) basal medium (Carolina) without sucrose and placed at 4°C in darkness for the next 48 hours. Upon stratifications they were grown under long day conditions in a growth chamber (CLF_CU-36L6, Percival, Germany), under following conditions: relative humidity of 70% and light intensity of 200 µmol/m2 s with 16 hours light at 22°C and 8 hours dark at 18°C. After seven days seedlings were transferred to the soil under long day conditions.

Preparation of genomic DNA and Nova-Seq 6000 sequencing

Genomic DNA of 52 BC2 plants presenting PT overgrowth/per EMS mutant line was extracted using a QIAGEN DNeasy Plant Mini Kit. DNA pool per EMS mutant candidate was obtained by mixing in equimolar concentrations DNA from each plant of the pool, with a total amount of 1.5 µg of pooled DNA. The Functional Genomic Center of the University of Zürich prepared fragment library and sequenced three EMS mutant candidates with the pair end (2 x 150 bp) Nova-Seq 6000 sequencing platform. In total 200M of reads were obtained.

Sequencing analysis and identification of causative SNPs

FASTQ-formatted raw sequencing reads were quality-checked with the FastQC application (http://www.bioinformatics.babraham.ac.uk/projects/fastqc/) and FastQC reports were combined using MultiQC (Ewels et al., 2016) (https://multiqc.info/). After removal of duplicate reads using samtools version 1.8 (Li et al., 2009) reads were then mapped to the TAIR10 reference genome (http://www.arabidopsis.org/) with bwa mem v0.7.15 (Li and Durbin, 2010). SNPs were called and variant reads called using Freebayes version 1.0.2 (Garrison and Marth, 2012). Variants with allele frequencies lower than 10% or higher than 90% were discarded from the analysis as well as variants with unexpectedly high read coverage. Variant effects were predicted using SnpEff version 4.3 (Cingolani et al., 2012). The number of obtained SNPs per EMS mutant sample after filtering was: 5,651 for ADZ8, 1,080 for ADZ12 and 5,189 for ADZ17. SNP density plots were generated using web application CandiSNP, available at http://candisnp.tsl.ac.uk.

Confirmation of mutation

To confirm causative SNPs of EMS mutant candidates C321T in *AT1G16570* (*TUN*); G1024A in *AT1G26370* (*RID1*); G716A in *AT2G40190* (*ALG11*), SNP region of each gene was amplified from all of the plants within respective DNA pool, as well as from Col-0 and H_20 controls. Primers used for amplification, followed by in-house Sanger sequencing (ABI 3730 DNA Analyzer) are listed in Tab. S4.

Seed Set Analysis, Crosses and Aniline Blue Staining

Seed set analysis was performed by cutting and opening fully expanded mature siliques and counting the numbers of developed seeds (“fertilized seeds”) versus white and shrunken ovules (“unfertilized seeds”). Crosses were performed accordingly: as a female parent young closed floral buds of *A. thaliana* were emasculated two days prior to hand-pollination. Only flowers with closed stamens and no pollen release were used for emasculation, to make sure that no self-pollination is occurring. For the male parent freshly opened flowers were used for pollination. We have used as male parent either *A. thaliana* pollen (intraspecific pollinations) or *A. lyrata* for interspecific pollinations. Assessment of the pollen tube overgrowth phenotype was done by aniline blue staining of pollen tubes (Huck, 2003). Two days after pollination sepals and petals were removed and siliques were fixed using 9:1 ethanol (EtOH): acetic acid solution overnight at 4°C. Stained siliques were analyzed using a Leica DM6000B epifluorescence microscope under a UV-light source (Leica Microsystems).

In vitro Pollen Tube Germination

In vitro pollen germination was done as described previously (Boavida and McCormick, 2007; Boisson-Dernier et al., 2013). Pollen grains were released from the open *A. thaliana* flowers (floral stage 15) and germinated into solid medium. Pollen tubes were imaged using Leica DM6000B (Leica Microsystems) microscope on the differential interfering contrast (DIC) channel.

Bioinformatic analysis

RNA-Seq and Microarray expression data was obtained from publicly available datasets (Borges et al., 2008; Honys and Twell, 2004; Pina et al., 2005; Schmidt et al., 2011; Wuest et al., 2010) using expression analysis tool developed in the lab. The R script is available at the GitHub platform (https://github.com/VimalRawat1010/Rscripts/blob/master/LabData/.RData. Polymorph 1001 Genome Variant Browser (Alonso-Blanco et al., 2016) was used to find high effect SNPs variants of *RID1*.

Statistical analysis

D'Agostino-Pearson normality test was used to determine if data is fitting Gaussian distribution. Statistical significance of normally distributed data was assessed using with either Student's t test or One-way ANOVA followed by Tukey's multiple comparisons test. Sample size (n) is given in the figure legends. Statistical testes were done with GraphPad Prism 8 software.

References

Adhikari, P.B., Liu, X., Wu, X., Zhu, S., and Kasahara, R.D. (2020). Fertilization in flowering plants: an odyssey of sperm cell delivery. Plant Mol Biol.

Alonso-Blanco, C., Andrade, J., Becker, C., Bemm, F., Bergelson, J., Borgwardt, K.M., Cao, J., Chae, E., Dezwaan, T.M., Ding, W., et al. (2016). 1,135 Genomes Reveal the Global Pattern of Polymorphism in Arabidopsis thaliana. Cell *166*, 481–491.

Boavida, L.C., and McCormick, S. (2007). TECHNICAL ADVANCE: Temperature as a determinant factor for increased and reproducible in vitro pollen germination in Arabidopsis thaliana: Temperature effect on Arabidopsis pollen germination. The Plant Journal *52*, 570–582.

Boisson-Dernier, A., Frietsch, S., Kim, T.-H., Dizon, M.B., and Schroeder, J.I. (2008). The Peroxin Loss-of-Function Mutation abstinence by mutual consent Disrupts Male-Female Gametophyte Recognition. Current Biology *18*, 63–68.

Boisson-Dernier, A., Roy, S., Kritsas, K., Grobei, M.A., Jaciubek, M., Schroeder, J.I., and Grossniklaus, U. (2009). Disruption of the pollen-expressed FERONIA homologs ANXUR1 and ANXUR2 triggers pollen tube discharge. Development *136*, 3279–3288.

Boisson-Dernier, A., Lituiev, D.S., Nestorova, A., Franck, C.M., Thirugnanarajah, S., and Grossniklaus, U. (2013). ANXUR Receptor-Like Kinases Coordinate Cell Wall Integrity with Growth at the Pollen Tube Tip Via NADPH Oxidases. PLoS Biol *11*, e1001719.

Borges, F., Gomes, G., Gardner, R., Moreno, N., McCormick, S., and Feijo, J.A. (2008). Comparative Transcriptomics of Arabidopsis Sperm Cells1[C][W]. *148*, 14.

Capron, A., Gourgues, M., Neiva, L.S., Faure, J.-E., Berger, F., Pagnussat, G., Krishnan, A., Alvarez-Mejia, C., Vielle-Calzada, J.-P., Lee, Y.-R., et al. (2008). Maternal Control of Male-Gamete Delivery in *Arabidopsis* Involves a Putative GPI-Anchored Protein Encoded by the *LORELEI* Gene. Plant Cell *20*, 3038–3049.

Cingolani, P., Platts, A., Wang, L.L., Coon, M., Nguyen, T., Wang, L., Land, S.J., Lu, X., and Ruden, D.M. (2012). A program for annotating and predicting the effects of single nucleotide polymorphisms, SnpEff. Fly *6*, 80–92.

Duan, Q., Kita, D., Li, C., Cheung, A.Y., and Wu, H.-M. (2010). FERONIA receptor-like kinase regulates RHO GTPase signaling of root hair development. Proc Natl Acad Sci USA *107*, 17821–17826.

Duan, Q., Kita, D., Johnson, E.A., Aggarwal, M., Gates, L., Wu, H.-M., and Cheung, A.Y. (2014). Reactive oxygen species mediate pollen tube rupture to release sperm for fertilization in Arabidopsis. Nat Commun *5*, 3129.

Duan, Q., Liu, M.-C.J., Kita, D., Jordan, S.S., Yeh, F.-L.J., Yvon, R., Carpenter, H., Federico, A.N., Garcia-Valencia, L.E., Eyles, S.J., et al. (2020). FERONIA controls pectin- and nitric oxide-mediated male–female interaction. Nature *579*, 561–566.

Escobar-Restrepo, J.-M., Huck, N., Kessler, S., Gagliardini, V., Gheyselinck, J., Yang, W.-C., and Grossniklaus, U. (2007). The FERONIA Receptor-like Kinase Mediates Male-Female Interactions During Pollen Tube Reception. Science *317*, 656–660.

Ewels, P., Magnusson, M., Lundin, S., and Käller, M. (2016). MultiQC: summarize analysis results for multiple tools and samples in a single report. Bioinformatics *32*, 3047–3048.

Feng, W., Kita, D., Peaucelle, A., Cartwright, H.N., Doan, V., Duan, Q., Liu, M.-C., Maman, J., Steinhorst, L., Schmitz-Thom, I., et al. (2018). The FERONIA Receptor Kinase Maintains Cell-Wall Integrity during Salt Stress through Ca2+ Signaling. Current Biology *28*, 666-675.e5.

Franck, C.M., Westermann, J., and Boisson-Dernier, A. (2018). Plant Malectin-Like Receptor Kinases: From Cell Wall Integrity to Immunity and Beyond. Annu. Rev. Plant Biol. *69*, 301–328.

Gachomo, E.W., Jno Baptiste, L., Kefela, T., Saidel, W.M., and Kotchoni, S.O. (2014). The Arabidopsis CURVY1 (CVY1) gene encoding a novel receptor-like protein kinase regulates cell morphogenesis, flowering time and seed production. BMC Plant Biol *14*, 221.

Galindo-Trigo, S., Blanco-Touriñán, N., DeFalco, T.A., Wells, E.S., Gray, J.E., Zipfel, C., and Smith, L.M. (2019). *Cr* RLK 1L receptor-like kinases HERK 1 and ANJEA are female determinants of pollen tube reception. EMBO Rep.

Garrison, E., and Marth, G. (2012). Haplotype-based variant detection from short-read sequencing. ArXiv:1207.3907 [q-Bio].

Ge, Z., Bergonci, T., Zhao, Y., Zou, Y., Du, S., Liu, M.-C., Luo, X., Ruan, H., García-Valencia, L.E., Zhong, S., et al. (2017). *Arabidopsis* pollen tube integrity and sperm release are regulated by RALF-mediated signaling. Science *358*, 1596–1600.

Greene, E.A., Codomo, C.A., Taylor, N.E., Henikoff, J.G., Till, B.J., Reynolds, S.H., Enns, L.C., Burtner, C., Johnson, J.E., Odden, A.R., et al. Spectrum of Chemically Induced Mutations From a Large-Scale Reverse-Genetic Screen in Arabidopsis. 10.

Honys, D., and Twell, D. (2004). Transcriptome analysis of haploid male gametophyte development in Arabidopsis. Genome Biology 13.

Hou, Y., Guo, X., Cyprys, P., Zhang, Y., Bleckmann, A., Cai, L., Huang, Q., Luo, Y., Gu, H., Dresselhaus, T., et al. (2016). Maternal ENODLs Are Required for Pollen Tube Reception in Arabidopsis. Current Biology *26*, 2343–2350.

Huang, G.-Q., Li, E., Ge, F.-R., Li, S., Wang, Q., Zhang, C.-Q., and Zhang, Y. (2013). Arabidopsis RopGEF4 and RopGEF10 are important for FERONIA-mediated developmental but not environmental regulation of root hair growth. New Phytol *200*, 1089–1101.

Huck, N. (2003). The Arabidopsis mutant feronia disrupts the female gametophytic control of pollen tube reception. Development *130*, 2149–2159.

Kessler, S.A., Shimosato-Asano, H., Keinath, N.F., Wuest, S.E., Ingram, G., Panstruga, R., and Grossniklaus, U. (2010). Conserved Molecular Components for Pollen Tube Reception and Fungal Invasion. Science *330*, 968–971.

Kim, Y., Schumaker, K.S., and Zhu, J.-K. (2006). EMS Mutagenesis of Arabidopsis. In Arabidopsis Protocols, J. Salinas, and J.J. Sanchez-Serrano, eds. (Totowa, NJ: Humana Press), pp. 101–103.

Konishi, M. (2003). Genetic analysis of adventitious root formation with a novel series of temperature-sensitive mutants of Arabidopsis thaliana. Development *130*, 5637–5647.

Kumar, S., Stecher, G., and Tamura, K. (2016). MEGA7: Molecular Evolutionary Genetics Analysis Version 7.0 for Bigger Datasets. Mol Biol Evol *33*, 1870–1874.

Leydon, A.R., Tsukamoto, T., Dunatunga, D., Qin, Y., Johnson, M.A., and Palanivelu, R. (2015). Pollen Tube Discharge Completes the Process of Synergid Degeneration That Is Initiated by Pollen Tube-Synergid Interaction in Arabidopsis. Plant Physiol. *169*, 485–496.

Li, H., and Durbin, R. (2010). Fast and accurate long-read alignment with Burrows–Wheeler transform. Bioinformatics *26*, 589–595.

Li, C., Yeh, F.-L., Cheung, A.Y., Duan, Q., Kita, D., Liu, M.-C., Maman, J., Luu, E.J., Wu, B.W., Gates, L., et al. (2015). Glycosylphosphatidylinositol-anchored proteins as chaperones and co-receptors for FERONIA receptor kinase signaling in Arabidopsis. ELife *4*, e06587.

Li, H., Handsaker, B., Wysoker, A., Fennell, T., Ruan, J., Homer, N., Marth, G., Abecasis, G., Durbin, R., and 1000 Genome Project Data Processing Subgroup (2009). The Sequence Alignment/Map format and SAMtools. Bioinformatics *25*, 2078–2079.

Liang, Y., Tan, Z.-M., Zhu, L., Niu, Q.-K., Zhou, J.-J., Li, M., Chen, L.-Q., Zhang, X.-Q., and Ye, D. (2013). MYB97, MYB101 and MYB120 Function as Male Factors That Control Pollen Tube-Synergid Interaction in Arabidopsis thaliana Fertilization. PLoS Genet *9*, e1003933.

Lindner, H., Raissig, M.T., Sailer, C., Shimosato-Asano, H., Bruggmann, R., and Grossniklaus, U. (2012). SNP-Ratio Mapping (SRM): Identifying Lethal Alleles and Mutations in Complex Genetic Backgrounds by Next-Generation Sequencing. Genetics *191*, 1381–1386.

Lindner, H., Kessler, S.A., Müller, L.M., Shimosato-Asano, H., Boisson-Dernier, A., and Grossniklaus, U. (2015). TURAN and EVAN Mediate Pollen Tube Reception in Arabidopsis Synergids through Protein Glycosylation. PLoS Biol *13*, e1002139.

Liu, X., Castro, C., Wang, Y., Noble, J., Ponvert, N., Bundy, M., Hoel, C., Shpak, E., and Palanivelu, R. (2016). The Role of LORELEI in Pollen Tube Reception at the Interface of the Synergid Cell and Pollen Tube Requires the Modified Eight-Cysteine Motif and the Receptor-Like Kinase FERONIA. Plant Cell *28*, 1035–1052.

Manzano, C., Pallero-Baena, M., Silva-Navas, J., Navarro Neila, S., Casimiro, I., Casero, P., Garcia-Mina, J.M., Baigorri, R., Rubio, L., Fernandez, J.A., et al. (2017). A light-sensitive mutation in Arabidopsis LEW3 reveals the important role of N-glycosylation in root growth and development. Journal of Experimental Botany *68*, 5103–5116.

Mecchia, M.A., Santos-Fernandez, G., Duss, N.N., Somoza, S.C., Boisson-Dernier, A., Gagliardini, V., Martínez-Bernardini, A., Fabrice, T.N., Ringli, C., Muschietti, J.P., et al. (2017). RALF4/19 peptides interact with LRX proteins to control pollen tube growth in *Arabidopsis*. Science *358*, 1600–1603.

Miyazaki, S., Murata, T., Sakurai-Ozato, N., Kubo, M., Demura, T., Fukuda, H., and Hasebe, M. (2009). ANXUR1 and 2, Sister Genes to FERONIA/SIRENE, Are Male Factors for Coordinated Fertilization. Current Biology *19*, 1327–1331.

Ngo, Q.A., Vogler, H., Lituiev, D.S., Nestorova, A., and Grossniklaus, U. (2014). A Calcium Dialog Mediated by the FERONIA Signal Transduction Pathway Controls Plant Sperm Delivery. Developmental Cell *29*, 491–500.

Ohtani, M., Demura, T., and Sugiyama, M. (2013). Arabidopsis ROOT INITIATION DEFECTIVE1, a DEAH-Box RNA Helicase Involved in Pre-mRNA Splicing, Is Essential for Plant Development. The Plant Cell *25*, 2056–2069.

Okuda, S., Tsutsui, H., Shiina, K., Sprunck, S., Takeuchi, H., Yui, R., Kasahara, R.D., Hamamura, Y., Mizukami, A., Susaki, D., et al. (2009). Defensin-like polypeptide LUREs are pollen tube attractants secreted from synergid cells. Nature *458*, 357–361.

Page, D.R., and Grossniklaus, U. (2002). The art and design of genetic screens: Arabidopsis thaliana. Nat Rev Genet *3*, 124–136.

Parker, J. (2001). Amino Acid Substitution. In Encyclopedia of Genetics, (Elsevier), pp. 57–58.

Pina, C., Pinto, F., Feijó, J.A., and Becker, J.D. (2005). Gene Family Analysis of the Arabidopsis Pollen Transcriptome Reveals Biological Implications for Cell Growth, Division Control, and Gene Expression Regulation. Plant Physiol. *138*, 744–756.

Qu, L.-J., and Qin, G. (2014). Generation and Identification of Arabidopsis EMS Mutants. In Arabidopsis Protocols, J.J. Sanchez-Serrano, and J. Salinas, eds. (Totowa, NJ: Humana Press), pp. 225–239.

Rotman, N., Gourgues, M., Guitton, A.-E., Faure, J.-E., and Berger, F. (2008). A Dialogue between the Sirène Pathway in Synergids and the Fertilization Independent Seed Pathway in the Central Cell Controls Male Gamete Release during Double Fertilization in Arabidopsis. Molecular Plant *1*, 659–666.

Schmidt, A., Wuest, S.E., Vijverberg, K., Baroux, C., Kleen, D., and Grossniklaus, U. (2011). Transcriptome Analysis of the Arabidopsis Megaspore Mother Cell Uncovers the Importance of RNA Helicases for Plant Germline Development. PLoS Biol *9*, e1001155.

Shangguan, L., Han, J., Kayesh, E., Sun, X., Zhang, C., Pervaiz, T., Wen, X., and Fang, J. (2013). Evaluation of Genome Sequencing Quality in Selected Plant Species Using Expressed Sequence Tags. PLoS ONE *8*, e69890.

Takeuchi, H., and Higashiyama, T. (2012). A Species-Specific Cluster of Defensin-Like Genes Encodes Diffusible Pollen Tube Attractants in Arabidopsis. PLoS Biol *10*, e1001449.

Wang, L., Yang, T., Lin, Q., Wang, B., Li, X., Luan, S., and Yu, F. (2020). Receptor kinase FERONIA regulates flowering time in Arabidopsis. BMC Plant Biol *20*, 26.

Wuest, S.E., Vijverberg, K., Schmidt, A., Weiss, M., Gheyselinck, J., Lohr, M., Wellmer, F., Rahnenführer, J., von Mering, C., and Grossniklaus, U. (2010). Arabidopsis Female Gametophyte Gene Expression Map Reveals Similarities between Plant and Animal Gametes. Current Biology *20*, 506–512.

Zhu, D.Z., Zhao, X.F., Liu, C.Z., Ma, F.F., Wang, F., Gao, X.-Q., and Zhang, X.S. (2016). Interaction between RNA helicase ROOT INITIATION DEFECTIVE 1 and GAMETOPHYTIC FACTOR 1 is involved in female gametophyte development in Arabidopsis. EXBOTJ *67*, 5757–5768.

Supplementary Figures and Tables

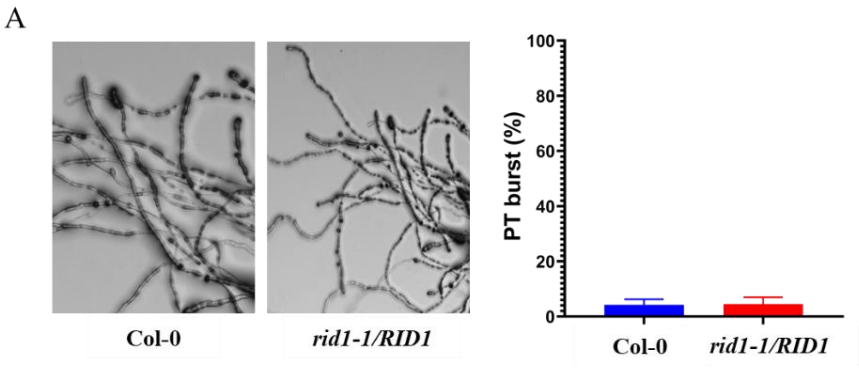

Figure S1. RID1 is not required for the maintenance of the PT integrity. Pollen *in vitro* germination assay of Col-0 and *rid1-1/RID1* mutant pollen. Column bar graph of PT bursting counts of Col-0 and *rid1-1/RID1* pollen. Pollen germination assays were performed three times. Sample size: Col-0 (n=1640) and *rid1-1/RID1* (n=196). Student's t-test (ns).

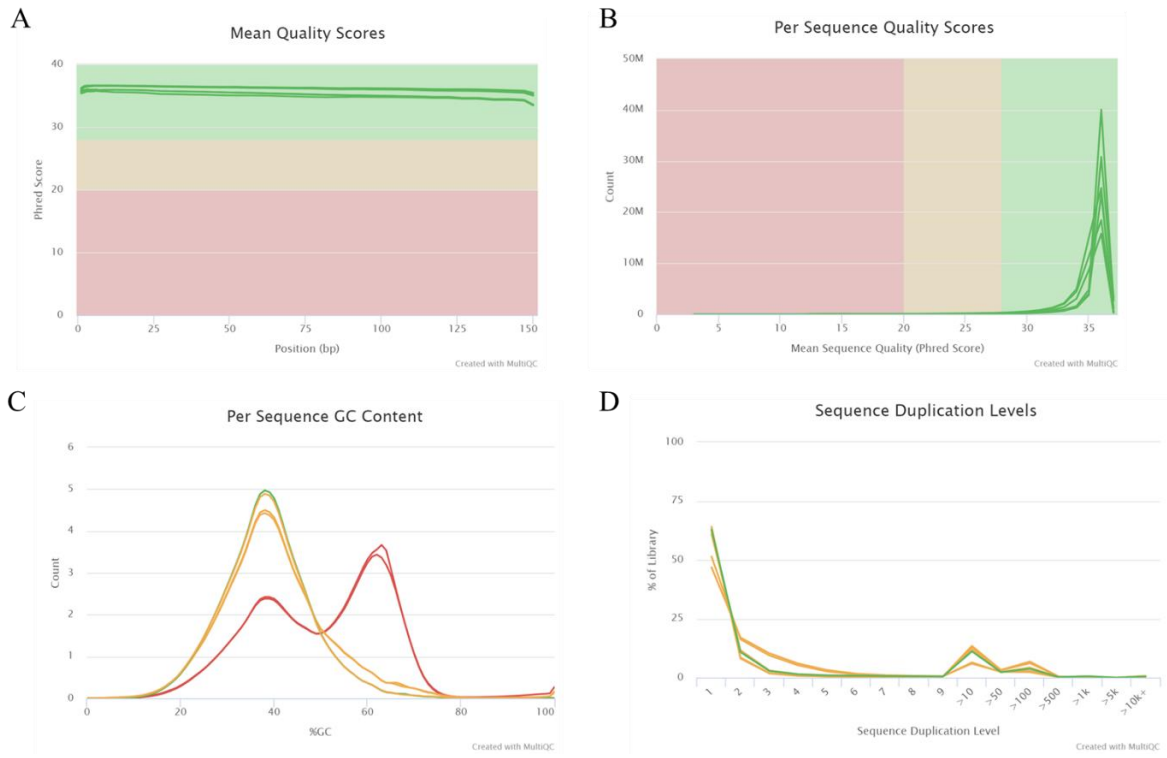

Figure S2. Sequencing quality of EMS mutant candidates. (A) Mean quality sequence scores for all three sequenced pools was of good quality across each base position in the read. **(B)** Per sequence quality score were in the good range, with a Phred score>35 for the largest proportion of obtained sequences. **(C)** Per sequence GC content revealed contamination and unexpected average content of GC for the ADZ12 sample (indicated in red) **(D)** Level of sequence duplication was in a good range (< 20%) for all three EMS mutant candidate.

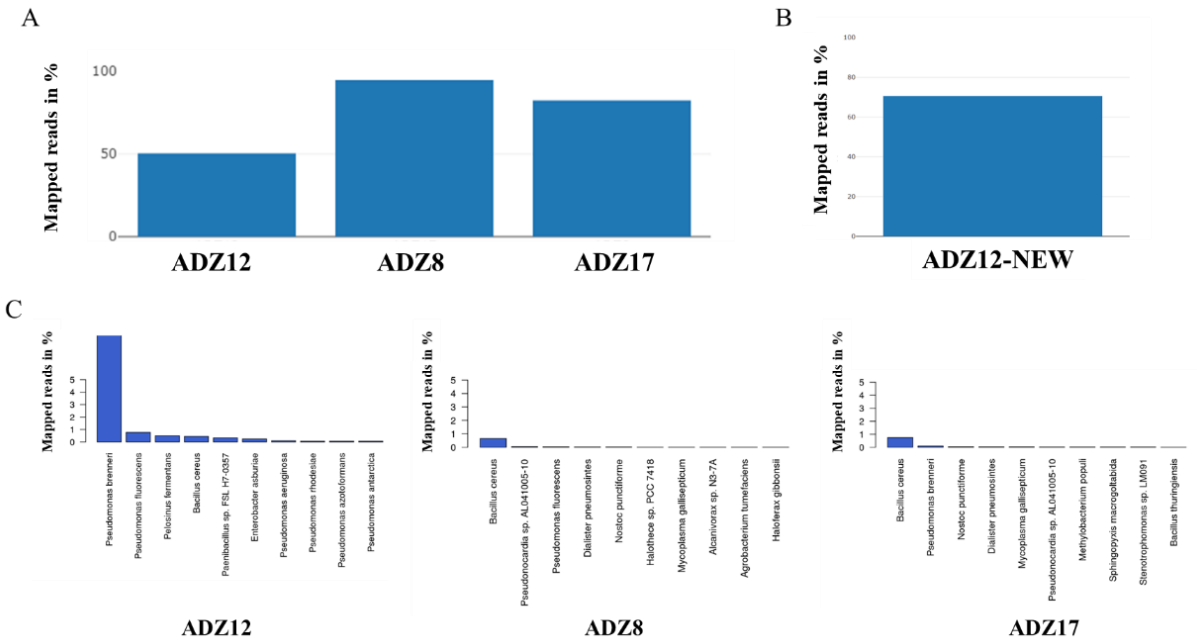

Figure S3. Mapping reads rates of EMS candidates. (A) Percentage of mapped reads for all three EMS candidates to the reference *A. thaliana* genome. ADZ8 and ADZ17 have typical mapping qualities (>85% of mapped reads to the reference), while ADZ12 had only 50%. **(B)** Resequencing of ADZ12 improved mapping rate for 15%. **(C)** Contamination of ADZ12 sample. Mapping to bacterial species revealed substantial contamination in ADZ12 with *Pseudomonas brenneri*.

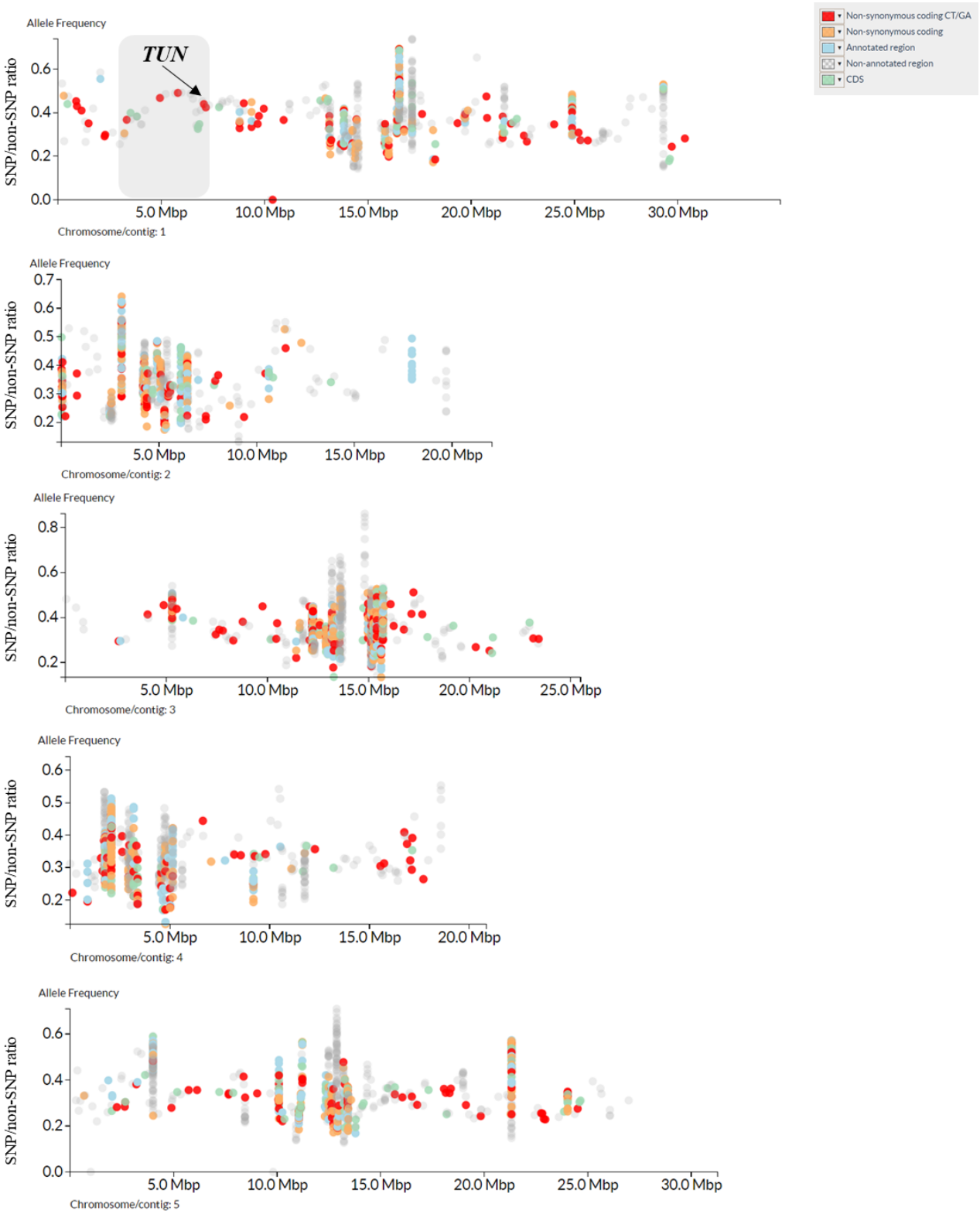

Figure S4. SNP/non-SNP ratio plots of ADZ8 EMS mutant candidate. Obtained SNP/non-SNP ratios of all heterozygous SNPs are plotted against respective chromosomal positions. Causative SNP should have a ratio of SNP/non-SNP of 0.5 (0.4 to 0.6), and outside this range are located non-causative SNPs. In the boxed area is genetically linked region of chromosome 1 with the causative SNP in *TUN*. CandiSNP tool was used to plot SNPs to their chromosomal positions. Legend is indicating type of effect SNPs have on the corresponding gene.

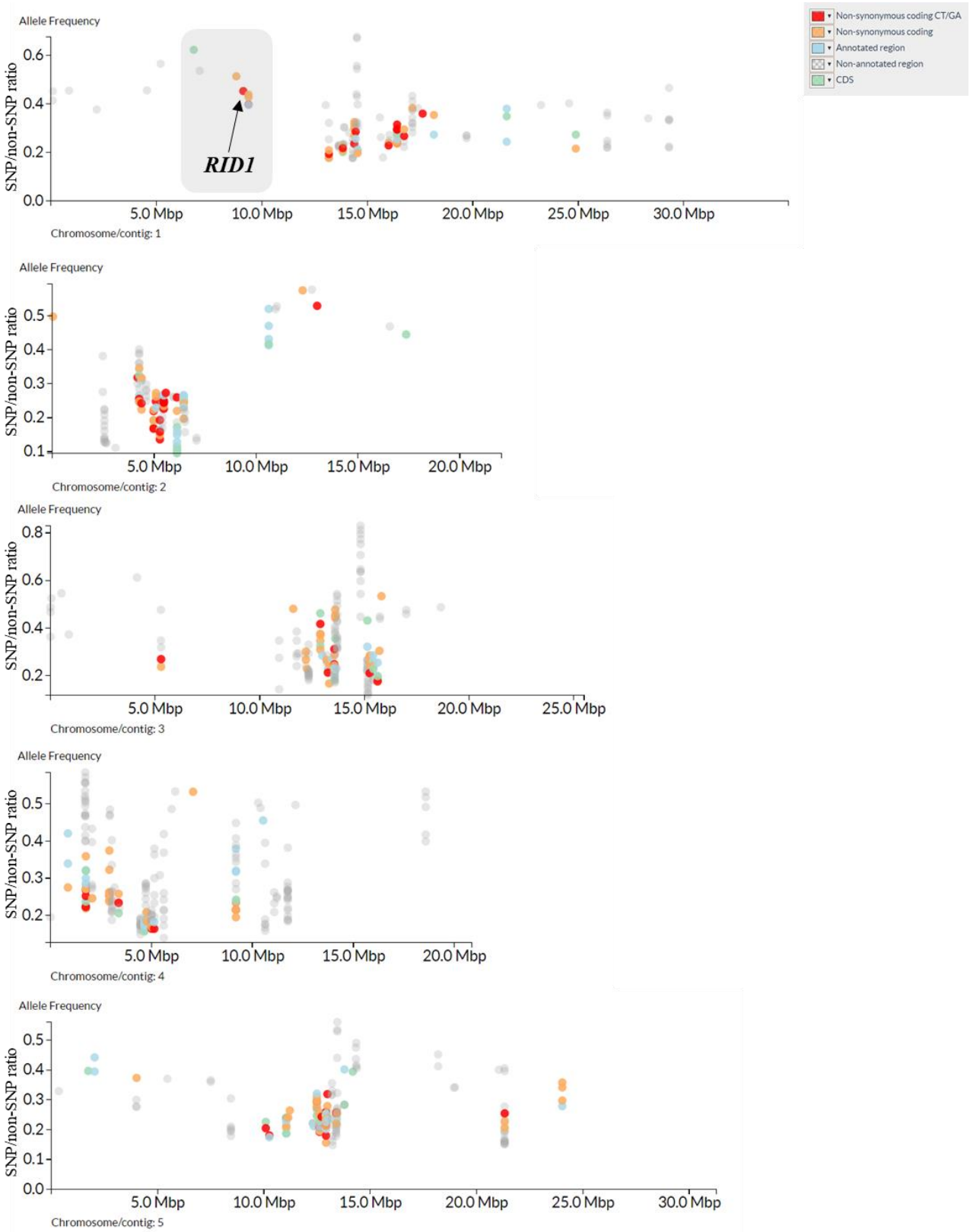

Figure S5. SNP/non-SNP ratio plots of ADZ12 EMS mutant candidate. Obtained SNP/non-SNP ratios for all ADZ12 heterozygous SNPs are plotted against respective chromosomal positions. Causative SNP should have a segregation ratio of SNP/non-SNP of 0.5 (0.4 to 0.6), while non-causative SNPs lie outside this range. Grey box is highlighting genetically linked region of chromosome 1 with the causative SNP in *RID1*. CandiSNP tool was used to plot SNPs to their chromosomal positions. Legend is illustrating the type of effect SNPs have on the corresponding gene.

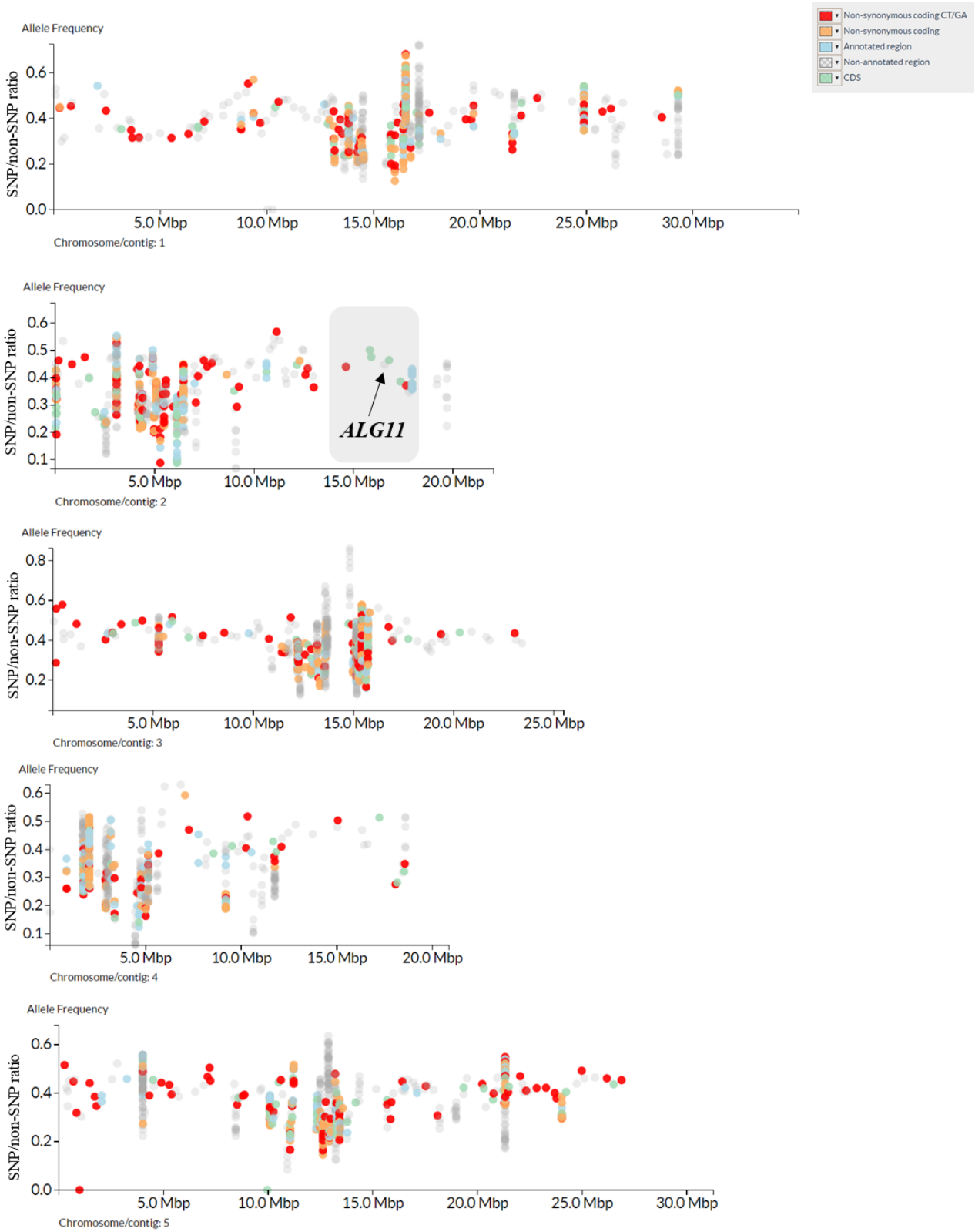

Figure S6. SNP/non-SNP ratio plots of ADZ17 EMS mutant candidate. Obtained SNP/non-SNP ratios of all heterozygous SNPs of ADZ17 are plotted against respective chromosomal positions. Causative SNP should have a SNP/non-SNP of 0.5 (0.4 to 0.6), while outside this range are positioned non-causative SNPs. The grey boxed area points out the genetically linked region of chromosome 1 with the causative SNP in *ALG11*. CandiSNP software tool was used to plot SNPs to their chromosomal positions. Legend is indicating type of effect SNPs have on the corresponding gene.

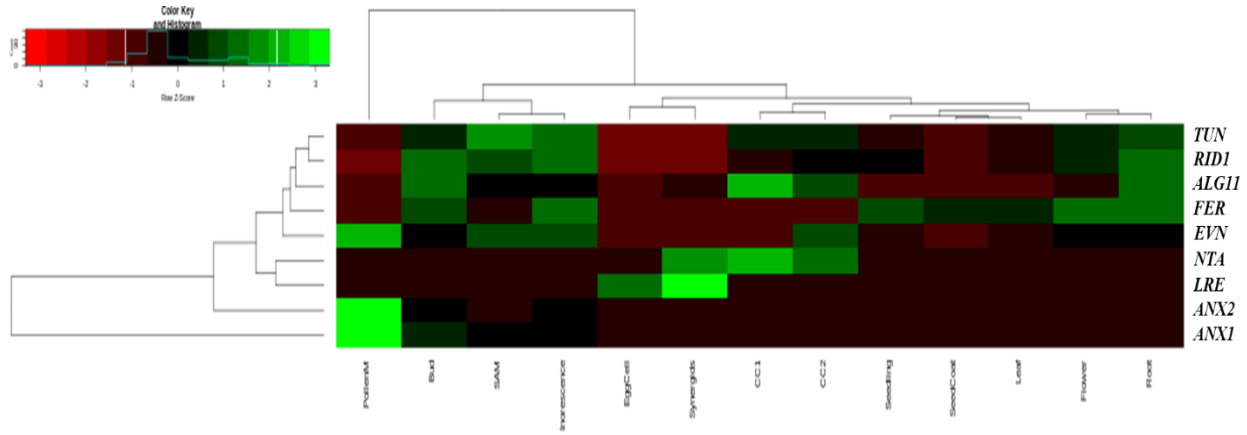

Figure S7. Expression data of mapped EMS candidates and PT reception players in different plant tissues. Heatmap of RNA-Seq data obtained from the previously published female gametophyte expression map (Wuest et al., 2010).

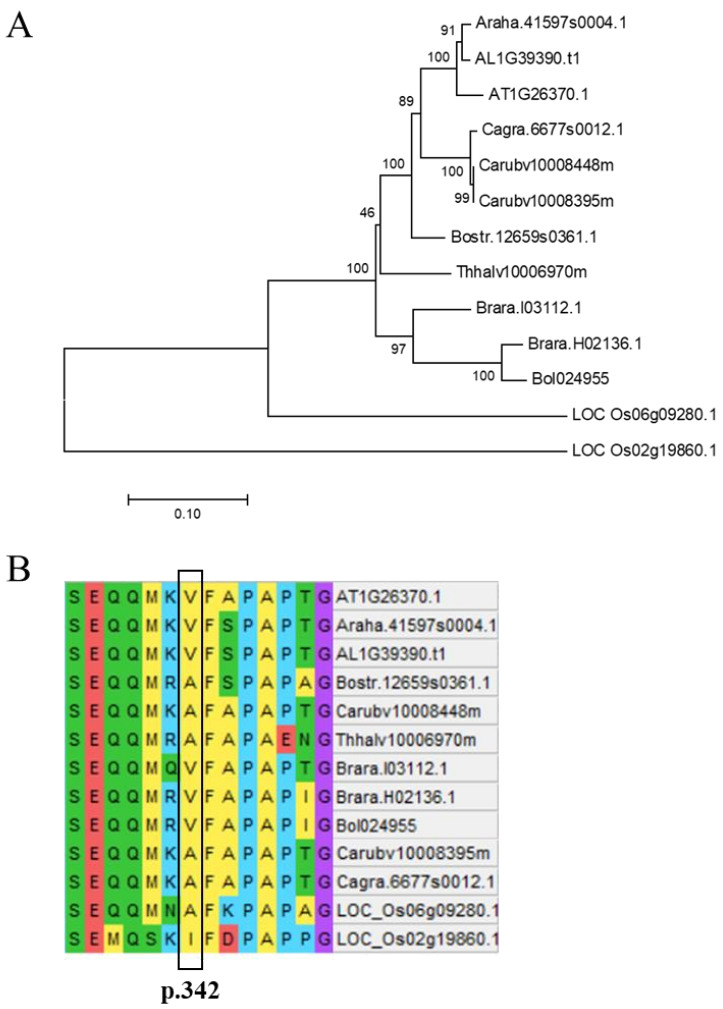

Figure S8. Phylogenetic analysis of RID1 conservation. **A)** Phylogenetic tree based on the full-length amino acid sequences of RID1 orthologs. Multiple alignments were performed using ClustalW2.0. Tree was reconstructed using Neighbor-Joining method, followed by bootstrap testing (1000 repetitions). The percentage of replicate trees in which the associated taxa clustered together in the bootstrap test are shown next to the branches Evolutionary analysis was conducted in MEGA7 (Kumar et al., 2016). **B)** Multiple protein sequence alignment of RID1 and its homologs with a focus on the EMS causative SNP position (p. 342).

Table S1. Normalized expression values of PT reception genes from RNA-Seq data. Data was obtained from the previously established gene expression map (Wuest et al., 2010).

AGI code	Gene name	Flower	PollenM	EggCell	Synergids	CC1	CC2	Seedling	Root	Leaf
AT1G16570	*TUN*	76.00	27.37	13.17	3.09	70.71	81.01	45.48	93.67	41.41
AT1G26370	*RID1*	65.05	0.39	2.79	1.93	36.47	51.44	59.78	108.77	39.08
AT2G17430	*NTA*	1.92	0.17	1.79	144.90	173.04	114.02	1.18	5.41	0.27
AT2G40190	*ALG11*	19.32	0.13	1.77	16.27	98.51	58.64	12.57	73.70	11.11
AT3G04690	*ANX1*	61.05	1493.15	6.76	4.77	0.53	0.53	32.59	24.78	18.00
AT3G45040	*EVN*	44.49	148.47	2.84	1.94	4.85	84.58	24.57	40.59	20.62
AT3G51550	*FER*	100.29	0.02	1.00	0.26	3.26	0.02	67.69	87.03	51.66
AT4G26466	*LRE*	0.19	0.19	111.82	222.02	1.32	2.74	0.86	0.19	0.26
AT5G28680	*ANX2*	5.97	497.79	0.37	0.26	0.03	0.03	0.23	0.03	0.04

Table S2. Normalized expression values of PT reception genes from Affymetrix Arabidopsis ATH1 arrays data. Microarray data was obtained from several studies (Borges et al., 2008; Honys and Twell, 2004; Pina et al., 2005; Schmidt et al., 2011).

AGI code	Gene name	Flowers	PollenM	Eggcells	Synergids	CCs	Seedling	Root_epidermis	Leaf
AT1G16570	*TUN*	8.38	8.93	8.52	8.08	8.71	8.62	8.97	8.10
AT1G26370	*RID1*	7.10	7.23	7.25	6.33	7.13	6.95	7.20	6.68
AT2G17430	*NTA*	3.87	4.42	4.92	8.39	6.21	4.12	4.28	3.90
AT3G04690	*ANX1*	4.28	10.89	3.89	4.65	3.79	3.37	3.46	3.47
AT3G45040	*EVN*	7.80	10.88	8.50	7.81	8.67	7.97	8.21	7.55
AT3G51550	*FER*	9.45	4.24	5.35	4.77	5.73	9.02	9.54	9.94
AT5G28680	*ANX2*	5.26	12.22	3.81	4.24	4.01	3.37	3.49	3.37

Table S3. List of T-DNA lines used in this study with respective molecular markers.

Locus	Mutant line	PCR genotyping
AT1G16570	adz8/ADZ8 (tun-2)	ADZ190/ADZ191
AT2G40190	adz17/ADZ17 (alg11-1)	ADZ156/ADZ157
AT1G26370	adz12/ADZ12 (rid1-1)	ADZ158/ADZ159
AT1G26370	GK-730B12 (rid1-2)	ADZ146/ADZ7147/ADZ186
AT1G26370	GK-310A05 (rid1-3)	ADZ144/ADZ145/ADZ186
AT1G19580	SALK_109391C (gamca-1)	ADZ148/ADZ149/ADZ184
AT1G19580	SALK_061105C (gamca-2)	ADZ150/ADZ151/ADZ184

Table S4. List of all primers and their respective sequences.

Primers	Primer Sequence (5’- 3’)
ADZ190	GTACCAGCGCCTGACATTTT
ADZ191	TGGCTCTGTTTTTCCAATTCA
ADZ156	CTCCTTGCTTATTTGGTGTT
ADZ157	CTGGATCCCTCACCTTCT
ADZ158	GGTTATTGGTTTGGTGATCT
ADZ159	CGATGTCTCCGCTATATT
ADZ144	ACATTCTGGTTTCGCACGGAATAA
ADZ145	AAGAAATGCTGATCACTGTTGCCG
ADZ146	ATACCTTCTTTGAAGCGTCTGTGC
ADZ147	AAGCTGATCATTATGTCTGCCAGT
ADZ148	TAGCGATTCTGGATTCGAATG
ADZ149	CATCCCATGCTTTTCAACAAC
ADZ150	AGCCTCAATGTTTGGTGTTTG
ADZ151	TTCAATTTCACACCAACCTCC
ADZ184	ATTTTGCCGATTTCGGAAC
ADZ186	ATATTGACCATCATACTCATTGC

CHAPTER 3 - RESULTS

N-linked glycosylation mediates gametophyte recognition during pollen tube reception in *Arabidopsis thaliana*

N-linked glycosylation mediates gametophyte recognition during pollen tube reception in *Arabidopsis thaliana*

Andrea Zupunski, Andrea Martinez-Bernardini, Stefan Wyder, Hiroko Shimosato-Asano, and Ueli Grossniklaus

Institute of Plant and Microbial Biology & Zurich-Basel Plant Science Center, University of Zürich, Zollikerstrasse 107, 8008 Zürich, Switzerland

Abstract

Double fertilization in flowering plants (angiosperms) and subsequent seed production rely on the successful transfer of sperm cells by pollen tubes (PT) to the embryo sack. Crucial role of receptor-like kinases during the PT reception was revealed with a discovery of *feronia* mutant in which PTs fail to rupture and instead keep overgrowing inside the embryo sack. Forward-genetic screen has been carried out to identify additional members of the FERONIA (FER) receptor-like kinase signaling pathway involved in PT reception. We have characterized a novel component of the FER pathway, ortholog of yeast ALG11, which encodes a putative alpha-1,2-mannosyltransferase and is a part of endoplasmic reticulum (ER) *N*-glycosylation pathway. Loss of ALG11 caused lethality, and heterozygous plants displayed *fer*-like PT overgrowth as well as loss of the PT integrity leading to the premature PT bursting. FER was properly localized to the filiform apparatus in the *alg11/ALG11* ovules, indicating that FER biogenesis was not compromised. Interspecific crosses between closely related species of the *Brassicaceae* family present a *fer*-like PT overgrowth phenotype, however underlying molecular mechanisms are scarce. Here we report that ALG11 is involved in the recognition of interspecific pollen similarly to ARTUMES (ARU) a first ever described component of interspecific PT reception pathway. Therefore, we have employed a reverse genetic approach and found additional ER-resident members of the *N*-glycosylation pathway to be involved in the recognition of interspecific pollen. Compared to the early processing steps occurring in the ER far less is known about the importance of Golgi associated *N*-glycan maturation on the plant development. Here we report the first ever connection of Golgi processing and the plant reproduction, more specifically the proper gametophyte recognition during pollen tube reception relies on the presence on complex-type glycans. Taken together we have found novel component of PT reception pathway, and further corroborated essential need for *N*-glycosylation during the establishment and maintenance of interspecific hybridization barriers.

Keywords: angiosperms; double fertilization; pollen tube reception; FERONIA; *N*-glycosylation pathway; endoplasmic reticulum; Golgi apparatus.

Introduction

Once a compatible pollen has landed on the stigma, an extensive journey to the female gametophyte can begin. Successful double fertilization depends on the proper communication between pollen and different maternal tissues, which enables pollen adhesion, hydration, pollen tube (PT) germination and growth through the transmitting tract (TT) (Adhikari et al., 2020; Dresselhaus et al., 2016).

Interaction among pollen grains and stigma involves an active molecular crosstalk between stigma localized heavily *N*-glycosylated receptor SRK (S-locus receptor kinase) and pollen-coat SCR (S-locus cysteine-rich) to allow further PT growth (Adhikari et al., 2020; Yamamoto et al., 2014). This receptor-ligand pair are key determinants of the self-incompatibility responses within *Brassicaceae* family. When *Arabidopsis lyrata* signaling pair SRK-SCR was introduces to the self-fertile *Arabidopsis thaliana* it generated self-incompatibility phenotype (Nasrallah, 2002). Once PTs have successfully penetrated stigmatic papilla cells, they continue growing through transmitting tract, guided by the ovular secreted cues.

Synergids cells are actively secreting cysteine-rich (CR) peptides such as LUREs and XIUQIU, and arabinogalactan polysaccharide AMOR, to promote PT navigation towards ovules (Mizukami et al., 2016; Okuda et al., 2009; Takeuchi and Higashiyama, 2012; Zhong et al., 2019). Pollen tubes plasma membrane-localized LRR-RLK (leucine-rich repeats receptor-like kinases) of two clades, POLLEN RECEPTOR LIKE KINASES (PRKs) or MALE DISCOVERER 1 (MDIS1) and MDIS1-INTERACTING RLK (MIK) are required to sense LURE1 and enable PT growth towards embryo sack (Takeuchi and Higashiyama, 2016; Wang et al., 2016). *Brassicaceae* family conserved XIUQUIs peptides attract PTs in a non-species-specific manner, while AtLURE1s and PRK6 ligand-receptor pair enables faster septum penetration of conspecific (*A. thaliana*) compared to heterospecific (*A. lyrata*) pollen. Taken together, AtLURE1 ligands and their male receptor PRK6 are required for the maintenance of reproductive isolation (Zhong et al., 2019).

Receptor like kinase (RLK) with more than 600 members in *A. thaliana*, play essential roles during each step of this extensive PT journey (Higashiyama, 2018; Kanaoka, 2018; Shiu and Bleecker, 2003). RLKs consist of a conserved intracellular kinase domain (ICD), a transmembrane domain (TMD) and a diverse extracellular domain (ECD) (Lindner et al., 2012a). Based on differences within their ECDs, RLK can be divided in 15 groups, with *Catharanthus roseus* RLK 1-like (*Cr*RLK1L) subfamily being the most extensively studied in the recent years (Galindo-Trigo et al., 2016). FERONIA (FER) the first functionally characterized member of the *Cr*RLK1L subfamily is a key player of pollen tube reception pathway. In the case of compatible pollinations (self-pollinations) once PT arrive to the proximity of synergid cells, extensive molecular cross talk occurs leading to the PT burst and release of two sperm cells. Subsequently double fertilization occurs enabling formation of embryo and endosperm (Dresselhaus and Franklin-Tong, 2013; Sankaranarayanan and Higashiyama, 2018). In the absence of FER, pollen tubes fail to burst in the synergid cells leading to the continuous growth of pollen tube inside the embryo sack (Escobar-Restrepo et al., 2007; Huck, 2003). Similar *fer*-like PT overgrowth (PTO) phenotype was observed in the interspecific crosses between closely related *Brassicaceae* family. *A. thaliana, A. lyrata* or *A. arenosa* (Escobar-Restrepo et al., 2007), suggesting that FER could play an active role also during interspecific pollen tube reception. Additionally the degree of sequence divergence in the FER extracellular domain is in direct correlation with the extent of interspecific PT overgrowth phenotype in crosses within *Brassicaceae* family (Escobar-Restrepo et al., 2007).

Since the discovery of FER, several other mutants displaying *fer*-like PTO phenotype were described, including *scylla, lorelei*, *nortia*, RNAi maternal *enodls*, abstinence by mutual consent (*amc*), and *myb97 myb101 myb120* (Boisson-Dernier et al., 2008; Capron et al., 2008; Hou et al., 2016; Kessler et al., 2010; Leydon et al., 2013; Liang et al., 2013; Rotman et al., 2008). Interestingly simultaneous loss of the closest homologs of FER, pollen expressed ANX1 and ANX2, leads to the opposite

phenotype of *fer* and causes premature PT bursting instead (Boisson-Dernier et al., 2009, 2013; Miyazaki et al., 2009).

Our group has previously performed an EMS screen to find novel components of the FER mediated PT reception pathway. Two EMS mutants with PTO were mapped to a putative UDP glycosyltransferase superfamily protein TURAN (TUN) and a dolichol kinase EVAN (EVN) (Lindner et al., 2012a). TUN and EVN are ER-localized members of *N*-glycosylation pathway, involved in the biosynthesis of the lipid linked oligosaccharide on the cytosolic side of the ER membrane (Aebi, 2013; Strasser, 2016). TUN and EVN also have roles during pollen development and PT integrity maintenance. PTs of *tun/TUN* are bursting upon germination, phenotype reminiscent of *anx1/anx2* pollen. TUN is needed for biogenesis of ANX1/2, however FER, LRE and NTA biogenesis was unaffected as well as their synergid localization in both *tun/TUN* and *evn/EVN* ovules (Lindner et al., 2012a). This study was the first showing vast importance of *N*-glycosylation for the proper PT reception. All members of the *Cr*RLK1L family have several putative *N*-glycosylation sites within their ECDs. However bare presence of predicted consensus motif does not imply protein *N*-glycosylation *in planta*. The key step of *N*-glycosylation is catalyzed by the OST complex which is transferring preassembled oligosaccharide ($NAcGlc_2Man_9Glc_3$) to the asparagine residue within consensus motif Asn-x-Ser/Thr (x≠P) of nascent polypeptides (Aebi, 2013). Glycoproteomic study (Zielinska et al., 2012) using *A. thaliana* inflorescence has detected presence of *N*-glycans at five predicted *N*-glycosylation sites within FER^{ECD}. In line with those observations, a recent crystallography study found three putative *N*-glycosylation sites to be occupied with *N*-glycans in FER^{ECD} (Xiao et al., 2019).

Further confirmation of *N*-glycosylation importance during gametophyte interaction came from the previous study in our group, in which the first known molecular factor exclusively involved in the regulation of interspecific pollen recognition was discovered (Müller et al., 2016). Mutants affected in ARTUMES (ARU) encoding a oligosaccharyltransferase 3/6 subunit (OST3/6), displayed significantly higher number of ovules with PTO in the comparison to the Col-0 when pollinated with the closely related *A. lyrata* (Müller et al., 2016). Even though biogenesis of FER was not affected in *aru* ovules, it is likely that FER is a target of OST complex, since *fer/FER* displayed similar interspecific pollen tube reception phenotype to *aru-1* (Müller et al., 2016).

Importance of OST complex has already been demonstrated, for instance loss of DEFECTIVE GLYCOSYLATION 1 (DGL1), an essential subunit of OST complex led to the embryo lethality. Weaker allele of DGL1 displayed reduced cell elongation, dwarfed phenotype, and 22 % of seed set abortion (Lerouxel et al., 2005). Similarly, simultaneous loss of two subunits of OST complex STT3A and STT3B led to the gametophytic lethality (Koiwa, 2003). Only recently Arabidopsis OST complex was purified using tandem affinity-tagged STT3a subunit and mass spectrometry (MS) analysis identified super complex formation (STT3a, OST1, HAP6, DGL1 and ribosome subunits) (Jeong et al., 2018). Loss of both OST1 isoforms (*ost1a/ost1b*) caused the gametophytic lethality, while mutation of DAD 1/2 (Defender Against apoptotic cell Death 1/2) led to the male gametophyte defects (Jeong et al., 2018).

Unlike severe phenotypes observed in the mutants affected in the enzymes of ER *N*-glycosylation pathway, loss of Golgi localized enzymes involved in *N*-glycans maturation is much better tolerated by the plant (Nagashima et al., 2018; Strasser, 2016). Key step of the complex type glycan formation is catalyzed by the β1,2-N-acetylglucosaminyltransferase I (GnTI/CGL1), which is recognizing final product of ER processing ($Man_5GlcNAc_2$) and adding a single *N*-acetylglucosamine (GlcNAc)

residue to the exposed α1,3-mannose (Aebi, 2013; Strasser, 2016). Mutants defective in GnTI, complex glycan less 1 (*cgl1*) are fully viable, even though all plant glycoproteins are of oligomannosidic type (Strasser, 2014). Regardless the fact that in plants around three quarters of all *N*-linked glycans are of the complex type, surprisingly little is known about their roles during plant growth and development (Strasser et al., 2004).

Here we report a novel component of the FER pollen tube reception pathway. Using SRM approach we have successfully mapped EMS mutant with *fer*-like PT overgrowth phenotype to the *ALG11* encoding an *N*-glycosylation ER-resident α1,2-mannosyltranferase. Mutant displayed 21% of *fer*-like PT overgrowth, 33% of pollen tube bursting as well as interspecific pollen tube reception defect. Reverse genetic approach revealed novel roles of the ER *N*-glycosylation enzymes ALG3 and ALG10 during interspecific pollen tube reception. Lastly, we report the first connection of Golgi associated *N*-glycan maturation to the gametophyte recognition during PT reception in *A. thaliana.*

Results

ALG11 is a novel component of PT reception pathway

Forward-genetic screen has been carried out to identify additional members of the FER signaling pathway required for the pollen tube reception. From an ethyl methanesulfunate (EMS)-screen several mutants with *fer*-like PTO phenotype have been identified (Lindner et al., 2015). Two of them, named TURAN and EVAN, were successfully identified using SNP ratio mapping (SRM) approach (Lindner et al., 2012) which is especially useful for the mapping of lethal or poorly transmitted mutations. Utilizing the same SRM approach on the uncharacterized EMS mutant candidate, revealed a stop codon in the third exon of the *AT2G40190* (*LEAF WILTING 3, LEW3*). *LEW3* was previously named due to the leaf wilting phenotype of a mutant isolated from an EMS screen (Zhang et al., 2009).

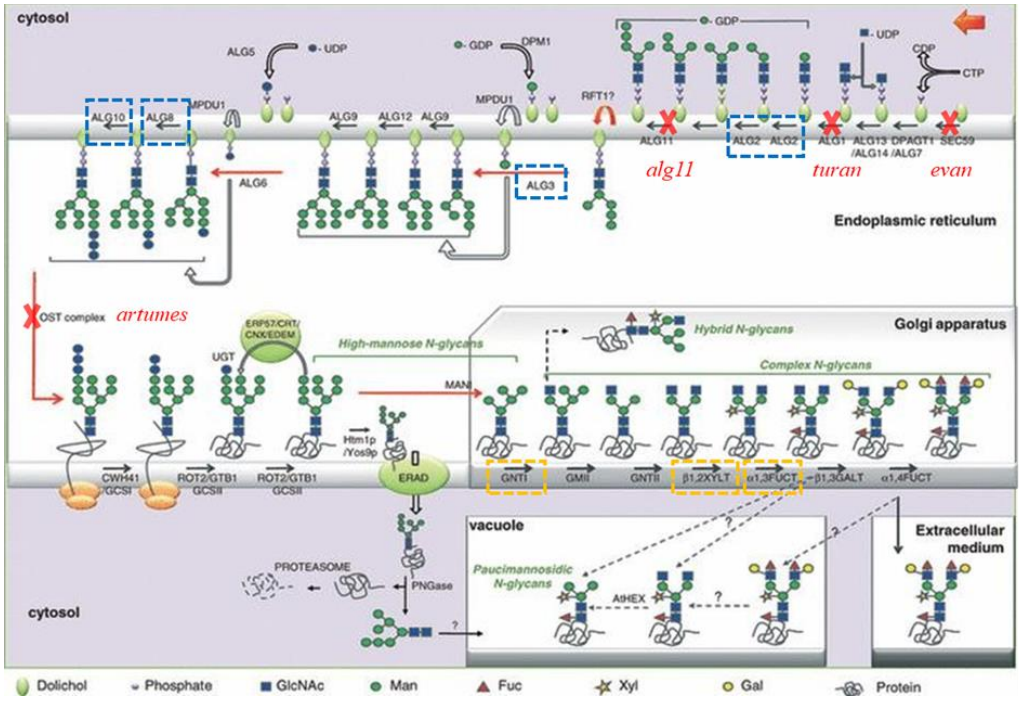

Figure 1. *N*-glycosylation in *A. thaliana*. Functionally characterized members of the *N*-glycosylation pathway with the name of the respective mutants are labeled in red. In the boxed area are indicated either endoplasmic

reticulum (blue box) or Golgi apparatus (orange) resident members that were investigated in this study. Image adapted from Gomord et al., 2010.

This gene encodes an alpha-1,2-mannosyltransferase of ER *N*-glycosylation pathway ortholog to yeast *ASPARAGINE-LINKED GLYCOSYLATION 11*, so it will be referred as *ALG11* in this chapter. It is involved in the *N*-glycan synthesis (Fig. 1) on the lipid carrier dolichylphosphate, catalyzing addition of mannoses only two steps after TURAN (TUN) processing (Aebi, 2013; Strasser, 2016). Previous study found that loss of ALG11 function leads to various developmental phenotypes including impaired cellulose synthesis, xylem collapse, increased sensitivity to osmotic stress and abscisic acid (ABA) treatment (Zhang et al., 2009). Additionally, a more recent study showed a light sensitive short root phenotype caused by impaired cell divisions and elongation of root cells (Manzano et al., 2017). However, none of the above-mentioned studies looked at the reduced fertility of ALG11 mutants. In order to confirm that fertility problems are due to *ALG11* mutation, two independent T-DNA insertion lines have been analyzed, *alg11-2* (SALK_000886), with the T-DNA insertion in its promoter region (Manzano et al., 2017), and *alg11-3* (SALK_106951) with an insertion in the fifth exon (Zhang et al., 2009) (Fig. 2A). Both T-DNA insertion lines showed the same *fer*-like PTO phenotype, as observed in the EMS line *alg11-1*, confirming the importance of ALG11 during PT reception (Fig. 2B/C).

To analyze if the fertility problem came from the female or male gametophyte, reciprocal crosses were performed. Mutant *alg11-1/ALG11* displayed PT overgrowth phenotype only when used as a female parent, while mutant pollen deposited on the wild type stigmas did not lead to the *fer*-like overgrowth phenotype (Fig. S1). Therefore, observed pollen tube overgrowth is caused by the female gametophytic issue, reminiscent of the previously described *tun/TUN* and *evn/EVN* (Lindner et al., 2015).

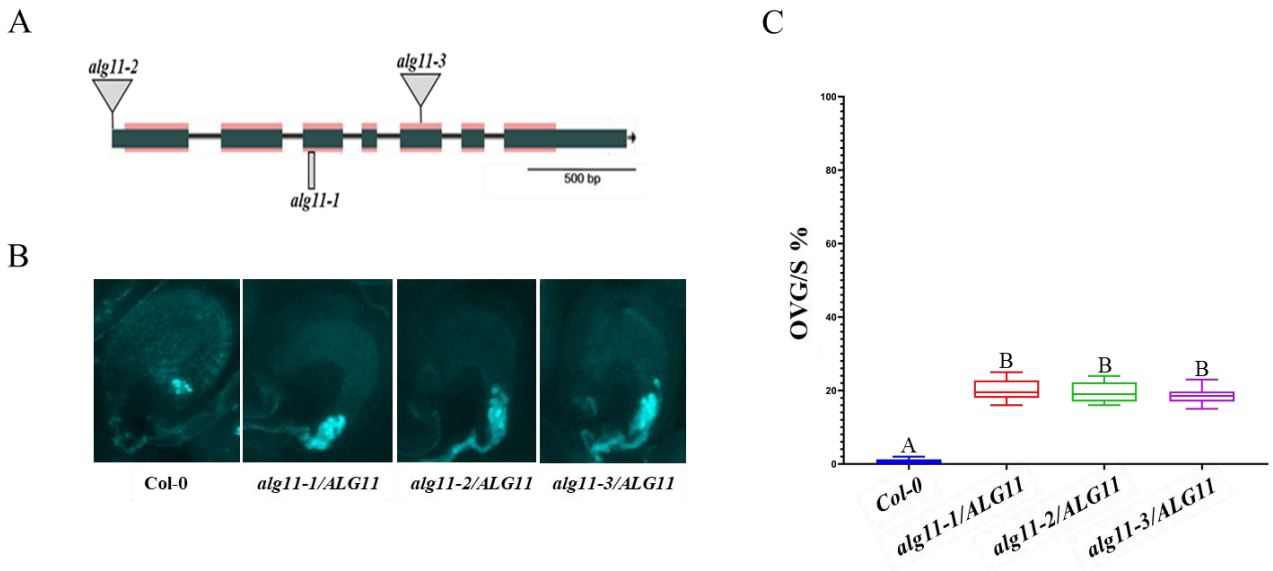

Figure 2. *alg11* mutants displays *fer*-like pollen tube overgrowth. (A) Schematic representation of *ALG11* locus with mutant alleles. Grey rectangle represents EMS causative SNP and grey triangles indicate T-DNA insertions. **(B)** Aniline blue staining of WT (Col-0) and mutant ovules reveals PT overgrowth in all three *ALG11* mutant alleles. **(C)** Intraspecific pollen tube reception of Col-0 and three mutant alleles of *ALG11*. Box plots represent the percentage of pollen tube overgrowth per silique (OVG/S). At least ten self-pollinated

siliques per genotype (five plants) were analyzed using aniline blue staining (n>2500 ovules per genotype). One-way ANOVA followed by Tukey's multiple comparison test (A-B ****P<0.0001).

We have checked if *ALG11* has a similar pattern of expression compared to the already known players of the PT reception pathway. Based on RNA-Seq data, *ALG11* tissue expression pattern shares the highest similarity with *TUN* and *FER* (clustering together), with a unique extraordinarily strong expression in central cells (Fig. 3C, Fig. S3, Tab. S1). The fact that *ALG11* has overlapping tissue expression pattern with *FER* is in line with the fact that *alg11* shows *fer*-like PTO. It is probable that due to the lower amount of ALG11, FER is inefficiently glycosylated, subsequently impacting receptor function. But a deeper analysis of FER N-glycosylation status in *alg11-1/ALG11* should be done.

Loss of ALG11 function leads to the salt stress hypersensitivity, with no additional vegetative growth phenotypes

Since *ALG11* was discovered through an EMS screen for mutants displaying *fer*-like PTO phenotype we wondered if the loss of ALG11 would phenocopy other *fer-4* vegetative phenotypes, namely root hair bursting, dwarfism, shorter petiole length, and anthocyanin accumulation (Duan et al., 2010; Guo et al., 2009). Firstly, using publicly available RNA-sequencing data we have checked whether *ALG11* is expressed in other tissues besides female gametophyte. *ALG11* is expressed throughout the plant, with the strongest expression in root, followed by seedling and leaves (Fig. 3C, Tab. S1). Therefore, since *ALG11* is broadly expressed, and having in mind that aberrant *N*-glycosylation is affecting 75% of secreted proteins (Lannoo and Van Damme, 2015; Medus et al., 2017), pleiotropic phenotypes could be expected. Firstly, we have checked if growth of root hairs is disrupted, however *alg11-1/ALG11* root hairs were fully developed and were able to reach the wild-type length (Fig. 3A). Additionally, petiole length, and shoot growth were all wild type like (data not shown).

Previously it was reported that loss of ALG11 led to the seed germination delay under salt or ABA treated conditions. Additionally swelling of the root tip under high salt stress was more prominent in the absence of *ALG11* compared to the wild type (Zhang et al., 2009). Recently it was demonstrated that during salt stress FER is required to sense cell wall (CW) loosening and accordingly regulate root growth. Hence in *fer-4* root cells exploded during recovery phase (Feng et al., 2018). Therefore, we have exposed *fer-4* and *alg11-1/ALG11* mutants to the high salinity conditions (140mM NaCl). Compared to the wild type Col-0 both *fer-4* and *alg11-1/ALG11* displayed significant inhibition of the primary root growth after only two days of treatment (Fig. 3B). Since it was proposed that these defects in *fer-4* can be rescued by supplementation with borate and calcium in the growth media (Feng et al., 2018), it remains to be tested if the same would apply for *alg11-1/ALG11*. Additionally, authors proposed that FER is binding CW pectin through its extracellular domain, based on the *in vitro* assays with the pectin backbone polymer polygalacturonic acid (PGA) (Feng et al., 2018). Knowing that FER extracellular domain is heavily glycosylated (detail description in the Chapter 4 of this thesis), it is conceivable that in the *alg11-1/ALG11* background FER is under- or miss-glycosylated, thus impacting FER`s ability to properly respond to the changes in CW upon exposure to the salt stress.

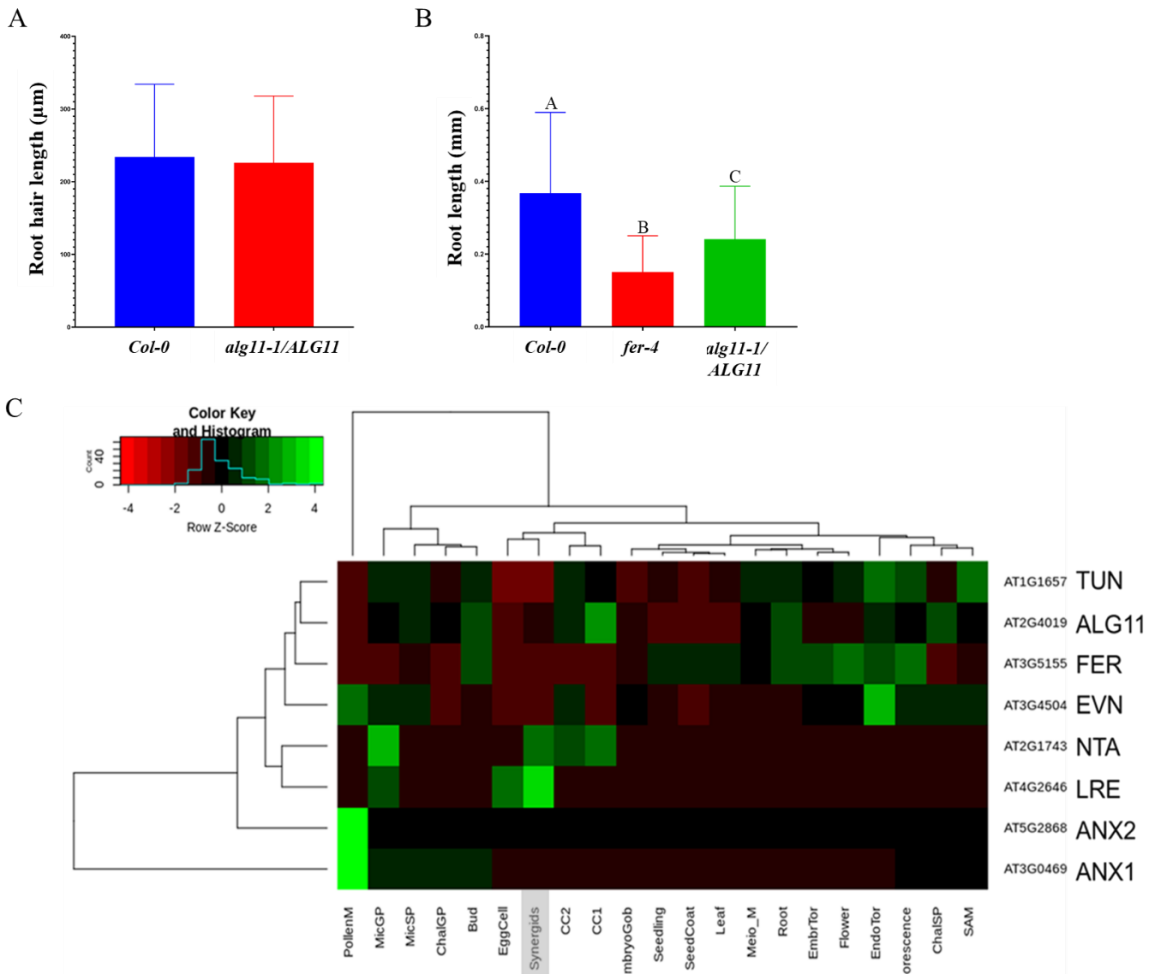

Figure 3. Loss of ALG11 leads to the hypersensitivity to salt stress. (A) Root hair length is not affected in *alg11-1/ALG11*. Images of 5 days old Col-0 and *alg11-1/ALG11*. Sample size Col-0 (n=140), *alg11-1/ALG11* (n=164). Mann-Whitney *U*-test (ns). **(B)** Primary root length of Col-0, *fer-4* and *alg11-1/ALG11* after two days of salt stress treatment (140 mM NaCl). Sample size: Col-0 (n=92), *fer-4* (86), *alg11-1/ALG11* (n=124). Kruskal-Wallis test followed by Dunn`s multiple comparison test (A-B ****P<0.0001; A-C *P=0.016; B-C *P=0.045). **(C)** Expression data of *ALG11* and PT reception players in different plant tissues. Heatmap of RNA-Seq data obtained from the previously published female gametophyte expression map (Wuest et al., 2010).

ALG11 is involved in both intra- and inter-specific pollen tube reception

With purpose of assessing fertility issues of *alg11-1/ALG11* plants, fully matured siliques were harvested for the seed set analysis. Visibly shorter siliques of mutant, compared to the wild type (Col-0), were indicative of a diminished fertility. Fully expanded siliques of *alg11-1/ALG11* were dissected, and the number of developed seeds was significantly reduced compared to the Col-0 (Fig. 4A). In order to get an insight in the pollen tube (PT) reception dynamics, PTs were visualized using aniline blue staining (Huck, 2003). In the case of *alg11-1/ALG11* 21% of targeted ovules displayed PT overgrowth, compared to less than 2% in the wild-type (Fig. 4B). Therefore, it can be concluded that ALG11 plays an important role during PT reception. It remains to be elucidated if the observed phenotype stems from the mis- or under- glycosylation of FER and/or other important PT reception players (LRE, HERK1, ANJEA).

Having in mind that mutation of OST3/6 subunit of OST complex led to the exclusive impairment of interspecific pollen tube reception (Müller et al., 2016) and FER being involved in both intra- and inter-specific PT reception (Müller et al., 2016) we hypothesized that loss of ALG11 would impact ability to distinguish between self and foreign pollen. In order to test this hypothesis, interspecific crosses with the closely related *Brassicaceae* species *A. lyrata* were performed. Wild type *A. thaliana* (ecotype Col-0) showed around 45 % of PT overgrowth when pollinated with heterospecific *A. lyrata* pollen. However, *alg11-1/ALG11* displayed significantly increased level of PT overgrowth compared to Col-0 (75%) (Fig. 4C). This suggests that ALG11 is important for the proper recognition of both self- (*A. thaliana*) and foreign- pollen (*A. lyrata*). The fact that *fer-4* complemented with FER lacking even single *N*-glycosylation site caused substantial impairment of the interspecific PT reception, additionally proves that *N*-glycosylation is necessary for the proper gametophyte recognition during PT reception (detailed description can be found in the Chapter 4 of this thesis).

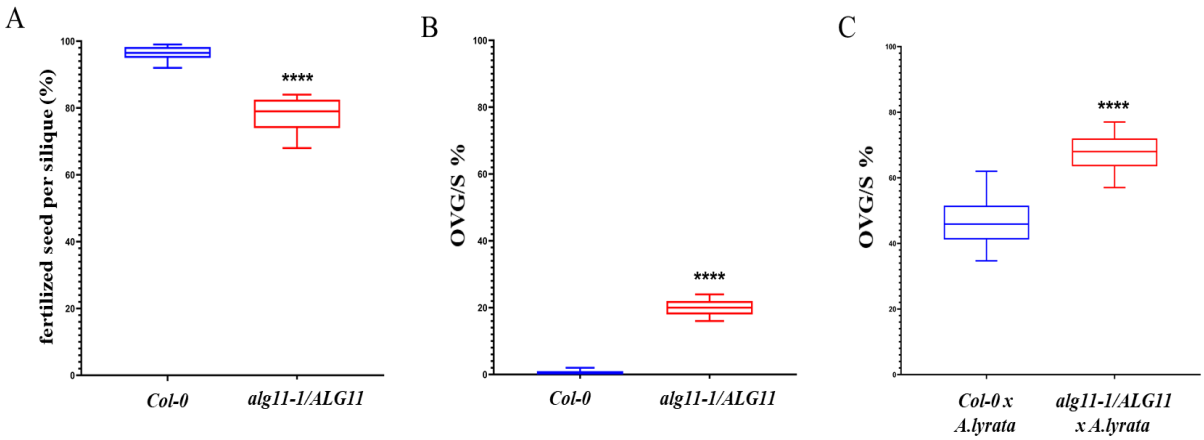

Figure 4. Mutation of ALG11 leads to a disruption of both intra- and inter-specific pollen tube reception. **(A)** Seed count analysis of Col-0 and *alg11-1/ALG11* was performed on the dissected mature siliques. At least five plants per line and five siliques per plant were analyzed (n>1250 seeds per line). Student's t-test ****P<0.0001. **(B)** Intraspecific PT reception of Col-0 and *alg11-1/ALG11*. Box plots represent the percentage of pollen tube overgrowth per silique. At least ten self-pollinated siliques from five plants of Col-0 and *alg11-1/ALG11* were analyzed with aniline blue staining (n>2500 ovules per genotype). Student's t-test ****P<0.0001. **(C)** PT overgrowth of Col-0 and *alg11-1/ALG11* in interspecific crosses with *A. lyrata*. Box plots represent percentage of PT overgrowth per silique of interspecific crosses. Siliques were harvested two days after pollination with *A. lyrata*, and at least three plants per line and five siliques per plant were analyzed using aniline blue staining (n>750 ovules per genotype). Student's t-test ****P<0.0001.

ALG11 is required for the pollen tube integrity maintenance

Along with the previously described female gametophytic *fer*-like PTO phenotype, aniline blue analysis of self-pollinated siliques revealed inability of many ovules to attract pollen tubes. This failure to lure PTs was reduced when flowers of *alg11-1/ALG11* were emasculated and pollinated with the wild type Col-0 pollen. Furthermore, offspring of self-pollinated *alg11-1/ALG11* consisted of only wild-type or heterozygous mutant plants. These observations pointed us to suspicion that mutation of ALG11 also affects the male gametophyte development. In order to test this hypothesis, *in vitro* pollen germination assays were performed (Boavida and McCormick, 2007; Boisson-Dernier et al., 2009; Franck et al., 2018).

Pollen development was normal, however 33% of *alg11-1/ALG11* PTs burst soon after germination, compared to less than 5% observed in the wild-type Col-0 (Fig. 5). This PT bursting phenotype is reminiscent of the *anx1/anx2* double mutants. ANX1/2 are pollen expressed, the closets homologs of FER, which act redundantly to ensure PT integrity during growth. Interestingly the same precocious PT bursting phenotype is observed in the *tun/TUN* in which ANXs is targeted to the ERAD pathway due to the aberrant *N*-glycosylation processing. (Boisson-Dernier et al., 2009, 2013; Lindner et al., 2015). It is probable that ANX1/2 biogenesis is similarly disrupted in the *alg11-1/ALG11*, since ALG11 acts on the substrate only two steps after TUN during *N*-glycosylation processing in the endoplasmic reticulum (Fig. 1) (Gomord et al., 2010; Strasser, 2016). Taken together these results expose ALG11`s importance for the maintenance of CW integrity of PTs and hence its strong impact on the male gametophytic fertility.

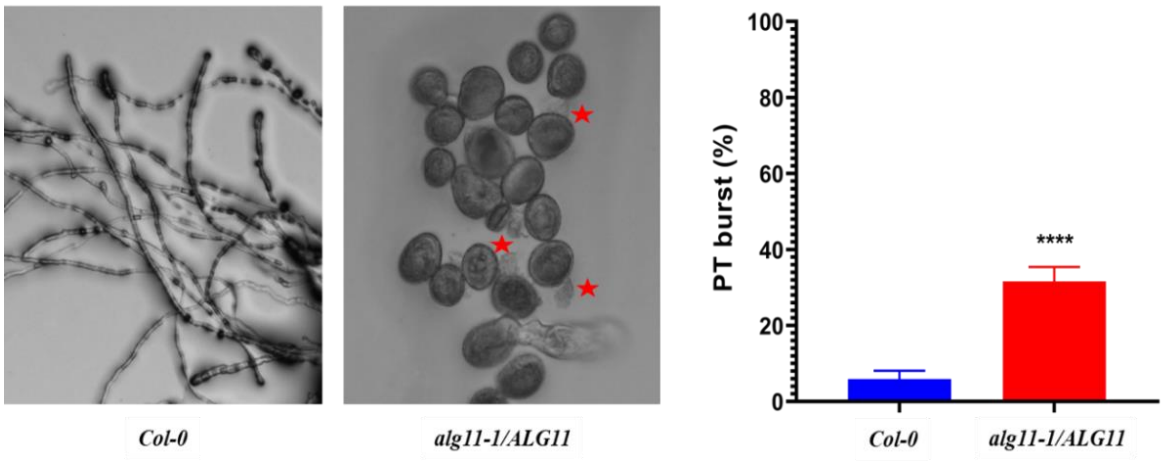

Figure 5. Loss of the ALG11 triggers pollen tube bursting phenotype. Pollen *in vitro* germination assay of Col-0 (on the left) and *alg11-1/ALG11* mutant pollen (on the right). Red stars indicate PT bursting and discharge of cytoplasm to the germination medium. Column bar graph of PT bursting counts of Col-0 and *alg11-1/ALG11* pollen. Pollen germination assays were performed three times. Sample size: Col-0 (n=180) and *alg11-1/ALG11* (n=610). Student's t-test ****P<0.0001.

Complementation of *alg11-1/ALG11*

With purpose of having a final validation of EMS causative SNP in *ALG11* gene being responsible for the observed PTO phenotype, complementation analysis was performed. Construct containing genomic region of *ALG11* (3 kb of promoter and the coding sequence) was transformed into the EMS obtained mutant *alg11-1/ALG11* (Tab.S4). T1 lines expressing ALG11 under its native promoter were fully complementing intraspecific PT reception defects (Fig. 6A), meaning that indeed EMS induced mutation of ALG11 was causative for the observed *fer*-like PTO phenotype. Furthermore interspecific PT reception was restored to the wild type level in the crosses with *A. lyrata* (Fig. 6B). Therefore it can be concluded that ALG11 is vital for the gametophyte recognition during PT reception.

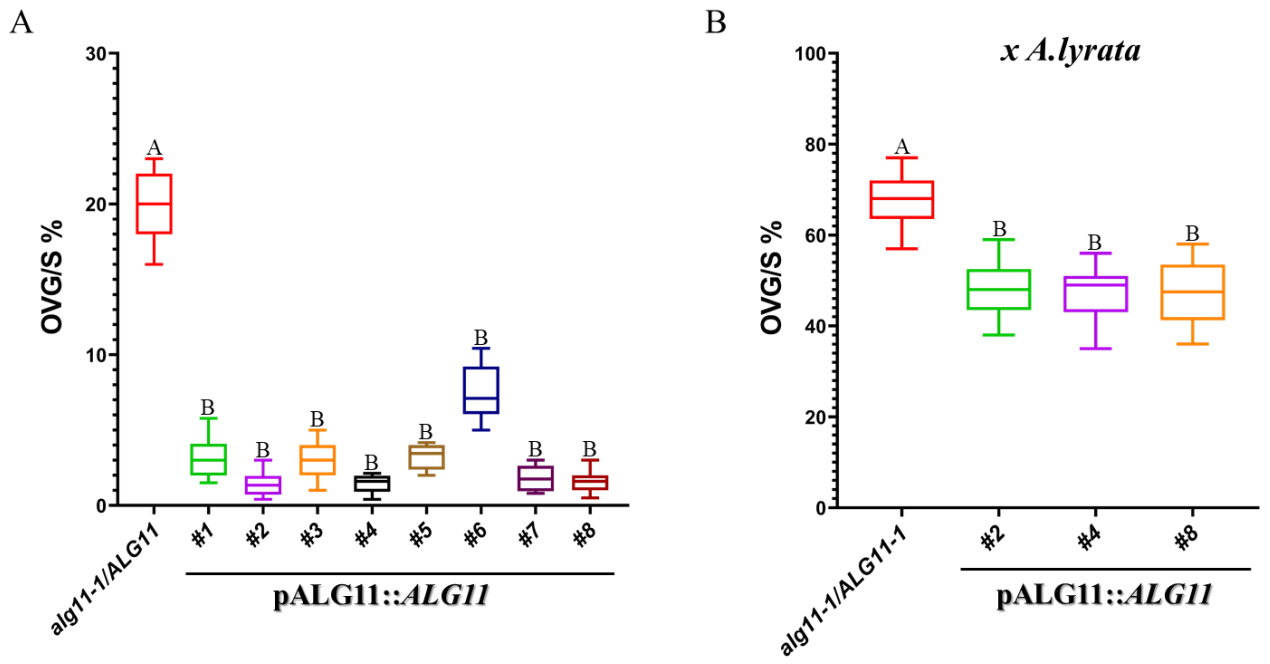

Figure 6. Complementation of *alg11-1* mutants. (A) Intraspecific PT overgrowth is complemented in T1 lines expressing pALG11:*AGL11*. Box plots represent the percentage of ovules with PT overgrowth per silique. Complementation ability was checked in eight independent T1 plants, for each T1 plant ten siliques were analyzed using aniline blue staining (n>500 ovules per T1 line). One-way ANOVA followed by Tukey's multiple comparison test (A-B ****P<0.0001) **(B)** Complementation of interspecific PT overgrowth in crosses with *A. lyrata*. T1 lines expressing ALG11 under its endogenous promotor were emasculated and pollinated two day later with *A. lyrata* pollen. Level of complementation was checked in three independent T1 plants, and for each T1 five siliques were collected two days after pollination and analyzed with aniline blue (n>250 ovules per T1 line). One-way ANOVA followed by Tukey's multiple comparison test (A-B ****P<0.0001).

FER-GFP localization in the female gametophyte is undisturbed in *alg11-1/ALG11* ovules

N-linked glycosylation is the most common posttranslational modification of secretory proteins, crucial for the proper folding as well as quality control and degradation of misfolded proteins (Liu and Li, 2014; Strasser, 2018). Therefore, we have hypothesized that stability and thus localization of FER could be impaired in the *alg11-1/ALG11 N*-glycosylation mutant background. To explore FER expression levels and localization in the female gametophyte, pFER:*FER-GFP* translational fusion was introduced into the *alg11-1/ALG11* mutant background (Tab. S4). Flowers (stage 12) of T1 plants (mutant or wild type segregants) were emasculated, and two days later pistils were dissected and imaged under confocal microscope. Confocal microscopy analyses revealed FER-GFP to be properly localized at the filiform apparatus of synergid cells (Fig. 7), as previously reported for the native FER expression (Escobar-Restrepo et al., 2007). This implies that observed *fer*-like PTO of *alg11-1/ALG11* is not caused by disrupted secretion of FER protein. However, even though FER is localized properly its under-/mis- glycosylation could hamper proper gametophyte recognition during PT reception.

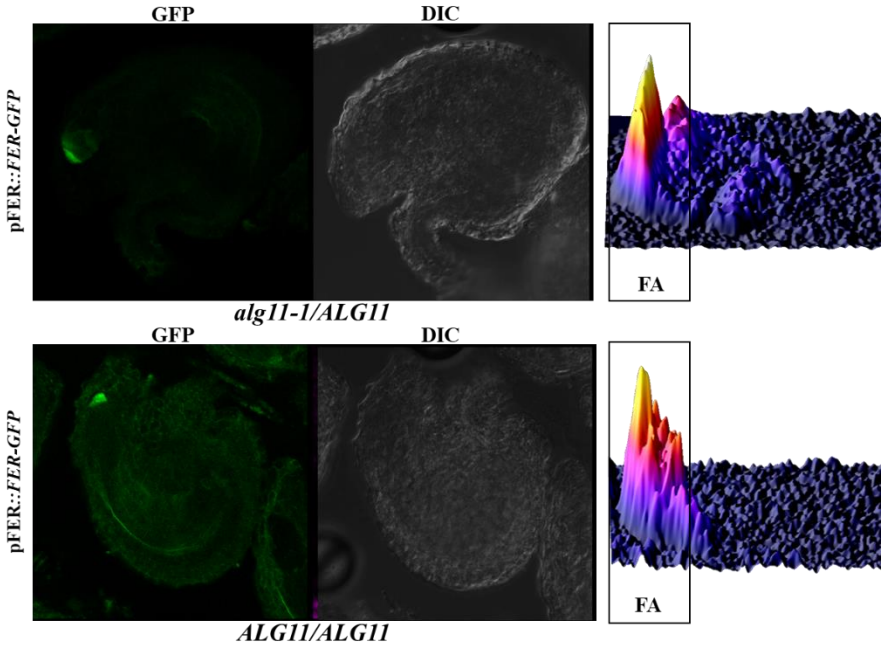

Figure 7. FER-GFP localization in the female gametophyte is undisturbed in *alg11-1/ALG11* ovules. Representative confocal images of ovules expressing FER-GFP in mutant background (top), or in wild-type (bottom). Surface plots of total synergid fluorescent signal intensity were made using ImageJ. Signal coming from the filiform apparatus (FA) is highlighted in the boxed areas.

ER resident ALG3 and ALG10 are required during interspecific pollen tube reception

TUN (homolog of the yeast ALG1) and ALG11 are both glycosyltransferases belonging to the asparagine-linked glycosylation (ALG) family. They are involved in the biosynthesis of the lipid linked oligosaccharide on the cytosolic side of the ER membrane (Aebi, 2013; Strasser, 2016). TUN is attaching the first mannose residue onto $GlcNAc_2$-PP-Dol, followed by ALG2 (*AT1G78800*) α1,6- and an α1,3-mannosylation and ALG11 addition of two α1,2-linked mannose residues. Synthesized oligosaccharide is subsequently flipped through the ER membrane by a putative RFT1 flippase for the further processing (Gomord et al., 2010).

Having in mind that TUN and ALG11 have overlapping female and male gametophytic defects, we employed reverse genetic approach to unravel functional importance of the previously uncharacterized ALG2 mannosyltransferase (Fig. 1). Based on the RNA-Seq and Microarray data, ALG2 is expressed in the female gametophyte, with especially strong expression in the egg cell (Fig. S3, Tab. S1, and Tab. S2). Two independent T-DNA lines (*alg2-1* and *alg2-2*), both having an insertion in the sixth exon, were analyzed. As ALG2 homozygous mutants were not possible to obtain, heterozygous mutant plants were analyzed. However limited number of plants have been checked (n=18), thus more extensive analysis is required to conclude its embryo lethality. Both intraspecific as well as interspecific pollen tube reception was unaffected, implying that ALG2 is not necessary for the gametophyte recognition (Fig. S2).

According to the evolutionary analysis no other homologs of ALG2 were found upon blasting of *A. thaliana* proteome. The closest related protein was ALG11, suggesting that ALG11 could act redundantly to ALG2 during mannosylation of lipid linked precursor (Fig. S4). Furthermore *N*-glycosylation pathway seems highly conserved in the distantly related bryophyte *Marchantia polymorpha*, and interestingly both ALG2 and ALG11 orthologs were found by blasting the *M. polymorpha* predicted proteome implying that ALG2 and ALG11 did not duplicate recently (Fig. S4).

Once the lipid-linked precursor ($Man_5GlcNAc_2$) is flipped to the luminal side of the ER, the first mannosylation step is catalyzed by an α1,3-mannosyltranferase ALG3 (Aebi, 2013; Lannoo and Van

Damme, 2015). Unlike ALG2, ALG3 has been studied extensively (Henquet et al., 2008; Kajiura et al., 2010), however mutants displayed no obvious phenotypes, and only recently were linked to immune responses thorough impact on the biogenesis of FLS2 receptor (Trempel et al., 2016). *ALG3* is highly expressed in the female gametophyte, with the strongest expression in the synergid cells from all analyzed *N*-glycosylation mutants (Fig. S3, Tab. S1. and Tab. S2). With intention to study its role during gametophyte interaction, we have obtained two T-DNA lines, with insertions in the third and the sixth exon (Fig. 8A). Similarly, to the *alg2/ALG2* T-DNA insertional mutants, disruption of ALG3 did not have an impact on the intraspecific pollen tube reception (Fig. 8B). However, *alg3-1* and *alg3-2* showed significantly higher level of PT overgrowth compared to the wild type control in crosses with closely related *A. lyrata* (Fig. 8C). Strength of the observed phenotype was undistinguishable in comparison to the previously described *aru* mutant (Müller et al., 2016).

Seeing the importance of the ER luminal processing, we have decided to test the role of yet uncharacterized α1,3-glucosyltransferases ALG8, expressed throughout the female gametophyte (Fig. S3, Tab. S1. and Tab. S2). However, neither of the two T-DNA lines, insertions in the 300-UTR-5 and the first exon, showed abnormalities in either intra- or inter-specific pollen tube reception (Fig. S2). It is probable that loss of ALG8 can be tolerated since ALG8 as well as ALG6 are glucosyltransferases catalyzing the same type of reactions on the lipid link oligosaccharide (LLO) precursor (Fig. 1). Similarly, to the above mentioned ALG2 and ALG11 phylogenetic analysis revealed that ALG6 and ALG8 are the closest homologs in *A. thaliana*, and additionally in *M. polymorpha* they each have an ortholog indicating that there was no recent duplication event (Fig. S4).

Final step of the LLO synthesis is catalyzed by an α1,2-glucosyltransferase ALG10. Upon addition of the terminal glucose fully assembled precursor is transferred by the OST complex from the lipid carrier to the asparagine residue within *N*-glycosylation motif of nascent polypeptide (Gomord et al., 2010; Nagashima et al., 2018). Loss of ALG10 function leads to defects in the leaf development and abiotic stress hypersensitivity (Farid et al., 2011). *ALG10* showed similar expression pattern with *ALG3* and *ALG2*, with extremely high expression in egg cell and very low in pollen (Fig. S3, Tab. S1. and Tab. S2). Having in mind that loss of ALG10 leads to drastic protein underglycosylation as well as activation of ERAD pathway, we hypothesized that biogenesis of members of PT reception pathway could be affected leading to a diminished PT recognition. Therefore. we have obtained two T-DNA lines, *alg10-1* and *alg10-2*, with insertions in the first and fifth exon (Fig. 8A). In line with the previously tested *N*-glycosylation mutants, neither of two T-DNA lines displayed impairment of intraspecific pollen tube reception (Fig. 8B). On the other hand, loss of ALG10 function led to the inability to recognize heterospecific (foreign) pollen, evident from the crosses with *A. lyrata* in which both *alg10-1* and *alg10-2* presented substantially higher proportion of PTO compared to the wild type control (Col-0) (Fig. 8C). These results show the importance of even single glucose residues for the optimal *N*-glycosylation of plant reproductive proteins.

Taken together we have dissected roles of several enzymes of ER *N*-glycosylation pathway and found two novel molecular components of interspecific pollen tube reception pathway: an α1,3-mannosyltranferase ALG3 and α1,2-glucosyltransferase ALG10. Additionally, our results point out that ER *N*-glycosylation pathway has roles beyond protein folding and quality control. Biogenesis of key proteins of the PT reception pathway was not affected since both *alg3* and *alg10* showed wild type like intraspecific PT reception. However, it is likely that those receptors are mis- under-

glycosylated leading to inability of *alg3* and *alg10* to recognize pollen from closely related *A. lyrata* during interspecifc pollinations.

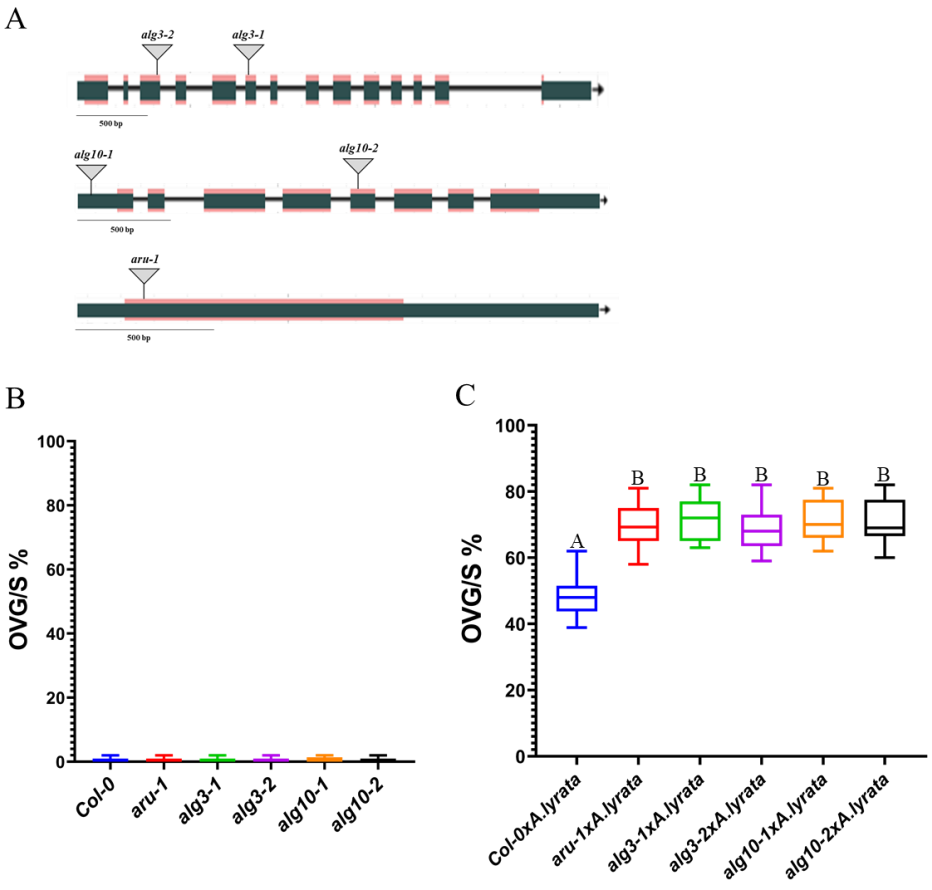

Figure 8. ER localized ALG3 and ALG10 *N*-glycosylation enzymes are required during interspecific pollen tube reception. **(A)** Gene model of *ALG3*, *ALG10*, and *ARU* with grey triangles depicting T-DNA insertions. **(B)** Intraspecific pollen tube reception is unaffected in the T-DNA insertion mutants of *ALG3* and *ALG10*. At least ten self-pollinated siliques from five plants of Col-0 and respective mutants were analyzed with aniline blue staining (n>2500 ovules per genotype). **(C)** Interspecific pollen tube reception with *A. lyrata* pollen is heavily disrupted in *alg3-1/2* and *alg10-1/2* ovules. As a positive control of interspecific barrier disruption, previously published *aru-1* was included in the crossing scheme (Müller et al., 2016). Box plots represent percentage of PT overgrowth per silique of interspecific crosses. Siliques of *A. lyrata* crosses were harvested two days after pollination, and at least three plants per line and five siliques per plant were analyzed using aniline blue staining (n>750 ovules per genotype). One-way ANOVA followed by Tukey's multiple comparison test (A-B ****P<0.0001).

Maturation of *N*-glycans in the Golgi is required for interspecific pollen tube reception

Complex glycan synthesis is initiated by β1,2-N-acetylglucosaminyltransferase I (GNTI/CGL1) (Fig. 1) which is thus responsible for the final *N*-glycan composition of all membrane-localized and secreted glycoproteins (Gomord et al., 2010; Nagashima et al., 2018). Despite being universally present in plants, for the long time complex glycans were thought to be completely dispensable for the plant growth and development (Strasser, 2014). CGL1 is evolutionary highly conserved and present even in some microalgae and mosses (Baïet et al., 2011; Koprivova et al., 2003). The only reported phenotype of the GNTI mutant, *cgl1* (*complex glycan less 1*), was a hypersensitivity to the salt stress (Kang et al., 2008), resulting in the inhibition of the primary root growth, phenotype reminiscent of *fer-4* (Feng et al., 2018). Complex plant *N*-glycans contain β1,2-xylose and α1,3-

fucose residues, whose addition is catalyzed by a core β1,2-xylosyltransferase (*XYLT*) and α1,3-fucosyltransferase (*FUT11/12*) (Nagashima et al., 2018; Strasser, 2016). Similarly, to the loss of *CGL1*, even triple mutant *xylt/fut11/fut12* displayed no visible developmental phenotype and is thus not critical for the proper plant growth. Only under salt stress conditions growth of the primary root is strongly inhibited, correspondingly to the *cgl1* and *fer-4* (Kang et al., 2008).

CGL1 is widely expressed within the plant, with the highest expression in root, followed by substantially high expression in egg and central cell (Fig. S3, Tab. S1. and Tab. S2). *XYLT*, *FUT11* and *FUT12* are also broadly expressed in plant tissues, but to a much lower degree in the female gametophyte compared to the *CGL1* (Fig. S3, Tab. S1. and Tab. S2). Evolutionary analysis based on the protein sequence homology revealed CGL1 to be uniquely present in *A. thaliana* proteome, while FUT11 and FUT12 are closest homologs and to the lower degree they display homology to XYLT (Fig. S5). Additionally, we have observed in *M. polymorpha* one ortholog clustering together in the case of CGL1 as well as XYLT, indicative of no recent duplication events (Fig. S5). However, for *A. thaliana* FUT11 and FUT12 only one ortholog was found in *M. polymorpha* (Fig. S5). Therefore, it is likely that during evolution duplication event happened leading to generation of two copies of ancestral gene, further implying that FUT11 and FUT12 have overlapping roles.

Having in mind that several enzymes of the ER mediated *N*-glycosylation pathway play a role in PT reception, and the high degree of conservation of Golgi resident enzymes we postulated that maturation in Golgi might be important for the gametophyte recognition during PT reception. In order to assess role of complex-type *N*-glycans in PT reception, we have obtained previously described EMS *cgl1-1* line as well as T-DNA line (*cgl1-2*) with the insertion in the thirteenth exon (Fig. 9A). We have detected full fertility of both mutant alleles, meaning that complex glycans are not needed for the intraspecific PT reception (Fig. 9B). On the other hand, both *cgl1* mutants presented significantly higher level of PTO phenotype in crosses with *A. lyrata* compared to the wild type control (Col-0) (Fig. 9C). Therefore, complex-glycans are needed for the proper recognition of heterospecific pollen.

Having in mind that XYLT, FUT11 and FUT12 are catalyzing downstream of CGL1 it would be expected that they do not impair intraspecific PT: As foreseen, we have observed full fertility of the self-pollinated *xylt/fut11/fut12* triple mutant (Fig. 9C). The fact that *xylt/fut11/fut12* shows significantly higher level of PTO, indistinguishable from *aru-1*, *cgl-1* and *cgl-2* is a further confirmation of the vital role of complex-type *N*-glycans during interspecific pollen tube reception. More than three quarters of all plant *N*-glycans are of the complex-type, which suggests their involvement in many aspects of plant life (Strasser, 2014). However, the only reported phenotype of *cgl1* so far was hypersensitivity to abiotic stress. Therefore, our study is shedding light into general importance of complex glycans for the *A. thaliana* and more specifically provides the first evidence for the reproductive proteins requiring proper Golgi maturation to fulfill their roles during PT reception.

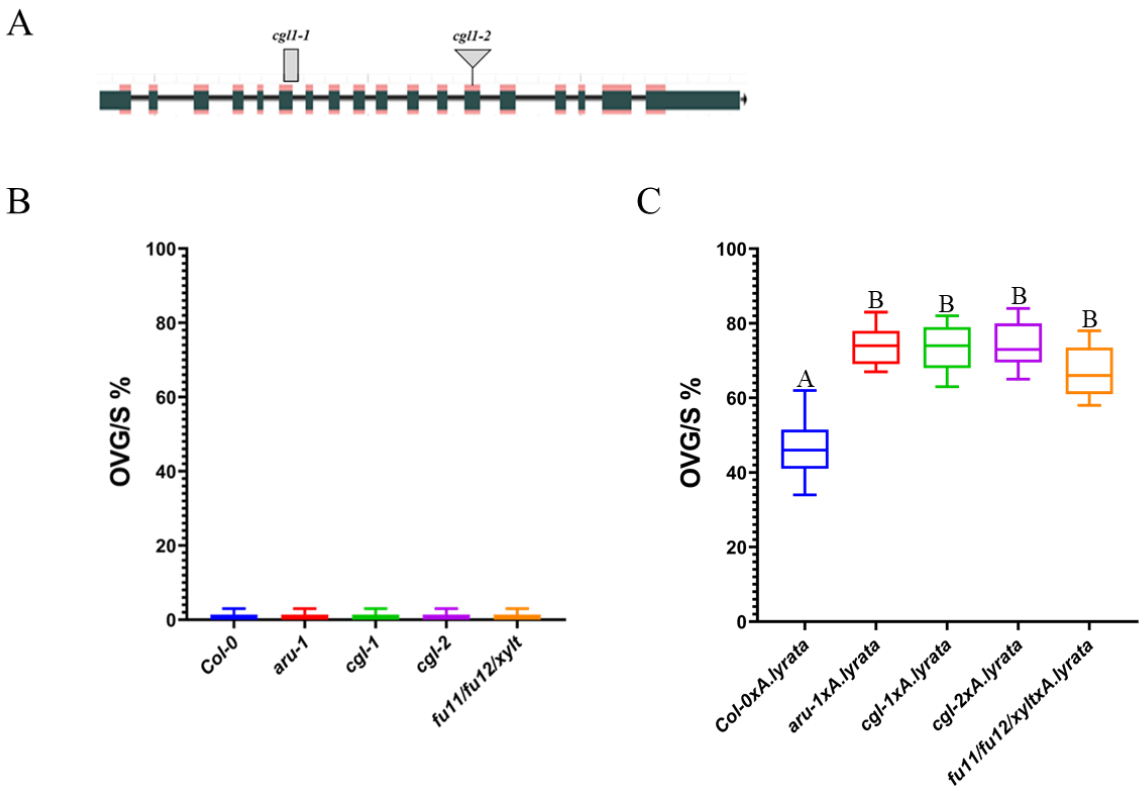

Figure 9. Maturation of *N*-glycans in the Golgi apparatus is required during interspecific pollen tube reception. (A) Schematic representation of CGL1 locus with mutant alleles, grey rectangle represents EMS causative SNP and grey triangle depicts T-DNA insertion line. **(B)** Intraspecific pollen tube reception of Golgi-localized enzymes is invariable in comparison to the wild type (Col-0). Ten self-pollinated siliques from five plants of Col-0 and indicated mutants were analyzed with aniline blue staining (n>2500 ovules per genotype). **(C)** Interspecific hybridization barrier is disrupted in the absence of complex glycans. Mutants affected in Golgi localized *N*-glycosylation enzymes were used as the female parent in crosses with *A. lyrata*. As the positive control of interspecific barrier impairment was used previously described *aru-1* (Müller et al., 2016). Box plots represent percentage of PT overgrowth per silique of interspecific crosses. *A. lyrata* pollinated siliques were assayed using aniline blue staining. At least three plants per line and five siliques per plant were included in the analysis (n>750 ovules per genotype). One-way ANOVA followed by Tukey's multiple comparison test (A-B ****P<0.0001).

Discussion

In this study we report identification of ALG11 (LEW3) as a novel component of FER-regulated PT reception pathway. ALG11 was one of the three remaining uncharacterized candidates from a forward genetic EMS screen, searching for the mutants with *fer*-like PTO phenotype. Using SNP ratio mapping (SRM) approach, we have successfully mapped EMS causative SNP to the third exon of *ALG11*. We have also mapped another EMS mutant candidate to the previously described *TURAN*, thus further confirming power of SRM approach. ALG11 (LEW3) has been characterized previously, however authors have not studied fertility defects. LEW3 was identified through an EMS screen for mutants showing leaf-wilting phenotype under standard growth conditions (Zhang et al., 2009).

ALG11 an alpha-1,2-mannosyltransferase is catalyzing addition of the two mannoses on the lipid carrier dolichylphosphate (Aebi, 2013; Lannoo and Van Damme, 2015; O'Reilly et al., 2006). In the yeast loss of ALG11 gene leads to the impaired growth and temperature induced lethality (Cipollo et al., 2001). In *A. thaliana* loss of ALG11 caused lethality, with heterozygous mutants displaying

impaired cellulose synthesis, thinner cell walls causing xylem collapse, global reduction in protein *N*-glycosylation, as well as higher sensitivity to osmotic stress or ABA treatment (Zhang et al., 2009). The more recent study has mapped mutant *limited root growth 1* (*lrg1*) to ALG11 unravelling its role during root growth and development (Manzano et al., 2017).

In line with the previously observed pleiotropic phenotypes of ALG11 mutants, here we report not only the female gametophytic PT overgrowth, but as well male gametophytic defect of pollen tube bursting, as well as defective interspecific pollen tube reception. Degree of PT overgrowth (PTO) in different alleles of *alg11* was consistent, with an EMS line presenting 22% of PTO (*alg11-1/ALG11*), and two independent T DNA lines 20% *alg11-2/ALG11* and 18% *alg11-3/ALG11* of PTO, further confirming correct mapping of EMS mutant. Similar degrees of PTO were previously observed for *tun/TUN* (12-15%) and *evn/EVN* mutants (20-28% PTO) (Lindner et al., 2015), implying an important role of early step processing on the cytosolic side of ER membrane during gametophyte recognition. On the other hand, the fact that most of the *fer-4* vegetative phenotypes are not phenocopied in the *alg11-1/ALG11*, could be explained by the remaining activity of ALG11 in heterozygous mutant. Since homozygous mutants cannot be obtained due to the embryo lethality, in the future expression of ALG11 can be downregulated using RNA interference (RNAi), to get a better understanding of the roles of ALG11 during vegetative growth and development.

The role of ALG2 mannosyltransferase during plant *N*-glycosylation was proposed based on the sequence homology with the yeast ALG2. However, complementation of yeast mutant *alg2* (Jackson et al., 1993) is needed to confirm that plant ALG2 is indeed a true ortholog and that it hence can perform predicted mannosylation steps. When loss of function ALG2 mutants were analyzed in *A. thaliana*, both intraspecific and interspecific PT recognition was wild type like. Potential explanation could lie in the fact that both ALG11 and ALG2 are mannosyltransferases, thus ALG11-mediated-manossylation could be sufficient for the further processing of lipid-linked oligosaccharide. Furthermore, the strong degree of conversation indicates that ALG2 and ALG11 might have overlapping functions. Redundancy issue can be addressed by generation of *alg2/alg11* double mutants in the future.

N-linked glycosylation is not only directly promoting proper protein folding but is also needed for the quality control and degradation of misfolded proteins (Helenius and Aebi, 2004; Liu and Li, 2014; Strasser, 2018). Therefore, we hypothesized that observed *fer*-like PTO phenotype of *alg11-1/ALG11* is stemming from an impaired biogenesis of FER. We have found FER to be properly localized to the filiform apparatus (FA), similarly to *tun/TUN*, *evn/EVN*, and *artumes* (*ost3-6*) ovules (Lindner et al., 2015; Müller et al., 2016). Even though FER biogenesis is not affected leading to proper localized at the FA, it cannot be excluded that mis- or under- glycosylation of FER does not impair recognition of putative ligands, or binding to coreceptors thereby reducing an extent of FER signaling response upon PT arrival.

Besides above mentioned female gametophytic defects, we have also found male gametophytic defect in *alg11-1/ALG11*. Pollen tubes of *alg11-1/ALG11* were bursting soon upon germination, phenotype reminiscent of *anx1/anx2* and *tun/TUN* mutants (Boisson-Dernier et al., 2009; Lindner et al., 2015). We have not checked expression of ANX1/ANX2 in the *alg11-1/ALG11* but it is probable that due to underglycosylation they are getting targeted to the ER associated degradation (ERAD) pathway, as it was reported for the *tun/TUN* mutants (Lindner et al., 2015). Therefore, further experiments are needed to conclude impact of *alg11* background on ANX1/ANX2 biogenesis. Since PT bursting of *alg11-1/ALG11* is less severe compared to *anx1 anx2* and *tun*, it could be checked if pollen tubes are

insensitive to the addition of ANX1/ANX2 ligands RALF4 and RALF19 peptides (Mecchia et al., 2017). Maintenance of the CW integrity during PT growth is controlled by additional component of ANX1/2 signaling pathway, a receptor-like cytoplasmic kinase (RLCK) MARIS (MRI) and Type One Protein Phosphatases (TOPP1) ATUNIS1/2 (AUN1/2) (Boisson-Dernier et al., 2015; Franck et al., 2018; Liao et al., 2016). Considering that constitutively active MRI^{R240C} can partially suppress *anx1/anx2* PT bursting phenotype (Boisson-Dernier et al., 2015) it would be interesting to test if similar rescue would occur in the case of *alg11-1/ALG11* or *tun/TUN* pollen. Ectopic expression of both wild-type MRI and MRI^{R240C} in the *N*-glycosylation mutant backgrounds would also answer the question if MRI^{R240C} is increasing stability of MRI and thus having a protective role from degradation via ERAD pathway.

We have employed reverse genetic approach to assess if additional ER-localized members of the *N*-glycosylation pathway play a role during pollen tube reception. We have found ALG3 and ALG10 to be important for the interspecific PT reception in crosses with closely related *Brassicaceae* species *A. lyrata*, while being unessential for the recognition of self-pollen. ALG3 catalyzes the first mannosylation step after core lipid-linked oligosaccharide precursor flipping to the luminal side of ER. Several pattern-recognition receptors (PRRs) were underglycosylated in *alg3*, however they were targeted to the plasma membrane and were able to trigger immune response to a lower extent compared to the wild-type. (Trempel et al., 2016). Therefore, in parallel with immune receptors, it is probable that in the *alg3* several PT reception members are mis- or under- glycosylated, but are still targeted to the FA, where upon arrival of intraspecific PTs they can trigger sufficiently enough FER-mediated signaling to induce PT burst. However, in the case of interspecific pollinations where heterospecific (*A. lyrata*) PTs are carrying different receptors and secreting ligands it could be that suboptimal level of functioning is not sufficient to induce PT burst, leading to PTO increase in *alg3*.

We have also characterized functional importance of ALG8 α1,3 glucosyltransferases in pollen tube reception. However, loss of ALG8 resulted in the normal wild type-like intra- and inter- specific PT reception, similarly to *alg2* mutants. It is of note that ALG6 and ALG8 catalyze two subsequent steps during processing of lipid linked oligosaccharide (Fig. 1), and additionally based on evolutionary analysis are highly conserved even in *M. polymorpha* (Fig. S4). Having in mind such an extent of conservation, it is likely that ALG6 and ALG8 act in a redundant way during PT reception, thus *alg6/alg8* double mutants should be generated in the future to get a full understanding of functional importance of these glucosyltransferases.

Mutation of ALG10, which catalyzes the addition of terminal glucose to the lipid-linked oligosaccharide (Aebi, 2013), led to the exclusive impairment of interspecific pollen tube reception, as observed in *alg3*. The fact that no impairment of intraspecific PT reception was found in *alg10* was a bit surprising, having in mind that in *alg10* ERAD pathway is activated (Farid et al., 2011). Loss of *alg10* additionally caused increased sensitivity to the salt stress as well smaller leaf size (Farid et al., 2011). Hence, we expected impaired biogenesis of PT reception pathway players (FER, LRE. ANJEA, HERK1, ENs), but this was most likely not the case having in mind the wild type like reception of self-pollen. Therefore, it could be that different members of the PT reception pathway are getting differently decorated in *alg3 and alg10* but still leading to the same inability to recognize interspecific pollen tubes.

Far less is known about impact of Golgi maturation on the plant development. Even though in *cgl1* mutant all complex glycans are lacking, no obvious phenotype was identified under standard growth conditions. Same was observed for the complex glycans devoid of β1,2-xylose and core α1,3-fucose

residues (Strasser et al., 2004). Intriguingly in the rice loss of GNTI caused severe developmental phenotypes and lethality before entering in the reproductive phase (Fanata et al., 2013). So far the only observed phenotype in *A. thaliana* for the *cgl1* is increased sensitivity to the salt stress, where primary root growth is substantially inhibited with aberrant root tip morphology (Kang et al., 2008). Triple mutant *fucTa fucTb xylT* displayed same salt hypersensitivity as the *cgl1*, suggesting that they have overlapping function during salt stress tolerance (Kang et al., 2008).

In this study we report a second ever biological role of CGL1 in *A. thaliana*, which was uncovered during interspecific crosses with *A. lyrata*, in which *cgl1* displayed increased PTO phenotype compared to the wild-type Col-0. We have also demonstrated that similarly to the salt stress response *fucTa fucTb xylT* mutants display *cgl1*-like increased PTO in interspecific pollinations. The only direct target of CGL1 so far identified is KORRIGAN1 (KOR1) a membrane-anchored endo -β-1,4-glucanase involved in the cellulose biosynthesis (Kang et al., 2008; Lane et al., 2001). Having in mind observed defects during interspecific PT reception, it is likely that loss of complex glycans from the receptor-like kinases such as FER/HERK1/ANJEA or their coreceptors GPI anchor proteins LRE, EN14 had a synergistic effect on their ability to promote recognition and reception of *A. lyrata* pollen. Additionally, it is possible that there is yet to be identified receptors at FA which are heavily *N*-glycosylated and which are substantially contributing to the successful reception of pollen. Further studies should be directed into establishing more direct link between CGL1 and PT reception players, through the biochemical evaluation of their *N*-glycosylation status, similarly to the elaborate characterization of KOR1 (Liebminger et al., 2013; Rips et al., 2014). Having in mind that KOR1 is essential for the CW synthesis, and that FER as well others members of the *Cr*RLK1l are proposed to function as the CW sensors (Boisson-Dernier et al., 2011), it can be postulated that impairment of complex glycans leads to the perturbation of apoplast localized proteins and ligands which can additionally hinder appropriate gametophyte recognition.

Material and Methods

Plant material

Wild-type *Arabidopsis thaliana* (Col-0), as well as T-DNA insertion lines used in the study, were obtained from The European Arabidopsis Stock Center (NASC). The *cgl1* ems line, published previously (von Schaewen et al., 1993) was a kind gift from Cristina Ortega-Villasante (Department of Biology, Universidad Autónoma de Madrid). Triple mutant line *fu11/fu12/xylt*, described previously (Strasser et al., 2004), was a generous gift from Richard Strasser (University of Natural Resources and Life Sciences, Vienna). *Arabidopsis lyrata ssp. lyrata* seeds were a kind gift from Detlef Weigel (Max Planck Institute for Developmental Biology, Tübingen).

Growth conditions

Seeds were surface sterilized using 3% NaOCl/0.01% Triton X-100 solution followed by 100% ethanol wash, and sterile drying. Seeds were plated using a toothpick on half-strength Murashige and Skoog (MS) basal medium (Carolina) without sucrose. Seeds were kept for two days at 4°C in darkness for synchronization, and then transferred to a growth chamber (CLF_CU-36L6, Percival,

Germany) with long-day conditions (16h light at 22°C; 8h dark at 18°C, approximate relative humidity of 70%, and light intensity of 200 μmol/m2 s). Seven days after germination seedlings were transferred to the soil. *A. thaliana* and *A. lyrata* were grown in the same greenhouse chamber under long-day conditions. *A. lyrata* plants were allowed to grow for two weeks, afterwards they were placed in the vernalization chamber (4°C, 16h light) for five weeks to induce flowering.

Pollen tube germination

In vitro pollen germination assay was performed as described previously (Boavida and McCormick, 2007; Boisson-Dernier et al., 2009). Pollen grains and pollen tubes were imaged using the differential interfering contrast (DIC) channel of a Leica DM6000B epifluorescence microscope (Leica Microsystems).

Seed Set Analysis, Crosses and Aniline Blue Staining

In order to quantify seed production, ten mature siliques were harvested per line and were cut opened with needles. Number of developed seeds ("fertilized seeds") versus unfertilized (white and shrunken ovules) was counted. *A. thaliana* flowers with closed stamens and no pollen release were used for emasculations. Two days later as a male parent were used newly opened flowers of either *A. thaliana* (intraspecific crosses) or *A. lyrata* (interspecific crosses). Assessment of pollen tube overgrowth phenotype was done using aniline blue staining of siliques harvested two days after pollination. Sepals and petals were removed and siliques were fixed using 9:1 solution of ethanol : acetic acid overnight at 4°C. Detailed protocol of aniline blue staining procedure was described previously (Huck, 2003). Stained carpels were visualized using a Leica DM6000B epifluorescence microscope (Leica Microsystems).

Root hair length analysis

Seedlings grown in the half-strength MS medium for five days after germination, were imaged using stereomicroscope Leica MZ FLIII. Root hairs were measured in the region of 1.5 to 3.5 mm from the primary root tip using ImageJ.

Root Growth Assay for the Assessment of Osmotic Stress Tolerance

Seedlings grown for five days after germination on the half-strength MS plates, were placed on the salt stress treatment plates (140mM NaCl). Exact position of the root tip was marked upon the placement on the treatment plates, which were then placed vertically and grown for two additional days. Plates were scanned using Epson Perfection 2450 scanner and changes in the root length were measured using ImageJ.

Plant transformation

Construct used for the complementation of EMS allele *alg11-1/ALG11* was previously published (Manzano et al., 2017) and it was a kind gift from Juan Carlos del Pozo (Centre for Plant Biotechnology and Genomics, Madrid). Details regarding the cloning of construct used for localization studies (*pFER*::FER-GFP) are described in the Chapter 4 of this thesis. For plant transformation expression clones were transformed into the competent *Agrobacterium tumefaciens* strain GV3101 (Koncz and Schell, 1986). *A. thaliana* transformation was done by floral dip method (Clough and Bent, 1998). Transgenics (Tab. S4) were selected using MS plates containing 25 µg/ml of hygromycin B (Invitrogen).

Confocal microscopy

Transgenic plants expressing pFER*::FER-GFP* translational fusion, were emasculated (floral stage 12) and carpel walls were removed from pistils 24-48h after emasculation. In order to visualize GFP expression, mature ovules were mounted on slides in 1M Glycine at pH 9.6 and imaged using Leica SP5 confocal microscope (Leica Microsystems). For GFP-fusion protein excitation was at 488 nm and emission was recorded from 500-550 nm. For chlorophyll autofluorescence, excitation was at 568 nm and emission was recorded from 590-650 nm. Single-focus plane images of 1024x1024 pixels were taken using a scan speed of 400 Hz.

Statistical analysis

D'Agostino-Pearson normality test was used to determine if data is fitting Gaussian distribution. Statistical significance of normally distributed data was assessed using One-way ANOVA followed by Tukey's multiple comparisons test. Data which did not pass normality test, was analyzed with Mann-Whitney or Kruskal-Wallis test followed by Dunn's multiple comparisons test. Sample size (n) is indicated in the figure legends. All statistical analysis was done with GraphPad Prism 8 software.

Bioinformatic analysis

RNA-Seq and Microarray expression data was obtained from publicly available datasets (Borges et al., 2008; Honys and Twell, 2004; Pina et al., 2005; Schmidt et al., 2011; Wuest et al., 2010) using expression analysis tool developed in the lab. R script is deposited at the GitHub platform (https://github.com/VimalRawat1010/Rscripts/blob/master/LabData/.RData). Multiple protein alignments were performed using ClustalW2 and phylogenetic trees were generated using Neighbor-Joining method (bootstrap test, 1000 replicates) in MEGA 7 software (Kumar et al., 2016).

References

Adhikari, P.B., Liu, X., Wu, X., Zhu, S., and Kasahara, R.D. (2020). Fertilization in flowering plants: an odyssey of sperm cell delivery. Plant Mol Biol.

Aebi, M. (2013). N-linked protein glycosylation in the ER. Biochimica et Biophysica Acta (BBA) - Molecular Cell Research *1833*, 2430–2437.

Baïet, B., Burel, C., Saint-Jean, B., Louvet, R., Menu-Bouaouiche, L., Kiefer-Meyer, M.-C., Mathieu-Rivet, E., Lefebvre, T., Castel, H., Carlier, A., et al. (2011). *N* -Glycans of *Phaeodactylum tricornutum* Diatom and Functional Characterization of Its *N* -Acetylglucosaminyltransferase I Enzyme. J. Biol. Chem. *286*, 6152–6164.

Boavida, L.C., and McCormick, S. (2007). TECHNICAL ADVANCE: Temperature as a determinant factor for increased and reproducible in vitro pollen germination in Arabidopsis thaliana: Temperature effect on Arabidopsis pollen germination. The Plant Journal *52*, 570–582.

Boisson-Dernier, A., Frietsch, S., Kim, T.-H., Dizon, M.B., and Schroeder, J.I. (2008). The Peroxin Loss-of-Function Mutation abstinence by mutual consent Disrupts Male-Female Gametophyte Recognition. Current Biology *18*, 63–68.

Boisson-Dernier, A., Roy, S., Kritsas, K., Grobei, M.A., Jaciubek, M., Schroeder, J.I., and Grossniklaus, U. (2009). Disruption of the pollen-expressed FERONIA homologs ANXUR1 and ANXUR2 triggers pollen tube discharge. Development *136*, 3279–3288.

Boisson-Dernier, A., Kessler, S.A., and Grossniklaus, U. (2011). The walls have ears: the role of plant CrRLK1Ls in sensing and transducing extracellular signals. Journal of Experimental Botany *62*, 1581–1591.

Boisson-Dernier, A., Lituiev, D.S., Nestorova, A., Franck, C.M., Thirugnanarajah, S., and Grossniklaus, U. (2013). ANXUR Receptor-Like Kinases Coordinate Cell Wall Integrity with Growth at the Pollen Tube Tip Via NADPH Oxidases. PLoS Biol *11*, e1001719.

Boisson-Dernier, A., Franck, C.M., Lituiev, D.S., and Grossniklaus, U. (2015). Receptor-like cytoplasmic kinase MARIS functions downstream of *Cr* RLK1L-dependent signaling during tip growth. Proc Natl Acad Sci USA *112*, 12211–12216.

Borges, F., Gomes, G., Gardner, R., Moreno, N., McCormick, S., and Feijo, J.A. (2008). Comparative Transcriptomics of Arabidopsis Sperm Cells1[C][W]. *148*, 14.

Capron, A., Gourgues, M., Neiva, L.S., Faure, J.-E., Berger, F., Pagnussat, G., Krishnan, A., Alvarez-Mejia, C., Vielle-Calzada, J.-P., Lee, Y.-R., et al. (2008). Maternal Control of Male-Gamete Delivery in *Arabidopsis* Involves a Putative GPI-Anchored Protein Encoded by the *LORELEI* Gene. Plant Cell *20*, 3038–3049.

Cipollo, J.F., Trimble, R.B., Chi, J.H., Yan, Q., and Dean, N. (2001). The Yeast *ALG11* Gene Specifies Addition of the Terminal α1,2-Man to the Man $_5$ GlcNAc $_2$ -PP-dolichol *N* -Glycosylation Intermediate Formed on the Cytosolic Side of the Endoplasmic Reticulum. J. Biol. Chem. *276*, 21828–21840.

Dresselhaus, T., and Franklin-Tong, N. (2013). Male–Female Crosstalk during Pollen Germination, Tube Growth and Guidance, and Double Fertilization. Molecular Plant *6*, 1018–1036.

Dresselhaus, T., Sprunck, S., and Wessel, G.M. (2016). Fertilization Mechanisms in Flowering Plants. Current Biology *26*, R125–R139.

Duan, Q., Kita, D., Li, C., Cheung, A.Y., and Wu, H.-M. (2010). FERONIA receptor-like kinase regulates RHO GTPase signaling of root hair development. Proc Natl Acad Sci USA *107*, 17821–17826.

Escobar-Restrepo, J.-M., Huck, N., Kessler, S., Gagliardini, V., Gheyselinck, J., Yang, W.-C., and Grossniklaus, U. (2007). The FERONIA Receptor-like Kinase Mediates Male-Female Interactions During Pollen Tube Reception. Science *317*, 656–660.

Fanata, W.I.D., Lee, K.H., Son, B.H., Yoo, J.Y., Harmoko, R., Ko, K.S., Ramasamy, N.K., Kim, K.H., Oh, D.-B., Jung, H.S., et al. (2013). N-glycan maturation is crucial for cytokinin-mediated development and cellulose synthesis in *Oryza sativa*. Plant J *73*, 966–979.

Farid, A., Pabst, M., Schoberer, J., Altmann, F., Glössl, J., and Strasser, R. (2011). *Arabidopsis thaliana* alpha1,2-glucosyltransferase (ALG10) is required for efficient N-glycosylation and leaf growth: *Arabidopsis alpha1,2-glucosyltransferase*. The Plant Journal *68*, 314–325.

Feng, W., Kita, D., Peaucelle, A., Cartwright, H.N., Doan, V., Duan, Q., Liu, M.-C., Maman, J., Steinhorst, L., Schmitz-Thom, I., et al. (2018). The FERONIA Receptor Kinase Maintains Cell-Wall Integrity during Salt Stress through Ca2+ Signaling. Current Biology *28*, 666-675.e5.

Franck, C.M., Westermann, J., Bürssner, S., Lentz, R., Lituiev, D.S., and Boisson-Dernier, A. (2018). The Protein Phosphatases ATUNIS1 and ATUNIS2 Regulate Cell Wall Integrity in Tip-Growing Cells. Plant Cell *30*, 1906–1923.

Galindo-Trigo, S., Gray, J.E., and Smith, L.M. (2016). Conserved Roles of CrRLK1L Receptor-Like Kinases in Cell Expansion and Reproduction from Algae to Angiosperms. Front. Plant Sci. *07*.

Galindo-Trigo, S., Blanco-Touriñán, N., DeFalco, T.A., Wells, E.S., Gray, J.E., Zipfel, C., and Smith, L.M. (2019). *Cr* RLK 1L receptor-like kinases HERK 1 and ANJEA are female determinants of pollen tube reception. EMBO Rep.

Gomord, V., Fitchette, A.-C., Menu-Bouaouiche, L., Saint-Jore-Dupas, C., Plasson, C., Michaud, D., and Faye, L. (2010). Plant-specific glycosylation patterns in the context of therapeutic protein production: PMP-specific glycosylation patterns. Plant Biotechnology Journal *8*, 564–587.

Guo, H., Li, L., Ye, H., Yu, X., Algreen, A., and Yin, Y. (2009). Three related receptor-like kinases are required for optimal cell elongation in Arabidopsis thaliana. Proceedings of the National Academy of Sciences *106*, 7648–7653.

Helenius, A., and Aebi, M. (2004). Roles of N-Linked Glycans in the Endoplasmic Reticulum. Annu. Rev. Biochem. *73*, 1019–1049.

Henquet, M., Lehle, L., Schreuder, M., Rouwendal, G., Molthoff, J., Helsper, J., van der Krol, S., and Bosch, D. (2008). Identification of the Gene Encoding the α1,3-Mannosyltransferase (ALG3) in *Arabidopsis* and Characterization of Downstream *N* -Glycan Processing. Plant Cell *20*, 1652–1664.

Higashiyama, T. (2018). Plant Reproduction: Autocrine Machinery for the Long Journey of the Pollen Tube. Current Biology *28*, R266–R269.

Honys, D., and Twell, D. (2004). Transcriptome analysis of haploid male gametophyte development in Arabidopsis. Genome Biology 13.

Hou, Y., Guo, X., Cyprys, P., Zhang, Y., Bleckmann, A., Cai, L., Huang, Q., Luo, Y., Gu, H., Dresselhaus, T., et al. (2016). Maternal ENODLs Are Required for Pollen Tube Reception in Arabidopsis. Current Biology *26*, 2343–2350.

Huck, N. (2003). The Arabidopsis mutant feronia disrupts the female gametophytic control of pollen tube reception. Development *130*, 2149–2159.

Jackson, B.J., Kukuruzinska, M.A., and Robbins, P. (1993). Biosynthesis of asparagine-linked oligosaccharides in Saccharomyces cerevisiae: the alg2 mutation. Glycobiology *3*, 357–364.

Jeong, I.S., Lee, S., Bonkhofer, F., Tolley, J., Fukudome, A., Nagashima, Y., May, K., Rips, S., Lee, S.Y., Gallois, P., et al. (2018). Purification and characterization of *Arabidopsis thaliana* oligosaccharyltransferase complexes from the native host: a protein super-expression system for structural studies. Plant J *94*, 131–145.

Kajiura, H., Seki, T., and Fujiyama, K. (2010). Arabidopsis thaliana ALG3 mutant synthesizes immature oligosaccharides in the ER and accumulates unique N-glycans. Glycobiology *20*, 736–751.

Kanaoka, M.M. (2018). Cell–cell communications and molecular mechanisms in plant sexual reproduction. J Plant Res *131*, 37–47.

Kang, J.S., Frank, J., Kang, C.H., Kajiura, H., Vikram, M., Ueda, A., Kim, S., Bahk, J.D., Triplett, B., Fujiyama, K., et al. (2008). Salt tolerance of Arabidopsis thaliana requires maturation of N-glycosylated proteins in the Golgi apparatus. Proceedings of the National Academy of Sciences *105*, 5933–5938.

Kessler, S.A., Shimosato-Asano, H., Keinath, N.F., Wuest, S.E., Ingram, G., Panstruga, R., and Grossniklaus, U. (2010). Conserved Molecular Components for Pollen Tube Reception and Fungal Invasion. Science *330*, 968–971.

Koiwa, H. (2003). The STT3a Subunit Isoform of the Arabidopsis Oligosaccharyltransferase Controls Adaptive Responses to Salt/Osmotic Stress. THE PLANT CELL ONLINE *15*, 2273–2284.

Koprivova, A., Altmann, F., Gorr, G., Kopriva, S., Reski, R., and Decker, E.L. (2003). N-Glycosylation in the Moss Physcomitrella patens is Organized Similarly to that in Higher Plants. Plant Biology *5*, 582–591.

Kumar, S., Stecher, G., and Tamura, K. (2016). MEGA7: Molecular Evolutionary Genetics Analysis Version 7.0 for Bigger Datasets. Mol Biol Evol *33*, 1870–1874.

Lane, D.R., Wiedemeier, A., Peng, L., Hocart, C.H., Birch, R.J., Baskin, T.I., Burn, J.E., Arioli, T., Betzner, A.S., and Williamson, R.E. (2001). Temperature-Sensitive Alleles of RSW2 Link the KORRIGAN Endo-1,4-□-Glucanase to Cellulose Synthesis and Cytokinesis in Arabidopsis. 11.

Lannoo, N., and Van Damme, E.J.M. (2015). Review/N-glycans: The making of a varied toolbox. Plant Science *239*, 67–83.

Lerouxel, O., Mouille, G., Andème-Onzighi, C., Bruyant, M.-P., Séveno, M., Loutelier-Bourhis, C., Driouich, A., Höfte, H., and Lerouge, P. (2005). Mutants in DEFECTIVE GLYCOSYLATION, an Arabidopsis homolog of an oligosaccharyltransferase complex subunit, show protein underglycosylation and defects in cell differentiation and growth: DGL1 is required for protein N-glycosylation. The Plant Journal *42*, 455–468.

Leydon, A.R., Beale, K.M., Woroniecka, K., Castner, E., Chen, J., Horgan, C., Palanivelu, R., and Johnson, M.A. (2013). Three MYB Transcription Factors Control Pollen Tube Differentiation Required for Sperm Release. Current Biology *23*, 1209–1214.

Liang, Y., Tan, Z.-M., Zhu, L., Niu, Q.-K., Zhou, J.-J., Li, M., Chen, L.-Q., Zhang, X.-Q., and Ye, D. (2013). MYB97, MYB101 and MYB120 Function as Male Factors That Control Pollen Tube-Synergid Interaction in Arabidopsis thaliana Fertilization. PLoS Genet *9*, e1003933.

Liao, H.-Z., Zhu, M.-M., Cui, H.-H., Du, X.-Y., Tang, Y., Chen, L.-Q., Ye, D., and Zhang, X.-Q. (2016). *MARIS* plays important roles in *Arabidopsis* pollen tube and root hair growth: *MRI* is required for tip growth. J. Integr. Plant Biol. *58*, 927–940.

Liebminger, E., Grass, J., Altmann, F., Mach, L., and Strasser, R. (2013). Characterizing the Link between Glycosylation State and Enzymatic Activity of the Endo-β1,4-glucanase KORRIGAN1 from *Arabidopsis thaliana*. J. Biol. Chem. *288*, 22270–22280.

Lindner, H., Müller, L.M., Boisson-Dernier, A., and Grossniklaus, U. (2012a). CrRLK1L receptor-like kinases: not just another brick in the wall. Current Opinion in Plant Biology *15*, 659–669.

Lindner, H., Raissig, M.T., Sailer, C., Shimosato-Asano, H., Bruggmann, R., and Grossniklaus, U. (2012b). SNP-Ratio Mapping (SRM): Identifying Lethal Alleles and Mutations in Complex Genetic Backgrounds by Next-Generation Sequencing. Genetics *191*, 1381–1386.

Lindner, H., Kessler, S.A., Müller, L.M., Shimosato-Asano, H., Boisson-Dernier, A., and Grossniklaus, U. (2015). TURAN and EVAN Mediate Pollen Tube Reception in Arabidopsis Synergids through Protein Glycosylation. PLoS Biol *13*, e1002139.

Liu, Y., and Li, J. (2014). Endoplasmic reticulum-mediated protein quality control in Arabidopsis. Front. Plant Sci. *5*.

Manzano, C., Pallero-Baena, M., Silva-Navas, J., Navarro Neila, S., Casimiro, I., Casero, P., Garcia-Mina, J.M., Baigorri, R., Rubio, L., Fernandez, J.A., et al. (2017). A light-sensitive mutation in Arabidopsis LEW3 reveals the important role of N-glycosylation in root growth and development. Journal of Experimental Botany *68*, 5103–5116.

Mecchia, M.A., Santos-Fernandez, G., Duss, N.N., Somoza, S.C., Boisson-Dernier, A., Gagliardini, V., Martínez-Bernardini, A., Fabrice, T.N., Ringli, C., Muschietti, J.P., et al. (2017). RALF4/19 peptides interact with LRX proteins to control pollen tube growth in *Arabidopsis*. Science *358*, 1600–1603.

Medus, M.L., Gomez, G.E., Zacchi, L.F., Couto, P.M., Labriola, C.A., Labanda, M.S., Bielsa, R.C., Clérico, E.M., Schulz, B.L., and Caramelo, J.J. (2017). N-glycosylation Triggers a Dual Selection Pressure in Eukaryotic Secretory Proteins. Sci Rep *7*, 8788.

Miyazaki, S., Murata, T., Sakurai-Ozato, N., Kubo, M., Demura, T., Fukuda, H., and Hasebe, M. (2009). ANXUR1 and 2, Sister Genes to FERONIA/SIRENE, Are Male Factors for Coordinated Fertilization. Current Biology *19*, 1327–1331.

Mizukami, A.G., Inatsugi, R., Jiao, J., Kotake, T., Kuwata, K., Ootani, K., Okuda, S., Sankaranarayanan, S., Sato, Y., Maruyama, D., et al. (2016). The AMOR Arabinogalactan Sugar Chain Induces Pollen-Tube Competency to Respond to Ovular Guidance. Current Biology *26*, 1091–1097.

Müller, L.M., Lindner, H., Pires, N.D., Gagliardini, V., and Grossniklaus, U. (2016). A subunit of the oligosaccharyltransferase complex is required for interspecific gametophyte recognition in Arabidopsis. Nat Commun *7*, 10826.

Nagashima, Y., von Schaewen, A., and Koiwa, H. (2018). Function of N-glycosylation in plants. Plant Science *274*, 70–79.

Nasrallah, M.E. (2002). Generation of Self-Incompatible Arabidopsis thaliana by Transfer of Two S Locus Genes from A. lyrata. Science *297*, 247–249.

Okuda, S., Tsutsui, H., Shiina, K., Sprunck, S., Takeuchi, H., Yui, R., Kasahara, R.D., Hamamura, Y., Mizukami, A., Susaki, D., et al. (2009). Defensin-like polypeptide LUREs are pollen tube attractants secreted from synergid cells. Nature *458*, 357–361.

O'Reilly, M.K., Zhang, G., and Imperiali, B. (2006). In Vitro Evidence for the Dual Function of Alg2 and Alg11: Essential Mannosyltransferases in N-Linked Glycoprotein Biosynthesis †. Biochemistry *45*, 9593–9603.

Pina, C., Pinto, F., Feijó, J.A., and Becker, J.D. (2005). Gene Family Analysis of the Arabidopsis Pollen Transcriptome Reveals Biological Implications for Cell Growth, Division Control, and Gene Expression Regulation. Plant Physiol. *138*, 744–756.

Rips, S., Bentley, N., Jeong, I.S., Welch, J.L., von Schaewen, A., and Koiwa, H. (2014). Multiple N-Glycans Cooperate in the Subcellular Targeting and Functioning of Arabidopsis KORRIGAN1. The Plant Cell *26*, 3792–3808.

Rotman, N., Gourgues, M., Guitton, A.-E., Faure, J.-E., and Berger, F. (2008). A Dialogue between the Sirène Pathway in Synergids and the Fertilization Independent Seed Pathway in the Central Cell Controls Male Gamete Release during Double Fertilization in Arabidopsis. Molecular Plant *1*, 659–666.

Sankaranarayanan, S., and Higashiyama, T. (2018). Capacitation in Plant and Animal Fertilization. Trends in Plant Science *23*, 129–139.

von Schaewen, A., Sturm, A., O'Neill, J., and Chrispeels, M.J. (1993). Isolation of a Mutant Arabidopsis Plant That Lacks N-Acetyl Glucosaminyl Transferase I and Is Unable to Synthesize Golgi-Modified Complex N-Linked Glycans. Plant Physiol. *102*, 1109.

Schmidt, A., Wuest, S.E., Vijverberg, K., Baroux, C., Kleen, D., and Grossniklaus, U. (2011). Transcriptome Analysis of the Arabidopsis Megaspore Mother Cell Uncovers the Importance of RNA Helicases for Plant Germline Development. PLoS Biol *9*, e1001155.

Shiu, S.-H., and Bleecker, A.B. (2003). Expansion of the Receptor-Like Kinase/Pelle Gene Family and Receptor-Like Proteins in Arabidopsis. Plant Physiol. *132*, 530–543.

Strasser, R. (2014). Biological significance of complex N-glycans in plants and their impact on plant physiology. Front. Plant Sci. *5*.

Strasser, R. (2016). Plant protein glycosylation. Glycobiology *26*, 926–939.

Strasser, R. (2018). Protein Quality Control in the Endoplasmic Reticulum of Plants. Annu. Rev. Plant Biol. *69*, 147–172.

Strasser, R., Altmann, F., Mach, L., Glössl, J., and Steinkellner, H. (2004). Generation of *Arabidopsis thaliana* plants with complex *N* -glycans lacking β1,2-linked xylose and core α1,3-linked fucose. FEBS Letters *561*, 132–136.

Takeuchi, H., and Higashiyama, T. (2012). A Species-Specific Cluster of Defensin-Like Genes Encodes Diffusible Pollen Tube Attractants in Arabidopsis. PLoS Biol *10*, e1001449.

Takeuchi, H., and Higashiyama, T. (2016). Tip-localized receptors control pollen tube growth and LURE sensing in Arabidopsis. Nature *531*, 245–248.

Trempel, F., Kajiura, H., Ranf, S., Grimmer, J., Westphal, L., Zipfel, C., Scheel, D., Fujiyama, K., and Lee, J. (2016). Altered glycosylation of exported proteins, including surface immune receptors, compromises calcium and downstream signaling responses to microbe-associated molecular patterns in Arabidopsis thaliana. BMC Plant Biol *16*, 31.

Wang, T., Liang, L., Xue, Y., Jia, P.-F., Chen, W., Zhang, M.-X., Wang, Y.-C., Li, H.-J., and Yang, W.-C. (2016). A receptor heteromer mediates the male perception of female attractants in plants. Nature *531*, 241–244.

Wuest, S.E., Vijverberg, K., Schmidt, A., Weiss, M., Gheyselinck, J., Lohr, M., Wellmer, F., Rahnenführer, J., von Mering, C., and Grossniklaus, U. (2010). Arabidopsis Female Gametophyte Gene Expression Map Reveals Similarities between Plant and Animal Gametes. Current Biology *20*, 506–512.

Xiao, Y., Stegmann, M., Han, Z., DeFalco, T.A., Parys, K., Xu, L., Belkhadir, Y., Zipfel, C., and Chai, J. (2019). Mechanisms of RALF peptide perception by a heterotypic receptor complex. Nature *572*, 270–274.

Yamamoto, M., Tantikanjana, T., Nishio, T., Nasrallah, M.E., and Nasrallah, J.B. (2014). Site-Specific *N*- Glycosylation of the S-Locus Receptor Kinase and Its Role in the Self-Incompatibility Response of the Brassicaceae. Plant Cell *26*, 4749–4762.

Zhang, M., Henquet, M., Chen, Z., Zhang, H., Zhang, Y., Ren, X., Van Der Krol, S., Gonneau, M., Bosch, D., and Gong, Z. (2009). LEW3, encoding a putative Î±-1,2-mannosyltransferase (ALG11) in N-linked glycoprotein, plays vital roles in cell-wall biosynthesis and the abiotic stress response in Arabidopsis thaliana: Protein.N-glycosylation, plant development and abiotic stress. The Plant Journal *60*, 983–999.

Zhong, S., Liu, M., Wang, Z., Huang, Q., Hou, S., Xu, Y.-C., Ge, Z., Song, Z., Huang, J., Qiu, X., et al. (2019). Cysteine-rich peptides promote interspecific genetic isolation in *Arabidopsis*. Science *364*, eaau9564.

Supplementary Figures and Tables

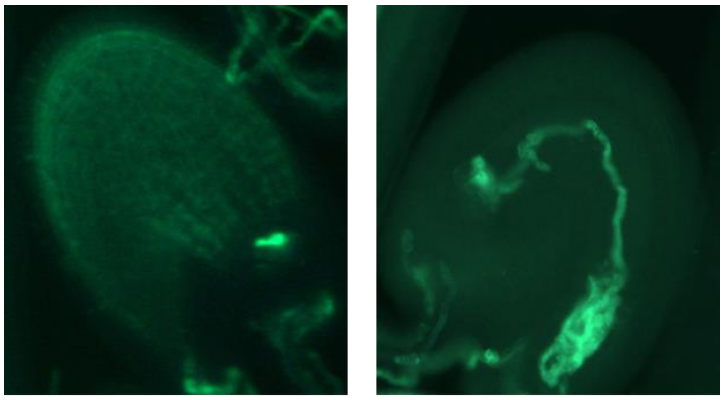

Figure S1. Mutation of the ALG11 leads to the female gametohytic PTO phenotype. Aniline blue staining of the callose within PT cell walls of siliques collected two days after pollination. On the left Col-0 ovule pollinated with *alg11-1/ALG11* pollen, and on the right *alg11-1/ALG11* ovule pollinated with Col-0 pollen.

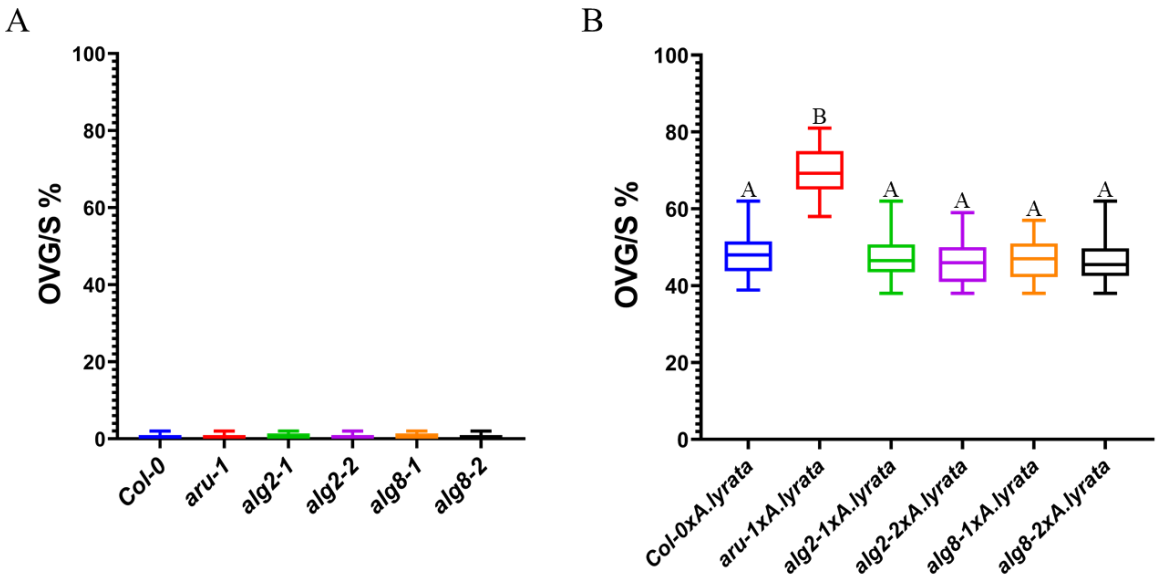

Figure S2. Pollen tube reception is undisturbed in *alg2* and *alg8* ovules. (A) Intraspecific pollen tube reception is unaffected in the mutants of ALG2 and ALG8 enzymes of *N*-glycosylation pathway. For each gene two independent T-DNA lines have been tested. At least ten self-pollinated siliques from five plants per genotype were analyzed with aniline blue staining (n>2500 ovules per genotype). **(B)** Interspecific pollen tube reception is indistinguishable from the wild type *A. thaliana* (ecotype Col-0). As a positive control interspecific crosses between *aru-1* (*artumes*) and *A. lyrata* have been performed, leading to the significantly higher level of PT overgrowth per silique. Three plants per line and five siliques per plant were analyzed using aniline blue staining (n>750 ovules per genotype). One-way ANOVA followed by Tukey's multiple comparison test (A-B ****P<0.0001).

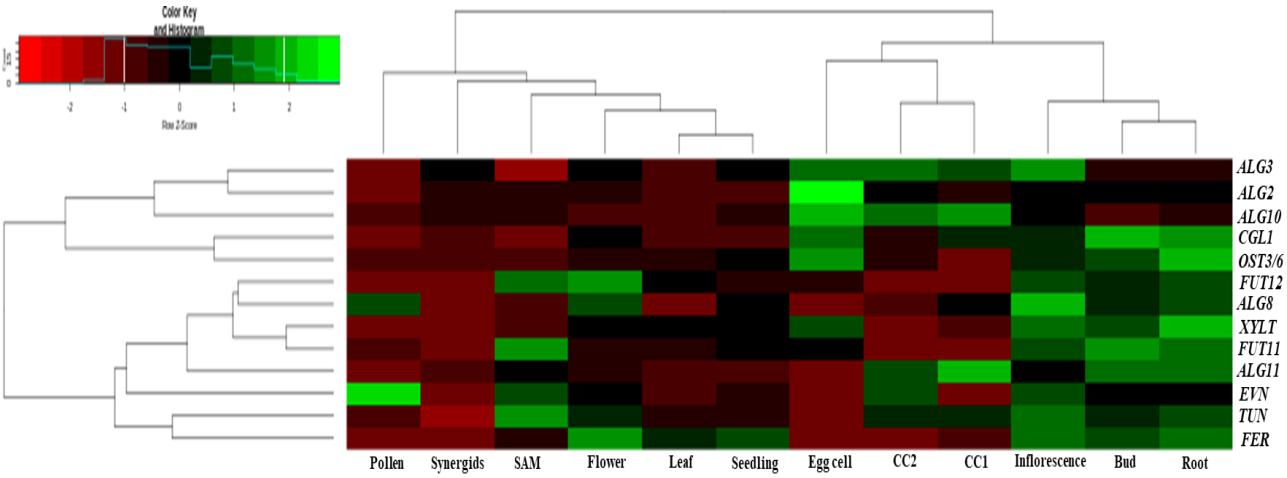

Figure S3. Expression data of *A. thaliana N*-glycosylation enzymes in different plant tissues. Heatmap of RNA-Seq data obtained from the female gametophyte expression map (Wuest et al., 2010).

Table S1. Normalized expression values of *N*-glycosylation genes from RNA-Seq data. Data was obtained from the previously established expression map (Wuest et al., 2010).

AGI code	Gene name	Flower	PollenM	EggCell	Synergids	CC1	CC2	Seedling	Root	Leaf
AT1G16570	*TUN*	76.00	27.37	13.17	3.09	70.71	81.01	45.48	93.67	41.41
AT1G49710	*FUT12*	76.26	0.64	19.70	3.48	0.13	0.13	23.12	52.92	26.58
AT1G61790	*OST3/6*	42.92	26.25	147.52	30.20	11.93	43.61	65.64	160.82	45.02
AT1G78800	*ALG2*	26.50	7.28	133.67	33.19	34.37	47.37	22.61	43.92	20.84
AT2G40190	*ALG11*	19.32	0.13	1.77	16.27	98.51	58.64	12.57	73.70	11.11
AT2G44660	*ALG8*	45.15	43.12	2.53	1.78	29.94	12.43	30.61	47.21	0.31
AT2G47760	*ALG3*	48.78	21.63	79.20	51.93	73.75	84.80	49.20	41.94	37.46
AT3G19280	*FUT11*	5.83	4.64	9.65	1.08	0.15	0.15	9.87	24.23	8.48
AT3G45040	*EVN*	44.49	148.47	2.84	1.94	4.85	84.58	24.57	40.59	20.62
AT3G51550	*FER*	100.29	0.02	1.00	0.26	3.26	0.02	67.69	87.03	51.66
AT4G38240	*CGL1*	65.73	17.87	127.27	36.45	88.77	48.83	38.63	152.43	42.86
AT5G02410	*ALG10*	11.77	0.24	184.38	37.76	170.96	126.20	27.36	24.65	21.43
AT5G55500	*XYLT*	18.24	0.07	28.70	0.69	3.25	0.07	17.63	49.58	16.80

Table S2. Normalized expression values of *N*-glycosylation genes from Affymetrix Arabidopsis ATH1 arrays data. Microarray data was obtained from several studies (Borges et al., 2008; Honys and Twell, 2004; Pina et al., 2005; Schmidt et al., 2011)

AGI code	Gene name	Flowers	PollenM	Eggcells	Synergids	CCs	Seedling	Root_epidermis	Leaf
AT1G16570	*TUN*	8.38	8.93	8.52	8.08	8.71	8.62	8.97	8.10
AT1G49710	*FUT12*	7.32	6.50	6.73	6.74	6.17	7.34	7.80	6.82
AT1G61790	*OST3/6*	10.60	10.63	7.59	7.34	7.40	10.77	11.48	10.49
AT1G78800	*ALG2*	6.95	6.18	6.82	6.59	6.53	6.69	7.74	6.94
AT2G44660	*ALG8*	7.42	9.25	7.40	6.48	5.76	7.33	7.85	7.17
AT2G47760	*ALG3*	7.83	8.75	8.47	7.49	7.72	8.11	8.35	7.52
AT3G19280	*FUT11*	5.24	5.38	5.98	5.49	4.85	5.23	5.82	5.13
AT3G45040	*EVN*	7.80	10.88	8.50	7.81	8.67	7.97	8.21	7.55
AT3G51550	*FER*	9.45	4.24	5.35	4.77	5.73	9.02	9.54	9.94
AT4G38240	*CGL1*	6.31	6.43	6.33	6.73	5.85	5.49	6.92	6.21
AT5G02410	*ALG10*	6.62	6.55	7.30	6.81	7.13	6.37	7.39	6.51
AT5G55500	*XYLT*	7.01	5.63	6.08	5.11	4.45	6.84	7.49	6.89

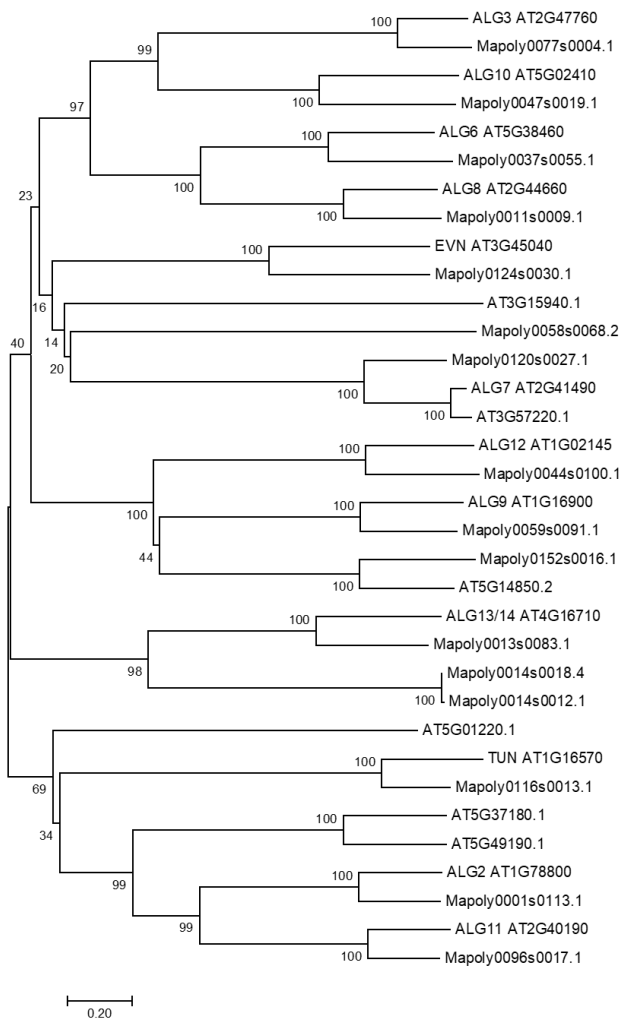

Figure S4. Phylogenetic analysis of ER-resident *N*-glycosylation enzymes from *A. thaliana* and *M. polymorpha*. Phylogenetic tree based on the full-length amino acid sequences of ER-resident *N*-glycosylation enzymes and putative *M. polymorpha* orthologs. Multiple alignments were performed using ClustalW2.0. Tree was reconstructed using Neighbor-Joining method, followed by bootstrap testing (1000 repetitions). The percentage of replicate trees in which the associated taxa clustered together are presented next to the branches. Evolutionary analysis was conducted in MEGA7 (Kumar et al., 2016).

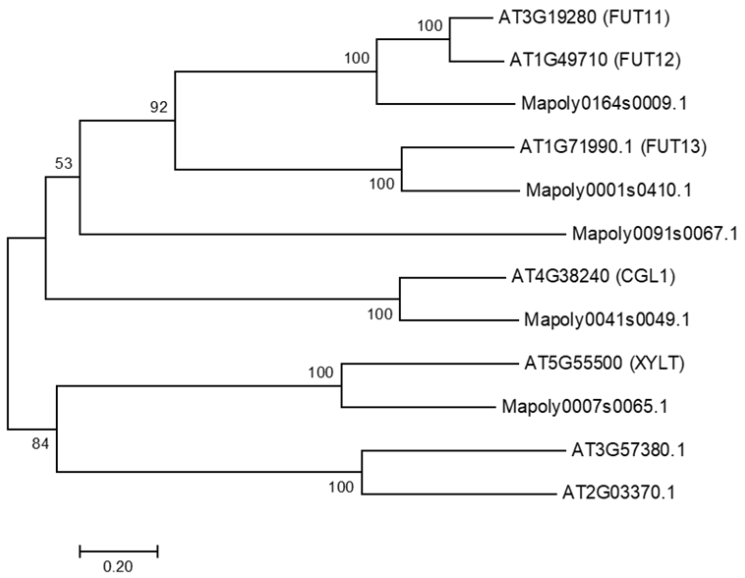

Figure S5. Phylogenetic analysis of Golgi apparatus *N*-glycosylation enzymes from *A. thaliana* and *M. polymorpha.* Phylogenetic tree based on the full-length protein sequences of Golgi apparatus resident *N*-glycosylation enzymes and their respective orthologs from *M. polymorpha*. Multiple alignments were performed using ClustalW2.0. Tree was generated using Neighbor-Joining method, followed by bootstrap testing (1000 replicates). The percentage of replicate trees in which the associated taxa clustered together are shown next to the branches. Evolutionary analysis was conducted in MEGA7 (Kumar et al., 2016).

Table S3. List of T-DNA lines used in this study and molecular markers.

Locus	Mutant line	PCR genotyping
AT2G40190	alg11/ALG11-1 *ems	ADZ156/ADZ157
AT2G40190	SALK_000886	ADZ140/ADZ141/ADZ184
AT2G40190	SALK_106951	ADZ142/ADZ143/ADZ184
AT2G47760	SALK_064006	ADZ63/ADZ64/ADZ184
AT2G47760	SALK_046061	ADZ65/ADZ66/ADZ184
AT5G02410	SAIL_515_F10	ADZ61/ADZ62/ADZ185
AT5G02410	SALK_051207C	ADZ132/ADZ133/ADZ184
AT1G61790	SALK_067271	ADZ71/ADZ72/ADZ184
AT4G38240	cgl1/cgl1-1 *ems	*WB detection
AT4G38240	SALK_073650C	ADZ76/ADZ77/ADZ184
AT1G78800	SALK_004198	ADZ152/ADZ153/ADZ184
AT1G78800	SALK_014293	ADZ154/ADZ155/ADZ184
AT2G44660	SAIL_586_C05	ADZ134/ADZ135/ADZ185
AT2G44660	SAIL_836_B11	ADZ136/ADZ137/ADZ185

Table S4. Transgenic lines with corresponding vectors used for transformation.

Transgenic line	Vector	Selection in bacteria	Selection in plants
alg11/ALG11-1 with pADZ77	pALG11::*ALG11*	Spectinomycin	Hygromycin
alg11/ALG11-1 with pADZ14	pFER::*FER-GFP*	Kanamycin	Hygromycin

Table S5. List of all primers and their respective sequences.

Primer	Primer Sequence (5'- 3')
ADZ61	GGGGCCGAATCTTAGTGATAG
ADZ62	ATGGAGCTGATGGAACTGATG
ADZ63	ATTGCAGCTGCCTTATGATTG
ADZ64	AAGCGTTGTCCATTTACGATG
ADZ65	AGAAGAAGCAAAAAGGCCAAG
ADZ66	TGGCACCTGAAATACGTAAGG
ADZ71	GAAGAACCTGGAGGGATCAAC
ADZ72	CGTTGAGAAGATCTGAATCGG
ADZ76	GCGTGATTTTTCTCCTCACTG
ADZ77	CGGGAAACTATAGGACGAAGC
ADZ132	AATGAAAATCGCTTTGCAGTG
ADZ133	ATTCCCATTGCAGTATTGCTG
ADZ134	ATGACTCACATTACGAACGGC
ADZ135	ACAGATTCGGCATTGTAATCG
ADZ136	CAGCTAAGATCCGAGTTCGTG
ADZ137	ATCGAAAGCAATAACCAACCC
ADZ140	AGGAGTGAACATGCGTAATGC
ADZ141	TTGTGAATCATGAGAATGCAAG
ADZ142	TGCAGTAAGCAGGTTTTGAGG
ADZ143	AACGGATTACACGGGTCTACC
ADZ152	GGTCAAGATGAGTGATCCGAG
ADZ153	GGCATCAACATTTGCCAATAC
ADZ154	GGTCAAGATGAGTGATCCGAG
ADZ155	GGATGGCTGATATGATCCTTG
ADZ156	CTC CTT GCT TAT TTG GTG TT
ADZ157	CTG GAT CCC TCA CCT TCT
ADZ184	ATTTTGCCGATTTCGGAAC
ADZ185	GCCTTTTCAGAAATGGATAAATAGCCTTGCTTCC

CHAPTER 4 - RESULTS

Importance of *N*-glycosylation for FER mediated signaling responses

Importance of *N*-glycosylation for FER mediated signaling responses

Andrea Zupunski, Andrea Martinez-Bernardini, and Ueli Grossniklaus

Institute of Plant and Microbial Biology & Zurich-Basel Plant Science Center, University of Zürich, Zollikerstrasse 107, 8008 Zürich, Switzerland

Abstract

Flowering plants owe their evolutionary success to the highly regulated guidance of the pollen tubes, ensuring the precise delivery of sperm cells to the female gametophyte. FERONIA (FER) receptor-like kinase is essential for the proper gametophyte communication and pollen tube (PT) reception. In the *fer* mutants PTs fail to rupture in synergid leading to overgrowth inside the embryo sac. A similar *fer-like* PT overgrowth (PTO) phenotype occurs during interspecific pollinations among closely related species of *Brassicaceae* family, pointing to the utilization of FER pathway. The FER extracellular ligand binding domain (ECD) contains ten putative *N*-glycosylation sites. Mass Spectrometry analysis was utilized to investigate FER *N*-glycosylation site occupancy and *N*-glycan composition. Four out of ten predicted sites were found to be occupied with *N*-glycans, two carrying high-mannose- and two complex-type *N*-glycans. Knowing that FER is *N*-glycosylated *in planta*, a large-scale mutagenesis approach was undertaken to assess functional importance of *N*-glycans during FER mediated signaling responses. We have found FER to be intolerant to the loss of *N*-glycans at the single positions during adaptation to the high salinity stress. This sensitivity was exacerbated in the heavily deglycosylated FER variants depleted of six and more *N*-glycosylation motifs. Root hairs development and growth were disturbed starting from the FER variant instantaneously depleted of six *N*-glycosylation motifs. The same hexapole mutant was fully fertile stemming from a complete restoration of the intraspecific PTO phenotype. Partial complementation of the intraspecific PTO was observed even in the FER variant depleted of nine out of the ten *N*-glycosylation sites, indicating extraordinarily high resilience of *N*-glycans depleted FER to ensure proper reception of the self-pollen. Contrasting to the intraspecific (self) pollinations, recognition of heterospecifc (foreign) pollen was heavily impaired even upon loss of *N*-glycans at the single positions, with more pronounced defects in the hexapole variant. *N*-glycosylation of FER`s extracellular domain is necessary for the recognition of both self and foreign pollen and the proper activation of downstream signaling cascade leading to the PT burst. Here we report the first evidence of *N*-glycosylation of the reproductive protein such as FER being important during the initiation of reproductive barrier establishment.

Keywords: Receptor kinase, CrRLK1L, synergid cells, pollen tube reception, *N*-glycosylation, interspecific pollination.

Introduction

Flowering plants (angiosperms) are one of the most successful and ubiquitously present groups of plants nowadays. One of the critical innovations that set them apart was their independence from water to enable sperm delivery (Kessler and Grossniklaus, 2011). Instead, PTs are responsible for the transportation of sperm cells to the female gametophyte, which is deeply embedded and protected within ovary sporophytic tissue (Bleckmann et al., 2014). Extensive PT journey starting from stigma papilla cells is highly regulated and can be blocked at any stage by different types of incompatibility systems (Dresselhaus and Franklin-Tong, 2013). After successful adhesion, hydration, and stigma invasion, pollen tubes continue their way through the transmitting tract towards the embryo sack (Higashiyama and Takeuchi, 2015). Active secretion of cysteine-rich (CR) peptides (LUREs and XIUQIU) by the synergid cells promotes micropylar PT guidance (Okuda et al., 2009; Takeuchi and Higashiyama, 2012; Zhong and Qu, 2019).

Once PT is successfully guided to synergids, extensive communication occurs leading to PT burst, and sperm cells release, enabling double fertilization, embryo, and endosperm formation (Dresselhaus et al., 2016). In the case of *feronia* mutants, this crosstalk is heavily disrupted, leading to PT failure to burst and PT overgrowth inside the embryo sack. FERONIA (FER) was named after the Etruscan goddess of fertility, since *fer* mutants exhibit severe fertility issues, with almost 80% of nonfertilized female gametophytes (Huck, 2003). FER is asymmetrically accumulated at the filiform apparatus where it interacts with GPI-anchor protein LORELEI (LRE) to control NADPH production of reactive oxygen species (ROS) in micropyle, and cytoplasmic Ca^{2+} signaling in synergids (Duan et al., 2014; Iwano et al., 2012; Liu et al., 2016; Ngo et al., 2014; Tsukamoto et al., 2010). FER is required for the NORTIA translocation from Golgi-associated compartments to filiform apparatus, where it modulates degree of cytosolic Ca^{2+} responses of synergid cells (Davis et al., 2017; Kessler et al., 2010). ENOLDs (EN) are also localized at the filiform apparatus, where EN14 binds with high affinity to FER ECD, and to the lower extent to LRE in order to promote FER-regulated PT burst (Hou et al., 2016). Newly described HERK1 and ANJEA form heterocomplexes with LRE and FER and thus synergistically contribute to the control of PT reception (Galindo-Trigo et al., 2019).

Discovery of *fer-like* PTO phenotype in the mutants affecting ER-localized members of the *N*-glycosylation pathway suggests an importance of posttranslational control of PT reception players. TURAN (TUN) encoding a putative UDP glycosyltransferase superfamily protein and EVAN (EVN) encoding a putative dolichol kinase affect respectively, PT integrity maintenance and pollen development. In *tun/TUN* ANX1/2 biogenesis is impaired, while FER, LRE and NTA synergid localization remained undisturbed (Lindner et al., 2015).

A similar PTO phenotype was observed in the interspecific crosses between closely related *Brassicaceae* species *A. thaliana* and *A. lyrata or A. arenosa* (Escobar-Restrepo et al., 2007). Interestingly the degree of interspecific PT overgrowth correlates with the sequence divergence of the FER extracellular domain (Escobar-Restrepo et al., 2007). GWAS study uncovered the role of OST3/6 (a subunit of the oligosaccharyltransferase complex 3/6) during interspecific PT reception (Müller et al., 2016). OST complex is catalyzing crucial step during *N*-glycosylation, the addition of preassembled oligosaccharide ($NAcGlc_2Man_9Glc_3$) to the asparagine residue within consensus motif N-x-Ser/Thr (x≠P) (Aebi, 2013). The mutation affected exclusively interspecific PT reception, with a significant increase of PTO in *ost3/6 (aru)* compared to the wild-type Col-0 when pollinated with *A. lyrata* (Müller et al., 2016). Biogenesis of FER, LRE, or NTA was not compromised in *aru*

background, with the PT reception players displaying wild type like synergid localization in *aru* ovules.

FER is the first functionally characterized member of the *Cr*RLK1L (*Catharanthus roseus* Receptor-Like Kinase 1-Like proteins) subfamily, named after the kinase, isolated from Madagaskar periwinkle (Schulze-Muth et al., 1996). *Cr*RLK1L subfamily consists of 17 closely related proteins (15 characterized so far), which have been considered as the cell wall (CW) surveillance system, with FER being a key regulator of reproduction, cell growth, development, abiotic and biotic stress responses and hormone pathways (Franck et al., 2018; Galindo-Trigo et al., 2016; Lindner et al., 2012; Nissen et al., 2016). Closest homologs of FER are pollen expressed ANXUR1 (ANX1) and ANXUR2 (ANX2), which act redundantly to ensure PT integrity through NADPH induced ROS production and Ca^{2+} gradient maintenance. Thereupon in *anx1 anx2* PTs are bursting prematurely, and delivery of sperm cells to female gametophyte is impaired (Boisson-Dernier et al., 2009, 2013; Miyazaki et al., 2009). Domain swap study between FER, ANX, and HERK1 showed functional equality of their intracellular domains in their ability to complement PT reception. Extracellular domains could not be interchanged, pointing to different ligands preferences. Even though FER kinase domain is essential for FER function, kinase-dead version (K565R) was able to complement PT reception defects (Kessler et al., 2015). However, the kinase-dead version of FER in roots was not able to induce typical to RALF1-Ca^{2+} mediated response (Haruta et al., 2018).

*Cr*RLK1L ECDs were shown to contain two malectin domains (MLDs), due to the low sequence homology with the ER-localized protein Malectin (Schallus et al., 2008). Malectin is highly conserved among all animals as well as with bacterial glycosylhydrolases, and it plays a role in the carbohydrate binding. Even though the initial assumption that *Cr*RLK1Ls recognize extracellular cues through the MLD binding to the CW polysaccharides (Boisson-Dernier et al., 2011), there was a lack of experimental evidence supporting it. The research took a turn once the RAPID ALKALINIZATION FACTOR1 (RALF1) was shown to be a ligand of FER in roots (Haruta et al., 2014). Since then, research on this small cysteine-rich peptide family of 37 members in Arabidopsis has flourished (Campbell and Turner, 2017). Many RALF–CrRLK1L ligand-receptor pairs have been described (Franck et al., 2018); however, the ligand of FER in the light of PT reception remains a mystery.

FER also plays a role during salt stress tolerance (Feng et al., 2018). Salt (NaCl) treatment leads to the remodeling of the CW components, mainly pectin, which needs to be recognized by the plant in order to control root growth. FER is sensing these perturbations by the binding to pectin, shown by *in vitro* assays. Once FER is absent, root cells are exploding like *mur1* in which pectin crosslinking is disrupted. Treatment with Ca^{2+} and borate, known as pectin cross-linkers, rescues these phenotypes (Feng et al., 2018). Another study in parallel has confirmed the importance of FER but also CW leucine-rich repeat proteins LRX3/4/5 during salt stress tolerance. LRX3/4/5 associate with RALF22/23 peptides in the apoplast. During salt stress LRX3/4/5 release RALF peptides presumably through S1P protease activation, which then conveys RALF22/23 interaction with FER and subsequent FER internalization (Zhao et al., 2018).

The fact that FER has ten putative *N*-glycosylation sites within the extracellular domain together with the notion that perturbation of the endoplasmic reticulum (ER) *N*-glycosylation pathway leads to a *fer*-like PTO phenotype, led us to believe that FER *N*-glycosylation is important for its function during gametophyte recognition. Since the sole presence of a predicted consensus motif does not imply protein *N*-glycosylation *in planta* (Strasser et al., 2016), we have performed Mass Spectrometry

(MS) analysis to check FER *N*-glycostatus. We were able to detect the addition of *N*-glycans on four out of ten putative N-glycosylation sites, N142 and N410 harbor high-mannose type glycans, and N46 and N330 harbor complex-type glycans. Having validation of FER *N*-glycosylation *in planta*, we have performed a systematic site-directed mutagenesis screen and generated FER mutant variants depleted of ascending number of *N*-glycosylation sites.

We have found that all the single FER *N*-glycosylation variants were able to complement *fer-4* vegetative growth defects (root hair bursting, petiole length, and dwarfism). Surprisingly even the octupole FER variant was able to fully complement *fer-4* fertility defects. On the other hand, starting from the hexapole FER variant root hair bursting of *fer-4* was no longer rescued, as well as the salt stress sensitivity. FER in different tissues shows a differential need for *N*-glycosylation, which is in line with FER having tissue-specific cofactors and functions. Even though FER *N*-glycosylation is not necessary for the recognition of conspecific pollen, mutation of individual sites caused the significant impairment of interspecific PT reception. This inability to distinguish between self (*A. thaliana*) and non-self (*A. lyrata*) pollen was further exacerbated in higher-order mutants. Therefore, we show that proper *N*-glycosylation of FER is crucial for the maintenance of the interspecific hybridization barrier.

Results

FER extracellular domain contains ten putative *N*-glycosylation sites highly conserved among *Brassicaceae* family

The importance of posttranslational modifications (PTMs) for the regulation of *Cr*RLK1L has been well established in the case of phosphorylation of the intracellular kinase domain (Kessler et al., 2015). Even though all 17 members of the *Cr*RLK1L family have several putative *N*-glycosylation sites within their ECDs (Lindner et al., 2012), their functional importance is still unknown. To get a better understanding of the extent of *N*-glycosylation within *A. thaliana Cr*RLK1L subfamily, protein sequences of all members were obtained and NetNGlyc1.0 software was used to identify putative *N*-glycosylation sites (Tab. S1). The number of predicted *N*-glycosylation sites varied from four in ANX2 to sixteen in THE1, and FER has ten predicted sites, with an average of eight potential *N*-glycosylation sites per member of *Cr*RLK1L subfamily. In order to asses level of *N*-glycosylation sites conservation among *Cr*RLK1L members, multiple alignments were performed and analysis revealed that from ten putative FER *N*-glycosylation sites the only conserved among all members of *Cr*RLK1L was N305, while site N330 was unique to FER, and N269 was only found in FER and MDS4 (Fig. 1A). Between the closest homologs of FER ANX1, and ANX2 (protein sequence identity of 54.3% and 50.9%) four and three *N*-glycosylation sites were conserved respectively, which is only slightly above the average (2.875 sites) among the *Cr*RLK1L family (Fig. 1A). This could indicate that highly conserved site N305 has a more general role, needed for the most of the members, such as to ensure proper protein folding and stability, while the more diverse sites are contributing to the more tissue/context specific roles of individual *Cr*RLK1l members.

In order to test how well FER *N*-glycosylation motifs are conserved between distantly related species, FER sequences from 42 species belonging to the same Orthologous Matrix (OMA) group (proteins all orthologous to each other) were aligned using OMA Browser (Altenhoff et al., 2013). We hypothesized that if an *N*-glycosylation site is crucial for the FER stability and conformation it should display high level of conservation, and potentially coincide with the most conserved sites within the

*Cr*RLK1L subfamily. While on the other hand *N*-glycosylation sites which are involved in conferring more FER specific roles should display higher level of preservation within FER OMA group compared to the *Cr*RLK1L members. Site N305 and N345 were conserved among all 42 species (Fig. S1). While site N305 was also conserved among all members of *Cr*RLK1L family thus possible being involved in protein stability, site N345 was conserved in 5 from 17 members of *Cr*RLK1L, potentially being important for more specific roles. Interestingly site N269 was conserved in 35/42 species of FER OMA group while it was one of the least conserved within *Cr*RLK1L, and it could potentially be more important for FER specific roles. The only site uniquely present in *A. thaliana* FER was site N46 (Fig. S1), while in *Cr*RLK1L subfamily it was not shared with ANX1/2, but it was the only site overlapping with both HERK1 and ANJEA.

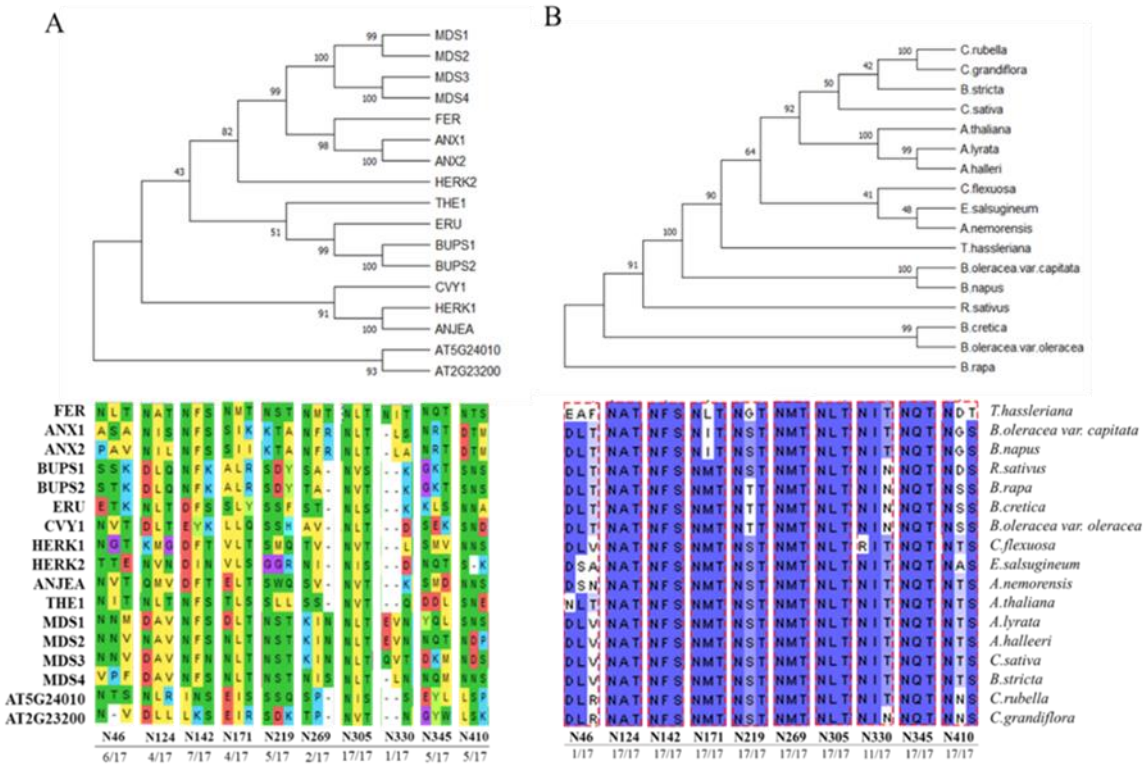

Figure 1. Overview of conservation levels of FER *N*-glycosylation sites. (A) Phylogenetic tree of 17 members of *Cr*RLK1L family (top). Multiple alignments of *Cr*RLK1L members protein sequences with indicated ten FER *N*-glycosylation sites. **(B)** Phylogenetic tree showing the relationships between FER orthologs within *Brassicaceae* family (top). Multiple alignments of FER orthologs protein sequences with indicated ten FER *N*-glycosylation sites (white represents no conservation; dark blue represents identical residues). All multiple alignments were done using ClustalW2.0 followed by tree reconstruction in MEGA 7 (protein sequence parsimony method). Multiple alignments and identity percentage was visualized using Jalview 2.11.0

In order to get an insight into species-specific patterns of *N*-glycosylation which could be important for the establishment of the interspecific hybridization barriers, we have compared level of FER *N*-glycosylation conservation among closely related species of *Brassicaceae* family. *A. thaliana* diverged only 6–13 Mya from the *A. lyrata/A. halleri* clade (Hohmann et al., 2015), which is also reflected not only in the protein sequence identity but also in the level of *N*-glycosylation motif conservation. Among *A. thaliana* and *A. lyrata/A. halleri* clade, nine out of ten putative *N*-glycosylation motifs are preserved, with the only difference of N46 (Fig. 1B). Since site N46 was the only one different between *A. thaliana* and *A. lyrata* it can be hypothesized that it could be involved

in the establishment of reproductive barrier. We wanted to get better understanding of *N*-glycosylation within *A. lyrata Cr*RLK1L subfamily to see if other members of the family display similar patterns observed for FER. Therefore, protein sequences of *A. thaliana Cr*RLK1L family members were blasted against *A. lyrata* proteome to identify *AlCr*RLK1L orthologs. Similar numbers of *N*-glycosylation sites and position within protein were observed in all members of *AlCr*RLK1L (Tab. S2).

FER is the crucial regulator of intraspecific pollen tube reception. Therefore, we hypothesized that if FER *N*-glycosylation is important to recognize self-pollen, and thus enable burst of only compatible pollen, *N*-glycosylation sites should be conserved within the species. To probe this hypothesis, we have used publicly available genomic data from 1135 *A. thaliana* accessions. Firstly, database was screened for the high-effect nonsynonymous SNPs leading to asparagine (*N*) amino acid change within predicted *N*-glycosylation motif. Since it is known that *N*-glycans can be covalently attached on the asparagine residue within N-X-S/T motif (X can be any amino acid except proline), loss of *N* to any other amino acid would mean that protein cannot acquire *N*-glycan at that position of polypeptide sequence (Aebi, 2013). According to our hypothesis, we have not found nonsynonymous SNPs affecting FER *N*-glycosylation sites among all 1135 accessions, and additionally there were no nonsynonymous changes affecting asparagine within the whole protein sequence (Tab. S3). All members of the *Cr*RLK1L family were analyzed in the same manner and only ERULUS (ERU) displayed such extreme level of conservation. In contrast, other members had tendency of a lower number of asparagine changes within *N*-glycosylation site when compared to the whole protein sequence. This implies that there is a strong selection pressure ensuring preservation of *N*-glycosylation sites, further indicating importance of *N*-glycans for the function of *Cr*RLK1L family members.

Confirmation of predicted *N*-glycosylation sites in FER *in planta*

FER protein structure consists of the variable ligand binding extracellular domain (ECD) with two malectin-like domains (MLD), transmembrane (TM) domain, and a highly conserved intracellular (ICD) S/T kinase domain (Boisson-Dernier et al., 2011). As previously mentioned, the extracellular domain of FER contains ten potential *N*-glycosylation sites (Fig 2A). MS analysis was performed to characterize FER *N*-glycosylation status *in planta*. Four out of ten putative *N*-glycosylation sites were occupied with *N*-glycans, two within MAL-A (N46 and N142), one in MAL-B (N330), and one in the extracellular juxtamembrane region (N410). *N*-glycosylation sites N142 and N410 harbor high-mannose type *N*-glycans ($Man_9GlcNAc_2$ to $Man_5GlcNAc_2$), and N46 and N330 harbor complex-type *N*-glycans ($GlcNAc_2Man_3XylFucGlcNac_2$) (Fig. 2B). Our results were consistent with the findings from the large-scale glycoproteomic study (Zielinska et al., 2012). Authors reported *N*-glycans attachment at five *N*-glycosylation sites, three overlapping: N46, N142, N330, and two differential N269 and N345, however site N345 was detected with a lower degree of confidence.

Additional confirmation of FER being *N*-glycosylated protein came from the crystallography study looking at heterotypic complex formation between RALF23, LLG2, and FER. *N*-glycans were found to be attached to FER^{ECD} at following positions: N142, N345 as well on the previously undetected N305 (FER^{ECD} was expressed in insect cells) (Xiao et al., 2019).

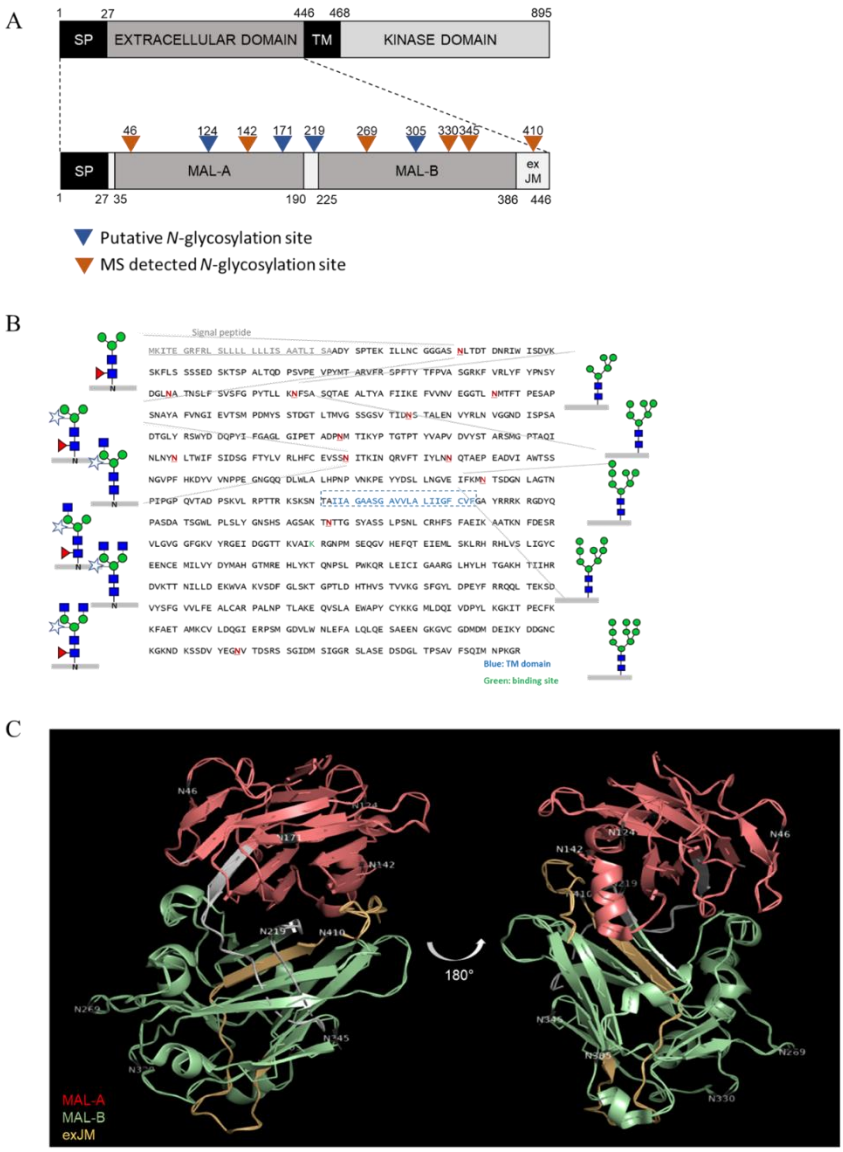

Figure 2. FERONIA receptor kinase is *N*-glycosylated. (A) Schematic diagram of the full-length FER protein sequence with a more detailed view of extracellular domain. SP, TM and ex JM stand for signal peptide, transmembrane domain and extracellular juxtamembrane region. MAL-A and MAL-B are malectin like domains. Numbers are labelling amino acid residues. Asparagines within *N*-glycosylation sites predicted to by glycosylated (NetNGlyc1.0) are depicted with blue triangles, while mass spectometry detected asparagines are marked with orange triangles. **(B)** Mass spectrometry analysis of FER-GFP. We have characterized four *N*-glycosylation sites, two harboring high type manose and two complex type glycans**. (C)** Crystal structure of FER extracellular domain (PDB ref. 6A5B) visualized with PyMOL. The protein structure is shown in ribbon type diagram (MAL-A domain colored red, MAL -B green and exJM domain yellow).

We have visualized all *N*-glycosylation sites within FER^{ECD} to test if they are surface exposed which would make them easily accessible for the oligosaccharyltransferase (OST) complex and increase their chances of being *N*-glycosylated *in planta.* We have found all *N*-glycosylation sites to be surface exposed, which is in line with MS detection of *N*-glycans at four positions (Fig. 2C). Recently also the closest homologs of FER ANX1/2 were crystallized, both being *N*-glycosylated, in the case of ANX1 three out of five potential sites were *N*-glycosylated (N132, N302, and N292), while ANX2 had all four out four predicted sites *N*-glycosylated (N133, N293, Ans303, N331) (Du et al., 2018; Moussu et al., 2018). Even though there is growing evidence of *Cr*RLK1L members being *N*-glycosylated, there is a lack of studies assessing importance of *N*-glycans for the protein stability, conformation, interaction with coreceptors/ligands in the tissue-specific context.

Systematic mutagenesis of FER *N*-glycosylation sites

In order to gain insight into the importance of *N*-glycosylation for the FER protein function, we have employed large scale site-directed mutagenesis approach to eliminate firstly all ten single *N*-glycosylation sites individually, followed by ascending number of targeted sites, up to a variant in which all ten sites were mutated (Tab. 1). *N*-glycosylation sites were abolished by replacing asparagine residue (N) within N-X-S/T consensus sequence with alanine (A), as done in previous studies (Yamamoto et al., 2014). We have decided to include all ten putative *N*-glycosylation sites since we have already detected four sites by MS (N46, N142, N330 and N410), two additional sites were detected in a previous glycoproteomic study (N269 and N345) (Zielinska et al., 2012), and crystal structure of FER revealed *N*-glycan presence on N305 (Xiao et al., 2019), while remaining three sites were found to be surface exposed in the FER^{ECD} (Fig. 2C). Firstly FER-GFP *N*-glycosylation variants` stability, expression and plasma membrane localization was detailly assessed. For the functional complementation tests FER-GFP *N*-glycosylation variants were introduced into the *fer-4* and improvement of phenotypes was assessed. We have assayed both vegetative as well as reproductive phenotypes to fully dissect importance of each *N*-glycosylation site in a tissue specific context.

Table 1. *N*-glycosylation site mutants of FER. Position of asparagine (N) within protein sequence is indicated.

Clone	Mutated site	Clone	Mutated site
M1	N46	**M16**	N269 + N305
M2	N124	**M17**	N269 + N345
M3	N142	**M18**	N305 + N345
M4	N171	**M19**	N46 + N142 + N330
M5	N219	**M20**	N46 + N142+ N124
M6	N269	**M21**	N46 + N142 + N171
M7	N305	**M22**	N46 + N142 + N124 + N171
M8	N330	**M23**	N46 + N142 + N330 + N410
M9	N345	**M24**	N46 + N142 + N330 + N410 + N269
M10	N410	**M25**	N46 + N142 + N330 + N410 + N269 + N345
M11	N46 + N142	**M26**	N46 + N142 + N330 + N410 + N269 + N345 + N124
M12	N46 + N330	**M27**	N46 + N142 + N330 + N410 + N269 + N345 + N124 + N171
M13	N46 + N410	**M28**	N46 + N142 + N330 + N410 + N269 + N345 + N124 + N171 + N219
M14	N142 + N330	**M29**	N46 + N142 + N330 + N410 + N269 + N345 + N124 + N171 + N305
M15	N330 + N410	**M30**	N46 + N142 + N330 + N410 + N269 + N345 + N124 + N171 + N219 + N305

FER-GFP intracellular trafficking and localization to the plasma membrane is not affected by the absence of *N*-glycans in up to three positions

Since it is known that main role of protein *N*-glycosylation is to ensure proper folding, stability and secretion (Liu and Li, 2014; Strasser, 2016) we have firstly analyzed whether loss of single *N*-glycosylation sites will have significant impact on the protein biogenesis. In order to localize protein within a plant cell *N*-glycosylation variants of FER-GFP translational fusions (pFER::*FER-GFP*) were transiently expressed in *Nicotiana benthamiana* epidermal cells. Confocal microscopy analysis revealed expected wild type FER-GFP localization to the plasma membrane (PM) (Fig. 3). We have then observed for eight out of ten FER variants to be exclusively localized at the PM, while FER-GFP variants M5 and M9 (Tab. 1) had predominant localization at the PM with a small cytoplasmic fraction (Fig. 3). In parallel localization of the four MS detected sites (M1, M3, M8 and M10, Tab. 1) was confirmed using *A. thaliana* mesophyll protoplasts. Either wild-type or single *N*-glycosylation mutant *FER-GFP* fusions under 35S viral promotor were transiently expressed in *A. thaliana* protoplasts (Tab. S6). We have observed that all FER variants were correctly located at the plasma membrane (Fig. S2). Therefore, loss of single *N*-glycan occupied sites *in planta* (N46, N142, N330, and N410) does not impact significantly protein folding and stability, since wild-type level of accumulation was observed.

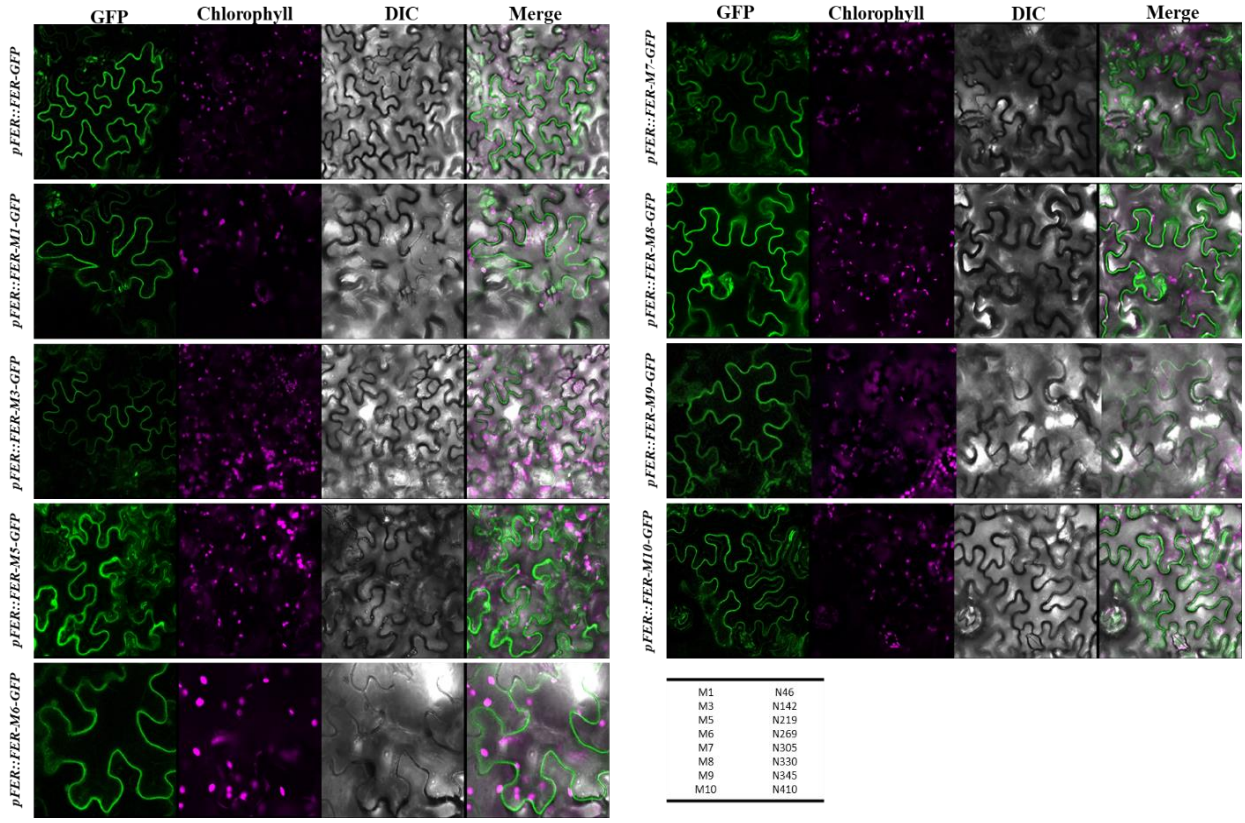

Figure 3. Subcellular localization of FER-GFP single *N*-glycosylation variants in *Nicotiana benthamiana* epidermal cells. Eight out of then FER-GFP *N*-glycosylation single mutants are exclusively targeted to the plasma membrane. GFP signal (green) and chlorophyll autofluorescence (magenta). Expression of FER-GFP variants was observed 3 days post-agroinfiltration.

Observing that loss of single *N*-glycosylation sites had almost no effect on the protein stability we wondered if different combination of double mutant variants would still properly be localized at the PM. We have firstly tested four different combinations of double mutants affecting MS detected sites (M11-M15, Tab. 1) and found all of them to entirely localize to the PM (Fig. S3). Therefore,

simultaneous introduction of two sites did not have a cumulative effect on protein stability. We then analyzed if various combinations of double mutant variants (M16-M18, Tab. 1) affected in sites found either in glycoproteomic study (N269 and N345) or crystallography study (N305) would have differential effect on protein localization at the PM.

Interestingly these three *N*-glycosylation sites are all residing within FER MAL-B domain. In line with the single N345 mutant (M9 variant), slight cytoplasmic localization with predominant PM targeting was observed for both double variants (M17 and M18, Tab. 1) which were depleted of site N345 (Fig. 4). Double variant M16 on the other hand showed unaffected PM localization (Fig. 4). Taken together only variants containing N345 mutated showed slight impairment of stability leading to reduced PM localization.

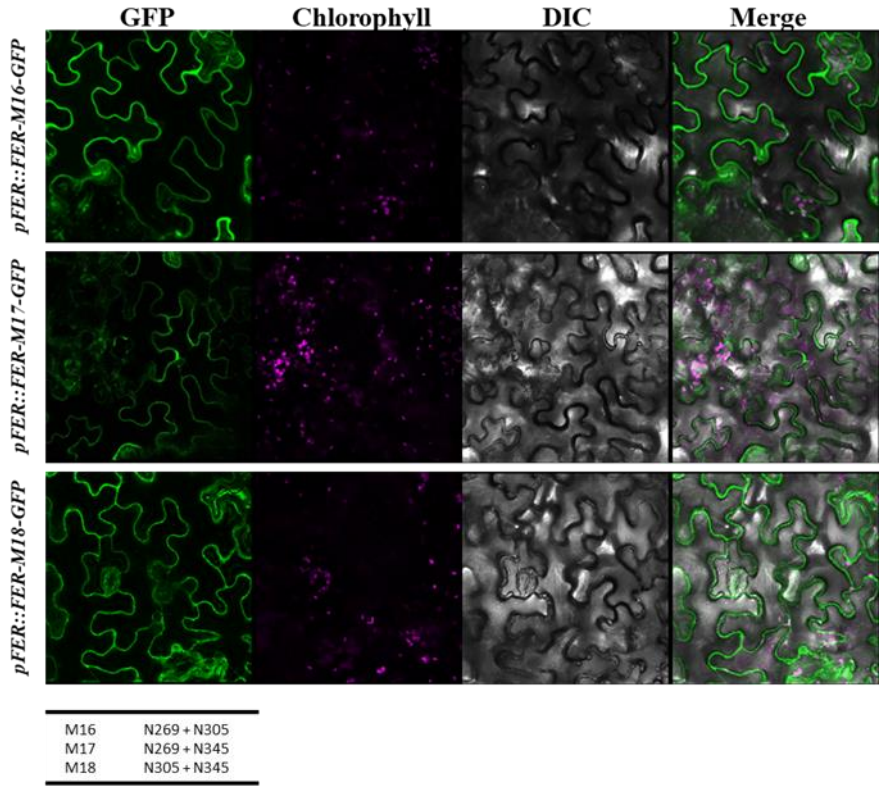

Figure 4. Subcellular localization of FER-GFP double *N*-glycosylation variants in *Nicotiana benthamiana* epidermal cells. FER-GFP N-glycosylation mutants predominantly localize to the plasma membrane. GFP signal in green and chlorophyll autofluorescence in magenta. Expression of FER-GFP variants was observed 3 days post-agroinfiltration using confocal microscope.

We then wondered if a coincident loss of three *N*-glycosylation sites would cause more severe impact on protein folding and stability. Thus, expression of three triple mutant variants (M19-M21, Tab.1) was analyzed in *N. benthamina*. M19 variant which was depleted of MS detected sites showed large cytoplasmic accumulations with still portion of protein being localized at the PM (Fig. S4). However, two other triple variants (M20 and M21, Tab.1) showed exclusive PM localization (Fig. S4). These variants had addition of N124 or N171 sites to the double variant M11 (Tab. 1), therefore it can be concluded that loss of these MAL-A residing *N*-glycosylation sites did not have detrimental impact on double mutant. In other to get better understanding of MAL-A *N*-glycosylation importance, variant depleted of all four MAL-A resident N-glycosylation sites was analyzed (M22, Tab. 1). Interestingly even quadruple variant completely devoid of MAL-A *N*-glycans was solely located to the PM (Fig. S4).

Simultaneous loss of four and more *N*-glycans interferes with the efficient targeting of FER-GFP to the PM

With purpose of assessing to which extent can loss of FER *N*-glycosylation be tolerated, we have generated high-end mutant variants (M23-M30, Tab. 1) and assessed subcellular localization in *N. benthamiana* leaves. Confocal analysis showed substantial accumulation in cytoplasmic streams already in variant M23 (Tab. 1), with still a remaining portion of protein being targeted to the PM (Fig. 5). Similar pattern of subcellular localization was observed for the quintuple M24 variant (Tab. 1) while starting from hexapole variant (M25, Tab. 1) level of protein degradation was exacerbated (Fig. 5). Confocal analysis revealed high degree of M25 being localized to not only cytoplasmic streams but also in perinuclear regions, indicative of ER retention (Fig. 5). From the hexapole variant onwards (M24-M30, Tab. 1) level of protein degradation was more prominent, with the highest proportion of fluorescent signal being detected in the perinuclear area (Fig. 5).

Since starting from quadruple variant (M23, Tab. 1) PM localization was disrupted (Fig. 5) while beginning from the hexapole variant (M25, Tab. 1, Fig. 5) level of the ER retention was substantial, colocalization assays of respective variants with an ER marker (*p35S::*ER-rk) were performed (Nelson et al., 2007). To begin with, expression of the wild-type FER-GFP cotransformed with an ER marker in tobacco leaves was analyzed. As expected, wild type FER-GFP was strictly targeted to the PM, thus no overlap was detected with ER marker (Fig. S5). However, confocal analysis revealed a substantial colocalization with ER marker for both M23 and M25 variants (Fig. S5). Overall, it can be concluded that simultaneous loss of four and more *N*-glycosylation sites FER has a strong impact on the protein folding, stability and secretion, while the degree of FER-GFP functionality can be only determined through the complementation studies in the loss of function *fer-4*.

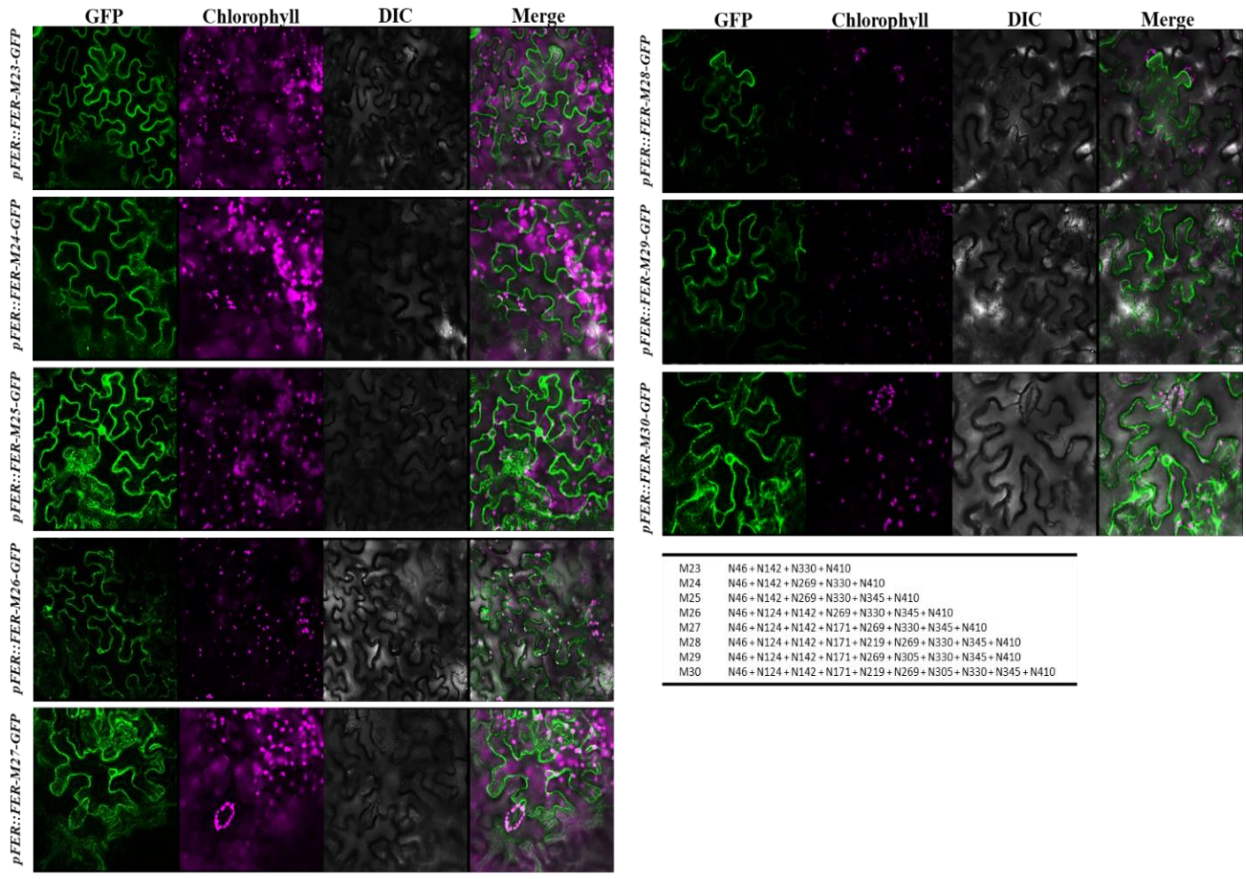

Figure 5. FER-GFP higher-end *N*-glycosylation variants in *N. benthamiana* epidermal cells. FER-GFP

quadruple and quintuple variants show partial membrane localization with cytosolic accumulations. Starting from the hexapole variant most of the signal is at perinuclear region suggesting ER retention. Expression was observed 3 days post-agroinfiltration using confocal microscope. GFP signal is depicted in green and Chlorophyll in magenta.

Simultaneous loss of five *N*-glycosylation sites do not affect FER mediated root hair development and growth

One of the most prominent *fer*-related defects is heavily impaired growth of root hairs (RHs), with a vast majority of RHs being either collapsed, burst, or short (Duan et al., 2010; Li et al., 2015). However, ligand of FER in the context of RHs development is still unknown, therefore it is unclear how FER perceives extracellular cues. As previously mentioned FER`s ECD contain two MLDs, hence it was postulated that FER directly binds CW polysaccharides (Boisson-Dernier et al., 2011).

Having in mind high degree of *in planta* FER^{ECD} *N*-glycosylation, we hypothesized that *N*-glycans mediate FER interaction with the environment (putative ligands/CW components) during RHs development and growth. In order to probe our hypothesis, we have introduced FER *N*-glycosylation expression clones (Tab. S10) to the homozygous *fer-4* to test their capability to rescue RHs bursting phenotype. Stable T1 transformants were selected and RHs length was measured five days after germination. As expected for *fer-4*, most of the RHs collapsed upon emergence, and those that grew burst after a while, leading to significantly shorter RHs length compared to the wild-type Col-0 (Fig. 6A). For each line (different FER variant) data from 10 T1 lines was pooled together since they were not behaving differently within respective line.

In the first place we checked whether wild-type FER (*pFER::*FER-GFP) can fully rescue *fer-4* RHs phenotype, meaning that translational fusion is functional (Fig. 6A). Since wild-type FER could restore RH growth, complementation capabilities of all ten single FER *N*-glycosylation variants were determined in the same manner. Total complementation of *fer-4* RHs phenotypes was detected for the eight variants that showed clear PM location (Fig 3 and Fig. 6). M5 and M9 variants previously showed mild accumulation in cytoplasm, but predominant PM targeting in tobacco (Fig. 3). M9 led to the complete rescue of *fer-4* RH defects, while variant M5 (N219) showed a mild reduction of complementation ability in comparison to the wild-type (Fig. 6). Taken together, loss of N219 caused a mild decrease in protein stability, but also affected FER function during RHs development. It is interesting to point out that site N219 is the only one residing between MAL-A and MAL-B domains in FER^{ECD} (Fig. 2A).

We have analyzed in the same fashion three double mutants M16-M18 (Tab. 1) which were targeted at N269, N345 and N305 *N*-glycosylation sites of the MAL-B domain. Similar to the single FER variants, all of the double mutants led to the full recovery of RHs bursting (Fig. 6). Therefore, a mild cytoplasmic fraction observed in tobacco of variants M17 and M18 (Fig. 4) did not have negative impact on the FER functionality in the context of RHs growth.

Furthermore, two triple (M20 and M21, Tab. 1) as well as quadruple mutant variant (M22) affecting MAL-A *N*-glycosylation sites resulted in a wild-type like RH length (Fig. 7). This was expected since targeting to the PM in localization assays was unaffected. Therefore, it can be concluded that simultaneous loss of all *N*-glycans within FER MAL-A does not impair FER stability, or ability to interact with potential ligand, leading to a full restoration of RHs growth.

On the other hand, we hypothesized that since we observed strong cytoplasmic signal in the quadruple variant M23 (Tab. 1, Fig. 5) as well as significant colocalization with ER marker (Fig. S5), that this destabilized version of FER would no longer be able to restore *fer-4* RHs phenotypes. Surprisingly, we have observed opposite, full complementation equivalent to wild type FER (Fig. 7). Furthermore, even quintuple mutant variant M24 (Tab. 1) could fully restore RHs bursting of *fer-4* seedlings (Fig. 7). Overall, it can be concluded that loss of *N*-glycosylation of FER is well tolerated by the root hair machinery, leading to the normal root hair development and growth.

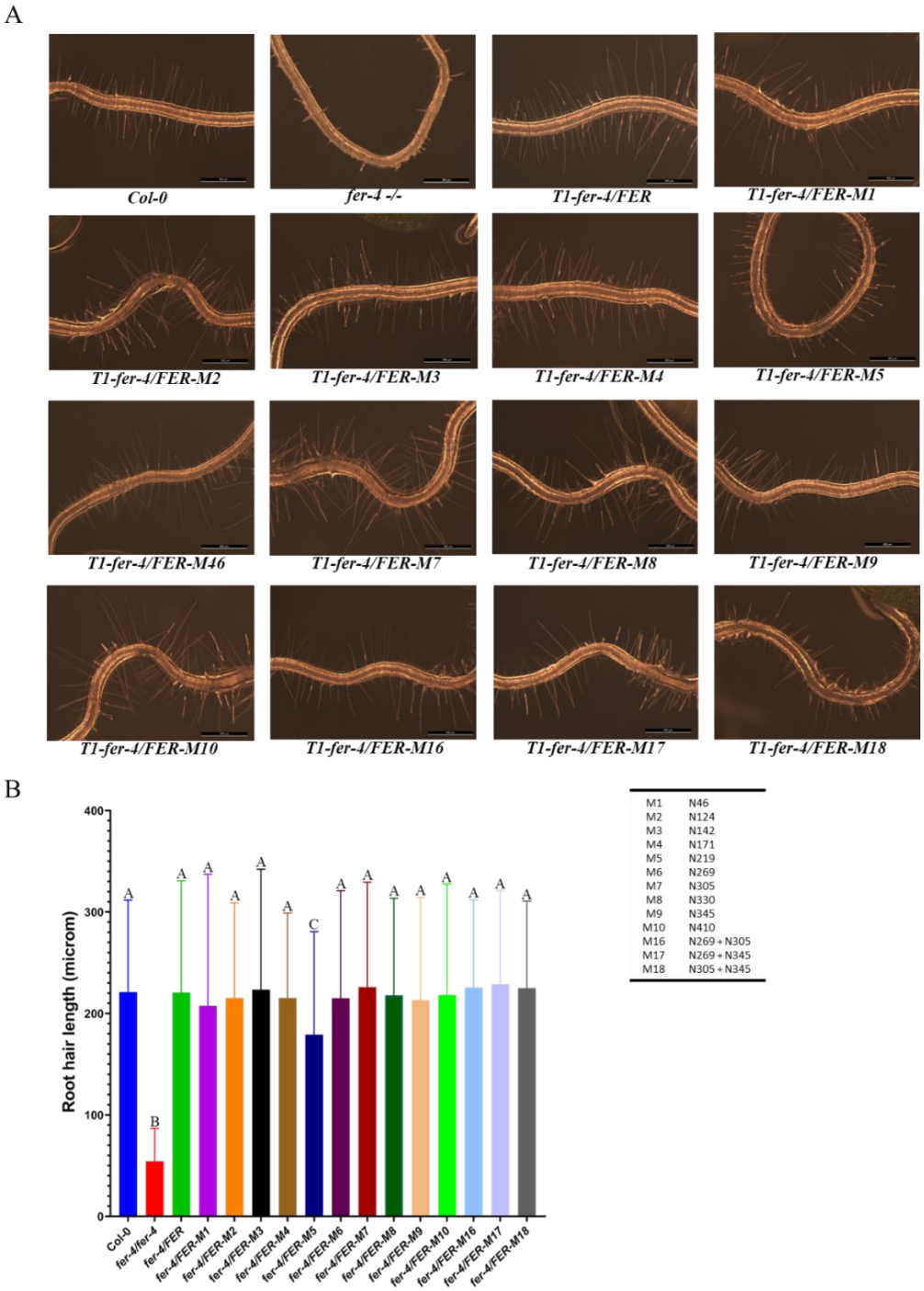

Figure 6. Root hair phenotypes of *fer-4* complemented with single and double FER-GFP *N*-glycosylation variants. (A) Images of 5 days old Col-0, *fer-4* and ten T1 seedlings/line were taken using Leica stereomicroscope. Phenotyping was done by measuring root hair length in the region of 1.5 to 3.5 mm from the primary root tip. **(B)** Quantification of root hair lengths.Col-0 (n=161), *fer-4* (n=110), *fer-4/FER* (n=245), *fer-4/FER-M1* (n=265), *fer-4/FER-M2* (n=142), *fer-4/FER-M3* (n=146), *fer-4/FER-M4* (n=160), *fer-4/FER-*

M5 (n=284), *fer-4/FER-M6* (n=152), *fer-4/FER-M7* (n=159), *fer-4/FER-M8* (n=163), *fer-4/FER-M9* (n=156), *fer-4/FER-M10* (n=151), *fer-4/FER-16* (n=258), *fer-4/FER-17* (n=247), *fer-4/FER-18* (n=253). Kruskal-Wallis test followed by Dunn`s multiple comparison test (A-B ****P<0.0001; A-C ****P<0.0001; B-C ****P<0.0001). Scale bar: 500µm.

FER mediated root hair growth is compromised after simultaneous loss of six *N*-glycosylation sites

Based on our subcellular localization studies in tobacco, hexapole variant FER-M25 (Tab. 1, Fig. 5) showed a high degree of protein degradation observed from a strong retention in the ER (Fig. S5). Since a fraction of FER at PM was observed we tested if the remaining proportion of FER is sufficient to complement *fer-4* RHs defects. We found an inability of FER-M25 variant to complement *fer-4* RHs bursting, however we have observed slightly differential complementation capabilities among different T1 lines. It is probable that difference in the complementation capabilities among T1s are stemming from varying amounts of expressed FER variant.

Copy number analysis using a digital droplet PCR (ddPCR) among T1s expressing M25 hexapole variant (Tab. 1) revealed one single T-DNA insertion line and two double insertion lines, while other had ascending number of insertions (Fig. S12). After obtaining T3 homozygous lines, it was discerned that the degree of complementation correlates with the copy number, thus double lines showed slightly better improvement of *fer-4* RHs burst compared to the single insertion line which was indistinguishable from *fer-4* (Fig. S6). Taken together it can be concluded that upon a loss of six *N*-glycosylation sites, FER-GFP stability is severely compromised leading to the inability to exit ER and the residual fraction at the PM can no longer compliment *fer-4* RHs growth defects. However, at this stage, it cannot be completely excluded that observed phenotypes are partially stemming from the heavily deglycosylated FER M25 variant being unable to properly sense its environment and thus mediate root har growth. Further localization analysis of M25-M30 variants is the seedling RHs will show whether a portion of FER can still be targeted to the PM.

Furthermore, we have found that addition of MAL-A resident sites M2 (N124) and M4 (N171) in the septuple (M26) and octupole (M27) mutant variants (Tab. S1) did not worsen complementation capabilities compared to the hexapole M25 (Fig. 7). This was in line with the previously observed PM targeting of quadruple MAL-A variant M22 (Fig. S4) as well as the full complementation of RHs bursting (Fig. 7). Thus, it is likely that sites M2 and M4 are not *N*-glycosylated *in planta*, or at least are not heavily occupied in the root hairs. Lastly, we detected that the nonuple (M28 and M29, Tab.1) and decuple (M30, Tab. 1) variants completely resembled *fer-4* even in a T1 hemizygous state (Fig. 7). Taken together it can be concluded that after the simultaneous loss of six *N*-glycosylation sites RHs bursting can no longer be complemented, probably due to the decreased protein stability.

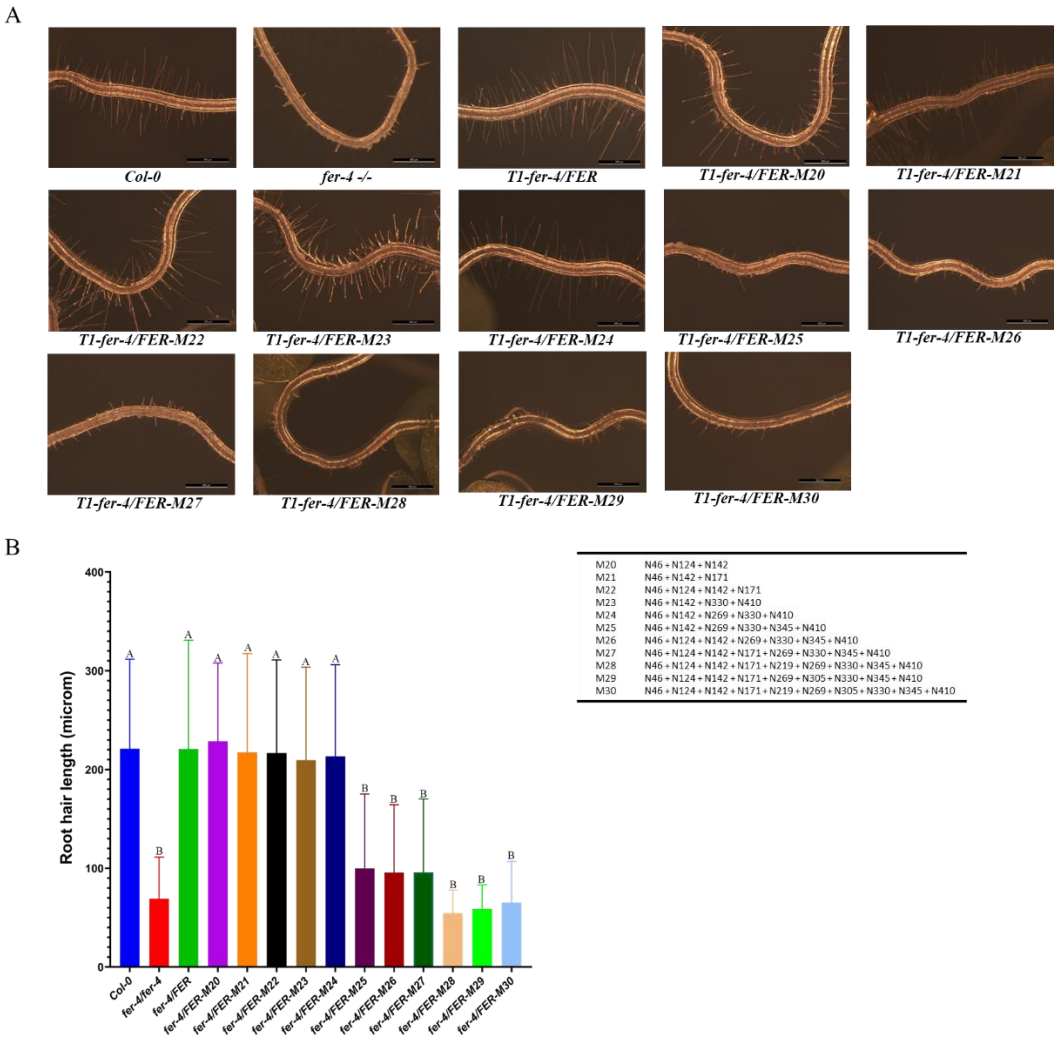

Figure 7. **Root hair phenotypes of *fer-4* complemented with high-order FER-GFP *N*-glycosylation variants. (A)** Images of 5 days old Col-0, *fer-4* and 10 T1 seedlings/line were taken using Leica stereomicroscope. M28 and M29 lines we had obtained reduced number of T1s, respectively six and three. Phenotyping was done by measuring root hair length in the region of 1.5 to 3.5 mm from the primary root tip. **(B)** Quantification of root hair lengths. Col-0 (n=161), *fer-4* (n=110), *fer-4/FER* (n=245), *fer-4/FER-M20* (n=148), *fer-4/FER-M21* (n=158), *fer-4/FER-M22* (n=184), *FER-M23/FER-M23* (n=265), *fer-4/FER-M24* (n=205), *FER-M25/FER-M25* (n=296), *fer-4/FER-M26* (n=215), *fer-4/FER-M27* (n=223), *fer-4/FER-M28* (n=46), *fer-4/FER-M29* (n=58), *fer-4/FER-M30* (n=181). Kruskal-Wallis test followed by Dunn`s multiple comparison test (A-B ****P<0.0001). Scale bar: 500µm.

FER-regulated vegetative growth of shoot and petioles is more tolerant to the loss of *N*-glycosylation

As mentioned previously FER is involved in the regulation of cellular elongation during vegetative growth, thus loss of FER leads to not only root hair burst, but also severe dwarfism and shorter petiole length (Guo et al., 2009; Li et al., 2016). Even though hexapole FER-M25 variant could not complement RHs bursting, on the other hand dwarfism and petiole length of *fer-4* were fully complemented (data not shown). Additionally, even variant lacking eight *N*-glycosylation sites (M27, Tab. 1) showed wild-type like vegetative growth and petiole length (data not shown). This is line with the observation that severity of RHs bursting is comparable between M25, M26 and M27 variants (Fig. 7). Despite inability to complement RHs bursting nonuple variants (M28 and M29, Tab. 1, Fig. 7), showed partial complementation of dwarfism and petiole length. However, severity of these

vegetative phenotypes was more pronounced in M28 (Tab. 1) which in addition to eight mutations had as well M5 variant (N219) targeted. This observation is in line with the variant M5 being the only single site in which RHs bursting was not fully complemented (Fig. 6). However, in the case of M28 variant only one transgenic plant survived transfer form selection plates to the adult stage, therefore these observations are tentative. In parallel M29 variant displayed higher degree of complementation compared to the M28, however due to low number of transgenics final conclusion cannot be derived at this stage. Only in the variant M30 (Tab. 1) which is lacking all ten *N*-glycosylation sites we observed complete loss of any complementation and all plants were *fer*-like in the terms of RHs bursting (Fig. 7), dwarfisms, anthocyanin accumulation and petiole length.

Salt stress responses are mediated by the *N*-glycosylation of FER extracellular domain

As already mentioned, FER is involved in the regulation of abiotic stress responses, with *fer-4* seedlings being extremely hypersensitive to the salt stress (Feng et al., 2018; Yu and Assmann, 2018; Zhao et al., 2018). Similar salt-induced phenotypes have been reported for the several mutants affected in the ER and/or Golgi apparatus resident enzymes of the *N*-glycosylation pathway (Farid et al., 2011, 2013; Kang et al., 2008; Koiwa, 2003; Liu et al., 2018). With all things considered, we hypothesized that *N*-glycosylation of FER^{ECD} is important for the FER mediated growth control under salt stress conditions.

Since it was reported that *fer-4* had strong hypersensitive phenotypes (inhibition of primary roots growth and reduced survival) under high salinity (140mM NaCl) (Feng et al., 2018), the ability of several *N*-glycosylation variants to complement *fer-4* salt-related growth defects was analyzed. Introduction of wild-type FER into *fer-4*, led to the restoration of both primary root length as well survival rates to the wild type level of Col-0 plants (Fig. 8). Survival rate was determined from the images taken upon salt stress treatment. We have considered seedlings sensitive if more than 50% of leaves went under prominent chlorosis (Fig. 8D). T2 plants expressing five different FER single *N*-glycosylation variants (M1, M5, M6, M7, M9, Tab. 1) were firstly screened. Single variants M1, M6, and M7 (Tab. 1) showed not only RHs bursting complementation but also exclusive targeting to the PM in tobacco (Fig. 3 and Fig. 6). M6 and M7 variants were able to recover salt stress induced inhibition of the root growth to the wild type level (Fig. S7). On the other hand, M1 (N46) could not restore *fer-4* salt stress hypersensitivity (Fig. S7). M5 variant (N219), which was not fully targeted to the PM in tobacco (Fig. 3), and it could not fully restore RHs bursting phenotype (Fig. 6), also the primary root growth was comparable to *fer-4* under salt stress conditions (Fig. S7). M9 variant (N345), which displayed cytoplasmic accumulations in tobacco (Fig. 3) but could entirely complement RHs bursting (Fig. 6) were as sensitivity to the high salinity as *fer-4* (Fig. S7).

Previous experiments were performed in a hemizygous T2 lines and in order to have a more conclusive findings we have obtained homozygous T3 plants expressing either wild type FER or the following *N*-glycosylation variants M1, M23 and M25 (Tab. 1). As mentioned previously ddPCR analysis was performed to find single insertion transgenic lines (Fig. S12). Therefore, in all following analysis single insertion lines for the wild type FER; M1 and M23 variants were used, while in M25 one single and two double were used. In order to have additional control of loss of function *fer-4*, T2 plants expressing M30 variant (Tab. 1) depleted of all ten FER *N*-glycosylation sites were included.

As expected, T3 lines expressing wild type FER were able to restore *fer-4* primary root growth as well as the survival defects (Fig. 8). Compared to the wild type FER and Col-0 which had around 95% of resistant seedlings, in the *fer-4* only 14% of seedlings were surviving under high salinity conditions. M1 variant (N46) had a diminished ability to recover *fer-4* salinity phenotypes, evident from both reduced absolute root length (Fig. 8A), as well as declination of relative root growth in comparison to the wild type FER variant (Fig. 8B). Survival rates were not fully complemented in T3 seedlings expressing M1, with approximately 84% of resistant seedlings (Fig. 8D). Even though similar survival rates were observed in the quadruple M23 variant (Tab. 1), absolute root length (Fig. 8A) and relative root length were more affected compared to M1 (Fig. 8B/C). T3 homozygous lines expressing hexapole variant FER-M25 displayed *fer-4* like growth of the primary root, evident from severe reduction of both absolute root length and the relative root growth (Fig. 8). Only survival rates could be partially complemented in M25 with 49% of resistant seedlings compared to the 14% observed in *fer-4* (Fig. 8D). As expected, decuple M30 (Tab. 1) displayed *fer*-like salt stress hypersensitivity (Fig. 8), with a slight increase of survival rates, however this should be confirmed once T3 lines expressing M30 are obtained. To summarize, FER requires *N*-glycosylation of its extracellular domain to adapt the root growth to the high salinity conditions.

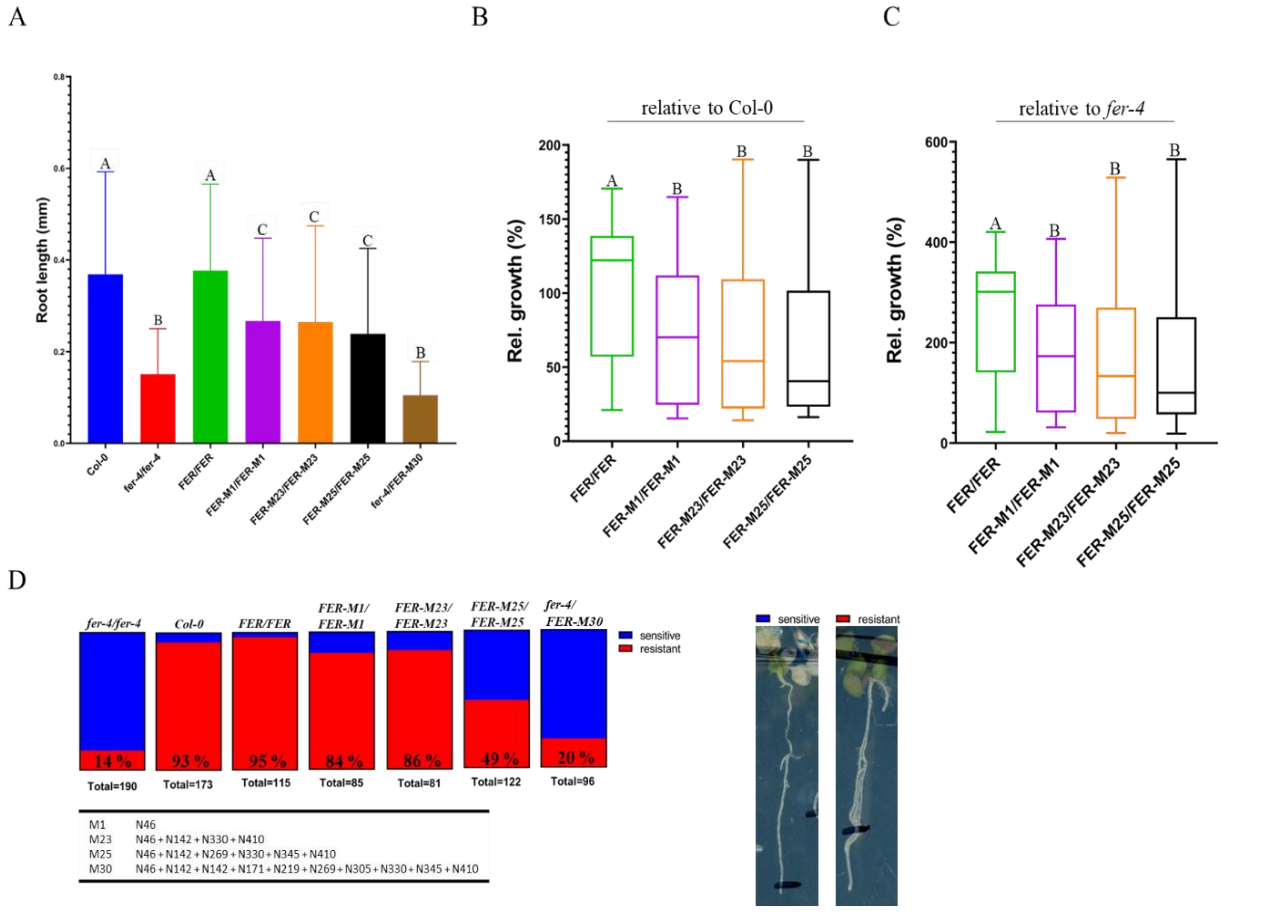

Figure 8. Complementation of *fer-4* salt sensitivity (140 mM NaCl) with different FER-GFP *N*-glycosylation variants. Images of 8 days old Col-0, *fer-4* and T3/T2 seedlings were taken using stereomicroscope. **(A)** Absolute root length. Phenotyping was done by measuring root growth upon transfer to the treatment plates (140 mM NaCl). Col-0 (n=170), *fer-4* (n=148), *FER/FER* (n=208), *FER-M1/FER-M1* (n=176), *FER-M23/FER-M23* (n=184), *FER-M25/FER-M25* (n=192), *FER-M30/FER-M30* (n=164). Kruskal-Wallis test followed by Dunn`s multiple comparison test (A-B ****P<0.0001; A-C **P<0.0043; B-C *P<0.034). **(B)** Relative root growth (compared to Col-0). One-way ANOVA followed by Tukey's multiple comparison test (A-B **P=0.0048). **(C)** Relative root growth (compared to *fer-4*). One-way ANOVA followed

by Tukey's multiple comparison test (A-B **P=0.0092). **(D)** Survival rate of Col-0, *fer*-4 and T3/T2 seedling was determined from images taken after the salt treatment. Examples of sensitive and resistant seedling.

Since salt stress conditions of 140mM NaCl have proven to be extremely severe with heightened decrease of *fer-4* seedlings survival, we decreased concentration of NaCl to try to alleviate harshness of treatment. After five days on 100mM NaCl several complementation lines displayed full complementation of the absolute root growth (Fig. 9A), visible as well from the proportion of relative root growth (Fig. 9B). Variant M5 previously showed *fer*-like primary root growth, while under milder conditions growth was almost fully complemented, with a slight difference compared to the other tested variants, however this mild reduction was not statistically significant (Fig. 9). The only evident disparity was found it the survival rates, in the case of M5 it reached 82% in the comparison to 90-95 % observed for M16, M17, M18 (Fig. 9C). T3 homozygous lines expressing hexapole M25 variant (Tab. 1) which previously exhibited high sensitivity to salt (Fig. 8) showed significantly improved survival rates (from 49% to 77% of resistant seedlings) as well as the absolute and relative root growth (Fig. 9 B/C).

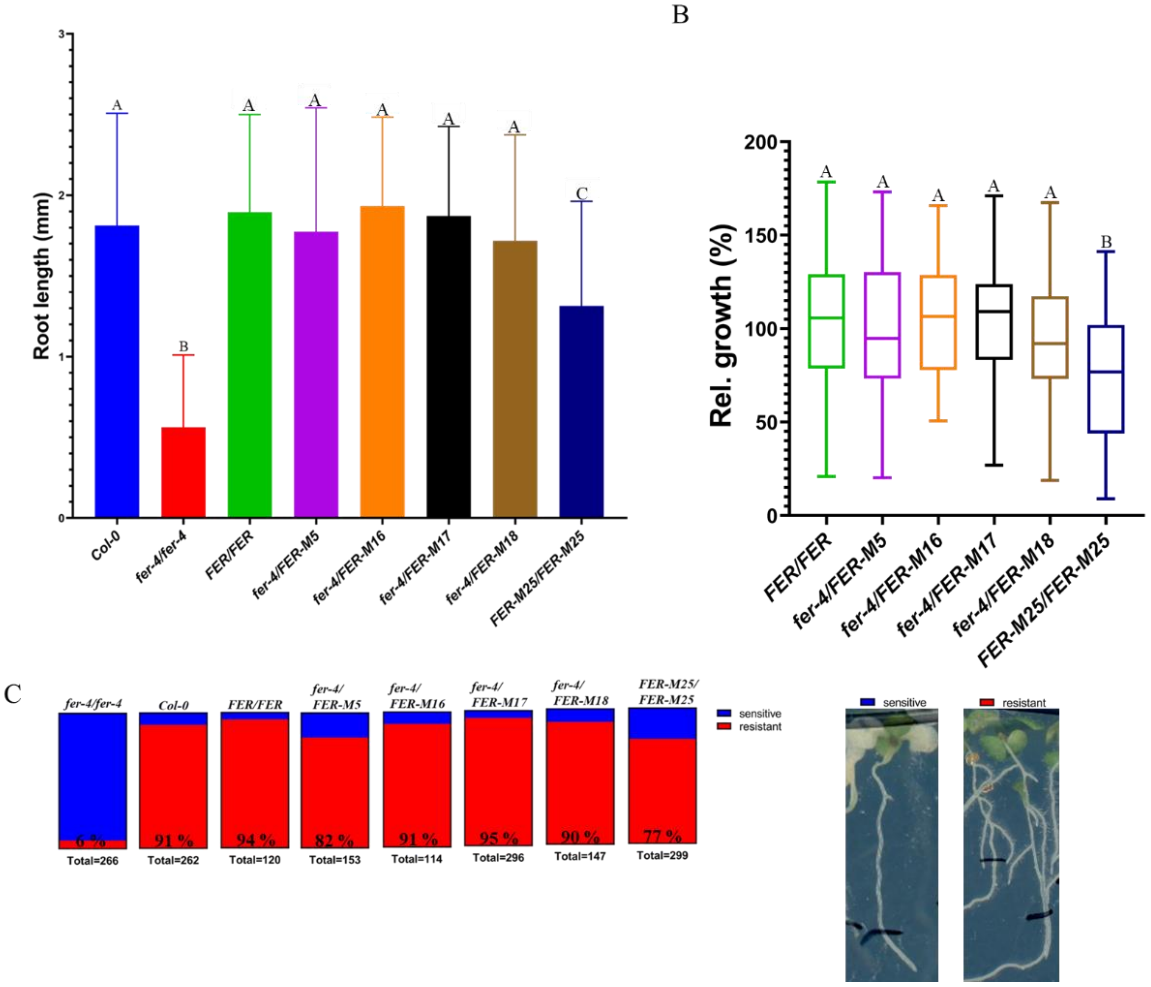

Figure 9. Complementation of *fer-4* salt sensitivity (100 mM NaCl) with different FER-GFP *N*-glycosylation variants. Images of 10 days old Col-0, *fer-4* and T3/T2 seedlings were taken using Leica stereomicroscope. **(A)** Absolute root length. Phenotyping was done by measuring root growth upon transfer to the treatment plates (100 mM NaCl). Col-0 (n=224), *fer-4* (n=206), *FER/FER* (n=145), *fer-4/FER-M5* (n=164), *fer-4/FER-M16* (n=158), *fer-4/FER-M17* (n=161), *fer-4/FER-M18* (n=149), *FER-M25/FER-M25* (n=194). Absolute length statistical significance was determined using Kruskal-Wallis test followed by Dunn`s multiple comparison test (A-B ****P<0.0001; A-C ****P<0.0001; B-C ****P<0.0001). **(B)** Relative root growth (compared to Col-0). One-way ANOVA followed by Tukey's multiple comparison test (A-B ****P<0.0001)

(C) Survival rate of Col-0, *fer*-4 and T3/T2 seedling was determined from images taken after the salt treatment. Examples of sensitive and resistant seedling.

Even though we have applied milder salt stress conditions, which improved sat tolerance of several complementation lines, survival rates of *fer-4* seedlings dropped from 14% to 6% (Fig. 9C). Potential explanation could lie in the prolonged duration of the treatment (from 3 to 5 days), therefore more optimization is needed to find conditions under which *fer-4* can be more tolerant to salinity so that more subtle changes of root growth could be decoupled from extremely low seedling survival. Taken together these results show that FER *N*-glycosylation has a protective role during salt stress responses, however it seems that contribution of N-glycosylation is only partial and that most of the FER interactions during salt stress are acting through protein-protein interactions.

FER mutant insensitivity to pectin inhibition is partially restored in hexapole N-glycosylation variant

As previously mentioned *Cr*RLK1Ls monitor dynamic changes in the CW to integrate extracellular cues with intracellular signaling responses (Boisson-Dernier et al., 2011; Höfte, 2015; Lindner et al., 2012). Mode of *Cr*RLK1L communication with the CW polysaccharides is very elusive. Two recent studies linked FER binding to pectin either in the context of CW monitoring during salt stress or in the light of PT reception (Duan et al., 2020; Feng et al., 2018). Another study connected vacuolar expansion during cellular elongation and sensing of the CW by the joint efforts of apoplastic leucine-rich repeat proteins (LRXs) and FER. Authors used epigallocatechin gallate (EGCG), to induce CW stiffening and reduce cellular elongation. Interestingly both *fer-4* and *lrx3/4/5* mutants were insensitive to the treatment, evident through continuation of cellular elongation despite of CW perturbations (Dünser et al., 2019).

Bearing these recent discoveries in mind we hypothesized that FER binding to pectin and/or other CW components is mediated by *N*-glycans within FER^{ECD}. Knowing that EGCG, natural inhibitor of pectin methyl esterases (PMEs) (Lewis et al., 2008) leads to an inhibition of vegetative growth, seedlings were grown for three days in the liquid MS supplemented with either EGCG or its mock. Upon treatment primary root elongation was measured as the output of vegetative growth. Even though in the previous studies already three days old seedlings were transferred to the liquid cultures (Dünser et al., 2019), in preliminary tests using 3 days old seedlings expected *fer-4* insensitivity to EGCG was observed, but also partial irresponsiveness of Col-0 to the EGCG treatment. Additionally, *fer-4* seedlings are very delicate at this early developmental stage, so to ensure that perturbations of root growth are stemming predominantly from the EGCG effect and not from deterioration of general seedlings fitness, five days old seedlings were used in the following experiments.

EGCG responsiveness was tested in the three double mutant variants targeting sites within FER MAL-B domain (M16, M17, M18, Tab. 1). All three double variants displayed wild type like sensitivity to an EGCG treatment resulting in the strong inhibition of the primary root growth, with 50% of relative growth reduction compared to a mock (Fig. S8). Mild responsiveness was also observed in *fer-4* seedlings (Fig. S8), with 78% or relative growth compared to the mock. Taken together it can be concluded that loss of two *N*-glycosylation sites does not impair ability of FER variants to recognize EGCG induced perturbations of pectic component of CW, while in *fer-4* significant inability to sense CW perturbation resulted in a continuation of the primary root growth (Fig. S8).

Before concluding that FER *N*-glycosylation is nonessential during the CW sensing, hexapole M25 mutant variant was analyzed in the same manner. Since M25 is heavily deglycosylated, leading to impaired PM targeting in tobacco (Fig. S5), inability to restore root hair burst (Fig. 7) as well as substantial salinity hypersensitivity (Fig. 8, Fig. 9), we speculated that responsiveness to EGCG will be impaired thus causing *fer*-like continuation of growth. To probe this hypothesis T3 homozygous seedlings expressing either wild type FER-GFP or M25 variant, as well as *fer-4* and Col-0 were grown for five days followed by the EGCG treatment for the next three days. When EGCG treated seedlings were compared to the mock, we observed that all tested lines were responsive to EGCG, including *fer-4* to a lower degree (Fig. 10A). With purpose of getting better understanding of the amplitude of response for each line, growth of each line was normalized to its mock. Regardless of slight EGCG sensitivity *fer-4* showed around 80% of relative root growth which was significantly higher in comparison to 50% root growth observed in Col-0 as well as T3 expressing wild-type FER (Fig. 10B). Very modest increase of relative root growth of 8% was detected for T3 lines complemented with M25 (Fig. 10B), suggestive of slight insensitivity to the EGCG. In a nutshell, one possibility could be that FER *N*-glycosylation is stabilizing binding to pectin/other CW components, but most of the interaction can still happen in the absence of six *N*-glycosylation sites.

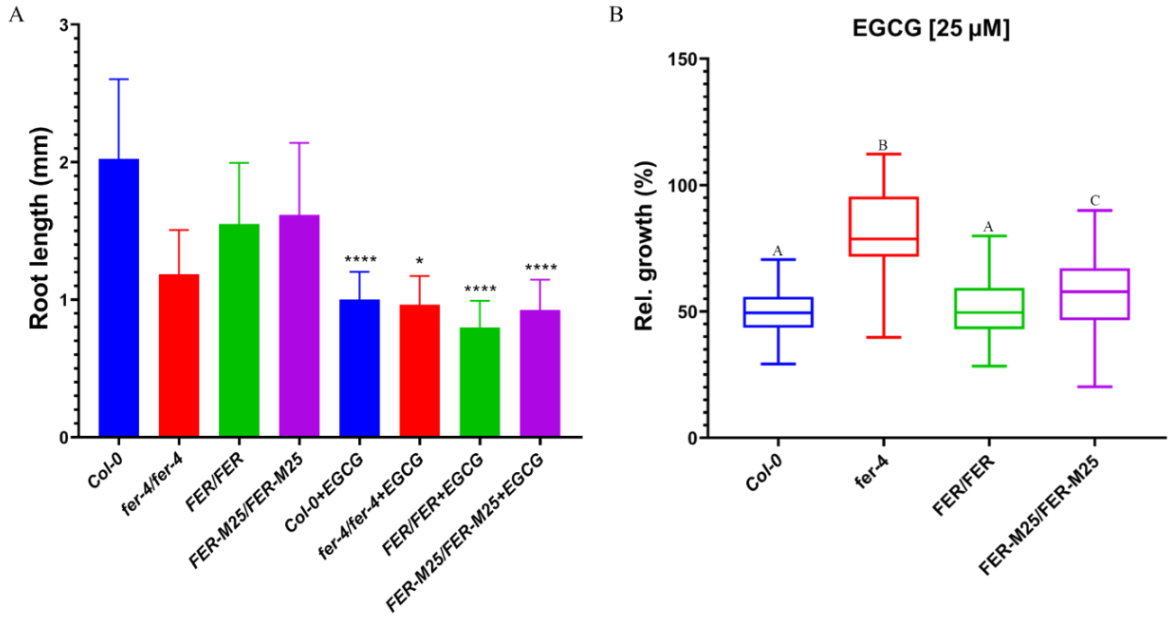

Figure 10. FER-GFP *N*- glycosylation hexapole mutant is sensitive to the EGCG effects on the cell wall integrity. Five days old seedlings were transferred to the EGCG supplemented liquid media. Three days later images of Col-0, *fer-4* and T2 seedlings were taken using Leica stereomicroscope and phenotyping was done by measuring root length. Col-0 (n=38), *fer-4* (n=43), *FER/FER* (n=74), *FER-M25/FER-M25* (n=120). **(A)** Mann-Whitney U test was done to compare absolute root length before and after EGCG treatment. Each genotype was analyzed separately, but here is present together in a graph (*P=0.0143; **** P<0.0001). **(B)** Relative root length after 3 days of EGCG treatment (each genotype normalized to the mock conditions). One-way ANOVA followed by Tukey's multiple comparison test (A-B ****P<0.0001; A-C *P=0.0274; B-D ****P<0.0001).

N-glycosylation of FER seems to be nonessential for the intraspecific pollen tube reception

Considering FER`s crucial role during intraspecific pollen tube reception (Escobar-Restrepo et al., 2007; Huck, 2003; Rotman et al., 2008) and the notion that perturbation of *N*-glycosylation pathway

leads to the similar *fer*-like PTO phenotype (Lindner et al., 2015; Müller et al., 2016), prompted us to believe that FER requires *N*-glycosylation during PT reception. In order to detect PTO phenotype, aniline blue staining was used to track the PT growth and ovule targeting. In the case of *fer-4* high proportion of PTs (~75%) does not stop its growth once in the proximity of synergids, but it continues overgrowing inside the embryo sack. On the other hand, in wild-type ovules PT stops it growth, burst and release sperm cell for fertilization, and only minor proportion displays PT overgrowth (up to 3%) (Fig. 9A).

To begin with, it was determined if T1s expressing wild type FER can complement PTO. In the T1 lines hemizygous insertion should segregate 1:1, therefore PTO should be reduced by half, which was observed (from 75% to 38% PTO). Systematic assessment of the FER *N*-glycosylation variants ability to complement *fer-4* PTO was undertaken, starting from the single variants up to a decuple variant completely lacking FER^{ECD} *N*-glycosylation motifs (Tab. 1). All FER single *N*-glycosylation variants (M1-M10, Tab. 1) fully complemented *fer-4* PT reception defect (Fig. 11 and Fig. S9). Loss of the single *N*-glycosylation site N219 (M5, Tab. 1) led to impaired complementation of root hair bursting as well as salt sensitivity, but in the context of PT reception was completely tolerated. Similarly, M1 and M9 variants (Tab. 1) could not recover salt stress hypersensitivity but turned out to be superfluous during gametophyte recognition (Fig. 11). This trend of FER *N*-glycosylation sites being unnecessary for the FER mediation of PT reception continued in double mutant (M16-M18, Tab. 1) variants as well (Fig. 11).

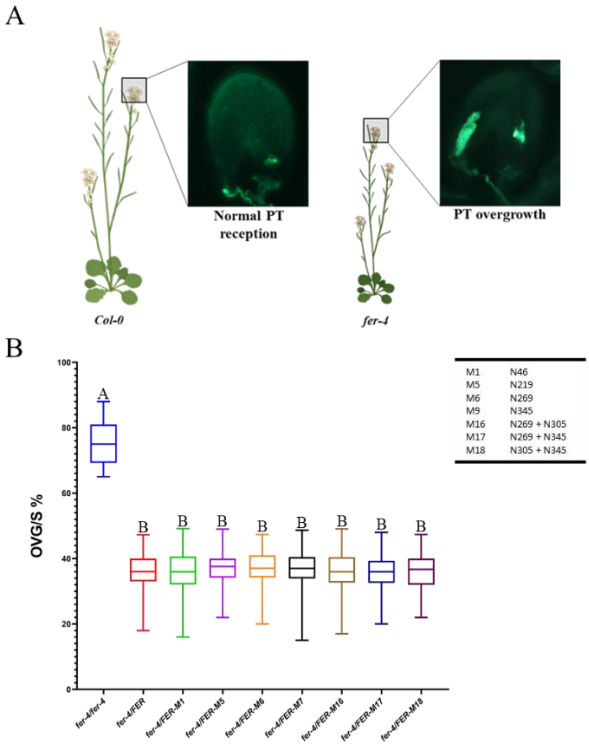

Figure 11. Complementation of *fer-4* intraspecific pollen tube reception with single and double FER-GFP *N* glycosylation variants. (A) Drawing of *A. thaliana* flowering plant, either wild- type Col-0 or *fer-4* mutant (BioRender). Aniline blue stained Col-0 ovule with normal PT reception, and *fer-4* ovule with PT overgrowth. **(B)** Intraspecific PT overgrowth of *N*-glycosylation complementation lines. Box plots represent the percentage of ovules with pollen tube overgrowth per silique. For each FER-GFP *N*-glycosylation complementation line data from 10 independent T1 plants is presented (>500 ovules counted per T1 plant). One-way ANOVA followed by Tukey's multiple comparison test (A-B ****P <0.0001).

Depletion of *N*-glycosylation within MAL-A domain (M22, Tab. 1) led to the full restoration of PTO (Fig. S9). We hypothesized based on the localization and salinity studies, that starting from quadruple M23 (Tab. 1) some extent of impaired PT reception could be observed. On the contrary, complete wild type degree of complementation was observed in the quadruple M23, quintuple (M24), hexapole (M25) and octuple (M27) variants (Fig. 12). These findings are suggesting that FER *N*-glycosylation is differentially regulated in root compared to the flower tissue.

Starting from nonuple variants M28 and M29 partial complementation of *fer-4* fertility was detected, with the 66% and 64% of PT overgrowth found in M28 and M29 respectively (Fig. S9). In line with these observations also vegetative phenotypes were partially complemented, however due to the low number of T1s, final conclusions cannot be drawn at this stage, but these preliminary data are pointing out that loss of *N*-glycosylation cannot be fully tolerated in the context of PT reception. Only M30 variant which was completely depleted of *N*-glycosylation within extracellular domain, fully resembled *fer-4* mutants in heavily impaired intraspecific reception (74% of PTO). It remains to be elucidated if in homozygous state some degree of complementation would be achieved.

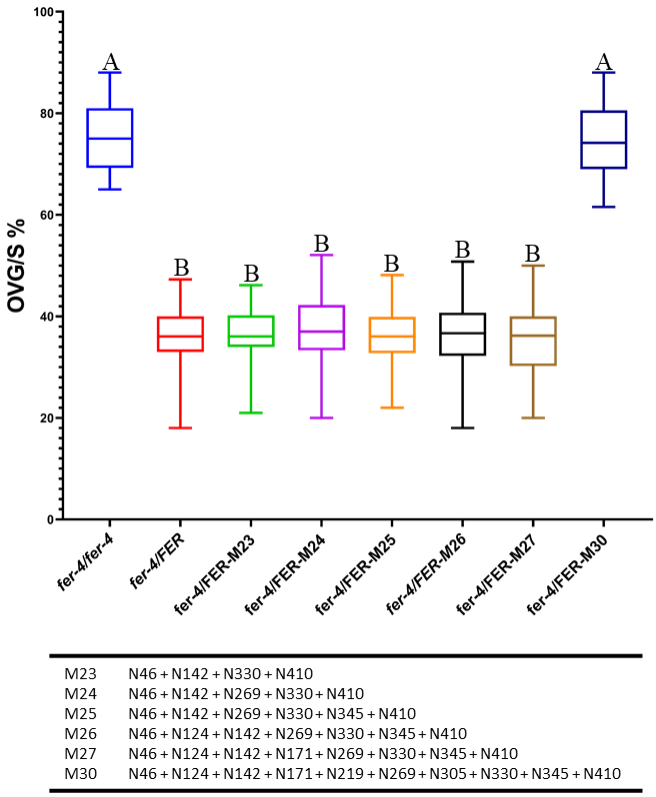

Figure 12. Complementation of *fer-4* intraspecific pollen tube reception with high-order FER-GFP *N* glycosylation variants. Box plots represent the percentage of ovules with pollen tube overgrowth per silique. For each FER-GFP *N*-glycosylation complementation line data from 5 independent T1 plants is presented (>500 ovules counted per T1 plant). One-way ANOVA followed by Tukey's multiple comparison test (A-B ****P < 0.0001).

Finally, we have analyzed previously described single-insertion T3 homozygous lines expressing either wild type FER; M1, M23 or M25 variants (Tab.1, Fig. S12) for their complementation capabilities of intraspecific PT overgrowth. As expected according to the complementation observed in the hemizygous T1 plants (Fig. 11 and Fig. 12), full complementation was achieved in all four variants leading to the wild type level of PTO (<3%) (Fig. S10). Therefore, it can be concluded that even heavily deglycosylated hexapole M25 variant was fully functional in the light of intraspecific PT reception.

FER *N*-glycosylation is required for the proper localization to the filiform apparatus

FER is broadly expressed, however in ovule it is accumulated to the filiform apparatus (FA) (dense folds of PM) of synergid cells (Escobar-Restrepo et al., 2007), where together with its coreceptor LRE and other PT reception players control ROS and Ca^{2+} signaling upon PT arrival, to enable PT burst (Duan et al., 2014; Hou et al., 2016; Kessler et al., 2015; Liu et al., 2016; Ngo et al., 2014; Tsukamoto et al., 2010). Therefore, polarized localization of FER is important to mediate its role during PT reception. Loss of *N*-glycosylation can lead to the protein stability decrease and targeting to the ER associated degradation (ERAD) pathway leading to inability of protein to be secreted to the plasma membrane (Li et al., 2009; Liu and Li, 2014). With intent to determine the importance of *N*-glycosylation for the polar secretion of FER to the FA, localization of different FER *N*-glycosylation variants (Tab. 1) was observed in the ovules of T1 complementation lines two days after emasculation.

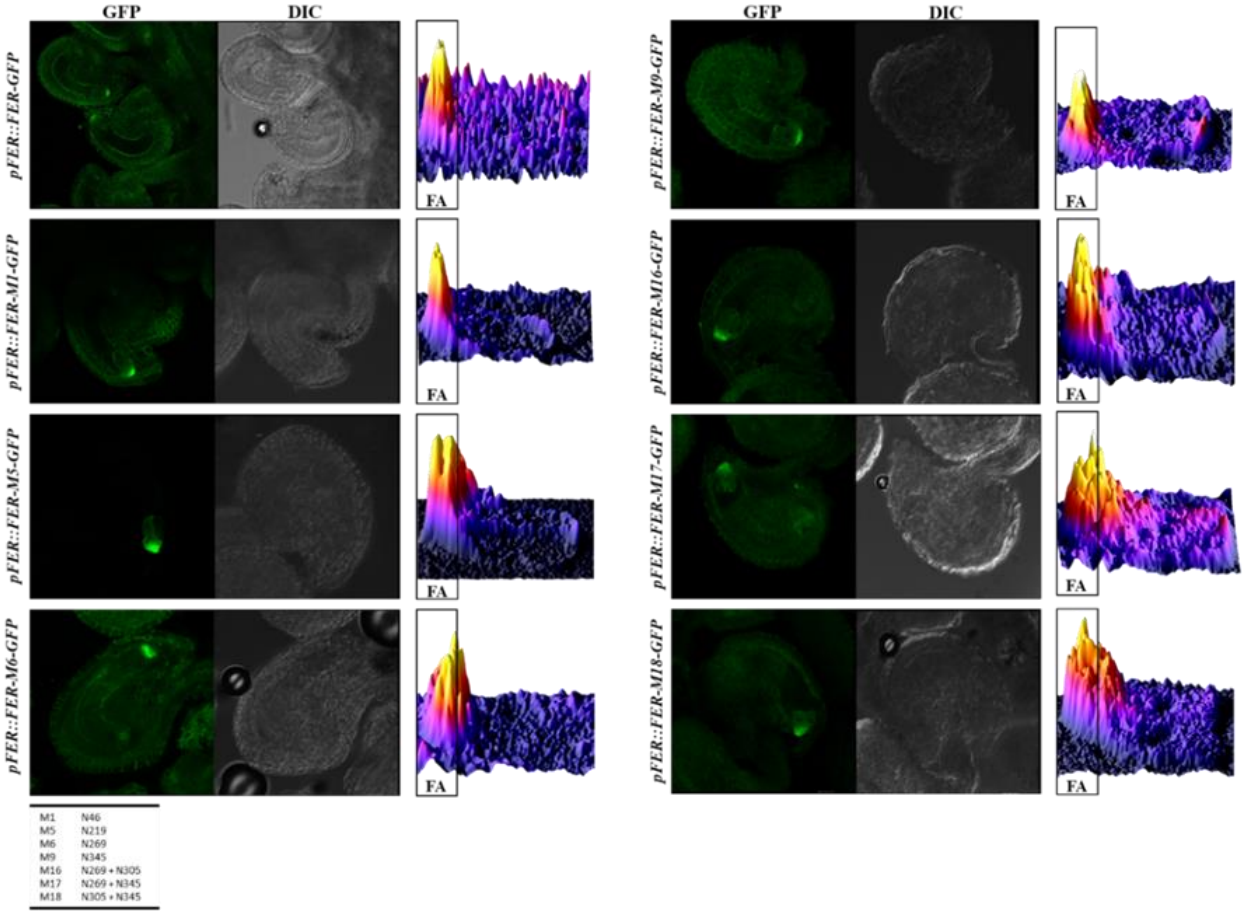

Figure 13. Single and double FER-GFP *N*-glycosylation variants are properly localized at the filiform apparatus of synergid cells. Flowers (floral stage 12) were emasculated and ovules were dissected out of the pistils 24 h later and observed under Leica SP5. Representative confocal images of ovules expressing different FER-GFP *N*-glycosylation variants are presented. Surface plots of total synergid GFP signal intensity were made in ImageJ. Signal coming from the FA is highlighted in the boxed areas. All depicted FER-GFP *N*-glycosylation variants fully complement *fer-4* pollen PT overgrowth phenotype.

In order to have a better insight of the GFP signal distribution, fluorescence intensity was visualized using surface plots which were representing only the area of synergid cells. Boxed section within the plots depicts area of the FA (~10 µm) while the remaining part represents signal coming from a

synergid cytoplasm (SC). In the wild-type FER due to its polar secretion most of the signal is restricted to the FA region (boxed section). The stronger effect *N*-glycosylation variant would have on the protein folding and stability, leading to ER retention, the stronger signal can be expected in the SC region.

All ten single *N*-glycosylation variants (Tab. 1) were stable and properly secreted resulting in the wild-type like localization at the FA (Fig.13 and Fig. S11). Similar degree of secretion was observed for triple and quadruple variants depleted of MAL-A *N*-glycosylation sites (M20-M22, Tab. 1) leading to the exclusive FA localization (Fig. S11). Double mutant variants of MAL-B *N*-glycosylation sites (M16-M18, Tab.1) showed predominant targeting to the FA, with a mild mislocalization found for M17 and M18 variants, in which SC signal in was slightly increased in a comparison to the wild type variant (Fig. 13). This mild impairment of secretion was in line with previously observed cytoplasmic accumulations in tobacco localization assays (Fig. 4).

Quadruple and quintuple variants (M23 and M24, Tab. 1) were predominantly targeted to the FA, but increased accumulation of signal was observed in SC (Fig. 14). Regardless this increase of protein degradation both M23 and M24 were fully functional during PT reception (Fig. 12). Having in mind strong colocalization with the ER marker of hexapole M25 variant (Fig. S5), as well as an inability to restore root hair growth (Fig. 7) and salt stress vegetative growth (Fig. 8, Fig. 9) we expected to find stronger degree of protein degradation compared to lower-end *N*-glycosylation variants (Fig. 13). Therefore, it was not surprising to detect higher signal intensity in the SC area of ovules expressing M25 variant (Fig. 14). Evident downregulation of FA signal intensity compared to the wild-type FER was observed, however the remaining fraction was enough to fully complement intraspecific PT reception (Fig. 12). Lastly, in both septuple and octuple variants (M26, M27, Tab. 1) secretion of FER-GFP was severely impaired, leading to the SC accumulation of signal and only miniscule fraction of FER-GFP at the FA. It is interesting that even these massively mislocalized variants (M25-M27) are still complete functional in their ability to restore the PT reception defects of *fer-4* (Fig. 12). Unfortunately, we could not observe localization of the nonuple mutant variants (M28, M29, Tab. 1), due to the low numbers of obtained T1s, we could not find a line expressing sufficiently strong signal for the confocal analysis.

Lastly, we have obtained ten T1s expressing M30 (Tab. 1) variant lacking all ten *N*-glycosylation sites. Interestingly very similar distribution of fluorescent signal was detected for the decuple M30 variant compared to M25-M27, suggesting that only small decrease of FER-GFP targeting to the FA is leading to the inability of M30 to compliment *fer-4* PTO (Fig. 12). Taken together it can be concluded that loss of *N*-glycosylation sites of FER caused the decreased stability of FER-GFP resulting in the impaired targeting to the FA, however even in octuple variants remaining amount of FER was fully adequate to restore the *fer-4* PTO.

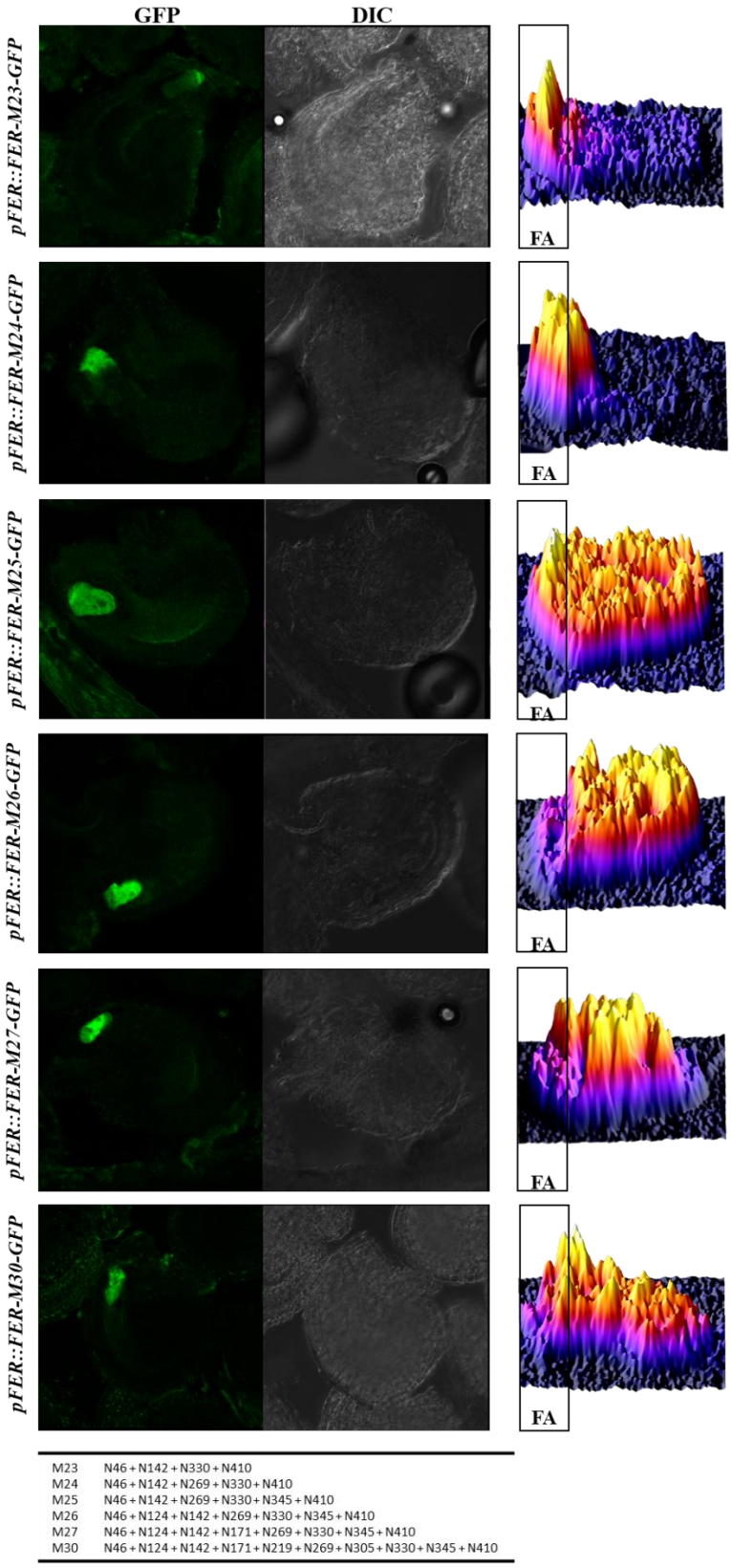

Figure 14. High-order FER-GFP *N*-glycosylation variants display impaired localization at the filiform apparatus of synergid cells. Flowers (floral stage 12) were emasculated and ovules were dissected out of the pistils 24 h later and observed under confocal microscope. Representative images of ovules expressing different FER-GFP *N*-glycosylation variants are presented. Surface plots of total synergid GFP signal intensity. Signal coming from the FA is highlighted in the boxed areas. FER-GFP *N*-glycosylation variants including M27 (8 N-glycosylation sites mutated) fully complement *fer-4* PT overgrowth phenotype. M30 (devoid of all 10 N-glycosylation sites) is no longer able to complement *fer-4* PT overgrowth phenotype.

N-glycosylation of FER ECD is vital during interspecific pollen tube reception

The fact that crosses between closely related *Brassicaceae* species display the *fer*-like PTO (Escobar-Restrepo et al., 2007), as well as the discovery of ER resident *N*-glycosylation mutant *aru* (*ost3/6*) causing an impairment of the interspecific pollen tube reception (Müller et al., 2016) prompted us to believe that FER might play a role in the maintenance of interspecific hybridization barriers. When a self-compatible *A. thaliana* (ecotype Col-0) is pollinated with a closely related self-incompatible *A. lyrata*, interspecific barrier is acting at the stage of pollen tube reception, leading to the PT overgrowth (Fig. 15A).

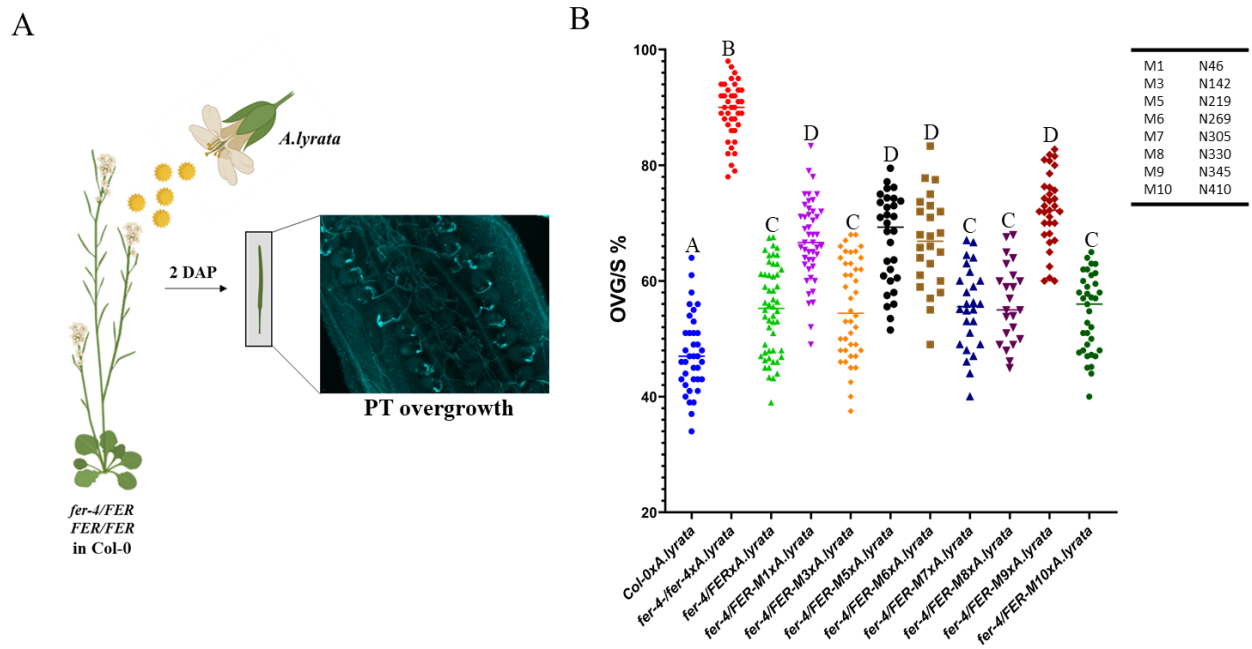

Figure 15. Complementation of *fer-4* interspecific pollen tube reception with single FER-GFP *N* glycosylation variants. (A) Drawing of interspecific cross between *A. thaliana* T1 complementation lines pollinated with *A. lyrata*. Aniline blue staining of silique with high proportion of PT overgrowth. Drawing was done using BioRender. **(B)** FER-GFP *N*-glycosylation complementation lines siliques pollinated with *A. lyrata*. Scatter plots represents data from 5 independent T1 lines/FER variant, and for each line at least 8 crosses were performed (each dot represents one silique). One-way ANOVA followed by Tukey's multiple comparison test (A-B ****P< 0.0001; A-C ***P=0.0001; A-D ****P< 0.0001; B-C ***P=0.0001; B-D ****P< 0.0001, C-D ****P< 0.0001).

Once a Col-0 is pollinated with heterospecific pollen (*A. lyrata*), around 47% of ovules remains unfertilized due to the inability of the female gametophyte to trigger burst of the foreign PTs, resulting in the PT overgrowth. When homozygous *fer-4* is pollinated with foreign pollen (*A. lyrata*), over 90% of the ovules present PT overgrowth, which in comparison to the Col-0 (47%) is markedly higher (Fig. 15B). To be certain of the active utilization of FER signaling during interspecific pollinations, we have checked whether wild type FER can improve interspecific PT overgrowth of *fer-4*. A significant reduction of the PT overgrowth (58%) in T1s expressing wild-type FER was observed, illustrating a direct role of FER in the recognition of interspecific pollen. Upon realization that FER does play an active role in the distinguishing between self- versus foreign pollen, we hypothesized that *N*-glycosylation of FER^{ECD} is required to mediate FER induced interspecific PT reception. Complementation capabilities of the single FER *N*-glycosylation variants (Tab. 1) were assayed in the interspecific crosses with *A. lyrata*. Four out of the eight single variants showed equivalent degree of the PTO compared to the wild type FER in the pollinations with *A. lyrata* (Fig. 15B). These four

variants (M3, M7, M8 and M10) previously displayed strict accumulation to the FA (Fig. S11). On the other hand, remaining four variants (M1, M5, M6 and M9) led to the significant increase of PTO compared to both Col-0 as well as of *fer-4* complemented with the wild type FER (Fig. 15B). The most prominent increase in the PTO compared to the wild type FER was detected in the M9 variant depleted of *N*-glycosylation site N345. This was interesting finding having in mind that intraspecific PT overgrowth was fully complemented, and that targeting to the FA was undisturbed (Fig. 13). Furthermore, we discovered that variants M1 and M6 (Tab. 1) which were exclusively localizing to FA (Fig. 13) displayed significantly higher degree of PTO in crosses with *A. lyrata* (Fig. 15). Lastly also variant M5 (N219) presented increased degree of PTO during interspecific pollinations, and again most of the detected signal was coming from FA (Fig. 13).

Seeing that already loss of the *N*-glycans at the single positions had a striking impact on the interspecific pollen recognition, we were curious to find out if this impairment in the interspecific PT reception would be further enhanced in the higher-order *N*-glycosylation mutants. All three double mutant combinations (M16-M18, Tab. 1) resulted in the increase of PTO in comparison to wild type control (Fig. 16). Cumulative effect was observed in the M16 which was devoid of M6 and M7 *N*-glycosylation sites (Tab. 1) in comparison to the single M6 variant (Fig. 15B). Interestingly even though quadruple variant affecting MAL-A located sites (M22, Tab. 1) showed higher PTO compared to the wild type FER, the extent of phenotype was slightly lower compared to the double mutants targeting MAL-B resident *N*-glycosylation sites. We have also compared the extent of interspecific pollination disruption between MAL-A depleted M22 and quadruple M23 variant targeted at MS detected sites residing within MAL-A and MAL-B domain.

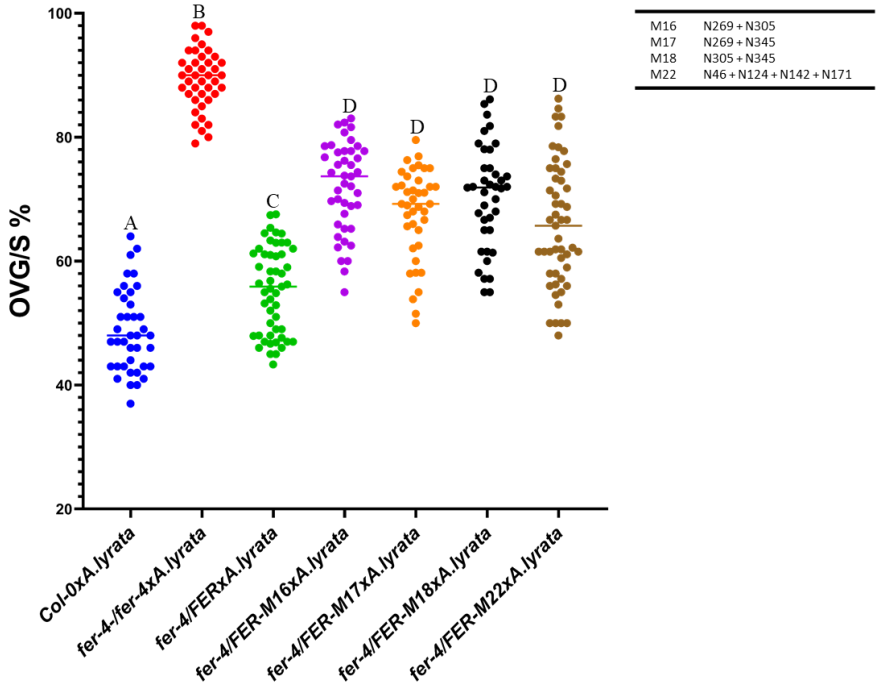

Figure 16. Complementation of *fer-4* interspecific pollen tube reception with double and quadruple FER-GFP *N* glycosylation variants. FER-GFP *N*-glycosylation complementation lines siliques pollinated with *A. lyrata*. Scatter plots represents data from 5 independent T1s/FER variant, and for each line at least 8 crosses were performed (each dot represents one silique). One-way ANOVA followed by Tukey's multiple comparison test (A-B ****P<0.0001; A-C ***P=0.0001; A-D ****P<0.0001; B-D ****P<0.0001).

Based on the slight impairment of M23 secretion, evidential from both tobacco (Fig. 5) and FA mislocalization (Fig. 14), we expected to find more pronounced disruption of the interspecific barrier

in the M23 variant compared to the M22 quadruple variant. To our surprise, this was not the case, and even though PTO was increased in comparison to the wild type FER it was equivalent to the M22 variant. Quintuple variant M24 (Tab. 1) similarly to the quadruple M22 and M23 variants displayed significantly higher increase of the PTO in interspecific pollinations (Fig. 17), however additive effect of M6 depletion in the M23 background was not very prominent, despite of the more pronounced cytoplasmatic accumulations within synergids (Fig. 14). Only when site M9 (Tab. 1) was introduced to the quintuple FER-M24, a substantial drop in the ability of T1 ovules expressing hexapole M25 variant to recognize foreign pollen was found (Fig. 17). Consistent with these findings was a significant drop of the M25 variant targeting to the FA and a pronounced accumulation in the SC region (Fig. 14). However, M25 was restoring to the wild type level intraspecific PT reception, thus the remaining fraction of FER at the FA can successfully accomplish reception of the self-pollen (Fig. 12, Fig. S10). Exact mechanism of the foreign pollen recognition/reception are under a veil of mystery; however, it seems that there is a vast need for the FER^{ECD} *N*-glycosylation to ensure activation of the FER signaling pathway upon arrival of the foreign pollen tubes.

Since octuple M27 variant can fully complement recognition of the self-pollen (Fig. 12), we aimed to uncover if this variant would deteriorate interspecific PT reception in comparison to the hexapole M25. The degree of PTO in the interspecific crosses with *A. lyrata* pollen was indistinguishable between M25 and M27 variant (Fig. 17). Even though both M25 and M27 variant presented substantial increase of the PTO in comparison to the wild type FER, the extent of PTO was still not as severe as in *fer-4*.

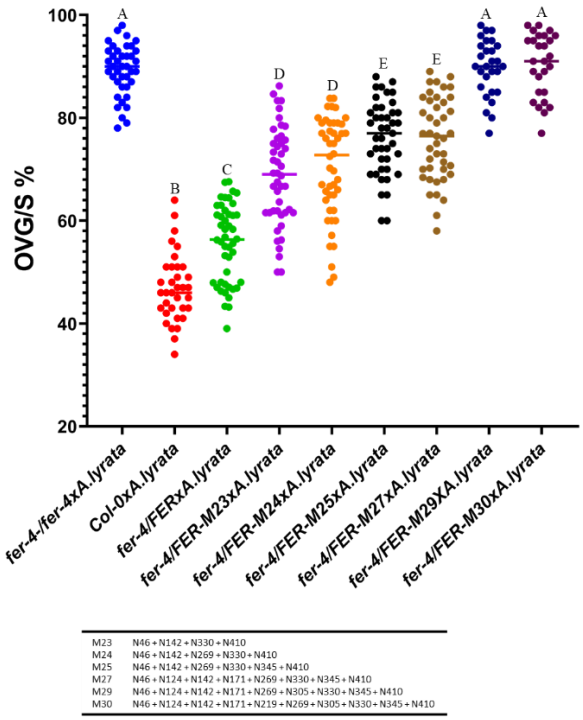

Figure 17. Complementation of *fer-4* interspecific pollen tube reception with high-order FER-GFP *N* glycosylation variants. FER-GFP *N*-glycosylation complementation lines siliques pollinated with *A. lyrata*. Scatter plots represents data from 5 independent T1 lines/FER variant, and for each line at least 8 crosses were performed (each dot represents one silique). One-way ANOVA followed by Tukey's multiple comparison test (A-B ****P<0.0001; A-C ****P<0.0001; A-D ****P<0.0001; A-E ****P<0.0001; B-C ****P<0.0001; B-D ****P<0.0001; B-E ****P<0.0001; C-D ****P<0.0001; C-E ****P<0.0001; D-E ***P=0.0002).

Only when T1s expressing nonuple variant M29 (N305 introduced to octuple variant) were pollinated with *A. lyrata*, level of the PTO matched the one of *fer-4*, leading to astonishing 90% of ovules presenting PTO (Fig. 17). However, only four T1s were obtained for M29 variant, and moreover T1s showed partial intraspecific complementation (Fig. S9), making it harder to uncouple recognition of self- versus foreign pollen.

Lastly, we have selected homozygous T2 plants from the ddPCR characterized T1 lines expressing either wild type FER, M1, M23 or M25 (Fig. S12). We have observed equal degree of PTO between Col-0 and T2 homozygous lines expressing the wild-type FER, meaning that introduction of FER decreased proportion of PTO from 90% observed in *fer-4* to 47% detected in the T2 *FER/FER* plants and Col-0 (Fig. 18). Additionally, three independent T2 lines (derived from the single insertion T1s, Fig.S12) all displayed equivalent degrees of PTO (Fig. 19A). When interspecific crosses were performed, significant increase in the degrees of PTO was observed for all three FER *N*-glycosylation variants (Fig. 18).

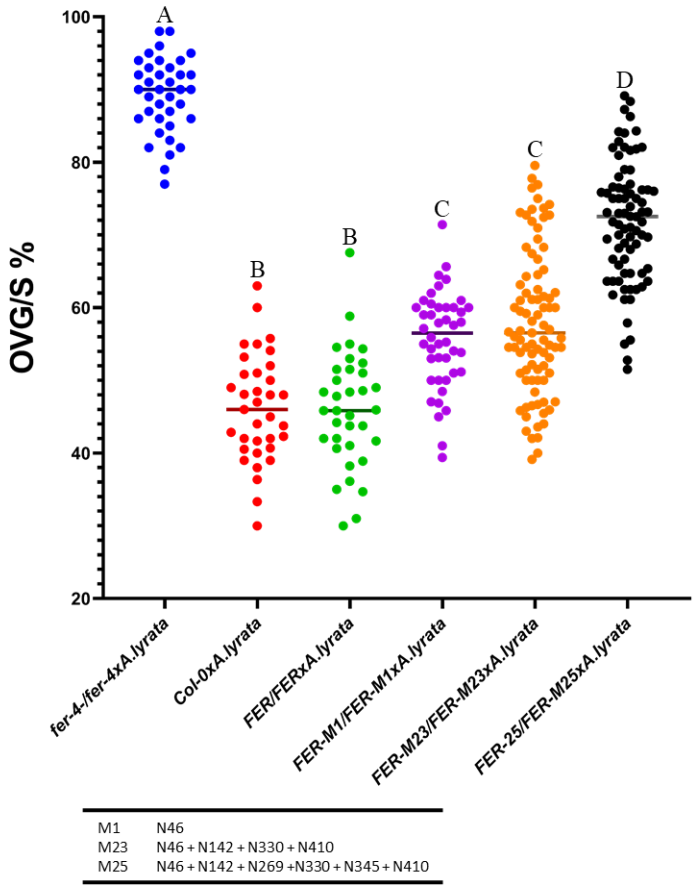

Figure 18. Single, quadruple and hexapole T2s homozygous lines present higher degree of PT overgrowth in interspecific crosses. *A. thaliana* T2 complementation lines were emasculated followed by hand-pollination with *A. lyrata* pollen. Scatter plots represents pooled data from 3 independent T2 lines/FER variant, and for each line at least 5 crosses were performed (each dot represents one silique). One-way ANOVA followed by Tukey's multiple comparison test (A-B ****P<0.0001; A-C ****P<0.0001; A-D ****P<0.0001; A-E ****P<0.0001; A-F ****P<0.0001; B-C ****P<0.0001; B-D ****P<0.0001).

Surprisingly, the extent of the PTO was almost equal between single M1 variant (N46) and quadruple M23 variant (Fig. 18). When individual T2s expressing M1 were analyzed almost identical degrees of PTO (~56%) were found among three independent T2 lines (Fig. 19B). Correspondingly in the T2 lines expressing M23 quadruple variant (Tab. 1) equivalent proportion of the PTO (~57%) was

detected among individual T2s (Fig. 19C). These results were a bit unexpected having in mind M23 quadruple variant`s impaired protein secretion, evidential from the increased accumulation of signal within synergids cytoplasm (Fig. 14). Homozygous T2 plants expressing hexapole M25 variant had not only significantly higher level of PT overgrowth (~73%) compared to the both Col-0 and wild-type FER which displayed ~47% of PTO, but also in the comparison to single (M1) and quadruple (M23) variant which had similar degree of PTO (56%) (Fig. 18 and Fig. 19). Having in mind that for the variant M25 we identified only one single insertion T1 line and several double insertion T1s (Fig. S12), we wondered if the observed level of complementation corresponds to the number of insertions.

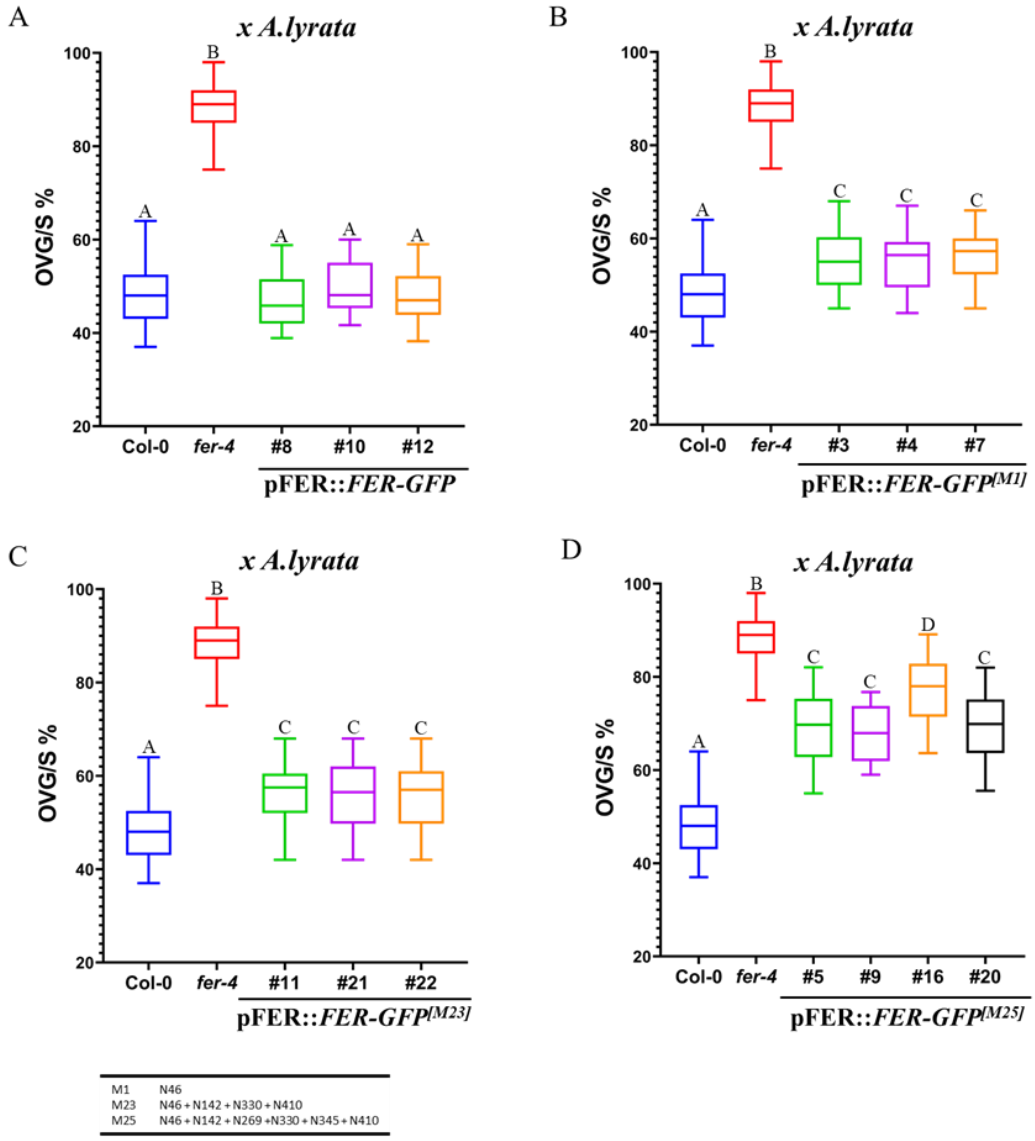

Figure 19. T2 complementation lines show higher level of PT overgrowth in interspecific crosses. Flowers (floral stage 12) from the T2 lines were emasculated followed by a hand-pollination with *A. lyrata* pollen. Scatter plots represent data from 3 plants/genotype and for each plant 5 crosses were performed. **(A)** T2 lines expressing wild type FER variant fully restore interspecific PT overgrowth to the Col-0 level. One-way ANOVA followed by Tukey's multiple comparison test (A-B ****P<0.0001). **(B)** T2s expressing M1 variant (N46) show higher degree of interspecific PT overgrowth in comparison to the Col-0. One-way ANOVA followed by Tukey's multiple comparison test (A-B ****P<0.0001; A-C ****P<0.0001; B-C ****P<0.0001). **(C)** T2s expressing quadruple M23 variant display higher proportion of interspecific PT overgrowth in comparison to the Col-0. One-way ANOVA followed by Tukey's multiple comparison test (A-B ****P<0.0001; A-C ****P<0.0001; B-C ****P<0.0001). **(D)** T2 lines expressing hexapole M25 variant display higher degree of interspecific PT overgrowth in comparison to the Col-0. Independent double insertion T2 lines (#5, #9, and #20) show significantly lower extent of PT overgrowth compared to the single insertion

T2 line (#16). One-way ANOVA followed by Tukey's multiple comparison test (A-B ****P<0.0001; A-C ****P<0.0001; A-D ****P<0.0001; B-C ****P<0.0001; B-D ****P<0.0001; C-D ***P=0.0005).

The highest number of insertions (~2.5) was detected in the line T2-9 and correspondingly the extent of the interspecific PTO was the lowest (~70%) among analyzed T2s expressing M25 (Fig. 19D). Furthermore, lines T2-5 and T2-20 (~2 insertions) displayed slightly increased level of PTO (~72%) compared to T2-9 (Fig. 19D). Finally, the single insertion line T2-16 showed the highest degree of PTO (77%) (Fig. 19D), which was also above the pooled value (73%) of all four T2s (Fig. 18). To summarize, we have found that in all variants degree of interspecific phenotype directly depends on the number of insertions proving once again that FER plays a major role during interspecific pollen tube reception. In a summary, only the properly glycosylated FER can fulfill its role during interspecific pollination, while even the loss of single *N*-glycans leads to impaired recognition of foreign pollen. Protein backbone and its carbohydrate decorations are both necessary during the sensing of the interspecific pollen tubes.

Discussion

Here we report the systematic characterization of *N*-glycans role for the mediation of FER signaling responses during vegetative growth, abiotic stress, and PT reception. We have performed a large-scale site-directed mutagenesis screen to assess importance of all ten *N*-glycosylation sites located in the FER`s extracellular domain (ECD). MS analysis revealed FER to be *N*-glycosylated *in planta* at four out of ten putative *N*-glycosylation sites, with attachment of high-mannose type *N*-glycans at positions N142 and N410 and complex-type *N*-glycans at N46 and N330. Only when *N*-glycans were simultaneously depleted at six positions RHs bursting of *fer-4* could no longer be complemented, while vegetative growth of shoot and leaves was undisturbed even in octupole mutant variant. On the other hand, we discovered high requirement for *N*-glycans presence during adaptation to the salt stress, where even loss of single *N*-glycans resulted in a substantial inhibition of the primary root growth. Additionally, we demonstrated that binding of FER to CW components is only partially stemming from *N*-glycans and majority of binding can be achieved in the absence of even six *N*-glycans. FER plays a key role during reproduction and we demonstrated that it is of fundamental importance for both intra- as well inter-specific PT reception.

Studies on the importance of the individual *N*-glycans for the functionality of receptor-like kinases are extremely scarce and most of them have been focused on the immune receptors (Häweker et al., 2010; van der Hoorn et al., 2005; Li et al., 2009; Nekrasov et al., 2009). Having in mind that FER is essential for several key aspects of a plant life, this study is filling up a large gap in our knowledge on the *N*-glycoproteins. As above mentioned, we have successfully mapped four (N46, N142, N330 and N410) out of the ten putative N-glycosylation sites. Our results were predominantly consistent to the previously reported *N*-glycans attachment at the five positions of FER (N46, N142, N330, N269 and low-confidence N345) (Zielinska et al., 2012). Knowledge on the other members of the *Cr*RLK1L members is completely lacking, but looking into detected *N*-glycopeptides from the above-mentioned study, we have found eight more *Cr*RLK1L members to have from one to five *N*-glycans occupied sites (Zielinska et al., 2012). Future studies are needed to perform more elaborate characterization of *N*-glycosylation status of each member and as well to dissect their functional

importance. In the recent crystallography study looking at complex formation between FER, LLG1, and RALF23, *N*-glycans were found to be attached at N142, N345 as well on the previously undetected N305, further confirming that FER is heavily glycosylated *in planta* (Xiao et al., 2019). Authors propose that detected *N*-glycans do not play a major role in the ligand binding, since they are located outside of the ligand binding cleft (Xiao et al., 2019), however it remains to be assessed empirically how important they really are for the stabilization of the complex formation between FER and its coreceptors and ligands.

Highly conserved *N*-glycosylation sites are more likely to be essential for the protein function and based on the FER sequence alignments from 42 species, sites N142, N305 and N345 were found to be the most conserved ones. In several studies it was reported that the heaviest impairment of protein stability and secretion was observed upon the loss of the most conserved *N*-glycosylation sites (van der Hoorn et al., 2005; Liebminger et al., 2013; Yamamoto et al., 2014). We have performed subcellular localization assays in *N. benthamiana* and *A. thaliana* protoplasts, and found for single FER variants, depletion of eight from ten sites to not have an impact on the plasma membrane (PM) targeting , while only loss of sites N219 and N345 displayed a mild disruption of the protein targeting to the PM. Slight mislocalizaton of site N345 could be explained by the fact that is completely conserved among all 42 species of the FER OMA group, while site N219 was only partially retained (21 out of 42 species). Interestingly N219 site is not located within MLDs, but in the interconnecting region, therefore depletion might have caused destabilization of FER^{ECD} 3D conformation, which remains to be further investigated. The only site uniquely present in *A. thaliana* was site N46, which was also the only different site compared to the closely related *A. lyrata*. As expected for the non-conserved site exclusive targeting to the PM was observed, which was previously reported for the heavily *N*-glycosylated S-locus receptor kinase (SRK) involved in the self-incompatibility response in *A. lyrata* (Yamamoto et al., 2014).

Starting from the triple mutant variants moderate impairment of protein secretion was detected. Quadruple variant depleted of all MAL-A resident *N*-glycosylation sites displayed PM targeting while in quadruple variant targeted at two MAL-B and two MAL-A located sites ER degradation was more prominent. This indicates that two MAL-A sites (N124 and N171) are not *N*-glycosylated *in planta*, which is in line with them not being detected in either of MS analysis or crystallography study. Starting from hexapole variant onwards a more prominent ER retention was observed, suggestive of failure of underglycosylated FER to pass ER-mediated quality control resulting in a protein degradation via ERAD pathway (Hüttner and Strasser, 2012).

However, it is thought-provoking that even FER depleted of eight *N*-glycosylation sites was fully functional in complementing vegetative growth phenotypes as well as the intraspecific PT reception. This findings indicate that FER protein is very robust, since for other proteins such as SRK and KORRIGAN1 (KOR1) it was reported that loss of *N*-glycosylation sites resulted in a prominent ER retention and diminished protein functionality (Rips et al., 2014; Yamamoto et al., 2014). Sensitivity for other *N*-glycoproteins was mostly determined indirectly, by checking their biogenesis in different *N*-glycosylation mutant backgrounds. For instance in the mutants affected in the subunit of the key enzyme of N-glycosylation pathway, *ost3/6* (*artumes*) biogenesis of EF-TU RECEPTOR (EFR) and endo-β-1,4-glucanase KOR1 was severely compromised, while receptor kinase BRASSINOSTEROID-INSENSITIVE1 (BRI1) was unaffected (Farid et al., 2013). Additionally, previous results from our lab clearly demonstrated FER`s stability in *artumes* background since it was properly targeted to the PM rich filiform apparatus (FA) (Müller et al., 2016).

Additional way to probe if FER can tolerate severe underglycosylation is to transfect protoplasts with FER-GFP, expose them to tunicamyin, a strong inhibitor of *N*-glycosylation pathway, and observe degrees of newly synthesized FER`s targeting to the PM, which previously exemplified large difference in the stability of two immune receptors (Häweker et al., 2010). In order to determine proportion of protein that could escape the ER and get to Golgi on their way to PM, protein extracts from transiently transformed tobacco can be treated with endoglycosidase H (EndoH), which cleaves only oligomannosidic *N*-glycans, thus the fraction of protein that managed to reach the PM would be insensitive to the treatment (Li et al., 2009; Nekrasov et al., 2009). More importantly the same type of biochemical experiments can be performed in different tissues of *fer-4* complementation lines to correlate level of stable FER with the degree of phenotype restoration.

Contrasting to the shoot growth and petiole length, RHs bursting phenotype could no longer be complemented starting from the hexapole mutant variant (M25). Loss of the single M5 variant (N219) also resulted in the mild disruption of the RHs growth. However, for M5 variant only T1s were analyzed, and phenotyping should be repeated once the homozygous single-insertion T2s are obtained. In the case of M25 variant abundance of FER at the PM should be detailly analyzed using confocal microscopy to discern if the observed phenotype stems predominantly from the lower abundance of FER at PM, or additionally from the lower capacity of FER to correctly bind to its coreceptors/ligands. Localization analysis should be performed as well in the variants which can still fully restore RHs growth. It is puzzling that quadruple (M23) and quintuple (M24) variant can completely restore RHs burst while hexapole variant is equivalent to the *fer-4* degree of RHs bursting. Perhaps protein abundance and *N*-glycosylation status of M23 and M24 variants is sufficient to trigger RAC/ROP downstream signaling in RHs, while in M25 compromised receptor can no longer activate signaling cascade leading to inability to restore RHs growth (Duan et al., 2010). Since recently it was demonstrated that RALF1 promotes root hair growth, the degree of RALF1 responsiveness among homozygous T3s expressing different *N*-glycosylation FER variants remains to be assessed in the future (Zhu et al., 2020). Furthermore, in the root hairs glycosylphosphatidylinositol (GPI)-anchored membrane protein LRE-like GPI-AP1 (LLG1) is required for the appropriate secretion of FER from the ER, hence *llg1* mutants display *fer-4* like RHs burst (Li et al., 2015). Having in mind that LLG1 bind to the extracellular juxtamembrane (exJM) region of FER to enable its trafficking from the ER (Li et al., 2015), we expected M10 variant targeted at the exJM resident N410 to be less capable of tethering to LLG1, thus leading to impaired of RHs growth and development. However, this was not the case, and not only that single M10 variant displayed normal RH growth but as well all higher-end mutants depleted of this site. Even though N410 was identified by mass spectrometry (MS) analysis to be *N*-glycosylated, the extent of *N*-glycosylation among different tissues can vary significantly (Zielinska et al., 2012), thus it is possible that this site is not heavily utilized in the RHs. Lastly, it should be considered that most of the FER-LLG1 interactions are protein based and thus loss of a single *N*-glycan can be well tolerated by plants.

To recapitulate we demonstrated that under standard growth conditions loss of *N*-glycans is very well tolerated, however upon exposure to abiotic stress such as high salinity, FER requires proper *N*-glycosylation of its ECD. Loss of *N*-glycans at single positions (N46, N219, N345), resulted in an inability of FER to sense salt-induced perturbations of the CW and to accordingly accommodate primary root growth. Salt stress causes upregulation of the unfolded protein response (UPR) hence it is conceivable that even slightly deglycosylated FER variants cannot correctly refold and are targeted to the ERAD pathway (Deng et al., 2013). FER-GFP protein abundance at the PM should be carefully examined before and after exposure to the salt stress to find out if observed inhibition of root growth

stems from disrupted secretion. Kifunensine, inhibitor of ERAD pathway, can be used to further dissect if observed salt sensitivity phenotypes of single mutants are independent from ERAD pathway (Liebminger et al., 2013). In the previous MS analysis site N46 was found to be the most heavily *N*-glycosylated (*N*-glycans presence was detected in 16 glycopeptides, compared to 4-5 for other sites) (Zielinska et al., 2012). Additionally, in our MS analysis we found N46 to be occupied with complex-type *N*-glycans and having in mind that loss of this site resulted in the exclusive PM localization it seems that this site is involved in more than ensuring the right protein conformation, stability and secretion. It is interesting that in mutants completely depleted of all complex-type *N*-glycans similar salt stress sensitivity was observed, without upregulation of the ERAD pathway (Kang et al., 2008). Besides N46 also N330 carries complex-type *N*-glycans, thus it could have overlapping roles with N46. Having in mind that in quadruple M23 variant (devoid of both N46 and N330) no obvious additive effect was observed, it is likely that N330 is not as heavily *N*-glycosylated in roots as N46, but further examination of T3s expressing M8 in salinity assays are needed to draw final conclusions.

Salinity hypersensitivity was the most pronounced in the hexapole M25 variant. Having in mind that localization studies in tobacco revealed impaired secretion of M25 to the PM, the abundance of protein both before and after salt treatment should be more precisely determined. Similar above-mentioned biochemical inhibition of the ERAD pathway is needed to reveal if stability of M25 would be significantly increased thus improving the ability to compliment *fer-4* salt hypersensitivity responses. To sum up *N*-glycosylation is essential during FER mediated adaptation to the salt stress. However, it is still unclear if *N*-glycosylation is mainly needed for the protein stabilization or also for the appropriate sensing of the extracellular matrix.

We have found that even heavily deglycosylated M25 variant FER is capable of CW perturbations sensing, further implying that *N*-glycans are not essential for the binding to pectin and that most of the binding is through protein backbone. In the previous study authors report complete irresponsiveness of *fer-4* to the CW perturbation, leading to even increased relative root growth (Dünser et al., 2019). Under our experimental conditions *fer-4* mutants were slightly sensitive to pectin perturbations, which could be explained by the different age of seedlings used in the assays. We have performed analysis on the 5 days old seedlings, in contrast to the previously used 3 days old seedlings. We have opted for later stage due to the observed partial unresponsiveness to CW disturbance even in wild type Col-0 at three days after germination. Therefore, the right developmental stage of seedlings as well as concentration of EGCG remains to be evaluated before analysis is carried out on more FER variants in homozygous state. Previously it was demonstrated *in vitro* binding of FER MALA and MALB to the polygalacturonic acid PGA (the backbone polymer of pectin) (Feng et al., 2018), thus similar type of analysis with inclusion of other CW components (cellulose/hemicellulose) should be done for different FER variants to fully understand the contribution of *N*-glycans during FER interaction with the CW components.

In contrast to the adaptation to the salt stress where FER even upon a loss of single *N*-glycans is no longer fully functional, we discovered that during intraspecific PT reception even simultaneous loss of eight *N*-glycosylation sites is well tolerated, resulting in a complete rescue of the *fer-4* PTO phenotype. This was astonishing having in mind severely impaired targeting to the FA starting from the hexapole FER variant. Interestingly FER mutant variant depleted of all ten *N*-glycosylation sites displayed similar subcellular localization compared to the fully functional octupole variants, indicating that even a miniscule fraction of FER at FA is sufficient to trigger downstream signaling and ensure successful reproduction. The only other study looking at the importance of individual *N*-

glycosylation sites for the functionality of a reproductive protein was performed on the vastly *N*-glycosylated S-locus receptor kinase (SRK). Contrasting to FER, role of SRK`s *N*-glycosylation was strictly restricted to ensure the correct targeting to the PM, hence mutants depleted of several *N*-glycosylation sites could no longer exit ER, leading to the complete protein dysfunctionality (Yamamoto et al., 2014)

Unfortunately, we have obtained low number of T1s expressing nonuple FER variants (M28 and M29) but in those T1s partial complementation of PTO was detected, with a moderately better complementation capability of M29 variant. More transgenics need to be recovered to firstly determine the exact degree of complementation (using single-insertion T-DNA lines) followed by a confocal analysis to quantify the amount of FER needed at FA for the successful reception of self-pollen. Since we observed significant drop in FA targeting between quintuple and hexapole variant, it seems that loss of M9 (N345) is essential for the stabilization of protein and secretion. It is interesting that same hexapole variant could not restore RHs burst, while in PT reception it was nonessential, indicating that requirements for the abundance of FER are varying considerably among different tissues. This finding is in line with previously reported kinase-dead version of FER being able to fully complement PT reception, while RALF1-mediated suppression of primary root was partially lost (Haruta et al., 2018; Kessler et al., 2015). Also in the root hairs LLG1 is responsible for chaperoning FER from ER, while in synergids its closest homolog LRE is ensuring correct targeting of FER (Li et al., 2015; Liu et al., 2016). Therefore, it is possible that LLG1 and LRE have different tolerance to the FER`underglycosylation, which remains to be further elucidated.

Contrary to the intraspecific pollinations where *N*-glycans are nonessential for the reception of self-pollen, we have observed a striking need for the correct FER^{ECD} *N*-glycan attachment for the recognition of heterospecific pollen (foreign). We have found loss of several single *N*-glycosylation sites to lead to the significantly higher proportion of PTO compared to wild-type FER in crosses with *A. lyrata*. It is important to note that all single *N*-glycosylation variants were correctly targeted to the FA in synergids, meaning that observed inability to recognize and induce interspecific PT burst came from a reduced ability of underglycosylated FER^{ECD} to bind to putative interspecific ligands. When we have analyzed conservation of *N*-glycosylation sites among 42 different species, the only *N*-glycosylation site uniquely present in *A. thaliana* was N46. Having in mind that N46 was the only site not conserved in *A. lyrata*, and observed significant increase in the PTO in crosses with *A. lyrata*, it can be concluded that loss of a single FER^{ECD} *N*-glycan contributes to the establishment of interspecific hybridization barrier. Furthermore, considering that M1 variant depleted of N46 was exclusively targeted to the PM, it implies that most of the observed phenotype stems from the lack of carbohydrates. Potential explanation could also lie in the above-stated fact that site N46 is the most heavily glycosylated of all detected sites in a previous glycoproteomic study (Zielinska et al., 2012). Further validation of the vast importance of N46 *N*-glycosylation site came from the observation that quadruple variant displayed equivalent level of PTO in interspecific pollinations, meaning that additions of three more sites have not influenced substantially inability to recognize interspecific pollen.

In the case of three remaining single sites (N219, N269, and N345) which displayed increased PTO in interspecific pollinations, all the analysis was performed in T1s, thus phenotyping should be repeated once homozygous T2s are obtained. The most pronounced increase in the PTO compared to the wild type was found in the single mutant devoid of N345. Having in mind that N46 harbors complex-type *N*-glycans, site occupancy of N345 remains to be determined before it can be concluded

which class of *N*-glycans is more important for the gametophyte recognition during interspecific pollinations. Furthermore, only when N345 was introduced to the quintuple variant a proportion of PTO compared to wild type was dramatically increased. One possible explanation is that due to severely impaired secretion of hexapole mutant variant, less protein accumulates at the FA, resulting in a more pronounced failure to recognize interspecific PTs. In order to further dissect importance of *N*-glycan presence versus protein abundance at FA, modified pistil feeding assays (Duan et al., 2014) can be performed. Emasculated pistils could be treated with kifunensine to inhibit ERAD pathway and allow higher abundance of hexapole variant at FA. Then interspecific pollinations can be performed and if higher amount of protein results in the same degree of PTO it would point out that *N*-glycosylation plays a more prominent role. Additionally similar assays can be performed using tunicamyin, potent inhibitor of *N*-glycosylation pathway, to asses FER`s ability to be targeted to FA, followed by pollination assays using both intra- and inter-specific pollen to assess whether this treatment would cause in the wild type ovules aberrant PT reception. Previously it was reported that treating stigmas with tunicamycin can break self-incompatibility (SI) responses in Brassicaceae, the most likely through the degradation of SRK (Sarker et al., 1988; Yamamoto et al., 2014).

Taken together our results are shedding light into how a single broadly expressed protein can have so many different roles throughout the plant. This diversification is partially achieved through the heavily *N*-glycosylated extracellular domain, which in different tissues as well as conditions communicates with diverse partners to achieve tissue-specific roles. Above all our study has an evolutionary importance since we have demonstrated that *N*-glycans are important for recognition of both self and foreign pollen during interspecific pollinations among recently diverged *A. thaliana* and *A. lyrata*.

Material and methods

Plant Material and Growth Conditions

Wild-type *Arabidopsis thaliana (L.) Heynh. var. Columbia* (Col-0), as well as T-DNA insertion line *fer-4* (GABI_106A06), were obtained from The European Arabidopsis Stock Center (NASC). *Arabidopsis lyrata ssp. lyrata* seeds were a kind gift from Detlef Weigel (Max Planck Institute for Developmental Biology, Tübingen). Seeds were surface sterilized in 3% NaOCl/0.01% Triton X-100 solution followed by 100% ethanol wash and sterile drying. Seeds were transferred on half-strength Murashige and Skoog (MS) basal medium (Carolina) plates without sucrose. Seeds were stored for 48 hours at 4°C in darkness for stratification and then grown under long-day conditions (CLF_CU-36L6, Percival, Germany) with a relative humidity of 70% and light intensity of 200 µmol/m2 s. Seven days post-germination seedlings were transplanted to the soil. Both *A. thaliana* and *A. lyrata* plants were grown in the same greenhouse growth chambers under long-day conditions. After two weeks in the growth chamber, *A. lyrata* plants were vernalized for five more weeks to induce flowering (4°C, 16h light).

Seed Set Analysis, Crosses, and Aniline Blue Staining

Seed production was quantified by placing mature siliques (produced in the main stem 5 weeks after the start of flowering) on double-sided sticky tape and cutting off valves along the replum. Both fertilized (plump) seeds and unfertilized (white, shrunken ovules) were counted. Crosses were performed accordingly: as a female parent young closed floral buds of *A. thaliana* (floral stage 12) were emasculated two days before hand-pollination. Only flowers with closed stamens and no pollen release were used for emasculation, to ensure that no selfing is occurring. As the male parent newly opened flowers of *A. lyrata* were used for pollination in interspecific crosses.

The determination of the pollen tube overgrowth phenotype was done by aniline blue staining of pollen tubes (Huck, 2003). Elongated siliques from either self-pollinated or *A. lyrata* hand-pollinated flowers were fixed using 9:1 ethanol (EtOH): acetic acid solution overnight at 4°C. Siliques were gently pressed onto the microscope slide and analyzed using a Leica DM6000B epifluorescence microscope (Leica Microsystems) using an UV-light source.

Root hair length analysis

Seedlings were grown in half-strength MS medium (MS unless otherwise indicated) and imaged five days after germination (DAG). Root hairs in the region of 1.5 to 3.5 mm from the primary root tip were imaged using stereomicroscope Leica MZ FLIII. The length of root hairs in the same focal plane was measured by ImageJ.

Root Growth Assay for Osmotic Stress Tolerance

Seedlings after five DAG were transferred from MS plates to the salt stress treatment plates, supplemented with either 140mM or 100mM NaCl. Upon transfer to the treatment plates position of root tip was marked, and plates were grown vertically for the next three days (140mM NaCl) or five days (100mM NaCl). Images were taken using a scanner (Epson Perfection 2450) and the change in root length was analyzed using ImageJ. Survival rates were counted as the proportion of seedlings that is resistant versus sensitive (more than 50% of chlorotic leaves).

EGCG Root Length Assay

Catechin-derivative (-)-epigallocatechin gallate (EGCG) was used to inhibit pectin methyl esterases (PME) activity. Seedlings were grown for five DAG on MS plates and then transferred to liquid half-strength MS medium supplemented with 25 μM EGCG (Sigma-Aldrich) or solvent (water). Upon transfer, seedlings were grown for another 72h in 12 well tissue culture plates (Greiner). After treatment seedlings were laid onto solid half-strength MS plates and pictures were acquired with Epson scanner. Root length was measured using ImageJ.

Mass Spectrometry analysis

Transgenic lines expressing FER-GFP in the wild-type Col-0 were used to perform *N*-glycosylation site occupancy analysis. Proteins isolated from rosette leaves, seedlings and flowers were separated

by a native SDS-PAGE and detected by the Coomassie Brilliant Blue staining. The corresponding size bands were extracted from gel, followed by enrichment using GFP trap columns. Proteinase digestion, glycopeptide enrichment, and MS analysis were done by Dr. Chia-Wei Lin (Prof. Markus Aebi group), at the Functional Genomics Center Zurich (FGCZ).

Molecular cloning

Site-directed mutagenesis of FER N-glycosylation sites (N modified to A) was done using Gateway pABD52 as a template with Q5® Site-Directed Mutagenesis Kit (New England Biolabs). pABD52 contains a 2688bp FER CDS without stop codon from Col-0 and it was kindly provided by Aurélien Boisson-Dernier (University of Cologne, Germany). Primers used for mutagenesis are listed in Tab. S5. The same kit was used to modify FER *N*-glycosylation sites of *35S*::FER-GFP plasmid later used for the transient protoplast transfection (Tab. S6). After mutagenesis, all the plasmids were sequenced at the in-house Sanger sequencer (ABI 3730 DNA Analyzer), to exclude the presence of PCR-generated errors (Tab. S8). Constructs were transformed into chemically competent E. coli DH5α or DB3.1 cells. The destination vector for LR reactions was modified plant Gateway vector pMDC83 (Curtis and Grossniklaus, 2003), where the original 2x35S-promoter was exchanged for FER promoter, to enable synergid specific expression of FER (Müller et al., 2016). Entry vector pABD52 (Tab. S7) and the modified destination vector were combined in a LR reaction using Gateway Cloning ® (Life Technologies). Resulting expression clones *pFER*::FER-GFP (Tab. S9) were transformed into Agrobacterium tumefaciens strain GV3101 (Koncz and Schell, 1986). To test the complementation ability of different expression clones, *fer-4* mutant plants were transformed using the floral dip method (Clough and Bent, 1998). Transformants were selected using MS plates containing 25 μg/ml of hygromycin B (Invitrogen).

T-DNA copy number determination

High purity genomic DNA was isolated from T1 transformants leaves (20 μg) with Mag-Bind® Plant DNA DS 96 Kit (Omega) using KingFisher Duo Prime System (ThermoFisher). Digital droplet PCR (ddPCR) reaction was prepared using 2ng of EcoR V-HF (NEB) digested gDNA, 500nM primers, 200nM probes and 1X QX200 ddPCR Probe no dUTPS Supermix (BioRad, Hercules, CA, USA). Antibiotic resistance gene (Hygromycin) was used for transgene detection. AT3G20740 (FIE) was used as single copy internal reference. Assay was performed as duplex using MGB probes (ThermoFisher). Auto DG QX200 System (Bio-Rad) was used for droplet generation. Resulted droplets plates were sealed and cycled in a deep-well thermocycler C1000 (BioRad) following standard manufacture's recommendation for ddPCR. Fluorescence was immediately detected with the reader and analyzed with the provided Quanta Soft version 1.7. Performance of each primer set was assessed prior experiment and CN of each individual was calculated based on ratio of T-DNA versus reference single copy gene. An additional reference gene was used to validate the single copy gene FIE. Resulting single T-DNA insertion lines were used for downstream analysis.

Transient expression of Arabidopsis thaliana leaf protoplasts and Tobacco epidermis cells

Protoplast were isolated from rosette leaves of three weeks old Arabidopsis thaliana wild-type (Col-0) plants grown under short-day conditions (Yoo et al., 2007). Leaves were cut into 1 mm strips, which were enzymatically digested (20 mM MES pH5.7; 1.5% cellulase R10; 0.4% macerozyme R10; 0.4 M mannitol; 20 mM KCl) for 2 hours. High quality concentrated plasmid DNA (2 µg) was transfected into 5×10^4 protoplasts using polyethylene glycol solution (0.4 g/ml PEG 4000, 0.8 M mannitol, 125 mM CaCl2). Upon 15 minutes of room temperature incubation, protoplasts were washed, resuspended in W5 solution (154 mM NaCl, 125 mM $CaCl_2$, 5 mM KCl, 2 mM MES at pH5.7) and placed in the growth cabinet (Percival) for the next 24 hours before imaging was performed.

Single colonies of Agrobacteria tumefaciens strain GV3101 containing either desired binary plasmid or p19 viral silencing suppressor (Voinnet et al., 2003) were grown overnight in LB medium containing the appropriate antibiotics. Overnight cultures (5ml) were spin down (15 minutes at 4000 rpm) and resuspended in the infiltration buffer (10 mM MES, 10 mM MgSO4, 0.2 mM acetosyringone at pH 5.7). After incubating for 2h at room temperature in darkness, OD600 was measured using a photometer (BioRad SmartSpec3000) and adjusted to 0.5. For the final agroinfiltration solution p19 culture and clones with desired binary plasmids were mixed 1:1. Well-watered 3-4 weeks old N.benthamiana plants were infiltrated with 1 ml needless syringe on the abaxial leaf surface. The ER-marker pER-rk (mCherry) and PM-rk (mCherry) used for transient transformation were obtained from the ABRC (Nelson et al., 2007).

Microscopy

Flowers from transgenic plants (floral stage 12) carrying complementation constructs, were emasculated and pistils were dissected 24-48h post emasculation to visualize GFP expression of mature ovules. Ovules were mounted on slides in 1M Glycine at pH 9.6 and imaged with Leica SP5 confocal microscope (Leica Microsystems). For GFP-fusion protein expression excitation was at 488 nm and emission was recorded from 500-550 nm. For chlorophyll autofluorescence, excitation was at 568 nm and emission was recorded from 590-650 nm. Single-focus plane images of 1024x1024 pixels were recorded with a scan speed of 400 Hz. Subcellular localization of *35S*::FER-GFP in protoplasts was checked 24h post-transfection using DM6000B epifluorescence microscope (Leica Microsystems). *N. benthamiana* leaves were collected three days after infiltration and small leave pieces were analyzed immediately using the Leica SP5 confocal microscope. Used excitation wavelengths were 488 nm for GFP and 561nm for RFP. Emitted light was recorded at 500-550nm for GFP and at 590-650nm for RFP.

Bioinformatic Analysis

Pymol 2.3.4 Molecular Graphics System was used to visualize crystal structure of FER^{ECD} (PDB code: 6A5B). Phytozome v12.1 was used to blast *A. thaliana* protein sequences (all members of *Cr*RLK1L family) against *A. lyrata* v2.1 proteome. NetNGlyc1.0 software (Gupta et al., 2004) was used to determine putative *N*-glycosylation sites of *Cr*RLK1L members of either *A. thaliana* or

respective *A. lyrata* orthologs. OMA Browser was used for inference of orthologs. Polymorph 1001 Genome Variant Browser (Alonso-Blanco et al., 2016) was used to find high effect SNPs variants within *N*-glycosylation sites of *Cr*RLK1L members. In order to visualize conservation of FER *N*-glycosylation sites within different species, multiple alignments were done using Clustal Omega followed by visualization in Jalview 2.11.0. Phylogenetic trees were built using protein sequence parsimony method (bootstrap test, 1000 replicates) in MEGA 7 software (Kumar et al., 2016).

Statistical analysis

All the datasets were firstly tested for normality using D'Agostino-Pearson normality test. Normally distributed datasets were analyzed with either Student's t test or One-way ANOVA followed by Tukey's multiple comparisons test. Nonparametric tests were used for data that did not pass normality test, either Mann-Whitney or Kruskal-Wallis test followed by Dunn's multiple comparisons test. Sample size (n) is given in the figure legends. Statistical analysis was performed using GraphPad Prism 8 software.

References

Aebi, M. (2013). N-linked protein glycosylation in the ER. Biochim. Biophys. Acta BBA - Mol. Cell Res. *1833*, 2430–2437.

Altenhoff, A.M., Gil, M., Gonnet, G.H., and Dessimoz, C. (2013). Inferring Hierarchical Orthologous Groups from Orthologous Gene Pairs. PLoS ONE *8*, e53786.

Bleckmann, A., Alter, S., and Dresselhaus, T. (2014). The beginning of a seed: regulatory mechanisms of double fertilization. Front. Plant Sci. *5*.

Boisson-Dernier, A., Kessler, S.A., and Grossniklaus, U. (2011). The walls have ears: the role of plant CrRLK1Ls in sensing and transducing extracellular signals. J. Exp. Bot. *62*, 1581–1591.

Campbell, L., and Turner, S.R. (2017). A Comprehensive Analysis of RALF Proteins in Green Plants Suggests There Are Two Distinct Functional Groups. Front. Plant Sci. *8*.

Davis, T.C., Jones, D.S., Dino, A.J., Cejda, N.I., Yuan, J., Willoughby, A.C., and Kessler, S.A. (2017). Arabidopsis thaliana MLO genes are expressed in discrete domains during reproductive development. Plant Reprod. *30*, 185–195.

Deng, Y., Srivastava, R., and Howell, S. (2013). Endoplasmic Reticulum (ER) Stress Response and Its Physiological Roles in Plants. Int. J. Mol. Sci. *14*, 8188–8212.

Dresselhaus, T., and Franklin-Tong, N. (2013). Male–Female Crosstalk during Pollen Germination, Tube Growth and Guidance, and Double Fertilization. Mol. Plant *6*, 1018–1036.

Dresselhaus, T., Sprunck, S., and Wessel, G.M. (2016). Fertilization Mechanisms in Flowering Plants. Curr. Biol. *26*, R125–R139.

Duan, Q., Kita, D., Li, C., Cheung, A.Y., and Wu, H.-M. (2010). FERONIA receptor-like kinase regulates RHO GTPase signaling of root hair development. Proc. Natl. Acad. Sci. *107*, 17821–17826.

Duan, Q., Kita, D., Johnson, E.A., Aggarwal, M., Gates, L., Wu, H.-M., and Cheung, A.Y. (2014). Reactive oxygen species mediate pollen tube rupture to release sperm for fertilization in Arabidopsis. Nat. Commun. *5*, 3129.

Duan, Q., Liu, M.-C.J., Kita, D., Jordan, S.S., Yeh, F.-L.J., Yvon, R., Carpenter, H., Federico, A.N., Garcia-Valencia, L.E., Eyles, S.J., et al. (2020). FERONIA controls pectin- and nitric oxide-mediated male–female interaction. Nature *579*, 561–566.

Dünser, K., Gupta, S., Herger, A., Feraru, M.I., Ringli, C., and Kleine-Vehn, J. (2019). Extracellular matrix sensing by FERONIA and Leucine-Rich Repeat Extensins controls vacuolar expansion during cellular elongation in *Arabidopsis thaliana*. EMBO J. *38*.

Escobar-Restrepo, J.-M., Huck, N., Kessler, S., Gagliardini, V., Gheyselinck, J., Yang, W.-C., and Grossniklaus, U. (2007). The FERONIA Receptor-like Kinase Mediates Male-Female Interactions During Pollen Tube Reception. Science *317*, 656–660.

Farid, A., Pabst, M., Schoberer, J., Altmann, F., Glössl, J., and Strasser, R. (2011). *Arabidopsis thaliana* alpha1,2-glucosyltransferase (ALG10) is required for efficient N-glycosylation and leaf growth: *Arabidopsis alpha1,2-glucosyltransferase*. Plant J. *68*, 314–325.

Farid, A., Malinovsky, F.G., Veit, C., Schoberer, J., Zipfel, C., and Strasser, R. (2013). Specialized Roles of the Conserved Subunit OST3/6 of the Oligosaccharyltransferase Complex in Innate Immunity and Tolerance to Abiotic Stresses. Plant Physiol. *162*, 24–38.

Feng, W., Kita, D., Peaucelle, A., Cartwright, H.N., Doan, V., Duan, Q., Liu, M.-C., Maman, J., Steinhorst, L., Schmitz-Thom, I., et al. (2018). The FERONIA Receptor Kinase Maintains Cell-Wall Integrity during Salt Stress through Ca2+ Signaling. Curr. Biol. *28*, 666-675.e5.

Franck, C.M., Westermann, J., and Boisson-Dernier, A. (2018). Plant Malectin-Like Receptor Kinases: From Cell Wall Integrity to Immunity and Beyond. Annu. Rev. Plant Biol. *69*, 301–328.

Galindo-Trigo, S., Gray, J.E., and Smith, L.M. (2016). Conserved Roles of CrRLK1L Receptor-Like Kinases in Cell Expansion and Reproduction from Algae to Angiosperms. Front. Plant Sci. *07*.

Galindo-Trigo, S., Blanco-Touriñán, N., DeFalco, T.A., Wells, E.S., Gray, J.E., Zipfel, C., and Smith, L.M. (2019). *Cr* RLK 1L receptor-like kinases HERK 1 and ANJEA are female determinants of pollen tube reception. EMBO Rep.

Guo, H., Li, L., Ye, H., Yu, X., Algreen, A., and Yin, Y. (2009). Three related receptor-like kinases are required for optimal cell elongation in Arabidopsis thaliana. Proc. Natl. Acad. Sci. *106*, 7648–7653.

Haruta, M., Sabat, G., Stecker, K., Minkoff, B.B., and Sussman, M.R. (2014). A Peptide Hormone and Its Receptor Protein Kinase Regulate Plant Cell Expansion. Science *343*, 408–411.

Haruta, M., Gaddameedi, V., Burch, H., Fernandez, D., and Sussman, M.R. (2018). Comparison of the effects of a kinase-dead mutation of FERONIA on ovule fertilization and root growth of Arabidopsis. FEBS Lett. *592*, 2395–2402.

Häweker, H., Rips, S., Koiwa, H., Salomon, S., Saijo, Y., Chinchilla, D., Robatzek, S., and von Schaewen, A. (2010). Pattern Recognition Receptors Require *N* -Glycosylation to Mediate Plant Immunity. J. Biol. Chem. *285*, 4629–4636.

Higashiyama, T., and Takeuchi, H. (2015). The Mechanism and Key Molecules Involved in Pollen Tube Guidance. Annu. Rev. Plant Biol. *66*, 393–413.

Höfte, H. (2015). The Yin and Yang of Cell Wall Integrity Control: Brassinosteroid and FERONIA Signaling. Plant Cell Physiol. *56*, 224–231.

Hohmann, N., Wolf, E.M., Lysak, M.A., and Koch, M.A. (2015). A Time-Calibrated Road Map of Brassicaceae Species Radiation and Evolutionary History. Plant Cell tpc.15.00482.

van der Hoorn, R.A.L., Wulff, B.B.H., Rivas, S., Durrant, M.C., van der Ploeg, A., de Wit, P.J.G.M., and Jones, J.D.G. (2005). Structure–Function Analysis of Cf-9, a Receptor-Like Protein with Extracytoplasmic Leucine-Rich Repeats. Plant Cell *17*, 1000–1015.

Hou, Y., Guo, X., Cyprys, P., Zhang, Y., Bleckmann, A., Cai, L., Huang, Q., Luo, Y., Gu, H., Dresselhaus, T., et al. (2016). Maternal ENODLs Are Required for Pollen Tube Reception in Arabidopsis. Curr. Biol. *26*, 2343–2350.

Huck, N. (2003). The Arabidopsis mutant feronia disrupts the female gametophytic control of pollen tube reception. Development *130*, 2149–2159.

Hüttner, S., and Strasser, R. (2012). Endoplasmic Reticulum-Associated Degradation of Glycoproteins in Plants. Front. Plant Sci. *3*.

Iwano, M., Ngo, Q.A., Entani, T., Shiba, H., Nagai, T., Miyawaki, A., Isogai, A., Grossniklaus, U., and Takayama, S. (2012). Cytoplasmic Ca2+ changes dynamically during the interaction of the pollen tube with synergid cells. Development *139*, 4202–4209.

Kang, J.S., Frank, J., Kang, C.H., Kajiura, H., Vikram, M., Ueda, A., Kim, S., Bahk, J.D., Triplett, B., Fujiyama, K., et al. (2008). Salt tolerance of Arabidopsis thaliana requires maturation of N-glycosylated proteins in the Golgi apparatus. Proc. Natl. Acad. Sci. *105*, 5933–5938.

Kessler, S.A., and Grossniklaus, U. (2011). She's the boss: signaling in pollen tube reception. Curr. Opin. Plant Biol. *14*, 622–627.

Kessler, S.A., Shimosato-Asano, H., Keinath, N.F., Wuest, S.E., Ingram, G., Panstruga, R., and Grossniklaus, U. (2010). Conserved Molecular Components for Pollen Tube Reception and Fungal Invasion. Science *330*, 968–971.

Kessler, S.A., Lindner, H., Jones, D.S., and Grossniklaus, U. (2015). Functional analysis of related Cr RLK 1L receptor-like kinases in pollen tube reception. EMBO Rep. *16*, 107–115.

Koiwa, H. (2003). The STT3a Subunit Isoform of the Arabidopsis Oligosaccharyltransferase Controls Adaptive Responses to Salt/Osmotic Stress. PLANT CELL ONLINE *15*, 2273–2284.

Kumar, S., Stecher, G., and Tamura, K. (2016). MEGA7: Molecular Evolutionary Genetics Analysis Version 7.0 for Bigger Datasets. Mol. Biol. Evol. *33*, 1870–1874.

Lewis, K.C., Selzer, T., Shahar, C., Udi, Y., Tworowski, D., and Sagi, I. (2008). Inhibition of pectin methyl esterase activity by green tea catechins. Phytochemistry *69*, 2586–2592.

Li, C., Yeh, F.-L., Cheung, A.Y., Duan, Q., Kita, D., Liu, M.-C., Maman, J., Luu, E.J., Wu, B.W., Gates, L., et al. (2015). Glycosylphosphatidylinositol-anchored proteins as chaperones and co-receptors for FERONIA receptor kinase signaling in Arabidopsis. ELife *4*, e06587.

Li, C., Wu, H., and Cheung, A.Y. (2016). FERONIA and her pals: functions and mechanisms. Plant Physiol. pp.00667.2016.

Li, J., Zhao-Hui, C., Batoux, M., Nekrasov, V., Roux, M., Chinchilla, D., Zipfel, C., and Jones, J.D.G. (2009). Specific ER quality control components required for biogenesis of the plant innate immune receptor EFR. Proc. Natl. Acad. Sci. *106*, 15973–15978.

Liebminger, E., Grass, J., Altmann, F., Mach, L., and Strasser, R. (2013). Characterizing the Link between Glycosylation State and Enzymatic Activity of the Endo-β1,4-glucanase KORRIGAN1 from *Arabidopsis thaliana*. J. Biol. Chem. *288*, 22270–22280.

Lindner, H., Müller, L.M., Boisson-Dernier, A., and Grossniklaus, U. (2012). CrRLK1L receptor-like kinases: not just another brick in the wall. Curr. Opin. Plant Biol. *15*, 659–669.

Lindner, H., Kessler, S.A., Müller, L.M., Shimosato-Asano, H., Boisson-Dernier, A., and Grossniklaus, U. (2015). TURAN and EVAN Mediate Pollen Tube Reception in Arabidopsis Synergids through Protein Glycosylation. PLOS Biol. *13*, e1002139.

Liu, Y., and Li, J. (2014). Endoplasmic reticulum-mediated protein quality control in Arabidopsis. Front. Plant Sci. *5*.

Liu, C., Niu, G., Zhang, H., Sun, Y., Sun, S., Yu, F., Lu, S., Yang, Y., Li, J., and Hong, Z. (2018). Trimming of N-Glycans by the Golgi-Localized α-1,2-Mannosidases, MNS1 and MNS2, Is Crucial for Maintaining RSW2 Protein Abundance during Salt Stress in Arabidopsis. Mol. Plant *11*, 678–690.

Liu, X., Castro, C., Wang, Y., Noble, J., Ponvert, N., Bundy, M., Hoel, C., Shpak, E., and Palanivelu, R. (2016). The Role of LORELEI in Pollen Tube Reception at the Interface of the Synergid Cell and Pollen Tube Requires the Modified Eight-Cysteine Motif and the Receptor-Like Kinase FERONIA. Plant Cell *28*, 1035–1052.

Müller, L.M., Lindner, H., Pires, N.D., Gagliardini, V., and Grossniklaus, U. (2016). A subunit of the oligosaccharyltransferase complex is required for interspecific gametophyte recognition in Arabidopsis. Nat. Commun. *7*, 10826.

Nekrasov, V., Li, J., Batoux, M., Roux, M., Chu, Z.-H., Lacombe, S., Rougon, A., Bittel, P., Kiss-Papp, M., Chinchilla, D., et al. (2009). Control of the pattern-recognition receptor EFR by an ER protein complex in plant immunity. EMBO J. *28*, 3428–3438.

Nelson, B.K., Cai, X., and Nebenführ, A. (2007). A multicolored set of in vivo organelle markers for co-localization studies in Arabidopsis and other plants: Fluorescent organelle markers. Plant J. *51*, 1126–1136.

Ngo, Q.A., Vogler, H., Lituiev, D.S., Nestorova, A., and Grossniklaus, U. (2014). A Calcium Dialog Mediated by the FERONIA Signal Transduction Pathway Controls Plant Sperm Delivery. Dev. Cell *29*, 491–500.

Nissen, K.S., Willats, W.G.T., and Malinovsky, F.G. (2016). Understanding CrRLK1L Function: Cell Walls and Growth Control. Trends Plant Sci. *21*, 516–527.

Okuda, S., Tsutsui, H., Shiina, K., Sprunck, S., Takeuchi, H., Yui, R., Kasahara, R.D., Hamamura, Y., Mizukami, A., Susaki, D., et al. (2009). Defensin-like polypeptide LUREs are pollen tube attractants secreted from synergid cells. Nature *458*, 357–361.

Rips, S., Bentley, N., Jeong, I.S., Welch, J.L., von Schaewen, A., and Koiwa, H. (2014). Multiple N-Glycans Cooperate in the Subcellular Targeting and Functioning of Arabidopsis KORRIGAN1. Plant Cell *26*, 3792–3808.

Rotman, N., Gourgues, M., Guitton, A.-E., Faure, J.-E., and Berger, F. (2008). A Dialogue between the Sirène Pathway in Synergids and the Fertilization Independent Seed Pathway in the Central Cell Controls Male Gamete Release during Double Fertilization in Arabidopsis. Mol. Plant *1*, 659–666.

Saijo, Y. (2010). ER quality control of immune receptors and regulators in plants: ER quality control of plant immune receptors. Cell. Microbiol. *12*, 716–724.

Sarker, R.H., Elleman, C.J., and Dickinson, H.G. (1988). Control of pollen hydration in Brassica requires continued protein synthesis, and glycosylation is necessary for intraspecific incompatibility. Cell Biol. 5.

Schallus, T., Jaeckh, C., Fehér, K., Palma, A.S., Liu, Y., Simpson, J.C., Mackeen, M., Stier, G., Gibson, T.J., Feizi, T., et al. (2008). Malectin: A Novel Carbohydrate-binding Protein of the Endoplasmic Reticulum and a Candidate Player in the Early Steps of Protein *N* -Glycosylation. Mol. Biol. Cell *19*, 3404–3414.

Strasser, R. (2016). Plant protein glycosylation. Glycobiology *26*, 926–939.

Takeuchi, H., and Higashiyama, T. (2012). A Species-Specific Cluster of Defensin-Like Genes Encodes Diffusible Pollen Tube Attractants in Arabidopsis. PLoS Biol. *10*, e1001449.

Tsukamoto, T., Qin, Y., Huang, Y., Dunatunga, D., and Palanivelu, R. (2010). A role for LORELEI, a putative glycosylphosphatidylinositol-anchored protein, in Arabidopsis thaliana double fertilization and early seed development: LORELEI functions in fertilization and seed development. Plant J. *62*, 571–588.

Xiao, Y., Stegmann, M., Han, Z., DeFalco, T.A., Parys, K., Xu, L., Belkhadir, Y., Zipfel, C., and Chai, J. (2019). Mechanisms of RALF peptide perception by a heterotypic receptor complex. Nature *572*, 270–274.

Yamamoto, M., Tantikanjana, T., Nishio, T., Nasrallah, M.E., and Nasrallah, J.B. (2014). Site-Specific *N*- Glycosylation of the S-Locus Receptor Kinase and Its Role in the Self-Incompatibility Response of the Brassicaceae. Plant Cell *26*, 4749–4762.

Yu, Y., and Assmann, S.M. (2018). Inter-relationships between the heterotrimeric Gβ subunit AGB1, the receptor-like kinase FERONIA, and RALF1 in salinity response: Synergism between G-protein subunit AGB1 and FERONIA in salinity response. Plant Cell Environ. *41*, 2475–2489.

Zhao, C., Zayed, O., Yu, Z., Jiang, W., Zhu, P., Hsu, C.-C., Zhang, L., Tao, W.A., Lozano-Durán, R., and Zhu, J.-K. (2018). Leucine-rich repeat extensin proteins regulate plant salt tolerance in *Arabidopsis*. Proc. Natl. Acad. Sci. *115*, 13123–13128.

Zhong, S., and Qu, L.-J. (2019). Peptide/receptor-like kinase-mediated signaling involved in male–female interactions. Curr. Opin. Plant Biol. *51*, 7–14.

Zhu, S., Martínez Pacheco, J., Estevez, J.M., and Yu, F. (2020). Autocrine regulation of root hair size by the RALF-FERONIA-RSL4 signaling pathway. New Phytol. nph.16497.

Zielinska, D.F., Gnad, F., Schropp, K., Wiśniewski, J.R., and Mann, M. (2012). Mapping N-Glycosylation Sites across Seven Evolutionarily Distant Species Reveals a Divergent Substrate Proteome Despite a Common Core Machinery. Mol. Cell *46*, 542–548.

Supplementary Figures and Tables

Table S1. Potential *N*-glycosylation sites of *A. thaliana Cr*RLK1L family. Software NetNGlyc 1.0 was used to determine putative glycosylation sites within protein extracellular domain.

Locus	Name	Position of Asparagine (N)	Number of sites
AT3G51550	FER	N46; N124; N142; N171; N219; N269; N305; N330; N345; N410	10
AT3G04690	ANX1	N114; N132; N292; N302; N330	5
AT5G28680	ANX2	N133; N293; N303; N331	4
AT4G39110	BUPS1	N170; N183; N254; N317; N382	5
AT2G21480	BUPS2	N169; N182; N253; N316; N381	5
AT5G61350	ERU	N81; N125; N252; N359; N365	5
AT2G39360	CVY1	N40; N45; N125; N146; N209; N244; N277; N331; N355; N401; N405; N458	12
AT3G46290	HERK1	N40; N146; N217; N280; N381; N458	6
AT1G30570	HERK2	N40; N57; N94; N122; N158; N268; N271; N305; N343	9
AT5G59700	ANJEA	N40; N216; N279; N380; N448; N455	6
AT5G54380	THE1	N41; N64; N74; N75; N113; N114; N118; N136; N143; N154; N168; N225; N242; N288; N353; N376	16
AT5G38990	MDS1	N46; N136; N158; N210; N256; N263; N297; N324	8
AT5G39000	MDS2	N49; N64; N138; N168; N216; N266; N300; N340; N437	9
AT5G39020	MDS3	N46; N61; N165; N202; N213; N263; N286; N293; N384; N401; N426	11
AT5G39030	MDS4	N59; N134; N164; N171; N212; N233; N261; N297; N401; N423	10
AT5G24010	-	N6; N41; N74; N204; N227; N291; N438	7
AT2G23200	-	N61; N149; N221; N246; N277; N289; N314; N352; N361; N394	10

Table S2. Potential *N*-glycosylation sites of *A. lyrata Cr*RLK1L family. Software NetNGlyc 1.0 was used to determine putative glycosylation sites within protein extracellular domain.

Locus	Name	Postion of Asparagine (N)	Number of sites
AL5G31990.t1	AlFER	N48; N120; N138; N167; N215; N265; N301; N326; N341; N406	10
AL3G14750.t1	AlANX1	N114; N132; N292; N302; N330	5
AL6G40700.t1	AlANX2	N115; N133; N293; N303; N331	5
AL7G11050.t1	AlBUPS1	N151; N164; N235; N298; N363	5
AL4G10660.t1	AlBUPS2	N16; N125; N138; N209; N272; N337	6
AL8G38020.t1	AlERU	N81; N125; N252; N294; N359; N365	6
AL4G36710.t1	AlCVY1	N40; N45; N124; N145; N150; N208; N243; N275; N329; N353; N399; N456	12
AL5G25190.t1	AlHERK1	N37; N144; N215; N278; N379; N447; N457	7
AL1G44610.t1	AlHERK2	N40; N57; N94; N122; N158; N248; N251; N285; N323; N441; N444	11
AL8G36220.t1	AlANJEA	N40; N217; N280; N381; N389; N449; N456	7
AL8G29710.t1	AlTHE1	N40; N63; N74; N113; N117; N135; N142; N153; N167; N224; N241; N287; N352; N375	14
AL7G51430.t1	AlMDS1	N92; N138; N142; N168; N216; N266; N300; N327; N406; N438	10
AL7G51422.t1	AlMDS2	N46; N61; N165; N202; N366; N381; N403; N406	8
AL7G52590.t2	AlMDS3/4	N8; N64; N90; N105; N151; N428	6
AL6G35330.t1	AlAT5G24010	N40; N73; N203; N226; N290; N437	6
AL4G13080.t1	AlAT2G23200	N45; N55; N62; N132; N204; N229; N261; N273; N298; N336; N345; N378	12

Table S3. Asparagine (N) variants of *Cr*RLK1L family members among *A. thaliana accessions*. Genomic data from 1135 natural accessions using Polymorph 1001 tool was screened to find nonsynonymous asparagine variants within *N*-glycosylation sites and throughout the whole protein sequence.

Locus	Name	N variants within ECDs	N variants within whole protein
AT3G51550	FER	no missense variants	0
AT3G04690	ANX1	p.N330	5
AT5G28680	ANX2	no missense variants	3
AT4G39110	BUPS1	no missense variants	2
AT2G21480	BUPS2	p.N182	4
AT5G61350	ERU	no missense variants	0
AT2G39360	CVY1	p.N40; p.N125	5
AT3G46290	HERK1	p.N40	1
AT1G30570	HERK2	p.N40; p.N482	6
AT5G59700	ANJEA	no missense variants	2
AT5G54380	THE1	no missense variants	3
AT5G38990	MDS1	p.N263	3
AT5G39000	MDS2	p.N300; p.N437	8
AT5G39020	MDS3	p.N286	10
AT5G39030	MDS4	p.N233; p.N261	13
AT5G24010	-	p.N41	6
AT2G23200	-	p.N246	7

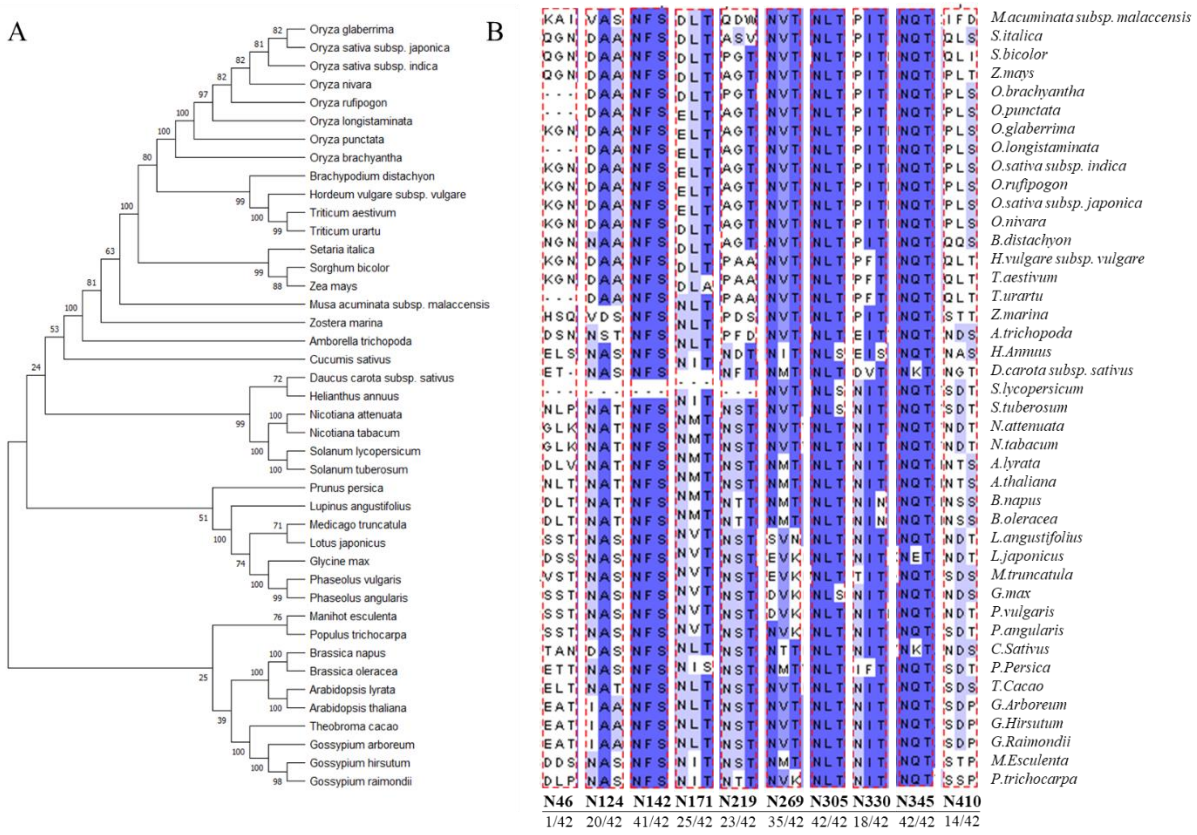

Figure S1. Protein conservation within FER ortholog group. (A) Phylogenetic tree showing the relationships between FER orthologs from 42 different species. Multiple alignments of FER protein orthologs were done using ClustalW2.0 followed by tree reconstruction in MEGA 7 (protein sequence parsimony method). **(B)** Conservation of FER protein N-glycosylation sites within ortholog group. Multiple alignment and identity percentage was visualized using Jalview 2.11.0 (white represents no conservation; dark blue represents identical residues). Proportion of *N*-glycosylation sites conservation among 42 species is indicated below each motif.

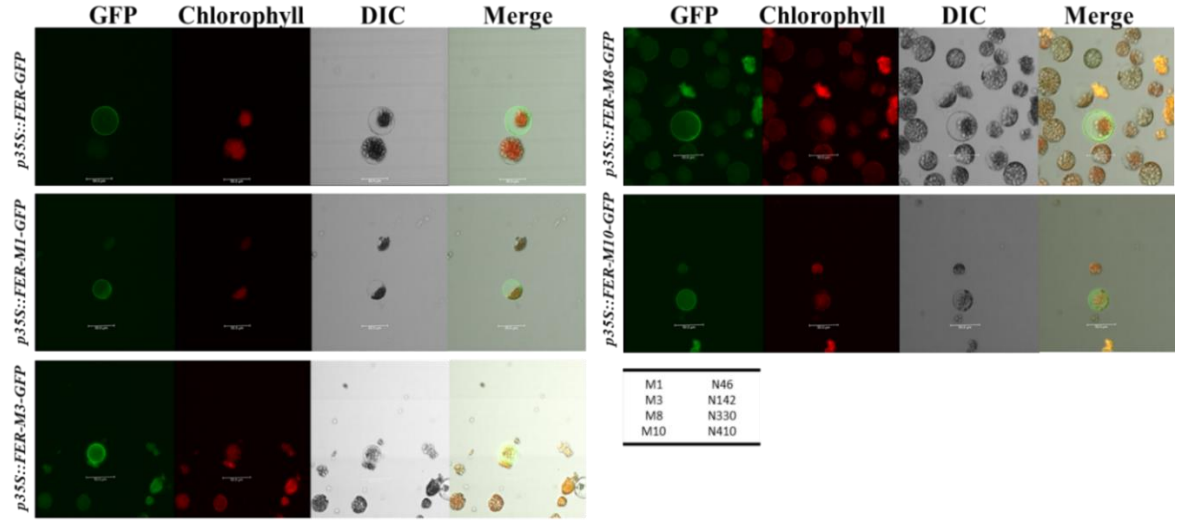

Figure S2. Subcellular localization of FER-GFP single *N*-glycosylation variants in *Arabidopsis* protoplasts. FER-GFP *N*-glycosylation mutants are localized solely in the plasma membrane (GFP signal in green and chlorophyll autofluorescence in red). Expression of FER-GFP variants was observed 24h post-transfection using epifluorescence microscope.

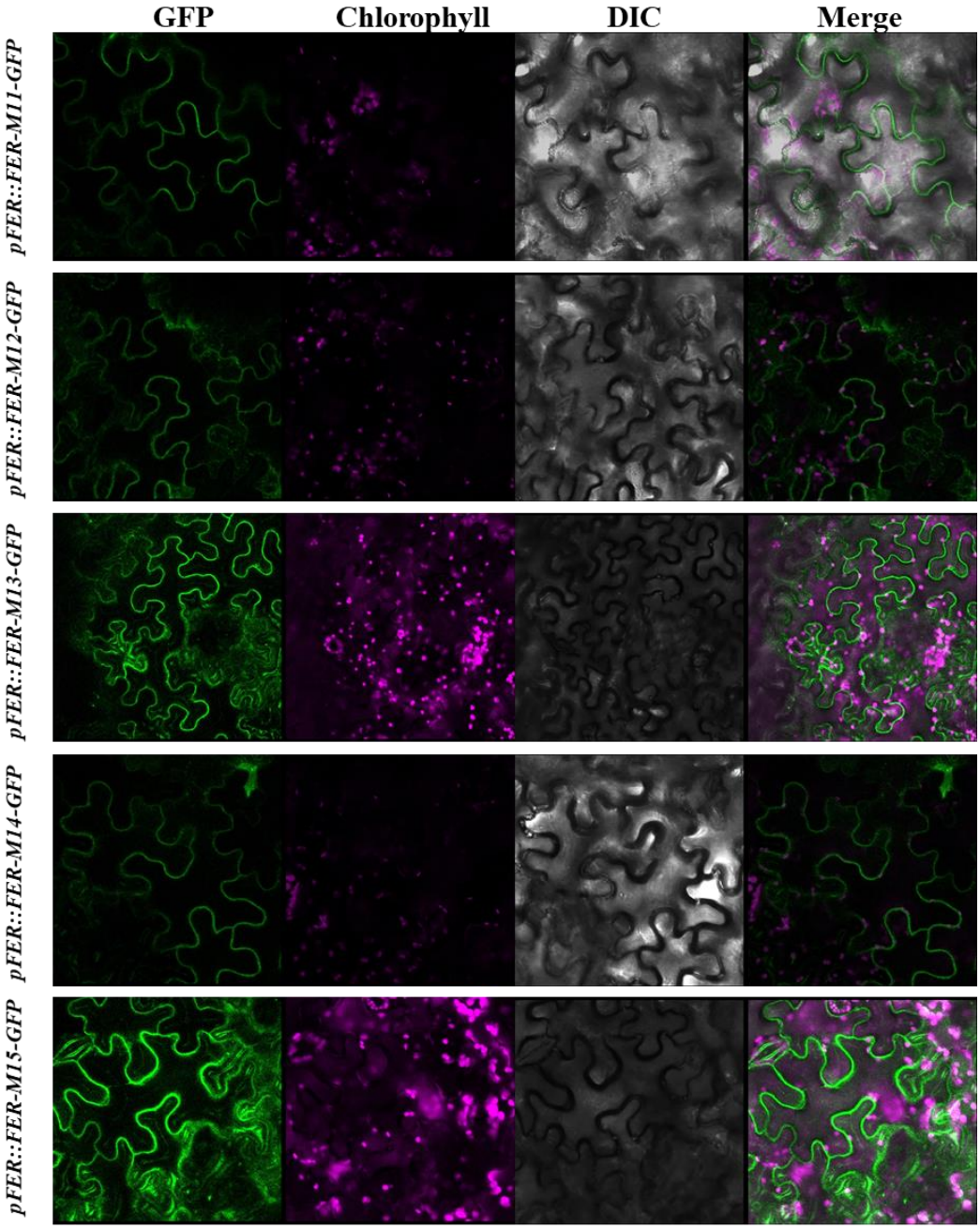

M11	N46 + N142
M12	N46 + N330
M13	N46 + N410
M14	N142 + N330
M15	N330 + N410

Figure S3. Subcellular localization of FER-GFP double *N*-glycosylation variants in *N. benthamiana* epidermal cells. Different combinations of double FER-GFP *N*-glycosylation mutants exclusively localize to the plasma membrane (GFP signal in green and chlorophyll autofluorescence in magenta). Expression of FER-GFP variants was observed three days post-agroinfiltration using confocal microscope.

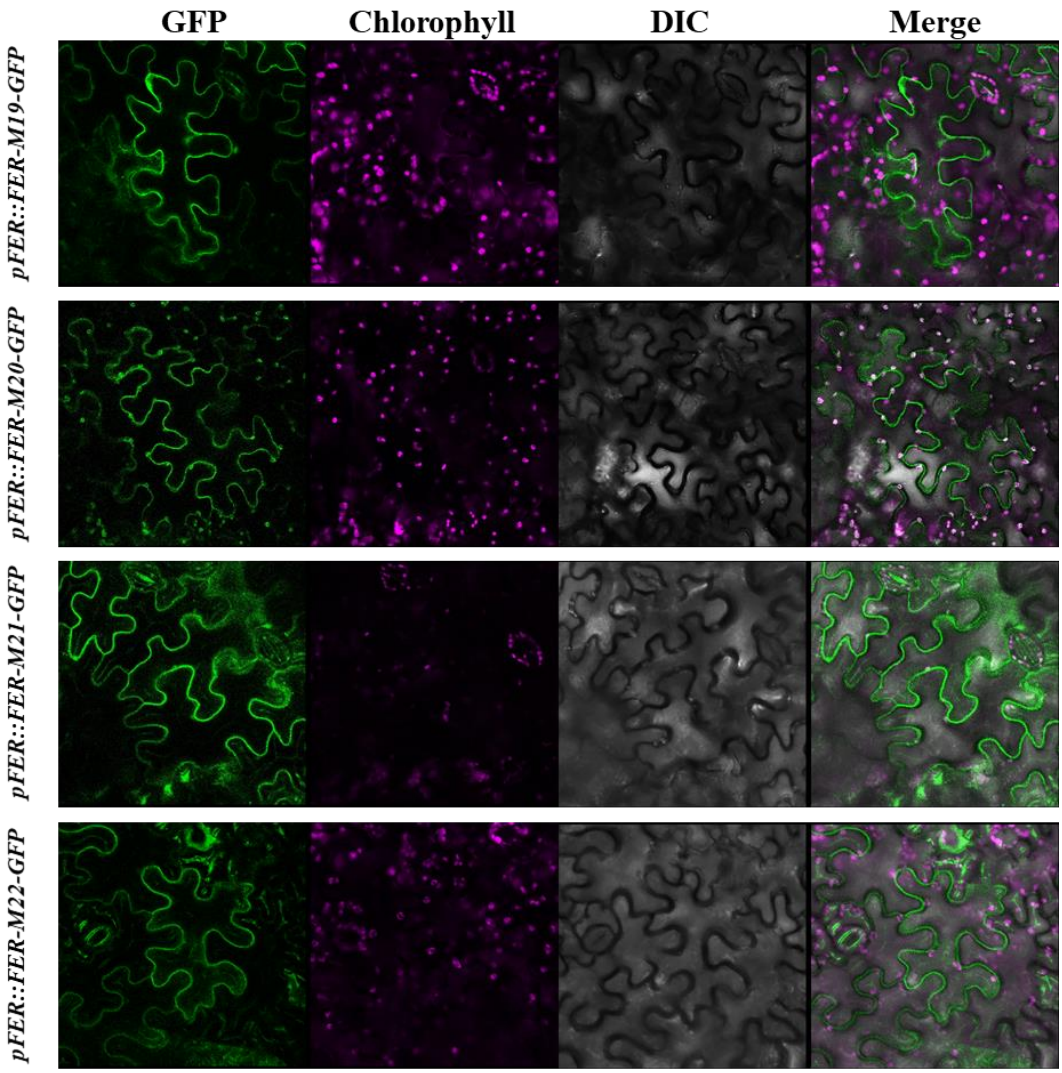

M19	N46 + N142 + N330
M20	N46 + N124 + N142
M21	N46 + N142 + N171
M22	N46 + N124 + N142 + N171

Figure S4. Subcellular localization of FER-GFP triple and quadruple *N*-glycosylation variants in *N. benthamiana* epidermal cells. Triple and quadruple FER-GFP *N*-glycosylation mutants predominantly localize to the plasma membrane with a small cytoplasmic fraction. GFP signal is depicted in green and chlorophyll autofluorescence in magenta. Expression of FER-GFP variants was observed three days post-agroinfiltration using confocal microscope.

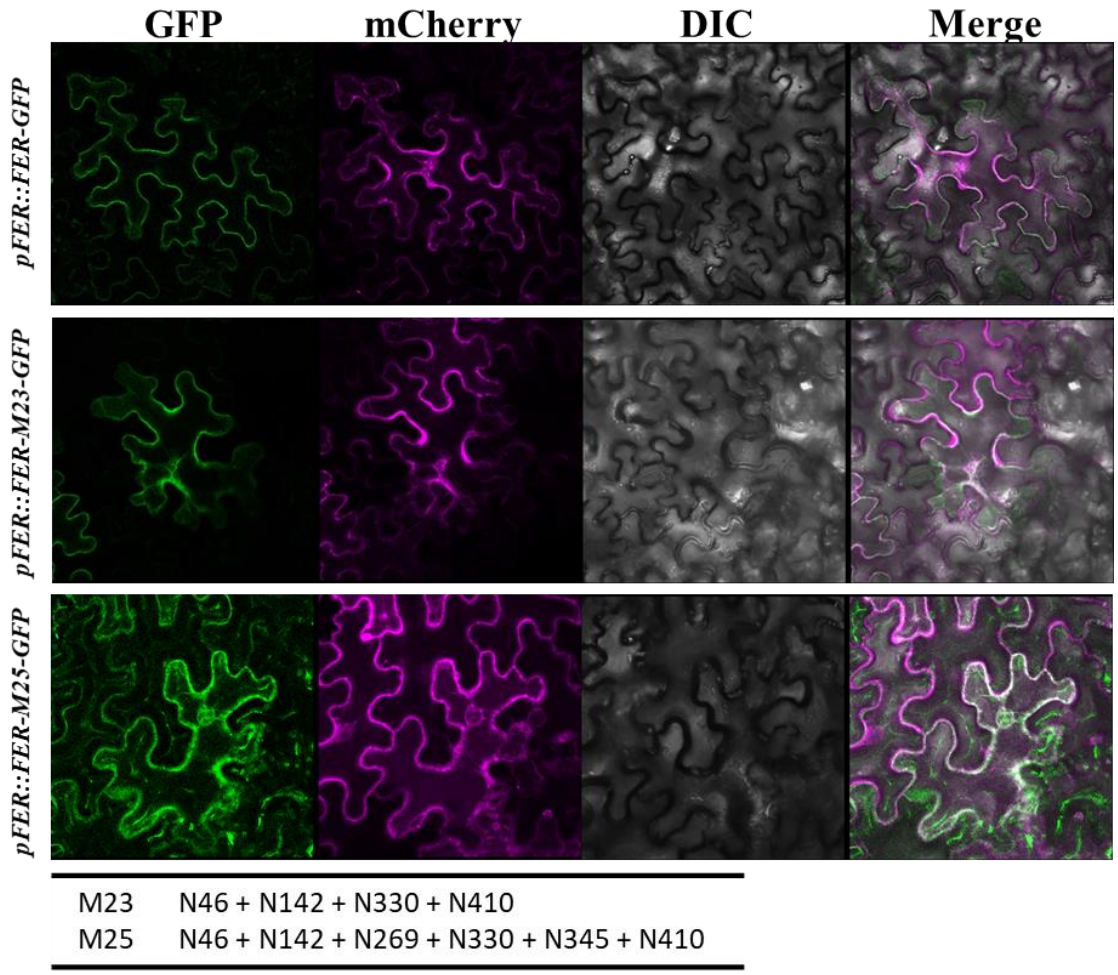

Figure S5. Colocalization of FER-GFP higher-end *N*-glycosylation variants with ER marker in *N. benthamiana* epidermal cells. Quadruple and hexapole FER-GFP *N*-glycosylation variants show significant overlap with pER-rk (mCherry), suggesting that large portion of FER-GFP is ER localized. GFP signal is depicted in green and mCherry in magenta. Expression was observed three days post-agroinfiltration using Leica SP5 confocal microscope.

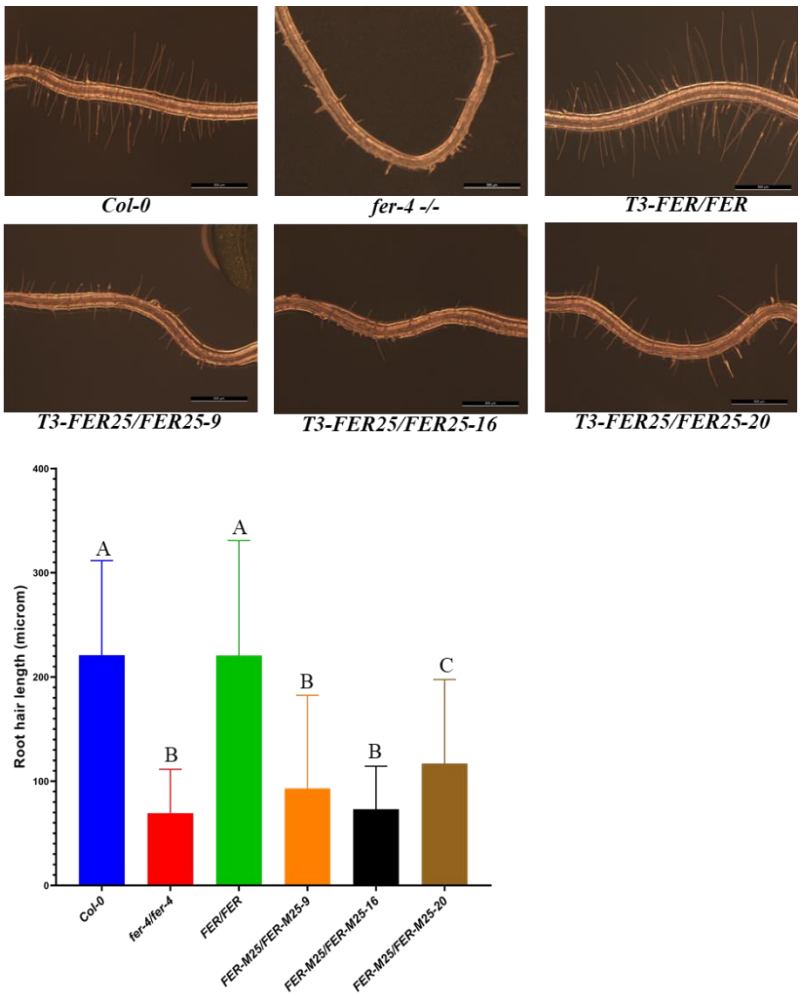

Figure S6. Root hair phenotype of *fer-4* complemented with hexapole FER-GFP *N*-glycosylation variant. Images of 5 days old Col-0, *fer-4* and T3 seedlings were taken using Leica stereomicroscope. Phenotyping was done by measuring root hair length in the region of 1.5 to 3.5 mm from the primary root tip. Col-0 (n=161), *fer-4* (n=110), *FER/FER* (n=155), *FER-M25/FER-M25-9* (n=302), *FER-M25/FER-M25-16* (n=290), *FER-M25/FER-M25-20* (n=278). Kruskal–Wallis test followed by Dunn's multiple comparison test (A-B ****P < 0.0001; A-C ****P < 0.0001; B-C ****P < 0.0001).

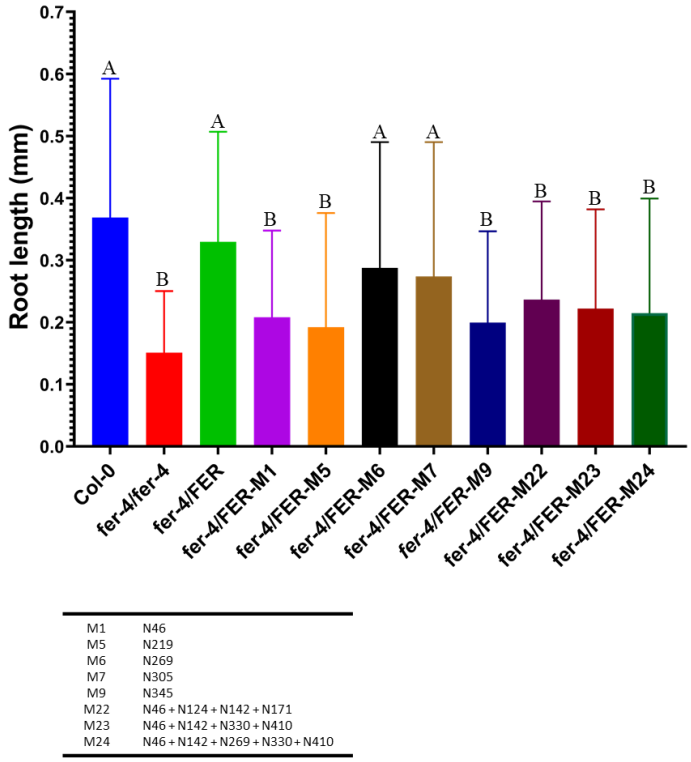

Figure S7. Complementation of *fer-4* salt sensitivity with different FER-GFP *N*-glycosylation variants. Images of 8 days old Col-0, *fer-4* and T2 seedlings were taken using stereomicroscope. Phenotyping was done by measuring root growth upon transfer to the treatment plates (140 mM NaCl). Col-0 (n=170), *fer-4* (n=148), *fer-4/FER* (n=123), *fer-4/FER-M5* (n=106), *fer-4/FER-M6* (n=118), *fer-4/FER-M7* (n=108), *fer-4/FER-M9* (n=116), *fer-4/FER-M22* (n=122), *fer-4/FER-M24* (n=110). Kruskal–Wallis test followed by Dunn's multiple comparison test (A-B ****P<0.0001).

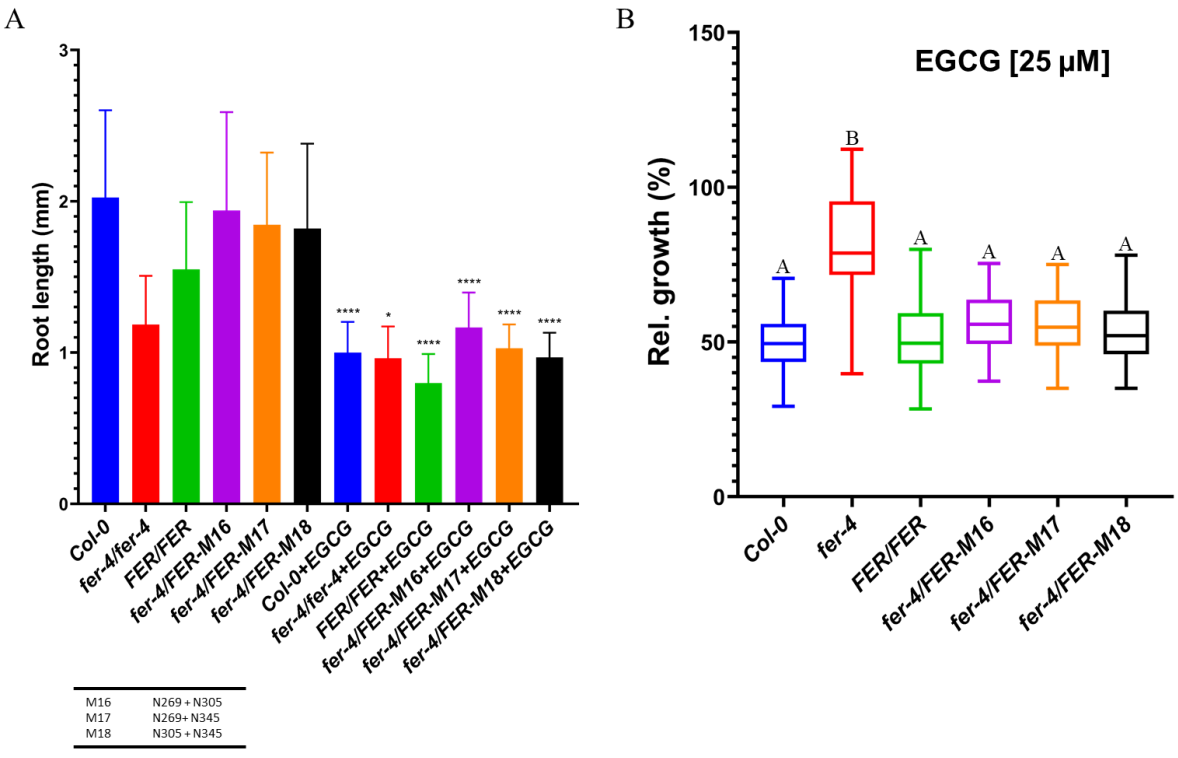

Figure S8. FER-GFP *N*-glycosylation variants are sensitive to the EGCG effects on the cell wall integrity. Five days old seedlings were transferred to the EGCG supplemented liquid media. Three days later images of Col-0, *fer-4* and T1 seedlings were taken using Leica stereomicroscope and phenotyping was done by measuring root length. Col-0 (n=38), *fer-4* (n=43), *fer-4/FER-M16* (n=29), *fer-4/FER-M17* (n=27), *fer-4/FER-M18* (n=31). **(A)** Mann-Whitney U test was done to compare absolute root length before and after EGCG treatment. Each genotype was analyzed separately, but here is present together in a graph (*P=0.0143; ****P<0.0001). **(B)** Relative root length after 3 days of EGCG treatment. One-way ANOVA followed by Tukey's multiple comparison test (A-B ****P<0.0001).

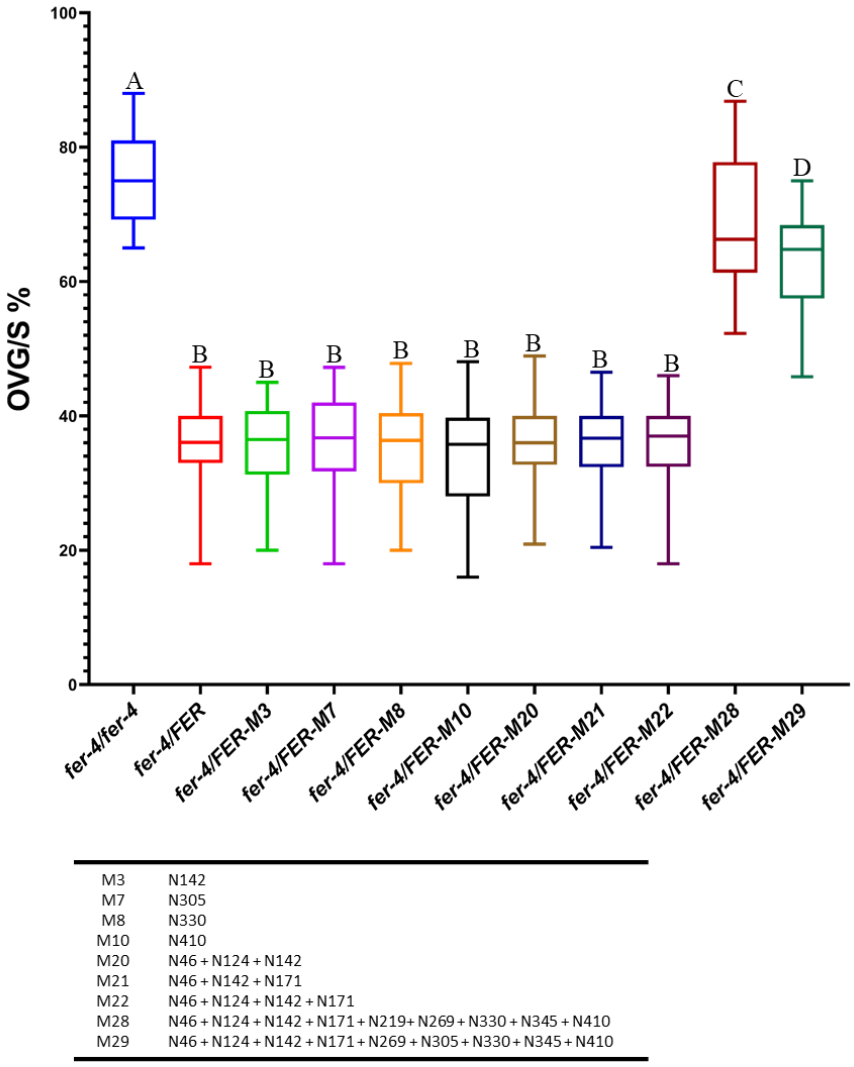

Figure S9. Complementation of *fer-4* intraspecific pollen tube reception with FER-GFP *N* glycosylation variants. Box plots represent the percentage of ovules with pollen tube overgrowth per silique. For each FER-GFP *N*-glycosylation complementation line data from 5 independent T1 plants is presented (>500 ovules counted per T1 plant). One-way ANOVA followed by Tukey's multiple comparison test (A-B ****P<0.0001; A-C *P=0.0337; A-D ****P<0.0001; B-C ****P<0.0001; B-D ****P<0.0001).

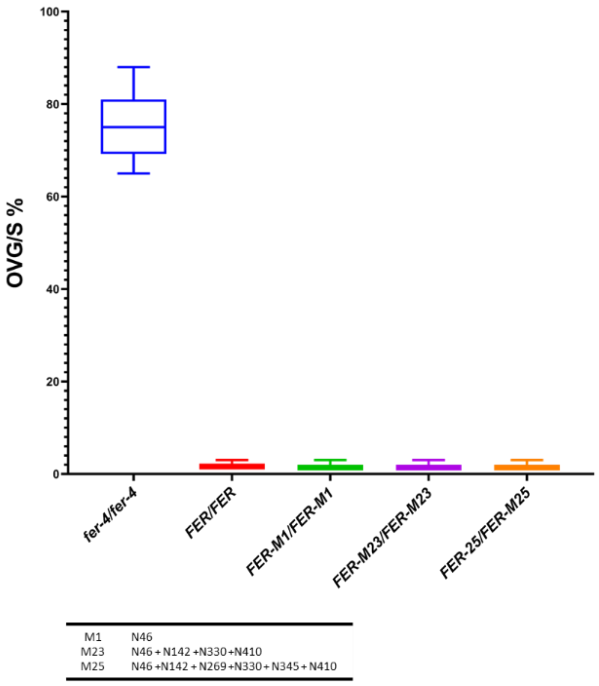

Figure S10. Full complementation of *fer-4* intraspecific pollen tube reception in T2 homozygous complementation lines. Box plots represent the percentage of ovules with pollen tube overgrowth per silique. For each FER-GFP *N*-glycosylation complementation line data from 10 independent T2 plants is presented (>500 ovules counted per T2 plant).

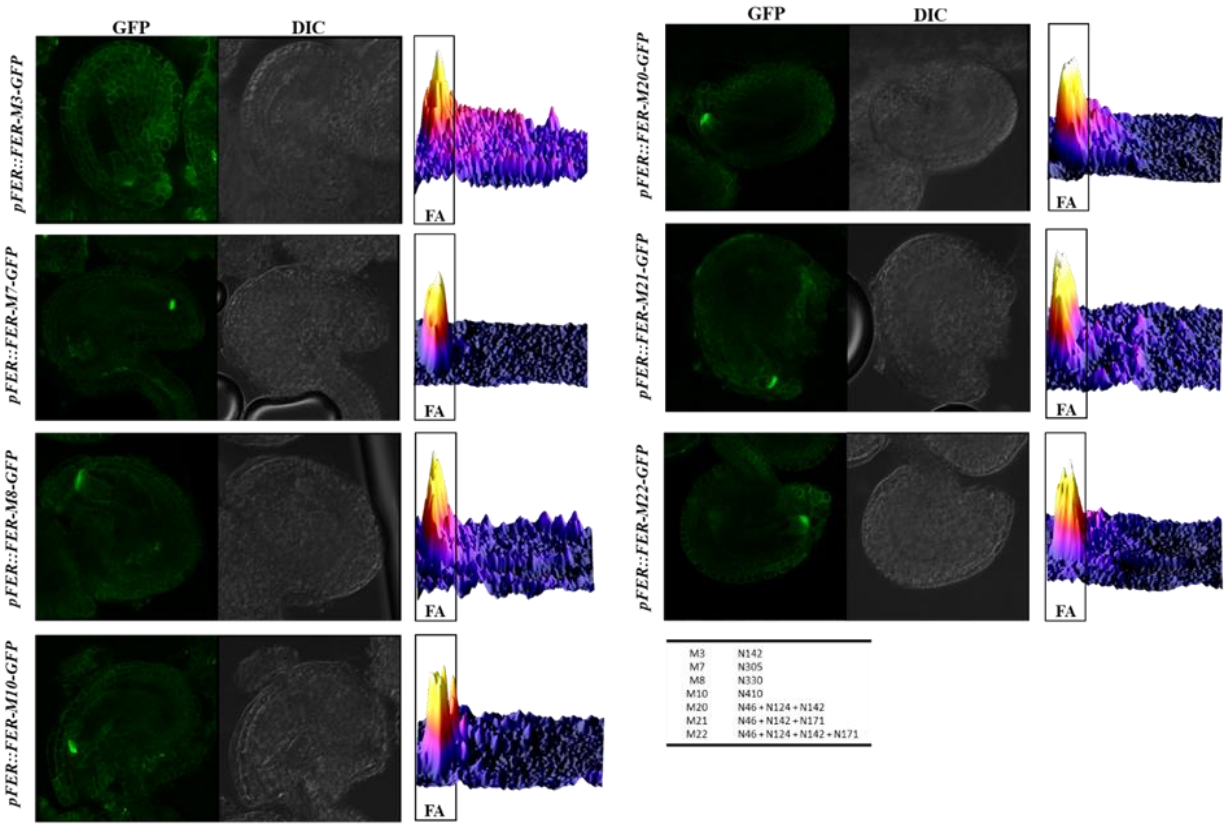

Figure S11. FER-GFP *N*-glycosylation variants are properly localized in the filiform apparatus of synergid cells. Representative confocal images of ovules expressing different FER-GFP *N*-glycosylation variants. Surface plots of total synergid GFP signal intensity. Signal coming from filiform apparatus (FA) is highlighted in the boxed areas. All depicted FER-GFP *N*-glycosylation variants fully complement *fer-4* pollen tube overgrowth phenotype.

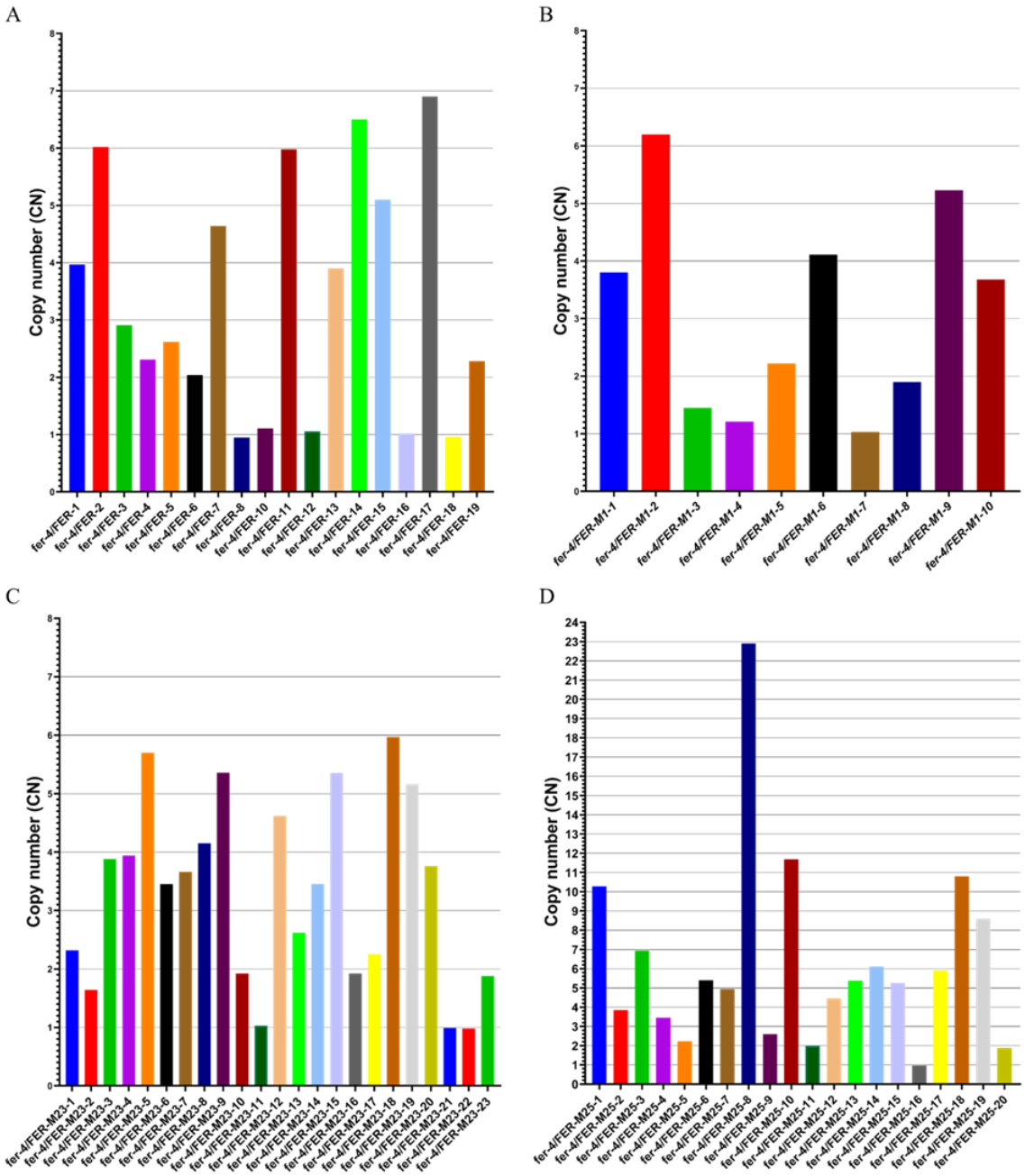

Figure S12. T-DNA insertion copy number of FER-GFP *N*-glycosylation variants complementation lines. Copy number was determined with ddPCR (hygromycin assay) **(A)** From 19 T1 complementation lines (FER-GFP) five had a single copy T-DNA insertion. **(B)** From 10 T1 lines (FER-GFP$^{[M1]}$) three had a single copy T-DNA insertion. **(C)** From 23 T1s (FER-GFP$^{[M23]}$) three had a single copy T-DNA insertion. **(D)** From 20 T1 lines (FER-GFP$^{[N25]}$) one had a single copy T-DNA insertion and two more lines had below 2 copies.

Table S4. Primers used for *fer-4* PCR genotyping.

Primer	Primer Sequence (5’- 3’)
ADZ124	ACTTCCTTTCACAACTGTGCTTAC
ADZ125	ATACGGGTTTGTATAGGTCGTGGT
ADZ126	ATAATAACGCTGCGGACATCTACATTTT

Table S5. Primers used for site-directed mutagenesis.

Primer	Description	Primer Sequence (5’- 3’)
ADZ164	N46A-F	TGGTGCTTCTgcTCTAACCGACAC
ADZ165	N46A-R	CCACCGCAATTCAATAGG
ADZ166	N124A-F	CGACGGTCTCgcCGCTACCAAC
ADZ167	N124A-R	TACGAGTTTGGGTAGAAG
ADZ168	N142A-F	TCTTCTCAAGgcTTTCAGTGCTTCTC
ADZ169	N142A-R	GTGTAAGGACCAAAGGAG
ADZ170	N171A-F	TGGAACGTTGgcCATGACGTTTAC
ADZ171	N171A-R	CCTTCAACGTTGACAACAAAC
ADZ172	N219A-F	TACTATTGATgcCAGTACTGCTCTTGAGAATG
ADZ173	N219A-R	ACAGAGCCAGATGATCCAAC
ADZ174	N269A-F	TGCTGATCCCgcCATGACGATTAAG
ADZ175	N269A-R	GTCTCTGGAATACCAAGTC
ADZ176	N305A-F	TCTCAACTACgcTCTTACTTGGATTTTCAGC
ADZ177	N305A-R	TTGATCTGAGCTGTTGGAC
ADZ178	N330A-F	GGTTTCTTCGgcTATCACTAAGATCAAC
ADZ179	N330A-R	TCACAGAAATGAAGTCTAAC
ADZ180	N345A-F	CTACCTCAACgcTCAAACTGCTGAG
ADZ181	N345A-R	ATTGTAAACACCCGTTGG
ADZ182	N410A-F	ATTCAAGATGgcTACTTCTGATGGTAATC
ADZ183	N410A-R	ATCTCCACTCCATTAAGAAG

Table S6. Constructs used for transient protoplast transfections.

Vector	Description	Selection in bacteria
pADZ1	35S:FER-GFP	Ampicillin
pADZ2	35S:FER$^{[N46A]}$-GFP	Ampicillin
pADZ3	35S:FER$^{[N142A]}$-GFP	Ampicillin
pADZ4	35S:FER$^{[N330A]}$-GFP	Ampicillin
pADZ5	35S:FER$^{[N410A]}$-GFP	Ampicillin

Table S7. List of donor vectors, with indicated positions of mutated asparagines (N) and bacterial selection.

Vector	Description	Selection in bacteria
pADZ8	FER w/o STOP	Genatamicin
pADZ10	$FER^{[N46A]}$ w/o STOP	Genatamicin
pADZ11	$FER^{[N142A]}$ w/o STOP	Genatamicin
pADZ12	$FER^{[N330A]}$ w/o STOP	Genatamicin
pADZ13	$FER^{[N410A]}$ w/o STOP	Genatamicin
pADZ19	$FER^{[N269A]}$ w/o STOP	Genatamicin
pADZ20	$FER^{[N345A]}$ w/o STOP	Genatamicin
pADZ23	$FER^{[N46A;N142A]}$ w/o STOP	Genatamicin
pADZ24	$FER^{[N46A;N330A]}$ w/o STOP	Genatamicin
pADZ25	$FER^{[N46A;N410A]}$ w/o STOP	Genatamicin
pADZ26	$FER^{[N142A;N330A]}$ w/o STOP	Genatamicin
pADZ27	$FER^{[N142A;N410A]}$ w/o STOP	Genatamicin
pADZ28	$FER^{[N330A;N410A]}$ w/o STOP	Genatamicin
pADZ29	$FER^{[N46A;N142A;N330A]}$ w/o STOP	Genatamicin
pADZ30	$FER^{[N46A;N142A;N410A]}$ w/o STOP	Genatamicin
pADZ31	$FER^{[N46A;N330A;N410A]}$ w/o STOP	Genatamicin
pADZ32	$FER^{[N142A;N330A;N410A]}$ w/o STOP	Genatamicin
pADZ33	$FER^{[N46A;N142A;N330A;N410A]}$ w/o STOP	Genatamicin
pADZ34	$FER^{[N46A;N142A;N330A;N410A;N269A]}$ w/o STOP	Genatamicin
pADZ35	$FER^{[N46A;N142A;N330A;N410A;N345A]}$ w/o STOP	Genatamicin
pADZ36	$FER^{[N46A;N142A;N330A;N410A;N269A;N345A]}$ w/o STOP	Genatamicin
pADZ51	$FER^{[N46A;N142A;N124A]}$ w/o STOP	Genatamicin
pADZ52	$FER^{[N46A;N142A;N171A]}$ w/o STOP	Genatamicin
pADZ53	$FER^{[N46A;N142A;N124A;N171A]}$ w/o STOP	Genatamicin
pADZ57	$FER^{[N46A;N142A;N330A;N410A;N269A;N345A;N124A]}$ w/o STOP	Genatamicin
pADZ58	$FER^{[N46A;N142A;N330A;N410A;N269A;N345A;N124A;N171A]}$ w/o STOP	Genatamicin
pADZ59	$FER^{[N46A;N142A;N330A;N410A;N269A;N345A;N124A;N171A;N219A]}$ w/o STOP	Genatamicin
pADZ60	$FER^{[N46A;N142A;N330A;N410A;N269A;N345A;N124A;N171A;N305A]}$ w/o STOP	Genatamicin
pADZ61	$FER^{[N46A;N142A;N330A;N410A;N269A;N345A;N124A;N171A;N219A;N305A]}$ w/o STOP	Genatamicin
pADZ67	$FER^{[N219A]}$ w/o STOP	Genatamicin
pADZ68	$FER^{[N305A]}$ w/o STOP	Genatamicin
pADZ69	$FER^{[N269A;N305A]}$ w/o STOP	Genatamicin
pADZ70	$FER^{[N269A;N345A]}$ w/o STOP	Genatamicin
pADZ71	$FER^{[N305A;N345A]}$ w/o STOP	Genatamicin

Table S8. Primers used for sequencing of final vectors

Primer	Primer Sequence (5'- 3')
ADZ192	TCCCCGATTCTTCAGGTATG
ADZ193	CGCCGTCATGTAAGGAACTT
ADZ194	CGTTCCCGAAGTTCCTTACA
ADZ195	CCTCGCGGTTGAATAAACAT
ADZ196	CGGCAAGGTTTACAGAGGAG
ADZ197	TTTGCAAGTGTTGGGTTCAA
ADZ198	GCAGCCCGAGGTTTACACTA
ADZ199	TGTCCATGTCACCGCATACT
ADZ200	GTTTTCCCAGTCACGACGTT
ADZ201	TGGGGCCTGCTTTGATAATA
ADZ202	TCGATCAAAAGGAGGCTACG
ADZ203	AAGCGATGAAATCGGAGAGA
ADZ204	ATTCAACCGCGAGGTCTATG
ADZ205	GATAGTGGAAGCCACCCTGA

Table S9. List of expression clones used for *fer-4* transformation with selection markers.

Expression clone	Description	Selection in bacteria	Selection in plant
pADZ14	pADZ8 in pADZ9	Kanamycin	Hygromycin
pADZ15	pADZ10 in pADZ9	Kanamycin	Hygromycin
pADZ16	pADZ11 in pADZ9	Kanamycin	Hygromycin
pADZ17	pADZ12 in pADZ9	Kanamycin	Hygromycin
pADZ18	pADZ13 in pADZ9	Kanamycin	Hygromycin
pADZ21	pADZ19 in pADZ9	Kanamycin	Hygromycin
pADZ22	pADZ20 in pADZ9	Kanamycin	Hygromycin
pADZ37	pADZ23 in pADZ9	Kanamycin	Hygromycin
pADZ38	pADZ24 in pADZ9	Kanamycin	Hygromycin
pADZ39	pADZ25 in pADZ9	Kanamycin	Hygromycin
pADZ40	pADZ26 in pADZ9	Kanamycin	Hygromycin
pADZ41	pADZ27 in pADZ9	Kanamycin	Hygromycin
pADZ42	pADZ28 in pADZ9	Kanamycin	Hygromycin
pADZ43	pADZ29 in pADZ9	Kanamycin	Hygromycin
pADZ44	pADZ30 in pADZ9	Kanamycin	Hygromycin
pADZ45	pADZ31 in pADZ9	Kanamycin	Hygromycin
pADZ46	pADZ32 in pADZ9	Kanamycin	Hygromycin
pADZ47	pADZ33 in pADZ9	Kanamycin	Hygromycin
pADZ48	pADZ34 in pADZ9	Kanamycin	Hygromycin
pADZ49	pADZ35 in pADZ9	Kanamycin	Hygromycin
pADZ50	pADZ36 in pADZ9	Kanamycin	Hygromycin
pADZ54	pADZ51 in pADZ9	Kanamycin	Hygromycin
pADZ55	pADZ52 in pADZ9	Kanamycin	Hygromycin
pADZ56	pADZ53 in pADZ9	Kanamycin	Hygromycin
pADZ62	pADZ57 in pADZ9	Kanamycin	Hygromycin
pADZ63	pADZ58 in pADZ9	Kanamycin	Hygromycin
pADZ64	pADZ59 in pADZ9	Kanamycin	Hygromycin
pADZ65	pADZ60 in pADZ9	Kanamycin	Hygromycin
pADZ66	pADZ61 in pADZ9	Kanamycin	Hygromycin
pADZ72	pADZ67 in pADZ9	Kanamycin	Hygromycin
pADZ73	pADZ68 in pADZ9	Kanamycin	Hygromycin
pADZ74	pADZ69 in pADZ9	Kanamycin	Hygromycin
pADZ75	pADZ70 in pADZ9	Kanamycin	Hygromycin
pADZ76	pADZ71 in pADZ9	Kanamycin	Hygromycin

CHAPTER 5 - DISCUSSION

Double fertilization is a distinctive characteristic of flowering plants (angiosperms), which are one of the most successful and ubiquitously present groups of plants nowadays. During process of double fertilization pollen tube (PT) bursts within the receptive synergid, sperm cells get released and fertilize egg and central cells enabling formation of embryo and endosperm (Sprunck, 2020). Successful double fertilization is hence essential for the high seed yield, which is of vast nutritional and agronomical importance in the crop plants (Bleckmann et al., 2014). Most of the progress in the past years in bettering our understanding of complex molecular and cellular mechanisms underlying successful plant reproduction have been made using the model plant species *A. thaliana* (Adhikari et al., 2020; Zheng et al., 2018). It has become evident that each step of the long PT journey from the stigma papilla cells through the pistil up to the embryo sack is tightly regulated by large set of sporophytic and gametophytic factors (Dresselhaus and Franklin-Tong, 2013). Essential role of receptor-like kinases during the double fertilization, has been revealed with a discovery of *feronia* mutant in which almost 80% of PTs fail to burst and release sperm cells, but instead they continuously grow within the embryo sack, which was described as a PT overgrowth (PTO) phenotype (Escobar-Restrepo et al., 2007; Huck, 2003). Since the discovery of FER only several gametophytic mutants with the distinguishing *fer*-like PTO have been uncovered, including *scylla, lorelei, nortia, RNAi enodls, evan, turan, herk1/anjea* double mutants, *ap1g* and *vha-a, amc*, and *myb97/myb101/myb120* triple mutants (Boisson-Dernier et al., 2008; Capron et al., 2008; Galindo-Trigo et al., 2019; Hou et al., 2016; Kessler et al., 2010; Leydon et al., 2013; Liang et al., 2013; Lindner et al., 2015; Rotman et al., 2008; Wang et al., 2017).

Even though in the last years there has been a progress in elucidating signaling cascade required for the successful PT reception, still there are many unanswered questions. For instance, the nature of ligand of FER during PT recognition and induction of PT burst is completely lacking. Additionally, surprisingly little is known on the downstream signaling components upon PT perception. So far there is not a single cytoplasmic receptor-like kinase or phosphatase reported to function downstream of FER in synergids. Furthermore, it is unclear how exactly FER regulates ROS production and Ca^{2+} signaling to enable PT burst. We have set out to answer some of these burning questions by analyzing EMS mutants with a classical *fer*-like PTO phenotype. Forward genetic screen was performed since it is the best way of finding novel signaling components in a completely unbiased fashion (Page and Grossniklaus, 2002). We have utilized a previously established SNP-ratio mapping approach (SRM) (Lindner et al., 2012) and identified a novel allele of *TUN*, which carried a causative SNP (c.321+1G>A), resulting in a splice donor variant of the first exon. Furthermore, the SNP/non-SNP ratio was 0,489 (very close to the expected ratio 0,5) and it allowed identification of causative SNP already by the visual inspection of plotted segregation ratios onto their chromosomal positions. The fact that we were able to map a known PT reception player further confirms our strategy to be not only rapid, easy to interpret but also extremely reliable (Lindner et al., 2012).

We have strong indications that a causative SNP (c.1024 G>A) in the second EMS mutant affected *RID1*, leading to a nonsynonymous amino acid change from valine to isoleucine V342I. We have obtained good overall sequence quality for all three EMS candidates, however in the case of sample ADZ12 mapping rates were lower, and around 50% of reads were mapping to the *A. thaliana* genome. Upon resequencing mapping rates were increased to 65%, which was sufficient to proceed with the downstream SRM analysis. We have obtained 1,079 heterozygous SNPs for ADZ12 sample. Upon plotting of segregation ratios to their chromosomal locations we have detected a typical rounded curve in chromosome 1 containing the *RID1* SNP. We did not want to rely only on the visual identification; hence we PCR amplified *RID1* from all 52 plants of the sequencing pool and obtained the same

heterozygous causative SNP. However, when we analyzed two independent T-DNA lines disrupting the *RID1*, we have obtained conflicting results. Only our EMS line (*rid1-1/RID1*) displayed 8% of PTO, while both T-DNA alleles displayed a severe disruption of PT guidance, and around 50% of ovules remained unfertilized, resulting in a seed abortion which was previously reported (Ohtani et al., 2013; Zhu et al., 2016). Upon a detailed characterization, we have found around 12% of non-targeted ovules in the *rid1-1/RID1*, and a total of 20% seed set abortion. Discrepancy of phenotype strength can be explained by the fact that in T-DNA lines protein is disrupted, while *rid1-1/RID1* EMS line had a single amino acid change. The final proof of correct identification of *RID1* will be obtained once functional RID1 is introduced into the *rid1-1/RID1* leading to the full complementation of reproductive phenotypes.

Having in mind that *RID1* encodes a RNA helicase important for the correct cellular specification of the female gametophyte (Ohtani et al., 2013; Zhu et al., 2016), a more detailed assessment of synergids identity/differentiation should be undertaken. For instance synergid-specific cell marker could be introduced in the *rid1-1/RID1* and expression should be analyzed in F2 generation, to asses if *rid1-1/RID1* embryo sacs are competent of expressing the synergid specific marker (Gross-Hardt et al., 2007). Furthermore, since MYB98 is expressed exclusively in the synergids with essential roles in the PT attraction through control of more than 83 downstream genes, expression of MYB98 should be carefully assessed in *rid1-1/RID1* ovules (Kasahara et al., 2005; Punwani et al., 2008). Very recently it was reported that two pre-mRNA processing factor 8 paralogs, PRP8A and PRP8B act in a redundant manner to regulate PT attraction. Double mutants *prp8a/prp8b* completely lost ability to attract PTs, while no obvious female or male gametogenesis defects were observed (Kulichová et al., 2020). RNA-seq analysis revealed that expression of MYB98, LUREs, and several CRPs was downregulated, indicative of aberrant synergid cell specification. Additionally, authors analyzed RALF peptide expression in *prp8a/prp8b*, and found RALF20 to be 5-times up-regulated, while RALF21, RALF28 and RALF29 were more than 5- times down-regulated. Lastly semi-RT-PCR intron profiling and frequency of exon-usage showed that FER and LER are correctly pre-mRNA processed in the *prp8a/prp8b* ovules (Kulichová et al., 2020). To summarize, it appears that spliceosome machinery plays surprisingly important role in the regulation of PT attraction, and most likely PT reception, which remains to be confirmed in the future by complementation of *rid1-1/RID1* mutant which displayed both defective PT guidance as well as the PTO phenotype.

Third EMS mutant was discovered to be the *ALG11* (*ASPARAGINE LINKED GLYCOSYLATION 11*), encoding an ER-resident enzyme of the *N*-glycosylation pathway. Causative EMS SNP (c.716G>A) led to the premature STOP codon generation in the third exon (T239*). Plotting of SNP segregation ratios to their chromosomal positions revealed a typical rounded curve in the chromosome 2, hence similarly to *TUN* already visual inspection allowed identification of causative SNP. Furthermore, we PCR amplified *ALG11* from all the mutants from the sequencing pool and found presence of causative heterozygous SNP in all of them. Correct identification of ALG11 was confirmed by detection of *fer*-like PTO phenotype in two previously described T-DNA lines (Manzano et al., 2017; Zhang et al., 2009). Similar extent of PTO was detected in *tun/TUN and evn/EVN* mutants, further confirming the vast importance of lipid-linked oligosaccharide (LLO) precursor biosynthesis occurring at the cytosolic part of endoplasmic reticulum (ER) membrane (Lindner et al., 2015; Schwarz and Aebi, 2011). Furthermore, functional ALG11 under its native promotor was introduced to the *alg11-1/ALG11* EMS line, resulting in a full complementation of PT reception defects. FER-GFP was properly localized at the filiform apparatus of synergid cells in *alg11-1/ALG11* (Escobar-Restrepo et al., 2007) indicating that biogenesis of FER was not impaired,

however the extent of mis- or under-glycosylation remains to be assessed using mass spectrometry and biochemical approaches. Furthermore, we have not checked localization of LRE and NTA, which in *tun/TUN, evn/EVN* and *artumes* were properly localizing to the FA of synergids (Lindner et al., 2015; Müller et al., 2016a), however it cannot be excluded that they would be differentially processed in the absence of ALG11. Lastly two homologs of FER from *Cr*RLK1L subfamily also expressed at the FA with a key role in PT reception, HERK1 and ANJEA, both have six *N*-glycosylation sites in their ECD. Therefore their biogenesis in *alg11-1/ALG11* background should be tested in the future, as they could be less stable compared to the FER (Galindo-Trigo et al., 2019). In a summary we have discovered a novel component of FER-mediated PT reception signaling cascade, which is a member of the *N*-glycosylation pathway in ER.

From the forward EMS genetic screen designed to find mutants with a *fer*-like PTO phenotype, already two alleles of *TUN*, two alleles of *EVN* and *ALG11* were found, all being ER resident enzymes of the *N*-glycosylation pathway (Lindner et al., 2015). This suggests that successful PT reception heavily relies on the properly *N*-glycosylated receptors and their ligands. However, finding of novel coreceptors/receptors/ligands of FER at synergids has proven to be particularly challenging. One of the possible explanations could be that broadly expressed FER which in different plant tissues intersects with multiple signaling pathways (Chen et al., 2020; Franck et al., 2018), also in synergids is forming large number of heteromeric complexes with different ligands, while being the key component. Having in mind that *N*-glycosylation is profoundly altering protein behavior, increasing their solubility, stability, biological half-life (J-Arey., 2012), it could be that in *N*-glycosylation mutants there is a simultaneous disruption of FER as well of its partners leading to a lower extent of binding/interaction.

One of the major hurdle of finding novel components of PT reception pathway is the large redundancy of underlying molecular players. For instance, importance of ENOLDs (ENs) was uncovered only when quintuple loss-of-function *RNAi-en* was obtained, while none of the single mutants had defects in PT reception, similarly role of FER`s homologs from the *Cr*RLK1L subfamily HERK1 and ANJEA became evident only in *herk1/anjea* double mutants, while single mutants had wild type PT reception (Galindo-Trigo et al., 2019; Hou et al., 2016). Since the initial discovery of RALF1 being ligand of FER in roots, many more RALF–*Cr*RLK1L ligand-receptor pairs have been described (Franck et al., 2018), but ligand of FER during PT reception remains a mystery. This could be explained by the fact that from 37 RALFs present in *A. thaliana*, more than 20 are expressed in the female gametophyte, and 12 are pollen-specific. Furthermore, application of maize PME inhibitor protein ZmPMEI1 induced PT burst *in vitro*, indicating that female gametophyte is utilizing this protein to destabilize PT integrity once PTs approach synergids. However in *A. thaliana* there are 71 putative *PMEI* genes, largely complicating their functional characterization (Palin and Geitmann, 2012; Woriedh et al., 2013). Even though challenging, development of new technologies such as CRISPR/Cas9 technology, will allow to simultaneously knock out several functionally redundant genes to get better understanding of molecular machinery underlying PT reception in *A. thaliana*.

Having in mind that from 10 known female-gametophytic mutants with *fer*-like PTO phenotype found during the last 17 years, three are mutants of the *N*-glycosylation pathway, it is evident that *N*-glycosylation has a vital role during gametophyte interactions. Potential strategy of finding novel members of the PT reception pathway could be through an EMS suppressor screens on either *tun/TUN, evn/EVN or alg11-1/ALG11*. Several studies reported differential impact of either *N*-glycosylation enzymes perturbation or of the components of the ER mediated quality control (ERQC)

on the biogenesis of immune receptors (Saijo, 2010; Tintor and Saijo, 2014). Therefore, it could be that some of the putative PT players will gain a second-site mutation rendering them constitutively active, and hence being able to override PT reception defects. Suppressor screens are the adequate strategy to find novel components of the signaling pathway of interest, and furthermore it would help uncovering interplay between PT reception and *N*-glycosylation pathway (Li and Zhang, 2016).

ALG11 is broadly expressed, and two previous studies reported diverse developmental phenotypes including delayed seed germination under osmotic stress and abscisic acid (ABA) treatment, impaired cellulose synthesis, abnormal primary cell walls, and light sensitive inhibition of the root growth (Manzano et al., 2017; Zhang et al., 2009). Mass spectrometry analysis of ALG11 allele *lew3/LEW3* revealed global reduction in protein *N*-glycosylation as well as accumulation of rare *N*-glycans $Man_3GlcNAc_2$ and $Man_4GlcNAc_2$, which typically do not occur in wild type plants (Zhang et al., 2009). In line with those pleiotropic phenotypes of *alg11-1/ALG11*, we have also observed increased PT bursting upon germination *in vitro*, reminiscent of *anx1/anx2* and *tun/TUN* mutants (Boisson-Dernier et al., 2013; Lindner et al., 2015). This indicates that ALG11 is also an important component of the cell wall (CW) machinery controlling PT growth. We have only analyzed PT growth *in vitro* and careful assessment of pollinated pistils will reveal at which stage do exactly *alg11-1/ALG11* abort their growth. Pollen-expressed members of the *Cr*RLK1L subfamily namely ANX1/2, BUPS1/2 and ERU display either precocious PT bursting, impaired polar growth through the pistil or inefficient PT targeting to the ovules (Boisson-Dernier et al., 2013; Schoenaers et al., 2017; Zhu et al., 2018). Having in mind that these proteins also have several putative *N*-glycosylation sites their biogenesis, and ability to bind RALF4/RALF19 ligands should be carefully evaluated in the future.

Having in mind the vast importance of TUN, EVN and ALG11 we have set out to find which additional components of the *N*-glycosylation machinery are required for the gametophyte recognition during PT reception. We have found that perturbation of enzymes which are catalyzing steps after ALG11 did not have disruptive effect on fertility, resulting in wild-type like PT reception and seed sets. This finding further pointed out the immense importance of a proper biosynthesis of oligosaccharide precursor ($Man_5GlcNAc_2$-PP-Dol) catalysed by EVN, TUN and ALG11 (Aebi, 2013). Similar *fer*-like PTO phenotype was reported in the interspecific crosses between closely related species of *Brassicaceae* family. Pollination of *A. thaliana* stigma with closely related *A. lyrata* or more distantly related *Cardamine flexuosa* pollen led to 55 % and 70% of PTO phenotype. Our group has previously performed a genome-wide association study (GWAS) utilizing natural variations in degree of PTO phenotype among 86 *A. thaliana* accessions when pollinated with *A. lyrata* pollen. Thus, ARTUMES (ARU) was identified which encodes oligosaccharyltransferase 3/6 subunit (OST3/6) involved in the crucial step of *N*-glycosylation (Müller et al., 2016). OST complex is catalyzing addition of preassembled oligosaccharide ($NAcGlc_2Man_9Glc_3$) to the asparagine residue within consensus motif Asn-x-Ser/Thr (x≠P) (Aebi, 2013). Mutations of OST3/6 affected exclusively interspecific PT reception, therefore upon pollination with *A. lyrata* both *aru-1* (84%) and *aru-2* (96%) displayed significantly higher number of ovules with PTO in the comparison to the Col-0 (58%) siliques (Müller et al., 2016).

Having in mind that loss of ARU resulted in the severely impaired recognition of the interspecific pollen, we have performed a systematic characterization of *N*-glycosylation mutants` ability to recognize heterospecific (foreign) pollen. We have found α-mannosyltransferases ALG3 and α-glucosyltransferases ALG10 to both similarly to *aru* be required exclusively for the recognition of interspecific pollen. ALG3 was the first identified glycosyltransferase from plants, which catalyzes

addition of one mannose residue on the $Man_5GlcNAc_2$ precursor upon its transfer to the ER lumen (Henquet et al., 2008). Mass spectrometry analysis revealed unique structural profile in *alg3* with rare *N*-glycan structure as well much lower amount of the complex-type *N*-glycans. Despite evident difference of *N*-glycosylation profile compared to the wild type, there was no obvious developmental phenotype, and *alg3* mutants were as well tolerant to the high temperature and salt stress (Kajiura et al., 2010).

Only recently it has been reported that several immune receptors are undergylcosylated in *alg3*, however their biogenesis was not impaired and even though calcium response to bacterial elicitors was slightly attenuated, the resistance remained intact (Trempel et al., 2016). Perhaps in *alg3* mutant known and putative PT reception players are underglycosylated, but with only slightly impaired biogenesis resulting in the wild-type localization to the FA. It could be proposed that such aberrant receptors can trigger FER-mediated signaling upon recognition of self-pollen, while heterospecific pollen due to different putative ligands can no longer pass the threshold, resulting in the inability to induce PT burst. Furthermore, it is important to keep in mind that in *alg3* some extent of complex-type *N*-glycans could be detected, indicating that there are compensatory mechanisms which were set in place to counteract deficiency of *N*-glycosylation. Additionally, it is known that GNTI can catalyze addition of N-acetylglucosamine residue to M3 structure (product with 3 mannose residues) but with a 20 times lower affinity compared to the M5 (product with 5 mannose residues), therefore aberrant oligosaccharide structures of *alg3* could be still processed but with a lower efficiency (Strasser et al., 2005).

Inactivation of α1,2-glucosyltransferase ALG10 led to the severe underglycosylation defect, activation of unfolded protein response, increased salt sensitivity as well as altered leaf size when grown on soil (Farid et al., 2011). Mass spectrometry analysis revealed impaired synthesis of lipid linked precursor, with a small fraction of rare *N*-glycan structures (Farid et al., 2011). Therefore, we expected to observe a more pronounced defects of PT reception players biogenesis, but this was not the case since reception of self-pollen was completely wild type like, while similarly to *alg3* and *aru* reception of interspecific pollen was heavily impaired. To encapsulate, loss of different ER-localized *N*-glycosylation enzymes results in partially overlapping phenotypes: defects in either intraspecific (*evn, tun, alg11*) or interspecific PT reception (*alg11, alg3, alg10, aru*), hypersensitivity to abiotic stress (*alg11, alg3, stt3a, aru*) and modulation of immune response through the substrate specific biogenesis of immune receptors (*alg3, ost3/6, stt3a*) (Farid et al., 2011, 2013; Koiwa, 2003; Trempel et al., 2016; Zhang et al., 2009). However even though many phenotypes are overlapping, still different mutants have also unique distinct defects such as leaf wilting of *alg11/lew3* or altered leaf size when grown on soil of *alg10*, which were not observed in other mutants. Therefore, it can be proposed that different members of the PT reception pathway are getting diversely decorated in *alg3, alg10* or *aru* backgrounds resulting in the same inability to recognize interspecific pollen tubes.

Current understanding of the plant *N*-glycan maturation in Golgi apparatus is surprisingly limited. In mammals GNTI plays a vital developmental role and loss of GNTI is embryo lethal in mice (Ioffe and Stanley, 1994). In humans disturbance of *N*-glycan processing is implicated in several type II CDGs disorders (Körner et al., 2008). Complex-type *N*-glycan modifications are conserved not only in higher plants but can also be found in distantly related microalgae and mosses, indicating that these modifications play important roles which have been preserved during the evolution (Baïet et al., 2011; Koprivova et al., 2003). In *A. thaliana* loss of GNTI results in normal growth under standard conditions, similar to *alg3*, and only under salt stress *cgl1* displayed inhibition of the primary root

growth, swelling of the root tip and callose accumulation, phenotypes similar to *lew3/alg11*, *stt3a*, and *alg10* (Kang et al., 2008). Typical decorations of plants are present in complex *N*-glycans and consist of the addition of β1,2 xylose, α1,3-fucose as well of generation of Lewis structure formed by attachment of β1,3 galactose and α1,4 fucose to the terminal glucose residue (Bencúr et al., 2005; Strasser, 2014; Strasser et al., 2004). We have found both *cgl1* as well as *xylt/fut11/fut12* triple mutants to be non-essential during the intraspecific PT reception. On the other hand, in interspecific crosses with *A. lyrata* substantially higher degree of PTO phenotype was observed for both *cgl1* as well as triple mutant performing processing steps downstream of *cgl1*. These results were in line with observation that in *alg3* in which no obvious phenotype could be detected, there was a significant impairment of interspecific pollen recognition. Additionally, *alg3 a*lmost completely lacked complex type *N*-glycans further confirming importance of these modifications. So far the only known target of GNTI is a membrane-anchored endo -β-1,4-glucanase KORRIGAN1 required for the cellulose biosynthesis (Kang et al., 2008; Lane et al., 2001). Therefore, future studies should be aimed at analyzing *N*-glycan composition of the known molecular PT reception players. Mass spectrometry (MS) can be utilized to reveal overall composition and most abundant type of *N*-glycans, as well as to assess *N*-glycan site occupancy in a more targeted approach (Farid et al., 2011, 2013; Liebminger et al., 2013; Yamamoto et al., 2014). Having in mind that MS analysis can be challenging especially when working with low abundant proteins, it could be coupled with biochemical and molecular approaches, such as lectin blots against Concanavalin A, which enables detection of high-mannose type *N*-glycans (Burén et al., 2011; Farid et al., 2013). Additional way to assess amount of complex-type *N*-glycans is by using anti-horseradish peroxidase (anti-HRP), which recognizes β-1,2-Xyl and core α-1,3-Fuc residues, typically present in complex-type *N*-glycans (Burén et al., 2011; Yamamoto et al., 2014). The ultimate goal would be the ability to perform live imaging and track changes of *N*-glycosylation during PT reception and newest advancement in chemoenzymatic glycan labeling (CeGL) techniques offer a promise in that direction (Farid et al., 2013).

To summarize, appropriate biosynthesis and *N*-glycan processing in both ER and Golgi apparatus is essential for the successful communication between gametophytes. The fact that we observed both intra- and inter-specific PT reception defects in the *alg11-1/ALG11* loss of function mutant implicates that early processing steps occurring at the cytosolic part of ER membrane have a more profound impact on the functionality of PT reception players. However, the fact that FER biogenesis is not impaired in *alg11-1/ALG11, tun/TUN and evn/EVN* suggest that both protein-protein interactions as well as carbohydrates-mediated recognition are crucial factors to ensure species-specific PT reception. *N*-glycans roles can be divided into three categories: structural (correct folding; protection from proteases, extracellular matrix organization); extrinsic (recognition of pathogen-associated molecular patterns) and intrinsic (ability to recognize same species antigens). Hence this ability of carbohydrates to differentiate between self vs non-self is especially important in the light of reproduction, how for plants as well for many other species (Varki, 2017). Glycans are important at many stages of mammalian fertilization, starting from oogenesis, spermatogenesis, sperm migration, maturation and early embryo development (Akintayo and Stanley, 2019; Cheon and Kim, 2015). Zona pellucida (ZP) is translucent matrix surrounding animal oocytes and it controls several aspects of fertilization including species-specific sperm recognition, induction of acrosome reaction and blocking of polyspermy. Several contradictory results proposed both protein-proteins as well protein -carbohydrate interactions to be vital during sperm binding to glycoproteins of ZP (Clark, 2010). This led to the establishment of a “domain-specific” model, which proposed a crucial role for both mechanisms (Clark, 2013).

References

Adhikari, P.B., Liu, X., Wu, X., Zhu, S., and Kasahara, R.D. (2020). Fertilization in flowering plants: an odyssey of sperm cell delivery. Plant Mol Biol.

Aebi, M. (2013). N-linked protein glycosylation in the ER. Biochimica et Biophysica Acta (BBA) - Molecular Cell Research *1833*, 2430–2437.

Akintayo, A., and Stanley, P. (2019). Roles for Golgi Glycans in Oogenesis and Spermatogenesis. Front. Cell Dev. Biol. *7*, 98.

Baïet, B., Burel, C., Saint-Jean, B., Louvet, R., Menu-Bouaouiche, L., Kiefer-Meyer, M.-C., Mathieu-Rivet, E., Lefebvre, T., Castel, H., Carlier, A., et al. (2011). *N* -Glycans of *Phaeodactylum tricornutum* Diatom and Functional Characterization of Its *N* -Acetylglucosaminyltransferase I Enzyme. J. Biol. Chem. *286*, 6152–6164.

Bencúr, P., Steinkellner, H., Svoboda, B., Mucha, J., Strasser, R., Kolarich, D., Hann, S., Köllensperger, G., Glössl, J., Altmann, F., et al. (2005). Arabidopsis thaliana β1,2-xylosyltransferase: an unusual glycosyltransferase with the potential to act at multiple stages of the plant N-glycosylation pathway. Biochemical Journal *388*, 515–525.

Bleckmann, A., Alter, S., and Dresselhaus, T. (2014). The beginning of a seed: regulatory mechanisms of double fertilization. Front. Plant Sci. *5*.

Boisson-Dernier, A., Frietsch, S., Kim, T.-H., Dizon, M.B., and Schroeder, J.I. (2008). The Peroxin Loss-of-Function Mutation abstinence by mutual consent Disrupts Male-Female Gametophyte Recognition. Current Biology *18*, 63–68.

Boisson-Dernier, A., Lituiev, D.S., Nestorova, A., Franck, C.M., Thirugnanarajah, S., and Grossniklaus, U. (2013). ANXUR Receptor-Like Kinases Coordinate Cell Wall Integrity with Growth at the Pollen Tube Tip Via NADPH Oxidases. PLoS Biol *11*, e1001719.

Burén, S., Ortega-Villasante, C., Blanco-Rivero, A., Martínez-Bernardini, A., Shutova, T., Shevela, D., Messinger, J., Bako, L., Villarejo, A., and Samuelsson, G. (2011). Importance of post-translational modifications for functionality of a chloroplast-localized carbonic anhydrase (CAH1) in Arabidopsis thaliana. PLoS One *6*, e21021–e21021.

Capron, A., Gourgues, M., Neiva, L.S., Faure, J.-E., Berger, F., Pagnussat, G., Krishnan, A., Alvarez-Mejia, C., Vielle-Calzada, J.-P., Lee, Y.-R., et al. (2008). Maternal Control of Male-Gamete Delivery in *Arabidopsis* Involves a Putative GPI-Anchored Protein Encoded by the *LORELEI* Gene. Plant Cell *20*, 3038–3049.

Chen, J., Zhu, S., Ming, Z., Liu, X., and Yu, F. (2020). FERONIA cytoplasmic domain: node of varied signal outputs. ABIOTECH.

Cheon, Y.-P., and Kim, C.-H. (2015). Impact of glycosylation on the unimpaired functions of the sperm. Clin Exp Reprod Med *42*, 77.

Clark, G.F. (2010). The Mammalian Zona Pellucida: A Matrix That Mediates Both Gamete Binding and Immune Recognition? Systems Biology in Reproductive Medicine *56*, 349–364.

Clark, G.F. (2013). The role of carbohydrate recognition during human sperm-egg binding. Human Reproduction *28*, 566–577.

Dresselhaus, T., and Franklin-Tong, N. (2013). Male–Female Crosstalk during Pollen Germination, Tube Growth and Guidance, and Double Fertilization. Molecular Plant *6*, 1018–1036.

Escobar-Restrepo, J.-M., Huck, N., Kessler, S., Gagliardini, V., Gheyselinck, J., Yang, W.-C., and Grossniklaus, U. (2007). The FERONIA Receptor-like Kinase Mediates Male-Female Interactions During Pollen Tube Reception. Science *317*, 656–660.

Farid, A., Pabst, M., Schoberer, J., Altmann, F., Glössl, J., and Strasser, R. (2011). *Arabidopsis thaliana* alpha1,2-glucosyltransferase (ALG10) is required for efficient N-glycosylation and leaf growth: *Arabidopsis alpha1,2-glucosyltransferase*. The Plant Journal *68*, 314–325.

Farid, A., Malinovsky, F.G., Veit, C., Schoberer, J., Zipfel, C., and Strasser, R. (2013). Specialized Roles of the Conserved Subunit OST3/6 of the Oligosaccharyltransferase Complex in Innate Immunity and Tolerance to Abiotic Stresses. Plant Physiol. *162*, 24–38.

Franck, C.M., Westermann, J., and Boisson-Dernier, A. (2018). Plant Malectin-Like Receptor Kinases: From Cell Wall Integrity to Immunity and Beyond. Annu. Rev. Plant Biol. *69*, 301–328.

Galindo-Trigo, S., Blanco-Touriñán, N., DeFalco, T.A., Wells, E.S., Gray, J.E., Zipfel, C., and Smith, L.M. (2019). *Cr* RLK 1L receptor-like kinases HERK 1 and ANJEA are female determinants of pollen tube reception. EMBO Rep.

Gross-Hardt, R., Kägi, C., Baumann, N., Moore, J.M., Baskar, R., Gagliano, W.B., Jürgens, G., and Grossniklaus, U. (2007). LACHESIS restricts gametic cell fate in the female gametophyte of Arabidopsis. PLoS Biol *5*, e47–e47.

Henquet, M., Lehle, L., Schreuder, M., Rouwendal, G., Molthoff, J., Helsper, J., van der Krol, S., and Bosch, D. (2008). Identification of the Gene Encoding the α1,3-Mannosyltransferase (ALG3) in *Arabidopsis* and Characterization of Downstream *N* -Glycan Processing. Plant Cell *20*, 1652–1664.

Hou, Y., Guo, X., Cyprys, P., Zhang, Y., Bleckmann, A., Cai, L., Huang, Q., Luo, Y., Gu, H., Dresselhaus, T., et al. (2016). Maternal ENODLs Are Required for Pollen Tube Reception in Arabidopsis. Current Biology *26*, 2343–2350.

Huck, N. (2003). The Arabidopsis mutant feronia disrupts the female gametophytic control of pollen tube reception. Development *130*, 2149–2159.

Ioffe, E., and Stanley, P. (1994). Mice lacking N-acetylglucosaminyltransferase I activity die at mid-gestation, revealing an essential role for complex or hybrid N-linked carbohydrates. Proceedings of the National Academy of Sciences *91*, 728–732.

J., B. (2012). The Role of Glycosylation in Receptor Signaling. In Glycosylation, S. Petrescu, ed. (InTech), p.

Kajiura, H., Seki, T., and Fujiyama, K. (2010). Arabidopsis thaliana ALG3 mutant synthesizes immature oligosaccharides in the ER and accumulates unique N-glycans. Glycobiology *20*, 736–751.

Kang, J.S., Frank, J., Kang, C.H., Kajiura, H., Vikram, M., Ueda, A., Kim, S., Bahk, J.D., Triplett, B., Fujiyama, K., et al. (2008). Salt tolerance of Arabidopsis thaliana requires maturation of N-glycosylated proteins in the Golgi apparatus. Proceedings of the National Academy of Sciences *105*, 5933–5938.

Kasahara, R.D., Portereiko, M.F., Sandaklie-Nikolova, L., Rabiger, D.S., and Drews, G.N. (2005). MYB98 Is Required for Pollen Tube Guidance and Synergid Cell Differentiation in Arabidopsis. Plant Cell *17*, 2981.

Kessler, S.A., Shimosato-Asano, H., Keinath, N.F., Wuest, S.E., Ingram, G., Panstruga, R., and Grossniklaus, U. (2010). Conserved Molecular Components for Pollen Tube Reception and Fungal Invasion. Science *330*, 968–971.

Koiwa, H. (2003). The STT3a Subunit Isoform of the Arabidopsis Oligosaccharyltransferase Controls Adaptive Responses to Salt/Osmotic Stress. THE PLANT CELL ONLINE *15*, 2273–2284.

Koprivova, A., Altmann, F., Gorr, G., Kopriva, S., Reski, R., and Decker, E.L. (2003). N-Glycosylation in the Moss Physcomitrella patens is Organized Similarly to that in Higher Plants. Plant Biology *5*, 582–591.

Körner, C., Lübbehusen, J., and Thiel, C. (2008). Congenital Disorders of Glycosylation. In Laboratory Guide to the Methods in Biochemical Genetics, N. Blau, M. Duran, and K.M. Gibson, eds. (Berlin, Heidelberg: Springer Berlin Heidelberg), pp. 379–416.

Kulichová, K., Kumar, V., Steinbachová, L., Klodová, B., Timofejeva, L., Juříček, M., Honys, D., and Hafidh, S. (2020). PRP8A and PRP8B spliceosome subunits act co-ordinately to control pollen tube attraction in Arabidopsis. Development dev.186742.

Lane, D.R., Wiedemeier, A., Peng, L., Hocart, C.H., Birch, R.J., Baskin, T.I., Burn, J.E., Arioli, T., Betzner, A.S., and Williamson, R.E. (2001). Temperature-Sensitive Alleles of RSW2 Link the KORRIGAN Endo-1,4-□-Glucanase to Cellulose Synthesis and Cytokinesis in Arabidopsis. 11.

Leydon, A.R., Beale, K.M., Woroniecka, K., Castner, E., Chen, J., Horgan, C., Palanivelu, R., and Johnson, M.A. (2013). Three MYB Transcription Factors Control Pollen Tube Differentiation Required for Sperm Release. Current Biology *23*, 1209–1214.

Li, X., and Zhang, Y. (2016). Suppressor Screens in Arabidopsis. In Plant Signal Transduction: Methods and Protocols, J.R. Botella, and M.A. Botella, eds. (New York, NY: Springer New York), pp. 1–8.

Liang, Y., Tan, Z.-M., Zhu, L., Niu, Q.-K., Zhou, J.-J., Li, M., Chen, L.-Q., Zhang, X.-Q., and Ye, D. (2013). MYB97, MYB101 and MYB120 Function as Male Factors That Control Pollen Tube-Synergid Interaction in Arabidopsis thaliana Fertilization. PLoS Genet *9*, e1003933.

Liebminger, E., Grass, J., Altmann, F., Mach, L., and Strasser, R. (2013). Characterizing the Link between Glycosylation State and Enzymatic Activity of the Endo-β1,4-glucanase KORRIGAN1 from *Arabidopsis thaliana*. J. Biol. Chem. *288*, 22270–22280.

Lindner, H., Raissig, M.T., Sailer, C., Shimosato-Asano, H., Bruggmann, R., and Grossniklaus, U. (2012). SNP-Ratio Mapping (SRM): Identifying Lethal Alleles and Mutations in Complex Genetic Backgrounds by Next-Generation Sequencing. Genetics *191*, 1381–1386.

Lindner, H., Kessler, S.A., Müller, L.M., Shimosato-Asano, H., Boisson-Dernier, A., and Grossniklaus, U. (2015). TURAN and EVAN Mediate Pollen Tube Reception in Arabidopsis Synergids through Protein Glycosylation. PLoS Biol *13*, e1002139.

Manzano, C., Pallero-Baena, M., Silva-Navas, J., Navarro Neila, S., Casimiro, I., Casero, P., Garcia-Mina, J.M., Baigorri, R., Rubio, L., Fernandez, J.A., et al. (2017). A light-sensitive mutation in Arabidopsis LEW3 reveals the important role of N-glycosylation in root growth and development. Journal of Experimental Botany *68*, 5103–5116.

Müller, L.M., Lindner, H., Pires, N.D., Gagliardini, V., and Grossniklaus, U. (2016a). A subunit of the oligosaccharyltransferase complex is required for interspecific gametophyte recognition in Arabidopsis. Nat Commun *7*, 10826.

Müller, L.M., Lindner, H., Pires, N.D., Gagliardini, V., and Grossniklaus, U. (2016b). A subunit of the oligosaccharyltransferase complex is required for interspecific gametophyte recognition in Arabidopsis. Nat Commun *7*, 10826.

Ohtani, M., Demura, T., and Sugiyama, M. (2013). Arabidopsis ROOT INITIATION DEFECTIVE1, a DEAH-Box RNA Helicase Involved in Pre-mRNA Splicing, Is Essential for Plant Development. The Plant Cell *25*, 2056–2069.

Page, D.R., and Grossniklaus, U. (2002). The art and design of genetic screens: Arabidopsis thaliana. Nat Rev Genet *3*, 124–136.

Palin, R., and Geitmann, A. (2012). The role of pectin in plant morphogenesis. Biosystems *109*, 397–402.

Punwani, J.A., Rabiger, D.S., Lloyd, A., and Drews, G.N. (2008). The MYB98 subcircuit of the synergid gene regulatory network includes genes directly and indirectly regulated by MYB98. The Plant Journal *55*, 406–414.

Rotman, N., Gourgues, M., Guitton, A.-E., Faure, J.-E., and Berger, F. (2008). A Dialogue between the Sirène Pathway in Synergids and the Fertilization Independent Seed Pathway in the Central Cell Controls Male Gamete Release during Double Fertilization in Arabidopsis. Molecular Plant *1*, 659–666.

Saijo, Y. (2010). ER quality control of immune receptors and regulators in plants: ER quality control of plant immune receptors. Cellular Microbiology *12*, 716–724.

Schoenaers, S., Balcerowicz, D., Costa, A., and Vissenberg, K. (2017). The Kinase ERULUS Controls Pollen Tube Targeting and Growth in Arabidopsis thaliana. Front. Plant Sci. *8*, 1942.

Schwarz, F., and Aebi, M. (2011). Mechanisms and principles of N-linked protein glycosylation. Current Opinion in Structural Biology *21*, 576–582.

Sprunck, S. (2020). Twice the fun, double the trouble: gamete interactions in flowering plants. Current Opinion in Plant Biology *53*, 106–116.

Strasser, R. (2014). Biological significance of complex N-glycans in plants and their impact on plant physiology. Front. Plant Sci. *5*.

Strasser, R., Altmann, F., Mach, L., Glössl, J., and Steinkellner, H. (2004). Generation of *Arabidopsis thaliana* plants with complex *N* -glycans lacking β1,2-linked xylose and core α1,3-linked fucose. FEBS Letters *561*, 132–136.

Strasser, R., Stadlmann, J., Svoboda, B., Altmann, F., Glössl, J., and Mach, L. (2005). Molecular basis of N-acetylglucosaminyltransferase I deficiency in Arabidopsis thaliana plants lacking complex N-glycans. Biochemical Journal *387*, 385–391.

Tintor, N., and Saijo, Y. (2014). ER-mediated control for abundance, quality, and signaling of transmembrane immune receptors in plants. Front. Plant Sci. *5*.

Trempel, F., Kajiura, H., Ranf, S., Grimmer, J., Westphal, L., Zipfel, C., Scheel, D., Fujiyama, K., and Lee, J. (2016). Altered glycosylation of exported proteins, including surface immune receptors, compromises calcium and downstream signaling responses to microbe-associated molecular patterns in Arabidopsis thaliana. BMC Plant Biol *16*, 31.

Varki, A. (2017). Biological roles of glycans. Glycobiology *27*, 3–49.

Wang, J.-G., Feng, C., Liu, H.-H., Feng, Q.-N., Li, S., and Zhang, Y. (2017). AP1G mediates vacuolar acidification during synergid-controlled pollen tube reception. Proc Natl Acad Sci U S A *114*, E4877–E4883.

Woriedh, M., Wolf, S., Márton, M.L., Hinze, A., Gahrtz, M., Becker, D., and Dresselhaus, T. (2013). External application of gametophyte-specific ZmPMEI1 induces pollen tube burst in maize. Plant Reprod *26*, 255–266.

Yamamoto, M., Tantikanjana, T., Nishio, T., Nasrallah, M.E., and Nasrallah, J.B. (2014). Site-Specific *N*- Glycosylation of the S-Locus Receptor Kinase and Its Role in the Self-Incompatibility Response of the Brassicaceae. Plant Cell *26*, 4749–4762.

Zhang, M., Henquet, M., Chen, Z., Zhang, H., Zhang, Y., Ren, X., Van Der Krol, S., Gonneau, M., Bosch, D., and Gong, Z. (2009). LEW3, encoding a putative Î±-1,2-mannosyltransferase (ALG11) in N-linked glycoprotein, plays vital roles in cell-wall biosynthesis and the abiotic stress response in Arabidopsis thaliana: Protein.N-glycosylation, plant development and abiotic stress. The Plant Journal *60*, 983–999.

Zheng, Y.-Y., Lin, X.-J., Liang, H.-M., Wang, F.-F., and Chen, L.-Y. (2018). The Long Journey of Pollen Tube in the Pistil. IJMS *19*, 3529.

Zhu, D.Z., Zhao, X.F., Liu, C.Z., Ma, F.F., Wang, F., Gao, X.-Q., and Zhang, X.S. (2016). Interaction between RNA helicase ROOT INITIATION DEFECTIVE 1 and GAMETOPHYTIC FACTOR 1 is involved in female gametophyte development in Arabidopsis. EXBOTJ *67*, 5757–5768.

Zhu, L., Chu, L.-C., Liang, Y., Zhang, X.-Q., Chen, L.-Q., and Ye, D. (2018). The Arabidopsis CrRLK1L protein kinases BUPS1 and BUPS2 are required for normal growth of pollen tubes in the pistil. Plant J *95*, 474–486.